



**Polymères contenant des paires de Lewis de type  
amine-borane, en tant que réservoirs d'hydrogène :  
relation structure/activité**

Audrey Ledoux

► **To cite this version:**

Audrey Ledoux. Polymères contenant des paires de Lewis de type amine-borane, en tant que réservoirs d'hydrogène: relation structure/activité. Polymers. Université de Lyon, 2016. English. NNT : 2016LYSE1234 . tel-01589242

**HAL Id: tel-01589242**

**<https://theses.hal.science/tel-01589242>**

Submitted on 18 Sep 2017

**HAL** is a multi-disciplinary open access archive for the deposit and dissemination of scientific research documents, whether they are published or not. The documents may come from teaching and research institutions in France or abroad, or from public or private research centers.

L'archive ouverte pluridisciplinaire **HAL**, est destinée au dépôt et à la diffusion de documents scientifiques de niveau recherche, publiés ou non, émanant des établissements d'enseignement et de recherche français ou étrangers, des laboratoires publics ou privés.



# **THÈSE de DOCTORAT DE L'UNIVERSITE DE LYON**

effectuée à

**l'Université Claude Bernard Lyon 1**

**Ecole Doctorale de Chimie de Lyon (ED206)**

**Spécialité Chimie**

Soutenue publiquement le 14 novembre 2016 par

**Audrey LEDOUX**

---

## **Lewis-pair amine-borane polymers as hydrogen reservoirs: structure/reactivity relationship**

---

Devant le jury composé de

**Dr. Sylviane Sabo-Etienne**, lab. LCC, Université de Toulouse

Rapporteur

**Prof. Daniel Taton**, lab. LCPO, Université de Bordeaux

Rapporteur

**Prof. Ian Manners**, University of Bristol

Examineur

**Prof. Catherine Journet-Gautier**, lab. LMI, UCBL Lyon

Examineur

**Dr. Emmanuel Lacôte**, lab. LHCEP, UCBL Lyon

Directeur de thèse

**Dr. Jean Raynaud**, lab. C2P2, UCBL Lyon

Co-encadrant de thèse



## UNIVERSITE CLAUDE BERNARD - LYON 1

### Président de l'Université

**M. le Professeur Frédéric FLEURY**

Président du Conseil Académique

M. le Professeur Hamda BEN HADID

Vice-président du Conseil d'Administration

M. le Professeur Didier REVEL

Vice-président du Conseil Formation et Vie Universitaire

M. le Professeur Philippe CHEVALIER

Vice-président de la Commission Recherche

M. Fabrice VALLÉE

Directeur Général des Services

M. Alain HELLEU

### *COMPOSANTES SANTE*

Faculté de Médecine Lyon Est – Claude Bernard

Directeur : M. le Professeur J. ETIENNE

Faculté de Médecine et de Maïeutique Lyon Sud – Charles Mérieux

Directeur : Mme la Professeure C. BURILLON

Faculté d'Odontologie

Directeur : M. le Professeur D. BOURGEOIS

Institut des Sciences Pharmaceutiques et Biologiques

Directeur : Mme la Professeure C. VINCIGUERRA

Institut des Sciences et Techniques de la Réadaptation

Directeur : M. X. PERROT

Département de formation et Centre de Recherche en Biologie Humaine

Directeur : Mme la Professeure A-M. SCHOTT

### *COMPOSANTES ET DEPARTEMENTS DE SCIENCES ET TECHNOLOGIE*

Faculté des Sciences et Technologies

Directeur : M. F. DE MARCHI

Département Biologie

Directeur : M. le Professeur F. THEVENARD

Département Chimie Biochimie

Directeur : Mme C. FELIX

Département GEP

Directeur : M. Hassan HAMMOURI

Département Informatique

Directeur : M. le Professeur S. AKKOUCHE

Département Mathématiques

Directeur : M. le Professeur G. TOMANOV

Département Mécanique

Directeur : M. le Professeur H. BEN HADID

Département Physique

Directeur : M. le Professeur J-C PLENET

UFR Sciences et Techniques des Activités Physiques et Sportives

Directeur : M. Y. VANPOULLE

Observatoire des Sciences de l'Univers de Lyon

Directeur : M. B. GUIDERDONI

Polytech Lyon

Directeur : M. le Professeur E. PERRIN

Ecole Supérieure de Chimie Physique Electronique

Directeur : M. G. PIGNAULT

Institut Universitaire de Technologie de Lyon 1

Directeur : M. le Professeur C. VITON

Ecole Supérieure du Professorat et de l'Education

Directeur : M. le Professeur A. MOUGNIOTTE

Institut de Science Financière et d'Assurances

Directeur : M. N. LEBOISNE





*Notre pouvoir ne réside pas dans notre capacité à refaire le monde, mais dans  
notre habileté à nous recréer nous-même.*

*Gandhi*



*À la mémoire de mon père, Gérard Guy Louis Marie Ledoux,  
Pour m'avoir transmis sa passion pour les Sciences et la Philosophie,  
Pour m'avoir appris que les miracles arrivent bien dans le Cœur que de ceux qui  
les attendent...  
Pour cette revanche qui est aussi la sienne.*



## Remerciements

---

Ma thèse, que j'ai effectuée dans le laboratoire C2P2, a été l'occasion pour moi de travailler sur un projet de recherche passionnant. J'ai eu la chance de travailler avec le Dr Emmanuel Lacôte et le Dr Jean Raynaud qui m'ont enseignés de nombreux savoirs tant sur le plan scientifique que sur le plan humain. Ainsi je tiens particulièrement à les remercier (et le mot est faible) pour m'avoir laissé la liberté de proposer mes idées, pour m'avoir transmis leurs exigences à l'égard du travail bien fait, pour leur bonne humeur, pour leur enthousiasme intarissable et pour leur écoute dans les moments qui se sont avérés nécessaires. Je tiens également à témoigner toute ma gratitude à l'égard de Dr. Chloé Thieuleux, de Dr. Alessandra Quadrelli ainsi qu'à M. Laurent Veyre qui ont partagés ma vie au laboratoire. Merci donc, pour votre disponibilité, pour nos discussions et pour tous vos conseils humains et professionnels. Je remercie également Dr. Christophe Boisson, Dr. Vincent Monteil, Dr. David Farrusseng et Pr. Eric Drockenmuller pour leurs collaborations et leurs conseils.

Ma thèse a été une expérience très riche en échanges avec les différents professionnels de mon laboratoire et avec nos collaborateurs à l'étranger. Je tiens à remercier le Pr. Todd Marder pour son accueil chaleureux dans son laboratoire en Allemagne et pour ses nombreux conseils, ainsi que Martin Eck et Emily Neeves qui ont été des rencontres mémorables. Merci aux Ingénieurs d'étude et aux Ingénieurs de recherche, en particulier Olivier Boiron pour m'avoir transmis son savoir avec tant d'enthousiasme, ainsi que Nesrine Cherni et Christine Lucas pour notre travail d'équipe au comité de sécurité du laboratoire et pour la gestion des déchets. Un énorme Merci aux étudiants et aux post-docs du C2P2. Merci à toi Stéphane Cadot pour m'avoir appris un dixième de tes nombreux savoirs, pour tes petits carrés de silicium en cadeaux et pour tous nos fous rires du vendredi soir. Merci à Reine Sayah à David Baudouin pour leur amitié, à Giuliana Rubulotta *la mia cara siciliana*, et en particulier, un grand merci à Delphine Crozet pour m'avoir montré le monde avec tant d'esprit et tant de courage. Merci à ma famille pour leurs encouragements dans les moments de travail les plus soutenus et enfin un très grand merci à Paolo Larini pour son soutien, son écoute et pour nos passionnantes discussions scientifiques et philosophiques dont je ne me lasserai jamais.



## List of Abbreviations

---

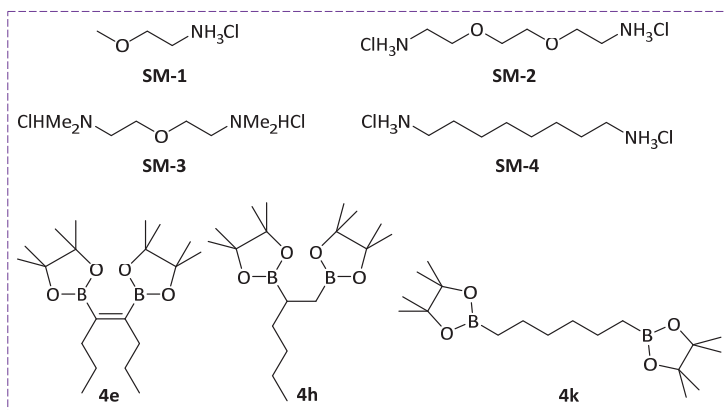
<b>AB</b>	Ammonia-borane
<b>ATR-IR</b>	Attenuated Total Reflectance - Infrared
<b>ATRP</b>	Atom Transfer Radical Polymerization
<b>BPO</b>	Benzoyl peroxyde
<b>BDE</b>	Bond Dissociation Energy
<b>DADB</b>	Diammoniate of Diborane
<b>DHB</b>	Dihydrogen Bonding
<b>DFT</b>	Density Functional Theory
<b>DOE</b>	Departement of Energy (USA)
<b>DSC</b>	Differential Scanning Calorimetry
<b>GC-MS</b>	Gas-Chromatography Mass-Spectroscopy
<b>MAS</b>	Magic Angle Spin
<b>NCI</b>	Non Covalent Interactions
<b>NH-BH</b>	Amine-borane with hydrogen substituted N and B
<b>C-NH-BH</b>	NH-BH inserted into an organic scaffold
<b>NMR</b>	Nuclear Magnetic Resonance
<b>Pin</b>	Pinacol
<b>ppm</b>	Part per million
<b>PVB</b>	Pinacol 4-vinylboronate
<b>RAFT</b>	Reversible Addition-Fragmentation Chain Transfer
<b>SEC</b>	Steric Exclusion Chromatography
<b>TGA</b>	Thermal Gravimetric Analysis
<b>TPD</b>	Temperature Program Desorption
<b>TS</b>	Transition State
<b>wt%</b>	Weight percent



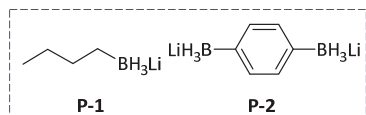
# Index

## Polyboramines (section 2)

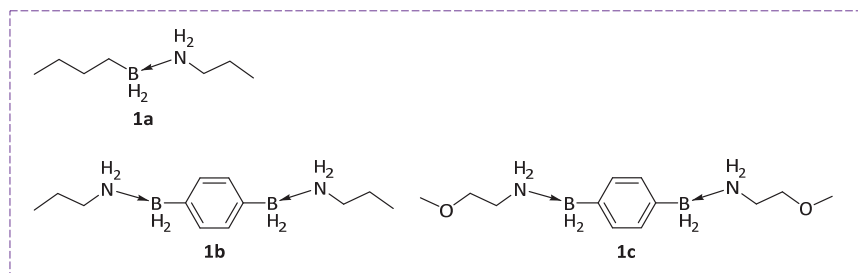
### Starting materials



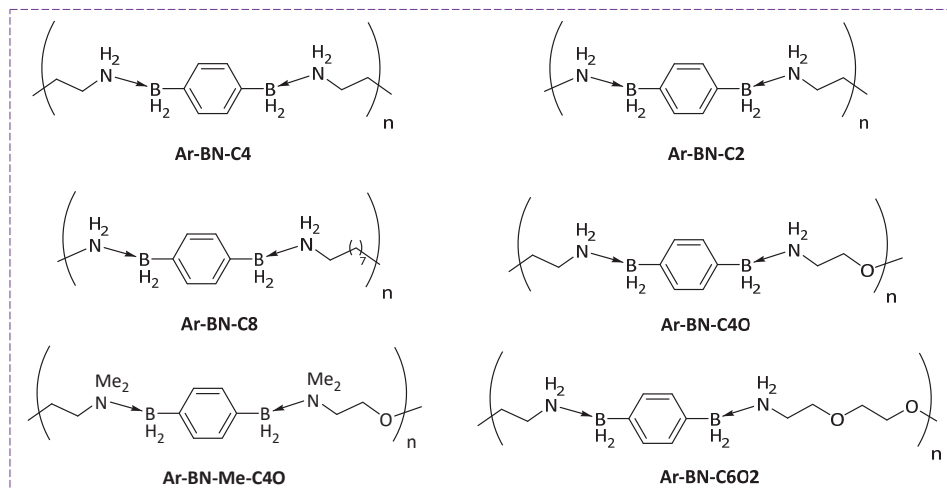
### Intermediates



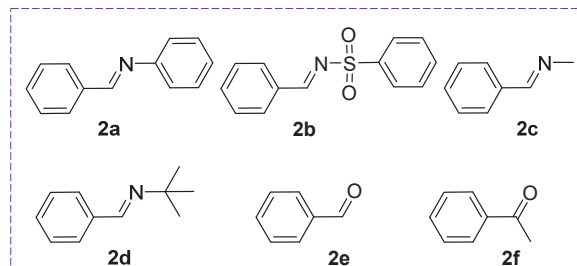
### Molecular bricks



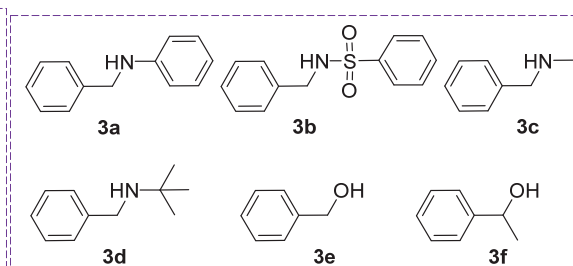
### Polyboramines



### Substrates

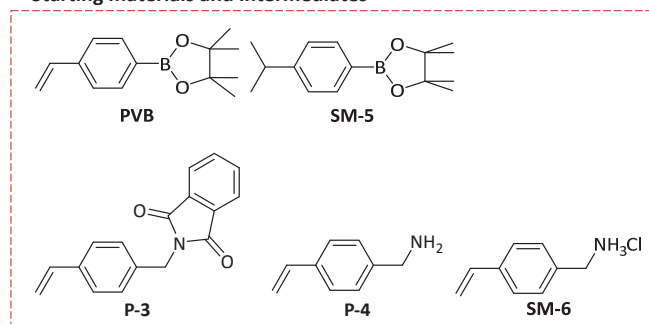


### Products

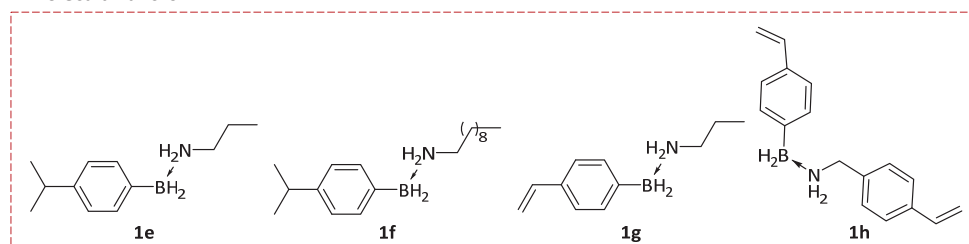


## Amine-borane functionalized (co)polymers (section 3)

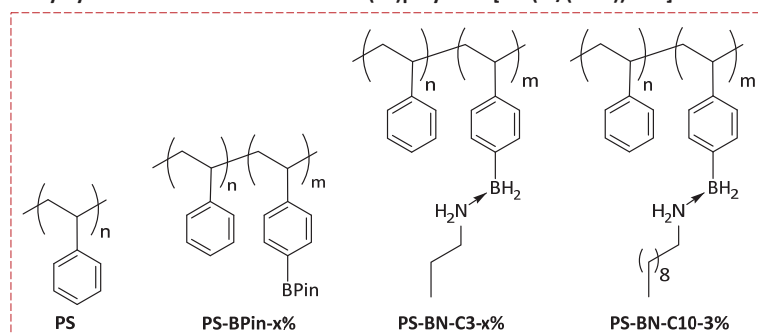
### Starting materials and intermediates



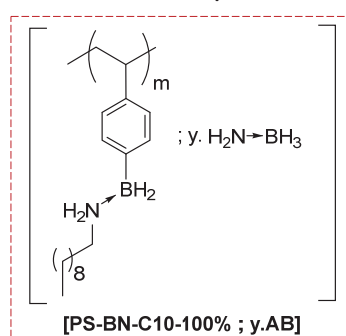
### Molecular bricks



### Polystyrene and boron functionalized (co)polymers [ $x = (m/(m+n)) \cdot 100$ ]



### Ammonia-borane doped amine-borane polymers



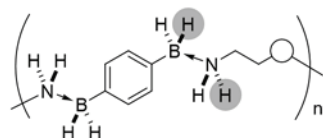
### General :

Structure between brackets "[ ]" are supposed intermediates or products and have not been formally identified.

## Résumé

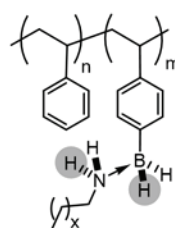
Le stockage et le relargage contrôlé du dihydrogène est devenu un domaine important de recherche visant à répondre à une demande énergétique grandissante. Bien que le borazane ( $\text{NH}_3\text{-BH}_3$ ) ait été identifié comme un candidat de choix dû à sa grande capacité de stockage (19.6 wt.%  $\text{H}_2$ ),<sup>i</sup> les chercheurs ont mis en évidence certaines limitations telles que des difficultés de mise en forme et des difficultés de régénération du matériau.<sup>ii, iii</sup> Nous avons tenté de répondre à ces problématiques en concevant de nouveaux polymères contenant des fonctions de type amine-borane dans leur chaîne principale (polyboramines) et sur les chaînes latérales, afin d'étudier l'influence du squelette polymère sur les propriétés du matériau et sa réactivité associée. Nos objectifs ont visé une facilité de synthèse et de mise en forme mais aussi l'éventualité d'une régénération simple et directe du réservoir après relargage du dihydrogène. Nous avons synthétisé ces polymères en une étape quantitativement et sélectivement à partir de fragments commerciaux ou facilement accessibles. Nous avons observé une influence conséquente de la matrice polymère sur les paramètres cinétiques et thermodynamiques de la déshydrogénation, à la suite de quoi nous avons étudié les paramètres structuraux influençant la réactivité. De plus les polymères obtenus après déshydrogénation ont montré d'intéressantes propriétés mécaniques et chimiques. Ces résultats nous ont encouragés à nous pencher vers le recyclage de ces réservoirs à hydrogène.

### Section 2



Amine-boranes en chaîne principale  
Polyboramines

### Section 3



Amine-boranes en chaîne latérale  
(co)polymères



## Réservoirs polymères d'hydrogène

<sup>i</sup> A. Staubitz, A. P. M. Robertson and I. Manners, Chem. Rev., 2010, 110, 7.

<sup>ii</sup> Z. Liu and T. B. Marder, Angew. Chem. Int. Ed. 2008, 47, 242.

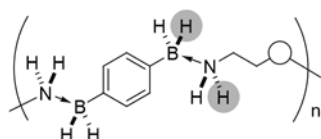
<sup>iii</sup> W. Luo, L.N. Zakharov, and S.Y. Liu, J. Am. Chem. Soc., 2011, 133, 13006.

## Abstract

Dihydrogen storage and controlled release has become an essential area of research aspiring to answer the ever-growing energetic demand. If ammonia-borane ( $\text{NH}_3\text{-BH}_3$ ) was early on identified as a premium candidate to constitute a  $\text{H}_2$  reservoir, due to its maximum storage capacity (19.6 wt.%  $\text{H}_2$ ),<sup>i</sup> researchers have then identified its shortcomings such as poor processability and troublesome material recycling.<sup>ii,iii</sup>

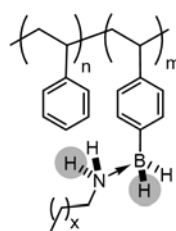
We have proposed to address these issues through the synthesis of new polymers containing the amine-borane motif in the main-chain (polyboramine) or as pendant moieties, harnessing improvements brought by the polymer backbone on the reactivity and material properties. We aimed at an ease of preparation, an enhanced processability but also an access to recyclable materials *via* simple re-hydrogenation techniques. We have synthesized these polymers from available organic building blocks by simple treatment of diammonium and bisboronic acids with  $\text{LiAlH}_4$ . We showed that the polymer matrix has a drastic effect on kinetic and thermodynamic parameters of the dehydrogenation process. We investigated the role of structural parameters on the reactivity. Moreover, polymers obtained after dehydrogenation ( $\text{H}_2$  release) still feature interesting mechanical and chemical properties. These results give us hope regarding the recycling of these hydrogen reservoirs.

### Section 2



Main-chain amine-borane polymers  
Polyboramines

### Section 3



Side-chain amine-borane (co)polymers



## Polymer hydrogen reservoirs

<sup>i</sup> A. Staubitz, A. P. M. Robertson and I. Manners, Chem. Rev., 2010, 110, 7.

<sup>ii</sup> Z. Liu and T. B. Marder, Angew. Chem. Int. Ed. 2008, 47, 242.

<sup>iii</sup> W. Luo, L.N. Zakharov, and S.Y. Liu, J. Am. Chem. Soc., 2011, 133, 13006.

## Résumé long en Français

---

Le développement des techniques de stockage de dihydrogène pour le domaine des transports est très prometteur car le dihydrogène utilisé comme « carburant » promet d'être une solution efficace, durable et non polluante.<sup>i</sup> En l'occurrence ce gaz génère de l'énergie par réaction avec l'oxygène pour produire de l'eau. Un des défis scientifiques majeurs pour ce faire est de mettre au point des solutions sûres et efficaces pour stocker et réémettre le dihydrogène. Le principal problème de ce dernier est qu'il requiert des températures et des pressions extrêmes pour pouvoir être stocké dans des volumes adaptés aux transports. Le stockage du dihydrogène moléculaire pose aussi d'importants problèmes de sécurité car il est inflammable et difficilement stockable de manière hermétique.

Les amine-boranes, tels que le borazane (ou ammonia-borane, Illustration 1) sont des composés chimiques très convoités dans le domaine des transports pour leur capacité à produire du dihydrogène après activation thermique ou catalysée. Elles constituent ainsi un réservoir solide de dihydrogène stabilisé, disponible dans des conditions normales à modérées de température et de pression.<sup>ii</sup>

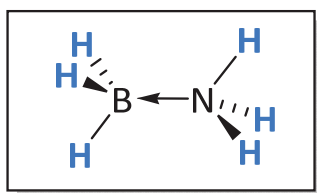


*Illustration 1. Exemple d'une amine-borane pouvant générer du dihydrogène: le borazane.*

Le borazane est le composé le plus étudié car il possède une haute capacité gravimétrique en dihydrogène (19.6 % massique) et se trouve proche des critères de stabilité fixés par le DOE (département of energy) des Etats-Unis<sup>ii</sup> (Tableau 1).

---

<sup>i</sup>Huang, Z.; Autrey, T., *Energy & Environmental Science* **2012**, 5, 9257-9268.

<sup>ii</sup> Staubitz, A.; Robertson, A. P. M.; Sloan, M. E.; Mannors, I., *Chem. Rev.* **2010**.

**Tableau 1.** Objectifs du « department of energy » (DOE) des États-Unis pour un système de stockage embarqué d'hydrogène et comparaison avec le borazane.<sup>i</sup>

Source Délais	Dihydrogène		Borazane
	2017	Objectifs finaux	Actuel
Capacité massique [% massique]	5.5	7.5	<b>19.6</b>
Stabilité [°C]	-40/60 (ensoleillement)	-40/60 (ensoleillement)	<b>Jusqu'à 85</b>
Min/max température d'émission [°C]	-40/85	-40/85	<b>85/200</b>
Temps de régénération [kg H <sub>2</sub> /min]	1.5	2.0	<b>Pas de régénération.</b>
Toxicité et sécurité	H <sub>2</sub> pur, stockage hermétique. (répondant aux limites en vigueur)		<b>Gaz toxiques, moussage.</b>

L'étude de ce composé a permis notamment de déterminer les mécanismes mis en jeu lors de la déshydrogénation. En effet, le borazane qui se présente à l'état solide à température ambiante, constitue un réseau de molécules stabilisées par des interactions dihydrogènes, d'énergie comparable aux liaisons hydrogènes conventionnelles.<sup>iii</sup> Le processus thermique de déshydrogénation du solide se fait selon un mécanisme bimoléculaire et autocatalytique au sein de ce réseau.<sup>iv</sup>

L'usage du borazane pour le stockage de l'hydrogène montre cependant plusieurs limitations<sup>i</sup> (Tableau 1) :

1) La processabilité : le matériau se présente sous forme d'une poudre très fine. Durant la déshydrogénation le matériau prend plusieurs fois son volume *via* un phénomène de « moussage » dû à une sublimation partielle des composants. Le résidu final est une poudre extrêmement fine et pulvérulente qui s'infiltre dans les systèmes d'appareillages (Illustration 2).

<sup>iii</sup> Feyereisen, M. W.; Feller, D.; Dixon, D. A., *The Journal of Physical Chemistry* **1996**, 100, 2993-2997.

<sup>iv</sup> Nguyen, V. S.; Matus, M. H.; Grant, D. J.; Nguyen, M. T.; Dixon, D. A., *The Journal of Physical Chemistry A* **2007**, 111, 8844-8856.

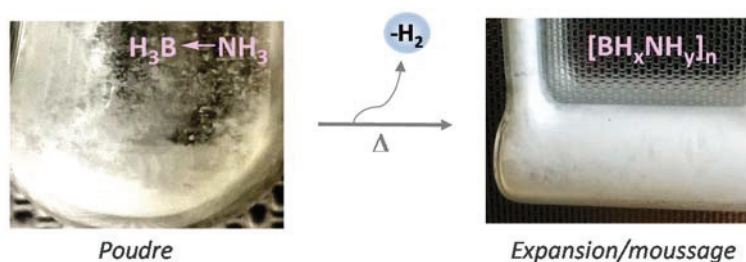


Illustration 2. Aspect du borazane avant (gauche) et après (droite) déshydrogénation.

2) Pollution du gaz émis : l'émission de dihydrogène par activation thermique s'accompagne de plusieurs gaz tels que  $B_2H_6$  et  $NH_3$  (Illustration 3), qui sont toxiques pour l'environnement et corrosifs pour les appareillages et les piles à combustible.

3) Irréversibilité du processus : le matériau obtenu après déshydrogénation est un mélange de polymères (Illustration 3) très réticulés et de très grande stabilité par rapport au borazane (réaction exothermique). De ce fait la régénération du borazane avec du dihydrogène n'a pas encore été décrite dans la littérature.

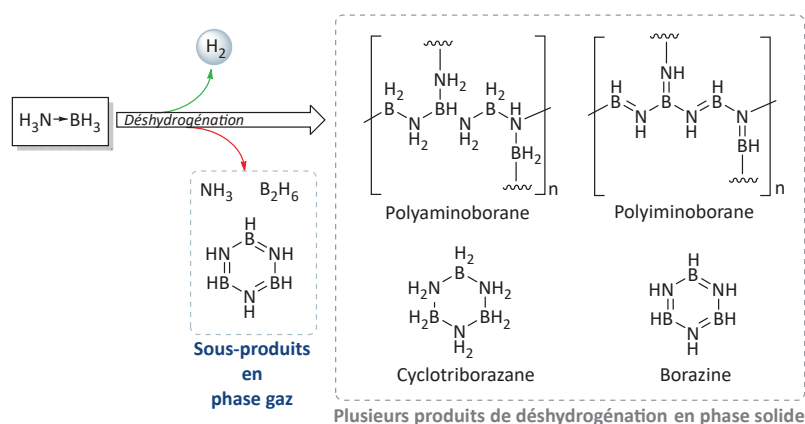


Illustration 3. Représentations des différents composants polluant la phase gaz ainsi que des produits obtenus après déshydrogénation du borazane.

Des améliorations ont été apportées quant aux problèmes de moussage et d'émission de gaz indésirables en modifiant le borazane. L'addition d'un substituant organique sur l'azote et/ou le bore a permis de résoudre ces deux points, tout en gardant une capacité massique en dihydrogène raisonnable ( $> 7\%$ ).<sup>v,vi,vii</sup> De plus, l'imprégnation du borazane sur des matériaux poreux (tels que la silice) a permis en plus de contrôler l'exothermicité de

<sup>v</sup> Zhang, L.; Li, S.; Tan, Y.; Tang, Z.; Guo, Z.; Yu, X., *Journal of Materials Chemistry A* **2014**, 2, 10682.

<sup>vi</sup> Li, L.; Gu, Q.; Tang, Z.; Chen, X.; Tan, Y.; Li, Q.; Yu, X., *Journal of Materials Chemistry A* **2013**, 1, 12263.

<sup>vii</sup> Luo, W.; Zakharov, L. N.; Liu, S.-Y., *J. Am. Chem. Soc.* **2011**, 133, 13006-13009.

la réaction.<sup>viii</sup> Cependant, la quantité massique du matériau en dihydrogène en est significativement réduite.

L'étude du borazane a permis également la compréhension des mécanismes mis en jeu. Le processus thermique de déshydrogénation du solide se faisant selon un mécanisme bimoléculaire et autocatalytique,<sup>i</sup> les températures exactes de déshydrogénation dépendent des conditions expérimentales (vitesse et durée de chauffe).<sup>ix</sup>

Cette thèse traite de la synthèse de polymères contenant des fonctions de type amine-borane (Illustration 4), soit dans la chaîne principale (section 2) soit en chaîne latérale (section 3). Au-delà du développement d'un matériau processable pouvant émettre du dihydrogène, notre approche s'est orientée vers la compréhension des effets du squelette polymère sur les paramètres cinétiques (température) et thermodynamiques de la réaction (enthalpie, nature des produits formés) en se basant sur nos observations expérimentales, corrélées à des études théoriques.

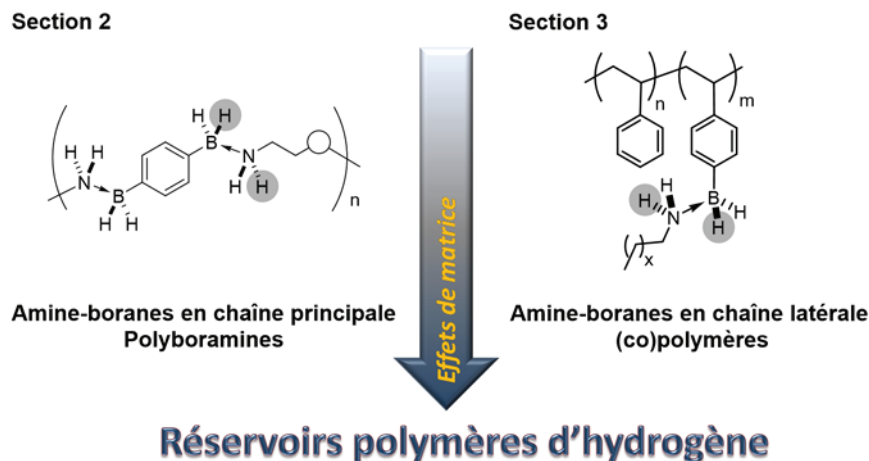


Illustration 4. Sujet de cette thèse.

Notre intérêt s'est porté vers l'élaboration de nouveaux types d'amine-boranes performants et prometteurs pour le stockage du dihydrogène. Nous avons voulu apporter de nouvelles connaissances sur la réactivité des amines-boranes de type NH-BH.

<sup>viii</sup> (a) Dündar-Tekkaya, E.; Yürüm, Y., *Int. J. Hydrogen Energy* **2016**, *41*, 9789-9795; (b) Kim, H.; Karkamkar, A.; Autrey, T.; Chupas, P.; Proffen, T., *J. Am. Chem. Soc.* **2009**, *131*, 13749-13755.

<sup>ix</sup> Wolf, G.; Baumann, J.; Baitalow, F.; Hoffmann, F. P., *Thermochim. Acta* **2000**, *343*, 19-25.



L'élaboration de ces polymères a requis la mise au point préalable d'une méthode générale d'obtention sélective et quantitative d'amine-boranes, à partir de réactifs facilement accessibles. C'est ainsi que nous avons mis au point une méthode de synthèse d'une grande gamme d'amine-boranes *via* une réaction « one-pot » entre un acide boronique (ou ester), un ammonium et du  $\text{LiAlH}_4$  (Illustration 5), qui ont été mis au point à partir d'études publiées dans la littérature.<sup>x,xi,xii</sup> Les sels d'aluminium générés ont été retirés par filtration. De plus, cette réaction permet d'utiliser les réactifs amines et boranes en quantité stoechiométrique ce qui a été crucial pour l'obtention de chaînes polymériques pour la synthèse des polyboramines (Illustration 4). Cette particularité a permis également de s'affranchir des étapes complexes de purification.

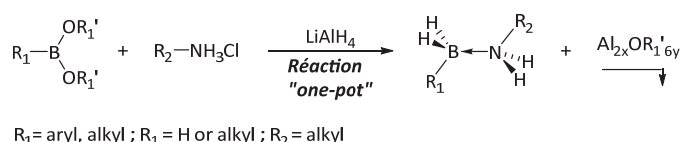


**Illustration 5.** Réaction de formation des amine-boranes en une étape mise au point pour la synthèse de polymères.

L'extension de cette méthodologie à la synthèse de polyboramines a été un succès (discussion dans la section 2) qui nous a permis de synthétiser une large gamme de polymères analogues à **Ar-BN-C4O** (représenté Illustration 6 à gauche) avec des masses moléculaires de l'ordre de  $\text{Mw} = 10^5$  Da et des températures de transition vitreuse autour de 60 °C. Afin de déterminer avec certitude le rôle du squelette polymère nous avons également synthétisé des analogues moléculaires, tels que **1b** (représenté Illustration 6, à droite) ayant le même environnement électronique que les amine-boranes des polymères.

<sup>x</sup> Hawthorne, M. F., *J. Am. Chem. Soc.* **1961**, *83*, 831-833

<sup>xi</sup> (a) Hawthorne, M. F., *J. Am. Chem. Soc.* **1958**, *80*, 4293-4296; (b) Hawthorne, M. F., *J. Am. Chem. Soc.* **1958**, *80*, 4291-4293.

<sup>xii</sup> Veeraraghavan Ramachandran, P.; Raju, B. C.; Gagare, P. D., *Org. Lett.* **2012**, *14*, 6119-6121.

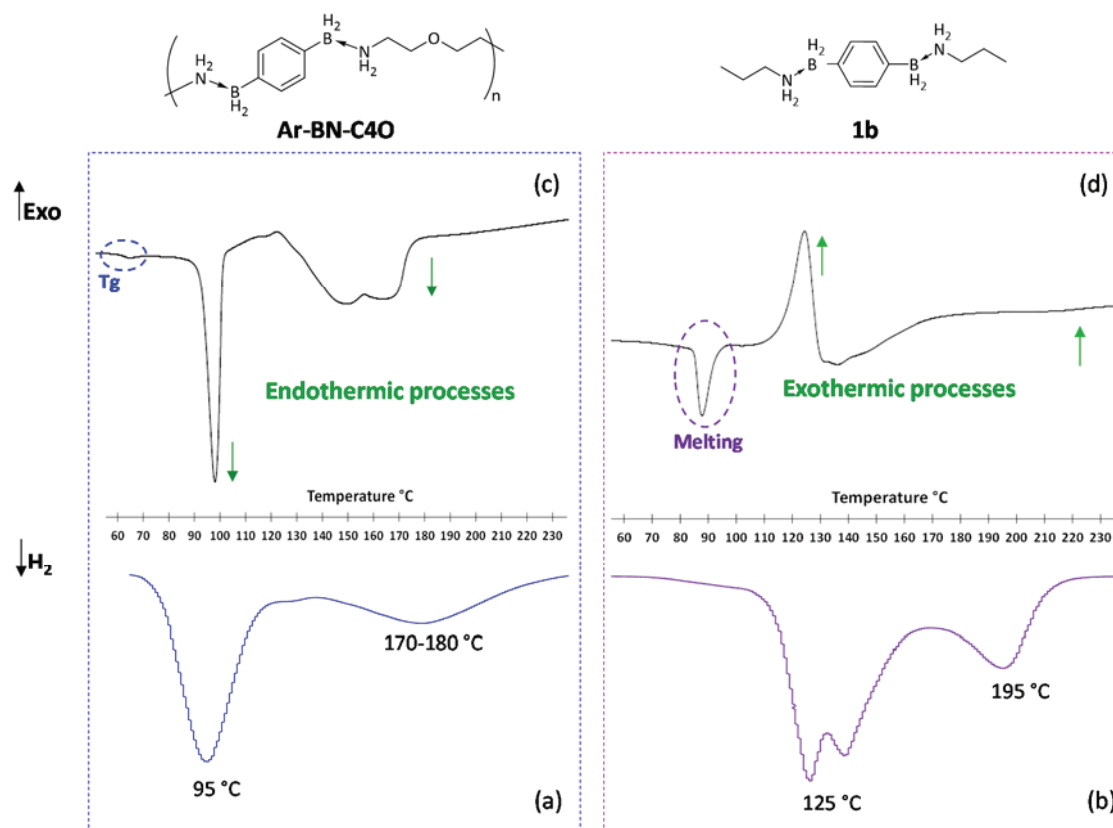
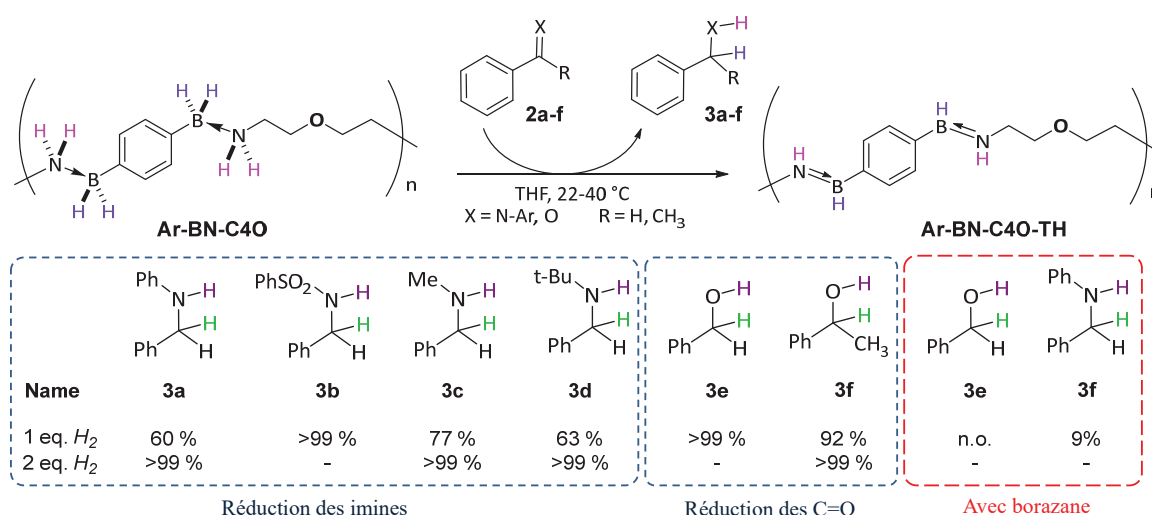


Illustration 6. Comparaison des spectres du polymère Ar-BN-C4O (gauche) et de la brique moléculaire 1b obtenus en TPD (a et b) et en DSC (c et d). Rampe de température : 30-250 °C, 5 °C/min.

L'analyse thermique de ces deux composés en TPD (Température programmed desorption, Illustration 6, a et b) et en DSC (differential scanning calorimetry, Illustration 6, c et d) a révélé des réactivités très différentes. Tandis que la brique moléculaire présentait une température de déshydrogénation et un profil calorimétrique typique, identique à ceux du borazane, le polymère s'est comporté de manière très différente. Outre l'abaissement de la température de déshydrogénation de 30 °C le polymère a présenté un processus de déshydrogénation exclusivement endothermique (Illustration 6, c) ce qui est une première à notre connaissance. De nombreuses analyses complémentaires sur différentes polyboramines ont permis de confirmer ce résultat et sont toujours en cours dans notre laboratoire. Sur le plan applicatif, l'endothermicité de la réaction de déshydrogénation suggère que les polymères formés après déshydrogénation sont moins stables thermodynamiquement que leurs analogues moléculaires (borazane, **1b**) dont la réaction de décomposition est exothermique. Ceci suggère une meilleure réactivité des polymères après déshydrogénation et par conséquent la possibilité d'envisager peut-être une « recharge » en hydrogène à partir du

matériau consommé. Sur le plan scientifique, cette observation suggère que l'environnement secondaire (la matrice) joue un rôle déterminant sur la réactivité des amibe-boranes, tant sur le plan cinétique que thermodynamique.

Les effets électroniques des substituants des polyboramines et de leurs analogues moléculaires ont été mis en évidence par réaction de transfert d'hydrogène sur des carbonyles. Les composés **Ar-BN-C4O** et **1b** se sont avérés plus réactifs que le borazane pour la réduction des imines en amines, avec une meilleure sélectivité pour le polymère (Illustration 7). Ces composés se sont également avérés capables de réduire quantitativement les aldéhydes et les cétones par réaction de transfert d'hydrogène. Cela différait du borazane pour lequel seule une réaction d'hydroboration était effectuée.<sup>xiii</sup>



**Illustration 7. Réaction d'hydrogénation par transfert direct.**

L'étude d'hydrogénation par transfert direct impliquant les polyboramines et analogues moléculaires a non seulement permis d'étendre la réaction à d'autres composés carbonylés, mais a surtout démontré que les effets électroniques des substituants étaient non-innocents dans la réactivité de ces composés. Plusieurs travaux sont en cours au sein de notre laboratoire sur le plan analytique, théorique et expérimental, afin de déterminer quels paramètres physicochimiques sont influencés par la matrice polymère dans la réactivité des polyboramines.

<sup>xiii</sup> Shi, L.; Liu, Y.; Liu, Q.; Wei, B.; Zhang, G., *Green Chemistry* **2012**, 14, 1372-1375.

Au cours de cette étude nous avons réalisé un autre type de polymère contenant des amine-boranes. Il s'agit de (co)polymères dont la structure est une chaîne polystyrène, fonctionnalisée statistiquement en position para du motif phényle par un groupement amine-borane de formule générale [alkyl-NH<sub>2</sub>-BH<sub>2</sub>-] (Illustration 8). La teneur en motifs fonctionnalisés a été variée de 0 % (PS) à 100 %. Deux familles de polymères ont ainsi été réalisées en modifiant la longueur de la chaîne alkyl substituant l'azote, c'est-à-dire, contenant les motifs [propyl-NH<sub>2</sub>-BH<sub>2</sub>-] et [decyl-NH<sub>2</sub>-BH<sub>2</sub>-]. Ces deux familles ont été désignées respectivement par **PS-BN-C3-x%** (Illustration 8, gauche) et **PS-BN-C10-x%** (Illustration 8, droite) avec **x (%)** la teneur en **m** motifs fonctionnalisés.

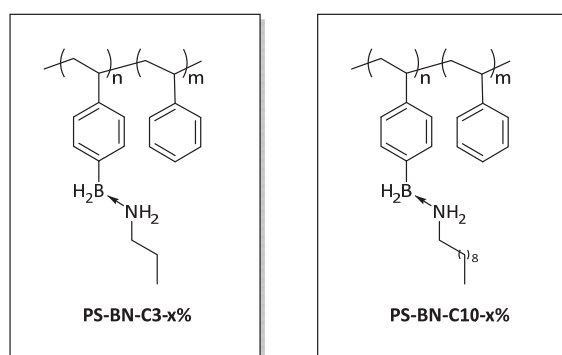


*Illustration 8. Représentation des deux familles de polymères synthétisés.*

Pour obtenir ces polymères, nous avons adopté une stratégie de (co)polymérisation / post fonctionnalisation (Illustration 9). La synthèse du polymère précurseur s'est effectuée par voie radicalaire non-contrôlée, en utilisant le styrène et le 4-vinylboronate de pinacol (PVB)) (co)polymère statistique, désigné **PS-BPin-x%**, avec **x (%)** la teneur en unités borées (Illustration 9, étape 1). Les fonctions boronates de ce polymère sont ensuite fonctionnalisées en amine-boranes via la réaction « one-pot », mise au point dans notre laboratoire (Illustration 9, étape 2).

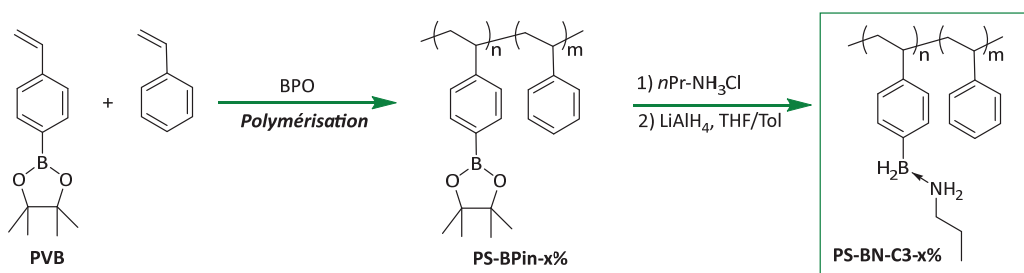


*Illustration 9. Stratégie de synthèse des polymères de type PS-BN-C3-x% et PS-BN-C10-x% de type polymérisation/post-fonctionnalisation. (Exemple pour la synthèse de PS-BN-C3-x%).*

Les températures de déshydrogénation de chaque polymère soumis à traitement thermique ont été corrélées à leur teneur en amine-borane (Illustration 10). Ces valeurs ont également été comparées aux briques moléculaires respectives, **1e** et **1f** (valeurs situées à droite sur le graphique ci-dessous). L'étude a montré une variation sur une gamme de 50 °C de la température de déshydrogénation suggérant une influence majeure de la teneur en amine-borane, du squelette polymère, ainsi que de la longueur de la chaîne alkyle substituant l'azote, sur la température de déshydrogénation. Une étude de la structure secondaire des polymères, avant et après déshydrogénation, a permis de démontrer que la présence des amine-boranes et notamment des interactions DHB qu'elles établissent entre elles modifiait de manière significative la structure secondaire du polymère et par conséquent son comportement physico-chimique.

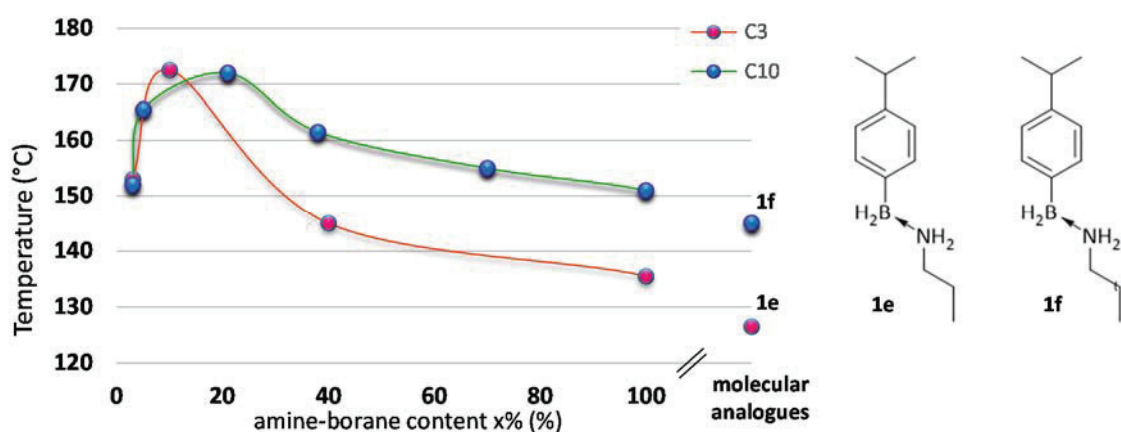


*Illustration 10. Evolution du pic de déshydrogénation pour chaque polymère appartenant à la famille PS-BN-C3-x% (en vert) et PS-BN-C10-x% (en rouge) et comparaison avec leur brique moléculaire respective 1e et 1f.*

Enfin, dans le but de maximiser la teneur en dihydrogène des matériaux polymères, nous avons dopé le polymère **PS-BN-C10-100%** avec du borazane (Illustration 11). Le profil de déshydrogénation obtenu n'est ni la superposition, ni la moyenne des deux matériaux de départ pris séparément. Cela suggère que le mélange des deux espèces crée un nouvel environnement chimique et donc une nouvelle réactivité. Des hypothèses concernant le réseau supramoléculaire établi par les DHB ont été mises en avant mais restent encore à être étudiées (Illustration 12).

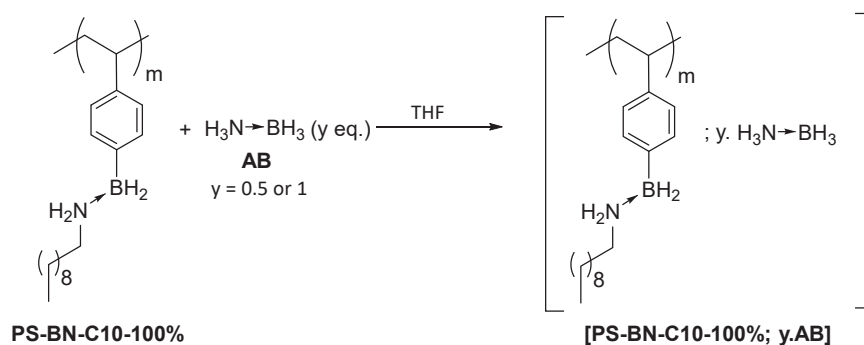


Illustration 11. Dopage du polymère PS-BN-C10-100% avec du borazane.

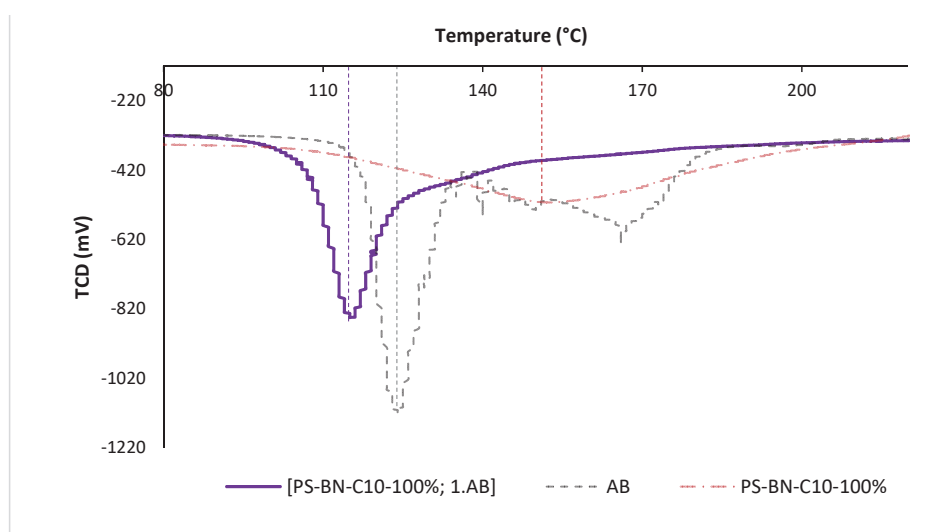


Illustration 12. Comparaison des profils de deshydrogénation des deux composant pris séparément (en pointillé) et du polymère dope (ligne).

Cette étude est actuellement poursuivie au sein de notre laboratoire pour développer des matériaux à haute teneur en hydrogène mais également dans le but de comprendre les facteurs structuraux qui peuvent modifier la réactivité des amine-boranes.

En conclusion, nous avons pu démontrer le rôle majeur des structures secondaires dans la réactivité des amine-boranes de type NH-BH. Ces structures impliquant de nombreux paramètres tels que la rigidité, l'amorphicité et les interactions DHB sont autant facteurs modifiant la cinétique et/ou la thermodynamique des réactions de deshydrogénation. L'identification et la mise en évidence des facteurs structuraux influençant la deshydrogénation des polymères amine-borane a permis d'apporter une vision complémentaire à la chimie des amine-boranes pour le stockage du dihydrogène et un pas supplémentaire vers une possible régénération du matériau applicable aux contraintes économiques et environnementales.

# Table of content

General introduction.....	35
Section 1: Bibliographical Review .....	36
Amine-borane reactivity for hydrogen release purposes – Factors influencing thermodynamics and kinetics.....	36
I. Introduction .....	37
II. Ammonia-borane and analogues: a molecular approach .....	37
II.1. The amine-borane Lewis-pair.....	37
II.1.a. The amine-borane bond.....	37
II.1.b. Dihydrogen release and dihydrogen bonding (DHB) .....	39
II.2. Factors influencing thermodynamic stability of the amine-borane bond: a discussion.....	41
II.2.a. Electronic and steric parameters governing the strength of the amine-borane bond.....	41
II.2.b. Isosterism and hydrocarbon-like skeletons: example of BNs and CBNs..	43
II.3. Synthesis of ammonia-borane and analogues .....	45
II.3.a. Reactions by ligand exchanges.....	45
II.3.b. Reactions of salt metathesis / H <sub>2</sub> release. Increasing efficiency.....	47
II.3.c. Reactions of salt metathesis / H <sub>2</sub> release. Use of a promoter. ....	48
II.3.d. Multistep-synthesis of intracyclic amine-borane. Synthesis of CBN molecules for hydrogen release purposes (C-BH-NH).....	49
II.3.e. One-pot synthesis of a large panel of CBN amine-boranes. ....	50
II.4. Ammonia-borane for hydrogen tanks .....	52
II.4.a. The challenge of developing hydrogen fuel cells.....	52
II.4.b. Promising characteristics of ammonia-borane (AB) and scientific issues	53
II.5. Thermal stepwise hydrogen release of ammonia-borane. ....	55

II.6.	Mechanistic insights on the thermal dehydrogenation of AB in the solid state.	
		59
II.6.a.	Key mechanistic points.....	59
II.6.b.	The two main mechanistic pathways of AB thermal dehydrogenation in the solid state. ....	60
II.7.	AB dehydrogenation with other media .....	62
II.7.a.	Ammonia-borane dehydrogenation in solution .....	62
II.7.b.	Metal catalyzed amine-borane dehydrocoupling .....	62
III.	Nitrogen and/or boron substituted amines-borane – electronic effects and reactivity in hydrogen release .....	63
III.1.	N and/or B-methyl-substituted amine-boranes .....	63
III.2.	Amine-boranes inserted in linear or cyclic organic scaffolds. Effects on the decomposition. ....	65
III.2.a.	C-BH-NH: hydrogen containing amine-boranes inserted in linear organic scaffolds	65
III.2.b.	C-BH-NH: amine-boranes inserted in cyclic organic scaffolds .....	67
IV.	Amine-borane embedded in an external matrix: modification of the dehydrogenation profile .....	68
V.	Conclusion .....	70
Section 2.....		73
Polyboramines: main-chain amine-borane .....		73
polymers as hydrogen reservoirs.....		73
I.	Introduction .....	74
II.	Literature precedents: polymers containing amine-boranes bonds in the main-chain .....	74
II.1.	Amine-boranes in the main-chain of organic polymers .....	74



II.2. Polyaminoboranes: boron-nitrogen isosters of polyolefins and key-intermediates in hydrogen release from amine-borane materials.....	77
III. This work: polyboramines for hydrogen release - Effects of the polymer scaffold	79
III.1. Structural and synthetic requirements .....	79
III.2. Development of a methodology for the straightforward access to $\text{NH}_2\text{-BH}_2$ amine-boranes.....	81
III.2.a. The two-step strategy.....	81
III.2.b. One-pot reaction allowing the straightforward access to amine-boranes	83
III.3. Application of the procedure to the polymerization .....	86
III.4. Characteristics of polyboramines / oligomers and molecular bricks.....	90
III.4.a. NMR and IR footprints.....	90
III.4.b. Steric exclusion chromatography (SEC).....	92
III.4.c. Glass transitions and fusion temperatures .....	94
III.4.d. Fluorescence properties.....	95
III.5. Transfer hydrogenation reaction: indicator of electronic effects of substituents	95
III.5.a. Introduction.....	95
III.5.b. This work: effect of substituent and polymer backbone on the hydrogenation of carbonyls.....	97
III.5.c. Transfer hydrogenation of N-benzylidene aniline: a comparative study	98
III.5.d. Scope of the hydrogen transfer reduction of imines .....	101
III.5.e. Hydrogen transfer reduction of aldehyde and ketones.....	104
III.5.f. Hypotheses on the polymer structure after transfer hydrogenation....	107
III.6. Polyboramines involved in thermal hydrogen release.....	108
III.6.a. Temperature of hydrogen-release and enthalpy of reaction. ....	108

III.6.b.	Quantitative analysis of dihydrogen delivery.....	113
III.6.c.	Evidences for a dehydrogenation peak.....	113
III.6.d.	Variation of the aliphatic chain within polyboramines .....	115
III.6.e.	Dehydrogenation of oligomers.....	116
III.6.f.	Characterization of dehydrogenated structures and hypotheses .....	119
III.7.	Mechanistic investigation.....	123
III.8.	Hypotheses related to the influence of polymer backbone in polyboramines supported by computational data.....	130
III.8.a.	Entropic effects.....	130
III.8.b.	End-of-chains and dissociation bond-energy .....	131
III.8.c.	Pre-organised backbone oriented structure.....	132
III.9.	Extension of the family of polyboramines, synthesis of bisboronic monomers and applications in polymerization. ....	133
III.9.a.	Metal-free diboration of alkenes. ....	133
III.9.b.	Copper-catalysed diboration of non-terminal alkynes.....	134
III.9.c.	Copper catalyzed C-Br boration .....	135
III.9.d.	Use of bisboron monomers in polymerization.....	135
IV.	Conclusion and perspectives .....	141
Section 3.....		143
Integration of pendant-chain amine-boranes within (co)polymers. Effect of the intrinsic structure.....		143
I.	Introduction .....	144
II.	Literature precedents: Amine-Borane containing polystyrenes .....	144
II.1.	Polymerization of 4-vinylphenylboronic acid/ester .....	146
II.1.a.	Free radical polymerization.....	146
II.1.b.	Atom transfer radical polymerization (ATRP) .....	147

II.1.c. Reversible addition-fragmentation chain transfer (RAFT).....	147
II.1.d. Ziegler-Natta polymerization .....	148
II.2. Strategies of functionalization.....	149
III. This work: Design of pendant-chain amine-borane polymers: dynamic structure / activity relationship.....	152
III.1. Establishment of a synthetic pathway .....	152
III.2. Synthesis characterization of PS-BN-C3 and PS-BN-C10 (co)polymers.....	155
III.2.a. Synthesis of PS-BN-C3-x% and effects of DHB.....	155
III.2.b. Synthesis of PS-BN-C10-x%.....	160
III.3. Thermally induced dehydrogenation: Impact of the polymer scaffold. ....	161
III.3.a. Thermally induced dehydrogenation of the molecular bricks .....	161
III.3.b. Thermally induced dehydrogenation: Impact of the polymer environment .....	163
III.4. PS-BN-C10-100%/AB hybrid polymers. A new type of high content solid hydrogen material .....	168
IV. Conclusion and perspectives .....	172
General conclusion and perspectives .....	173
References .....	178
Section 4:.....	182
Experimental data.....	182
I. Material and methods .....	183
II. Polyboramines: synthesis and characterization .....	185
II.1. Synthesis of precursors: experimental procedures and characterizations...	185
Procedure 1: synthesis of ammoniums chloride from aliphatic diamines .....	185
II.2. Synthesis of pinacol bisboranonates monomers .....	186
II.2.a. Procedure 2: Diboration of 1,2-hexene .....	186

II.2.b.	Procedure 3: Diboration of 4-octyne .....	187
II.2.c.	Procedure 4: Diboration of dibromohexene .....	187
II.3.	Synthesis of amine-borane molecular bricks: experimental procedures and characterizations .....	188
II.3.a.	Procedure 5: synthesis of borohydride derivatives from aliphatic boronic acids or pinacol boronates.....	188
II.3.b.	Procedure 6: synthesis of borohydride derivatives from aromatic boronic acids / boronic acid pinacol ester. ....	189
II.3.c.	Procedure 7: Synthesis of (N-alkyl)amine-(B-alkyl or aryl)boranes by salt metathesis / H <sub>2</sub> release.....	189
II.3.d.	Procedure 8: one-pot synthesis of (N-alkyl)amine-(B-alkyl/aryl)boranes from (1,4-benzene)bisboronic acid and amines hydrochloride .....	190
II.4.	Synthesis of polyboramines: experimental procedures and characterizations	192
II.4.a.	Procedure A: synthesis of poly[(N,N'-alkylene)diamine-(1,4-benzene)bisborane] from (1,4-benzene)bisboronic acid and diamine hydrochloride.....	192
II.4.b.	Procedure B: Synthesis of poly[(alkyl)diamine-(1,4-benzene)bisborane] from pinacol (1,4-benzene)bisboronate and diamine hydrochloride. ....	193
II.4.c.	Procedure C: Synthesis of other poly[(diethylenediamine-(aliphatic)-bisborane] from a pinacol bisboronate and diethylenediamine hydrochloride .	196
II.5.	NMR spectra .....	198
II.5.a.	Amines hydrochloride .....	198
II.5.b.	Pinacol bisboronate monomers .....	200
II.5.c.	Lithium trihydridoborates .....	202
II.5.d.	Amine-boranes N and B mono-substituted .....	204
II.5.e.	Polyboramines.....	206
II.6.	ATR-IR spectra .....	213

II.6.a.	Polyboramines and molecular analogues .....	213
II.6.b.	Transfer hydrogenation.....	215
II.7.	SEC (steric exclusion chromatography) .....	216
II.7.a.	SEC-THF of polymer Ar-BN-C4O .....	216
II.7.b.	SEC-THF of oligomer Ar-BN-C4O-olig .....	216
II.7.c.	SEC-DMF of a dehydrogenated polymer: Ar-BN-C4O-Dh .....	217
III.	Polyboramines: transfer hydrogenation on carbonyls .....	218
III.1.	Experimental procedures of transfer hydrogenation .....	218
III.1.a.	Procedure 9 .....	218
III.1.b.	Procedure 10: for viscous amine-boranes.....	219
III.2.	Characterization of transfer hydrogenation products .....	219
III.3.	Representative NMR spectra.....	221
III.3.a.	<sup>1</sup> H NMR monitoring .....	221
III.3.b.	<sup>11</sup> B NMR monitoring .....	224
IV.	Polyboramines: Thermal dehydrogenation studies.....	225
IV.1.	DSC (differential scanning calorimetry).....	225
IV.1.a.	Polymers .....	225
IV.1.b.	Molecular brick:.....	227
IV.1.c.	Oligomer: .....	228
IV.2.	TPD (H <sub>2</sub> temperature-programmed desorption).....	228
IV.2.a.	Polymer (Ar-BN-C4O).....	228
IV.2.b.	Molecular brick (1b) .....	230
IV.2.c.	Oligomer (Ar-BN-C4O-olig) .....	231
IV.3.	IR-in situ .....	231
IV.3.a.	Polymer.....	231
IV.3.b.	Oligomer .....	232

IV.4.	TGA (thermal gravimetric analysis) .....	232
IV.4.a.	Hydrogen quantification.....	232
IV.4.b.	Calcination .....	233
IV.5.	$^{11}\text{B}$ MAS-NMR of dehydrogenated materials .....	235
V.	Functional polystyrenes: synthesis and characterization.....	236
V.1.	Synthesis of precursors: experimental procedures and characterizations...	236
V.1.a.	Procedure 9: esterification of boronic acids with pinacol .....	236
V.1.b.	Procedure 10: Gabriel reaction on 4-vinylbenzene moieties .....	237
V.2.	Synthesis of molecular bricks: characterizations .....	239
V.3.	Free radical polymerization: Synthesis PS-BPin-x%. Experimental procedures and characterizations. ....	241
	Procedure D: Free radical copolymerization of styrene and PVB .....	241
V.4.	Post-functionalization: Synthesis PS-BN-C3-x% and PS-BN-C10-x%. Experimental procedures and characterizations .....	244
V.5.	Ammonia-borane doping .....	250
V.6.	NMR Spectra.....	252
V.6.a.	Precursors.....	252
V.6.b.	Molecular bricks .....	255
V.6.c.	Polymers PS and PS-BPin-x%.....	259
V.6.d.	PS-BN-C3-x%.....	265
V.6.e.	PS-BN-C10-x%.....	267
V.7.	ATR-IR .....	272
V.7.a.	Molecular bricks .....	272
V.7.b.	Polymers.....	273
V.8.	SEC (steric exclusion chromatography) .....	275
V.9.	DSC (differential scanning calorimetry).....	277

V.10. TGA (thermal gravimetric analysis).....280

V.11. TPD .....281

    V.11.a. Molecular bricks .....281

    V.11.b. Polymers PS-BN-C3-x% .....281

    V.11.c. Polymers PS-BN-C10-x% .....282

    V.11.d. AB-doped PS-BN-C10-100%.....283

## General introduction

With this work, we have tried to broaden the scope of amine-borane chemistry, concerning their use for hydrogen storage purposes. At first, this has been achieved through the synthesis of new polymers containing amine-boranes function in their backbone. These new entities showed enhanced dehydrogenation profiles both compared to their molecular counterpart as well as the golden standard, ammonia-borane. We foresaw the influence of the macromolecular structure on the thermal dehydrogenation in the solid state. For this reason, our aim was focused in understanding the interplay between molecular and macromolecular effects, employing both experimental and theoretical approach.

**Section 1** is a bibliographical review aiming at highlighting electronic and structural parameters influencing amine-borane reactivity. This section first present amine-boranes and their methods of synthesis. Then, ammonia-borane dehydrogenation and associated physicochemical properties are introduced as well as principal mechanistic pathways of dehydrogenation. At last, the effect of substituent or material support of amine-boranes on dehydrogenation properties is investigated.

**Section 2** report the synthesis of polymers containing amine-borane function in the main chain that we called Polyboramines (published). We described their behavior under solid-state thermal dehydrogenation and transfer hydrogen reactions on carbonyls. A comparison was done with molecular analogues and with ammonia-borane.

**Section 3** report the synthesis of polymers having polystyrene backbone, containing amine-borane pendant-functions as well as ammonia-borane doped polymers. We mapped their behavior under solid-state thermal dehydrogenation.

**Section 4** is the experimental section.



## **Section 1: Bibliographical Review**

**Amine-borane reactivity for hydrogen release purposes – Factors influencing thermodynamics and kinetics**

## I. Introduction

Amine-borane chemistry is showing an ever growing interest, due to its numerous potential applications.<sup>1</sup> In particular, amine-boranes are well suited hydrogen storage materials due to their light weight and propensity for bearing multiple protic (N–H) and hydridic (B–H) hydrogens.<sup>2</sup> The dehydrogenation of amine-borane in the solid state involves multiple mechanisms<sup>3</sup> and is dependent of Boron and Nitrogen substituents as well as the chemical environment.<sup>4</sup>

## II. Ammonia-borane and analogues: a molecular approach

### II.1. The amine-borane Lewis-pair

#### II.1.a. The amine-borane bond

Amine-boranes are formed by a boron-nitrogen bonding which results from the overlap between the two electrons of the nitrogen lone pair and the vacant p-orbital of the boron atom (Figure 1). According to the Lewis theory, the bonding generates the apparition of formal charges, positive on the nitrogen and negative on the boron. The bonding is accompanied by a modification of the boron geometry from planar trigonal to tetrahedral with a change in hybridization from  $sp^2$  to  $sp^3$  (Figure 1).<sup>1a,5</sup>

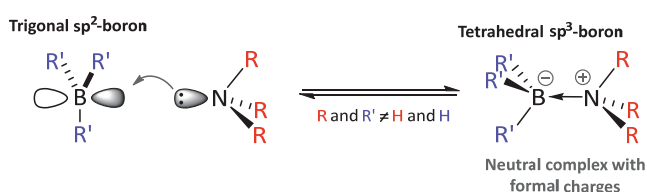


Figure 1. Formation of the amine-borane complex

Amine-boranes constitute a specific class of chemical species because they possess their own chemistry.<sup>6</sup> For instance, they are promising organocatalyst,<sup>1b,1c,7,8</sup> metal-free hydride, hydrogen transfer<sup>9,10</sup> for the reduction of organic molecules and dihydrogen reservoirs in the sector of alternative energies.<sup>1a, 2,11</sup> In addition, they have been source of

inspiration in the past decades since they present analogies with carbon-carbon bond (Figure 2).

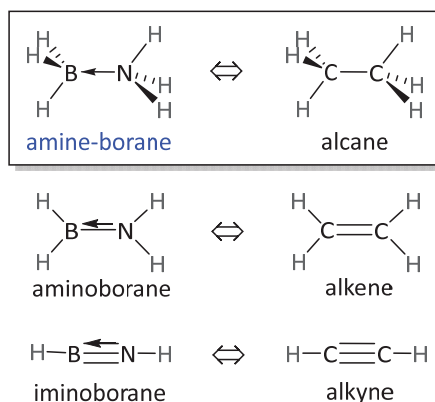


Figure 2. Structural analogy between boron-nitrogen and carbon-carbon bonds

Comparative studies<sup>12,13</sup> suggested that the two bonds are isoelectronic as well as isosteric. In fact boron, nitrogen and carbon atoms belonging to the same period, display the same valency and hybridization when they are involved in amine-borane and carbon-carbon bond (Figure 2). The same analogy is also relevant for aminoboranes and iminoboranes similar to alkenes and alkynes respectively.

However, despite these similarities boron-nitrogen bond and carbon-carbon bond display strong differences in terms of reactivity due to their relative strength and polarization. As a representative example (Figure 3), ammonia-borane (AB) is strongly polarized and has a dipole moment of 5.2 D while ethane is completely apolar (0 D).

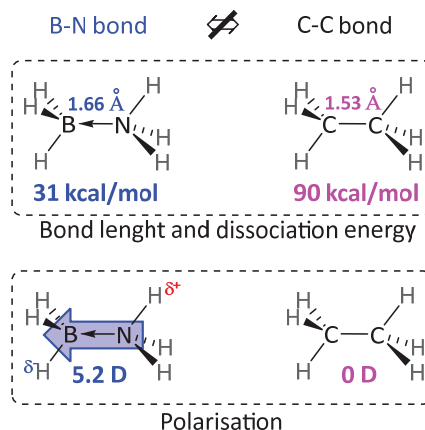


Figure 3. Divergences between B-N and C-C bonds illustrated with AB and ethane physical values.

This strong polarization modifies also the electronic density of substituents both located on boron and nitrogen. Indeed, the intrinsic polarization of the amine-borane bond generates electronically depleted nitrogen substituents ( $\delta^+$ ) while boron substituents are electronically enriched ( $\delta^-$ ). In the case of AB (Figure 3), the N-B bond polarization results in the presence of both hydridic and protic hydrogens on the same molecule.

### II.1.b. Dihydrogen release and dihydrogen bonding (DHB)

Amine-boranes bearing both B-H and N-H hydrogen atoms are part of a sub-class of amine-boranes recently named “Boron-Nitrogen-Hydrogen” compounds<sup>14</sup> that we will call BH-NH in this manuscript. These moieties are prone to losing dihydrogen by various stimuli (e.g. thermic or catalytic activation). They represent a promising class of compounds for hydrogen storage applications.<sup>14</sup>

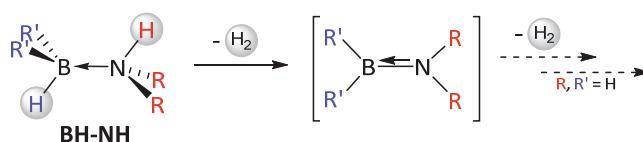


Figure 4. BH-NH compounds as potential reservoirs of dihydrogen

In particular, NH-BHs are commonly found to display intermolecular interactions between hydrogens, called “dihydrogen bonding” (DHB). The latter arises from attractive interactions between hydrogens ( $\delta^+\text{H} \cdots \text{H}\delta^-$ ),<sup>15</sup> represented Figure 5.

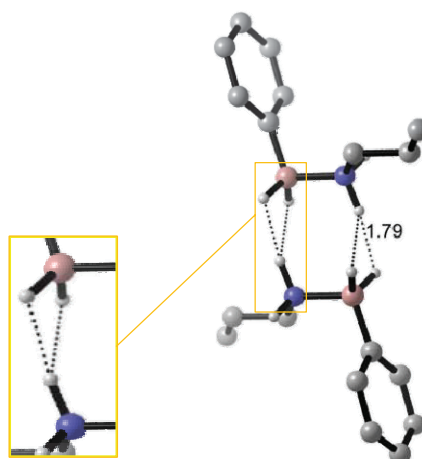


Figure 5. DHB interactions represented on an amine-borane dimer.

DHBs bring additional stabilization by allowing the formation of a network of coordinated molecules. In fact, the presence of DHBs can explain why AB is a solid at room temperature whereas ethane is in its gaseous form unless the two molecules display comparable molecular weights.<sup>16</sup>

DHBs have been illustrated at the molecular level, on the *n*-propylamine-phenylborane<sup>17</sup> dimer, which has been studied in this manuscript (Figure 6, left). DFT calculations (B97D3, 6-311++G[d,p]) showed that DHB induces a head-to-tail conformation of an amine-borane dimer as the state of minimum energy (Figure 5 and Figure 6, left). Weak interactions within the dimer can be highlighted by non-covalent interactions (NCI) mapping (Figure 6, right). NCI are represented by different areas between the two amine-borane molecules. The semi-quantitative color-scale, from red (very repulsive), to green (neutral), to blue (very attractive) evidences the attractive nature of DHBs that is illustrated by a blue area between B- and N- hydrogen atoms.

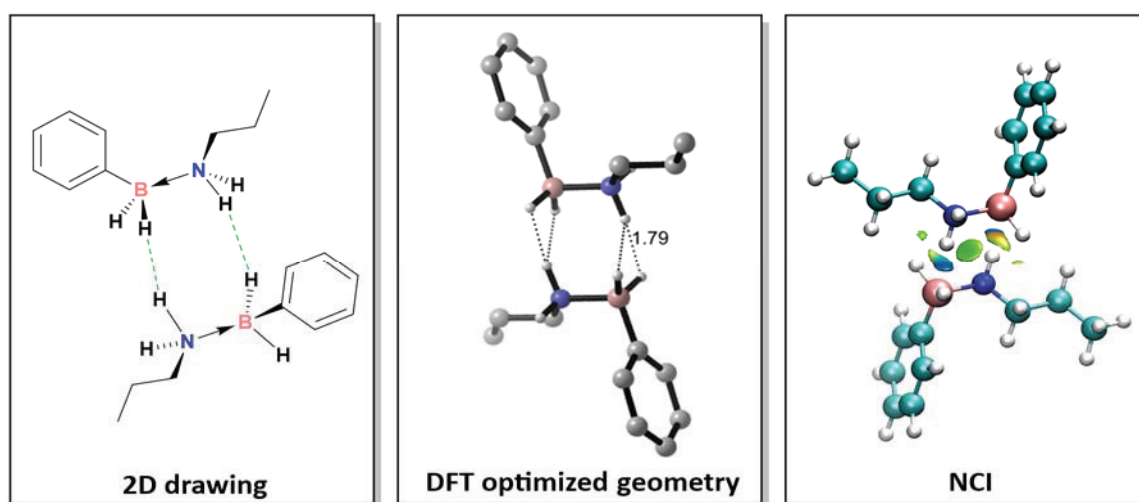


Figure 6. Representation of a dihydrogen bonding (DHB) in a dimer. (a) Drawing. (b) DFT geometry optimization<sup>17</sup> (c) Non-Covalent Interactions (NCI). Blue volume: attractive NCI; Red volume: repulsive NCI.

DHBs play a determinant role in affecting the conformation of molecules. By comparison, the most stable conformation of the butane molecule is well known to be the anti, while the BN-isoster of butane,  $\text{H}_3\text{N}-\text{BH}_2-\text{NH}_2-\text{BH}_3$  is stabilized by an intramolecular DHB in the gauche conformation.<sup>16</sup> Moreover DHBs play a key role in the reactivity of amine-boranes, particularly for solid-state hydrogen release because they are involved in the dehydrogenation pathways. Another fundamental parameter differentiating a traditional covalent bond from a Lewis acid-base adduct is the energy of the bond itself. An amine-

borane N-B bond is roughly three to six times weaker than a C-C bond. As a representative element of comparison, ammonia-borane has a gas-phase dissociation enthalpy ( $\Delta H_{dis}$ ) of 27.2 kcal/mol at 25°C whereas ethane is 90.1 kcal/mol. In the case of amine-boranes the bond strength are particularly affected by electronic and steric parameters of both boron and nitrogen substituents.

## II.2. Factors influencing thermodynamic stability of the amine-borane bond: a discussion.

### II.2.a. Electronic and steric parameters governing the strength of the amine-borane bond.

In amine-borane complexes, the bond strength is known to be mainly correlated to the respective Lewis-acidity and Lewis-basicity of boron and nitrogen atoms. The latter are influenced for the most part by the electronegativity of their substituents. For instance,  $\text{MeNH}_2\text{-BH}_3$  is more stable than  $\text{NH}_3\text{-BH}_3$  (AB) by 4 kcal/mol<sup>1a,12</sup> due to the donating inductive effect of the methyl substituent, that enhance the Lewis-basicity of the nitrogen. In contrary,  $\text{NH}_3\text{-MeBH}_2$  is less stable than AB because the methyl substituent decreases the Lewis-acidity of the boron atom. On this basis, a general trend can be observed (Table 1) according to dissociation enthalpy calculated for diversely methyl-substituted amine-boranes.<sup>12</sup> Of note, electron withdrawing groups at the boron can conversely enhance the dative bonding by reinforcing the Lewis-acidity at boron center.

Table 1. Calculated dissociation enthalpies in gas phase. Electronic and steric influences.

$\text{NH}_x\text{Me}_y\text{-BH}_3$	$\text{NH}_3\text{-BH}_3$	$\text{NH}_2\text{Me-BH}_3$	$\text{NHMe}_2\text{-BH}_3$	$\text{NMe}_3\text{-BH}_3$
$\Delta H^0_{dis}{}^a$	$31.1 \pm 1$	$35.0 \pm 0.8$	$36.4 \pm 0.8$	$34.8 \pm 0.8$
$\text{NH}_x\text{Me}_y\text{-BMe}_3$	$\text{NH}_3\text{-BMe}_3$	$\text{NH}_2\text{Me-BMe}_3$	$\text{NHMe}_2\text{-BMe}_3$	$\text{NMe}_3\text{-BMe}_3$
$\Delta H^0_{dis}{}^a$	$13.8 \pm 0.3$	$17.6 \pm 0.2$	$19.3 \pm 0.2$	$17.6 \pm 0.2$

<sup>a</sup>  $\Delta H^0_{dis}$  (kcal/mol) is the gas phase dissociation enthalpy<sup>12</sup>

However, the strength of the amine-borane dative bond can be also affected by steric effects. N- and/or B- trimethyl substituted amine-boranes are good representative examples.<sup>12</sup> As reported on Table 1  $\text{Me}_3\text{N-BH}_3$  is less stable than  $\text{NH}_2\text{Me-BH}_3$  and  $\text{NHMe}_2\text{-BH}_3$ , whereas the sum of inductive effects brought by methyl substituents is more important. Moreover, the amine-borane dissociation enthalpy significantly drops by more than half from  $\text{NH}_3\text{-BMe}_3$  to  $\text{NH}_3\text{-BH}_3$  (AB).

After, numerous achievements were done in the past year in the field of computational modeling, a consistent study has been reported in 2006 by Bessac and Franking.<sup>18</sup> To describe the amine-borane bond they used a BP86 functional, uncontracted slater-type orbitals and numerous sets to describe the polarization. They reported that the B-N bond dissociation energy of amine-boranes was composed of two major components:  $\Delta E_{\text{prep}}$  and  $\Delta E_{\text{int}}$  (Table 2), where  $\Delta E_{\text{prep}}$  was the energy required to modify the two initial species in two fragments having the geometry and the electronic state they have in the amine-borane complex. In particular,  $\Delta E_{\text{prep}}$  contained the distortion energy of pyramidalization, for the boron fragment to pass from a  $\text{sp}_2$  trigonal to a  $\text{sp}_3$  tetrahedral geometry.  $\Delta E_{\text{int}}$  was the global interaction energy to join the two fragments, which mainly contained the Lewis acid/base attraction.

**Table 2. Comparison of calculated gas phase dissociation enthalpies (1989) and DFT-calculated energies considering several additives parameters (2006). Importance of the distortion parameter.**

$-\text{D}_e = \Delta E_{\text{int}} + \Delta E_{\text{prep}}$

	$\text{NH}_3\text{-BH}_3$	$\text{NMe}_3\text{-BH}_3$	$\text{NH}_3\text{-BMe}_3$	$\text{NMe}_3\text{-BMe}_3$
$\Delta H_{\text{dis}}^0$ <sup>a</sup>	31.1 (± 1)	34.8 (± 0.5)	13.8 (± 0.3)	17.6 (± 0.2)
$D_e$ <sup>b</sup>	31.8	36.2	12.7	9.5
$-\Delta E_{\text{int}}$	44.6	51.4	27.7	31.3
$-\Delta E_{\text{prep}}$	-12.7	-15.1	-15.2	-21.8

<sup>a</sup> Calculated gas phase dissociation enthalpy ( $\Delta H_{\text{dis}}^0$ ) in kcal/mol<sup>12</sup>; <sup>b</sup> Dissociation energy obtained by computational studies considering two major components ( $-\text{D}_e = \Delta E_{\text{int}} + \Delta E_{\text{prep}}$ ) in kcal/mol<sup>18</sup>

The results first confirmed that the traditional calculation of the gas-phase dissociation enthalpy did not always correlate to the bond strength. Neither the distance between boron and nitrogen nor the relative Lewis acid/base parameters correlated cleanly with the bond strength according to Franking and co-workers.<sup>18</sup> In fact, the amine-borane bond energy was reported as the sum of an “interaction” term ( $\Delta E_{\text{int}}$ ) involving both electrostatic and orbital interactions as well as Pauli repulsions and a “preparation” term ( $\Delta E_{\text{prep}}$ ) that contained the energy of pyramidalization. However, it was confirmed that Lewis acidity and basicity of the fragments were sufficient to estimate less sterically hindered amine-borane complexes. For this reason, the dissociation energy calculated by DFT ( $D_e$ , Table 2) was found to match reasonably well with the gas phase dissociation enthalpy ( $\Delta H^0_{\text{dis}}$ , Table 1) calculated by A. Haaland (no more than 6% errors). Although, for sterically hindered trimethyl-substituted amine-boranes, a significant error has been found. The  $\Delta H^0_{\text{dis}}$  parameter was no more reliable because the  $\Delta E_{\text{prep}}$  factor was not taken in account. A summary of concepts determining amine-borane stability have been illustrated below (Figure 7).

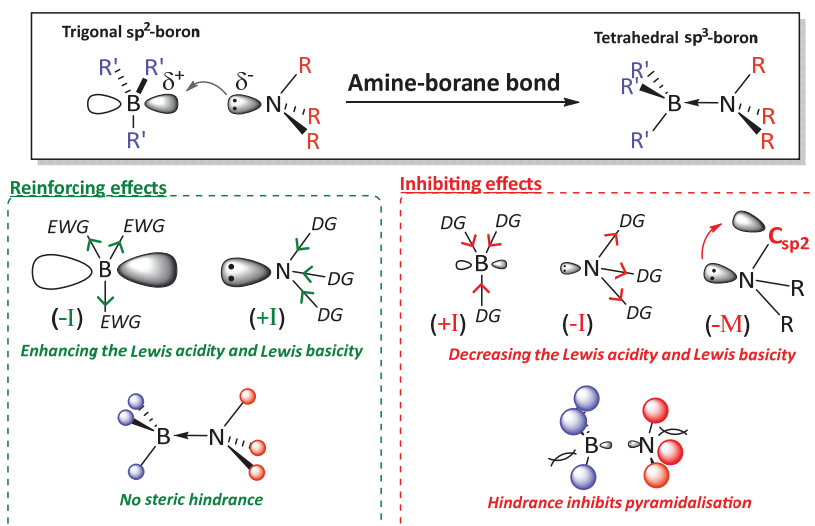


Figure 7. Inductive, mesomeric and steric effects on amine-borane bonding. *I*: inductive effects, *M*: mesomeric effects.

## II.2.b. Isosterism and hydrocarbon-like skeletons: example of BNs and CBNs

By taking advantage of the C-C / B-N isosterism, organic-like molecules have been synthesized by formally replacing one or several carbon-carbon sections by their boron-



nitrogen analogues. In the literature, these compounds have been generally called "BN-isosteres"<sup>19</sup> and among them, the carbon-boron-nitrogen (CBN) subclass referred to organic molecules that were partially functionalized with a boron-nitrogen section.

The first BN-isostere was reported by Alfred Stock and Erich Pohland in 1926 with the synthesis of the borazine<sup>20</sup> (Figure 8). This "inorganic benzene" was synthesized in the gas phase by reaction of diborane with ammonia. Later, the polyborazylene<sup>21</sup> analogue of the graphene as well as boron-nitrogen carbon nanotubes (BNNTs)<sup>22</sup> have been studied for their enhanced stability and their electronic properties with respect to their carbon-carbon counterpart.

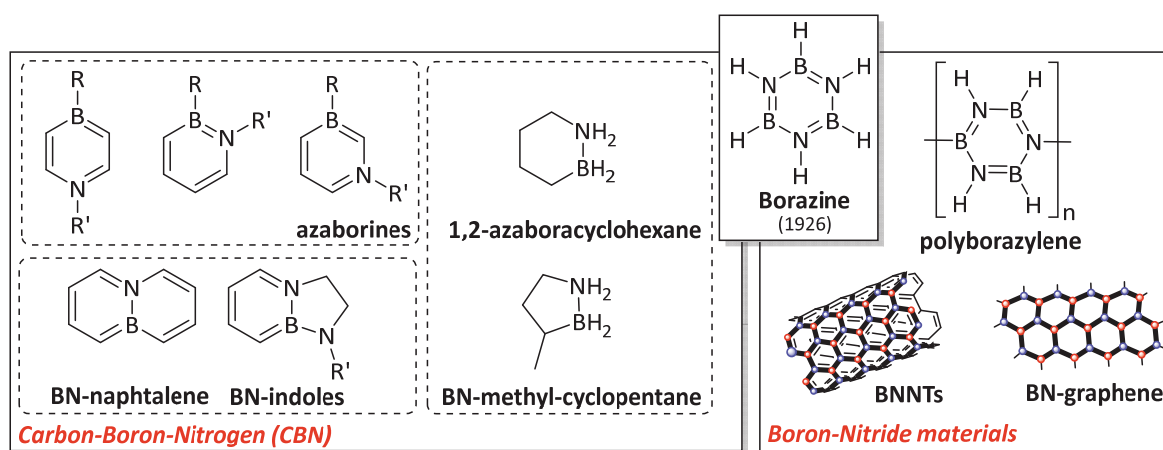


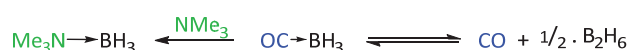
Figure 8. Non-exhaustive examples of Carbon-Boron-Nitrogen (CBN) molecules and Boron-Nitride materials.

Beyond these examples, a lot of organic molecules containing one or two boron-nitride functions in their structure and thus belonging to the family of CBN molecules were reported.<sup>19,23,24</sup> Most of them are the hybrid organic-inorganic analogues of arenes (e. g. azaborine) and cyclic backbone as cyclohexane<sup>4c,24a</sup> or cyclopentane<sup>23b</sup> (Figure 8). They exhibited a greatly enhanced reactivity with respect to their organic counterpart and they tended to form oligomers and polymers.<sup>4c,23b</sup> CBN molecules containing hydrogen atoms on Boron and Nitrogen (called C-BH-NH in this manuscript) and have been subject of many studies for hydrogen storage applications.<sup>25</sup> (This topic have been discussed in further details in the chapter III, section 1). These molecules are accessible through different ways of synthesis.

## II.3. Synthesis of ammonia-borane and analogues

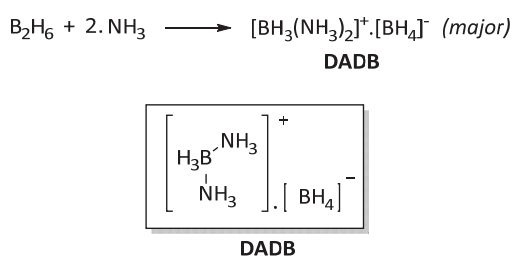
### II.3.a. Reactions by ligand exchanges.

The first synthesis of an amine-borane containing the trihydridoborane ( $\text{BH}_3$ ) has been reported by Stock in 1937.<sup>26</sup> He investigated the equilibrium between diborane  $\text{B}_2\text{H}_6$  and CO to form  $\text{BH}_3\text{CO}$ . He found that adding trimethylamine afforded quantitatively the amine-borane complex (Scheme 1).



*Scheme 1. The first synthesis of an amine-borane complex*

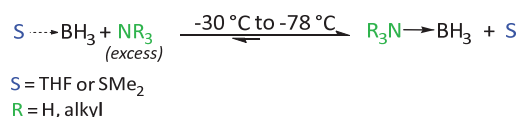
Later, it was reported that the diborane reacted with amines in the gas phase or in solution to give various amine-boranes of the form  $\text{R}_x\text{H}_{3-x}\text{N}-\text{BH}_3$ .<sup>27</sup> However, despite its high efficiency, this reaction has strong drawbacks in terms of safety since diborane and CO are highly toxic and diborane is even a pyrophoric gas. Moreover, this method did not lead to the AB selectively. The reaction between diborane and ammonia produced in majority the diammoniate of diborane (DADB), a ionic dimer of AB<sup>28</sup> (Scheme 2).



*Scheme 2. Synthesis of the DADB dimer from the reaction between diborane and ammonia.*

To synthesize the AB, the use of  $\text{BH}_3 \cdot \text{THF}$  or  $\text{BH}_3 \cdot \text{SMe}_2$  have been an alternative to provide the  $\text{BH}_3$  moieties in solution. These borane complexes are more stable than  $\text{BH}_3 \cdot \text{CO}$  and consequently safer. They have been used with an excess of ammonia at temperatures between  $-78^\circ\text{C}$  and  $-30^\circ\text{C}$ , to produce AB in good yields by displacement of the THF or  $\text{SMe}_2$  ligand (Scheme 3).<sup>29,30</sup> The resulting AB was purified by sublimation. The reaction was formally a Lewis-acid/Lewis-base exchange, thus the use of an excess of amine

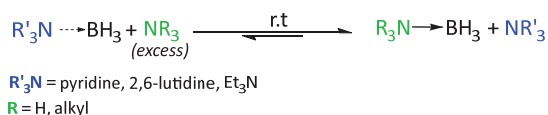
maximized the displacement of the equilibrium. This methodology provided amine-boranes in high yield and good purity because all the by-products were gas and/or volatiles and were thus, easily removable.



*Scheme 3. Synthesis of amine-borane from weakly associated borane complexes*

However, extending this method to other amines that may involve a higher boiling point could be an issue for purifications. In addition, for reaction requiring stoichiometric conditions the ligand-displacement method did not seem to be adapted although the equilibrium could be also displaced by continuous removal of the volatiles.<sup>31</sup> Finally, as noticed by A. Stautbitz *and co.*,<sup>1a</sup> the weakly associated complexes BH<sub>3</sub>·THF and BH<sub>3</sub>·SMe<sub>2</sub> was still likely to release toxic, flammable and/or malodorous gas such as BH<sub>3</sub> or SMe<sub>2</sub>. Consequently, the use of this methodology for large-scale syntheses presented a safety issue in terms of storage and handleability.

Amine-borane complexes have been synthesized ~~from other amine-boranes~~ by Lewis base-amine exchange<sup>32</sup> ~~from other amine-borane starting materials~~ (Scheme 4).



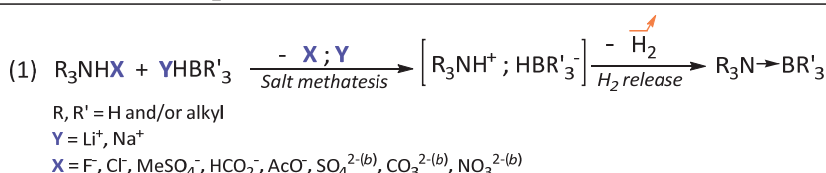
*Scheme 4. Synthesis of amine-borane by amine exchange.*

The equilibrated<sup>2</sup> reaction was displaced when the formed complex was stronger than the initial one. As discussed previously, the strength of amine-borane dative bonds was mainly determined by electronic effects influencing Lewis-acidity or basicity. But, in some cases other parameters such as steric hindrance significantly decreased the amine-borane bond strength. For instance, lutidine-borane and triethylamine-borane have been reported to be excellent starting materials to synthesize alkylamine-boranes, using classical equilibrium displacement techniques if required. This method had the advantage to be safer with respect to the method described above and to be possibly implemented at room temperature.

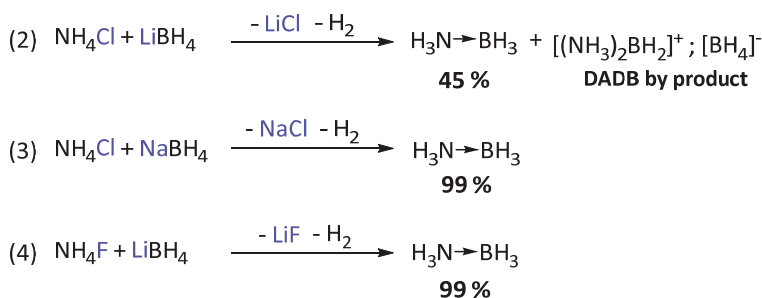
### II.3.b. Reactions of salt metathesis / H<sub>2</sub> release. Increasing efficiency.

~~Another procedure~~ Reactions between ammonium and hydridoborate salts ~~in polar aprotic solvents such as THF, Et<sub>2</sub>O, or dioxane~~ enabled the synthesis of amine-boranes under mild conditions, between 0 and 40 °C, quantitatively and with a high selectivity.<sup>11,33</sup> The reaction was carried out using stoichiometric amounts of starting materials. Salt metathesis and H<sub>2</sub> release were the driving forces of the reaction (Scheme 5).

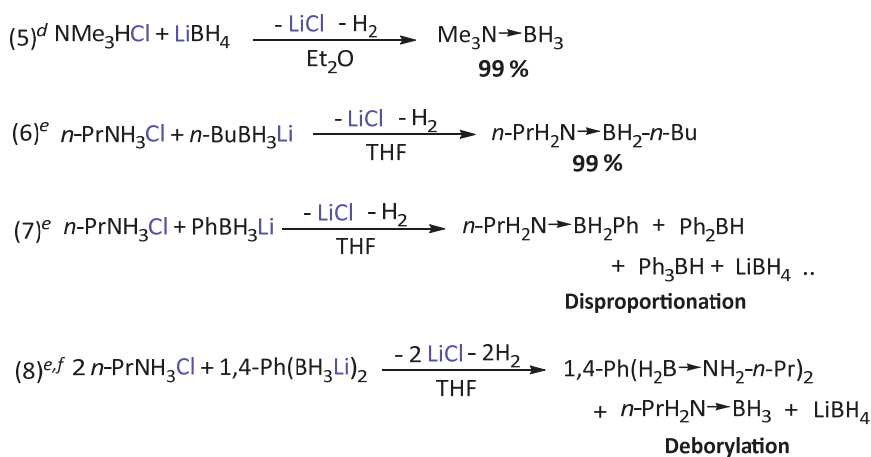
#### Salt metathesis / H<sub>2</sub> release general pathway<sup>a</sup>



#### Influence of counter-ions<sup>c</sup>



#### Influence of substituents



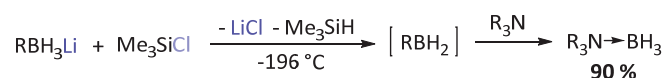
**Scheme 5. Synthesis of amine-boranes by subsequent salt metathesis/ dihydrogen release. General pathway.**

(a) see ref. <sup>33g</sup>; (b) with 2 ammonium counterpart; (c) conditions: NH<sub>3</sub>-THF, 25°C, see ref. <sup>1a,33b,33g</sup>; (d) see ref. <sup>1a,33e</sup>; (e) this work; (f) see ref. <sup>17</sup>.

The counter-ion of both ammonium and hydridoborate played an important role on the conversion and/or on the selectivity. In most of cases, starting materials were a chosen ammonium chloride (either commercially available or prepared from the corresponding amine and anhydrous HCl) and a lithium hydridoborate (affordable by treatment of a boronic acid/ester with  $\text{LiAlH}_4$ ).<sup>33d</sup> The majority of amine-boranes have been synthesized using these precursors (Scheme 5, eq. 5, 6), except for the synthesis of the AB itself which was particularly prone to form the DADB by-product (Scheme 5, eq. 2). In that case, the use of  $(\text{NH}_4)_2\text{SO}_4$  or  $\text{NH}_4\text{F}$  with  $\text{LiBH}_4$  as well as  $\text{NH}_4\text{Cl}$  with  $\text{NaBH}_4$  led to the completely selective formation of AB<sup>11,33g</sup> (Scheme 5, eq. 3, 4). During the synthesis of amine-phenylboranes derivatives, a split of the boron-carbon bond could be observed during the reaction<sup>17</sup> (Scheme 5, eq. 7, 8) and consequently other methods were considered.

### II.3.c. Reactions of salt metathesis / $\text{H}_2$ release. Use of a promoter.

Wagner and co-workers<sup>34</sup> reported conditions under which a ditopic B-aryl substituted amine-borane, bis(1,4-benzeneborane-dimethylethylamine), has been synthesized from the bis(trihydridoborate) precursor. The reaction temperature was set at  $-196^\circ\text{C}$ , then the system was allowed to warm up to room temperature in the presence of an excess of dimethylethylamine and trimethylchlorosilane. The chlorosilane acted as an external promoter to form the bis(dihydroborane) *in situ*, which was subsequently trapped by the amine to give the desired bis(amine-borane) in 90% yield (Scheme 6).



*Scheme 6. Synthesis of amine-borane: use of a promoter*

The reaction produced LiCl salt and gaseous  $\text{Me}_3\text{SiH}$  that offered the advantage to use a free amine instead of an ammonium salt. Other promoters have been reported in the literature such as  $\text{I}_2$ , HCl or MeI.<sup>35,36</sup>

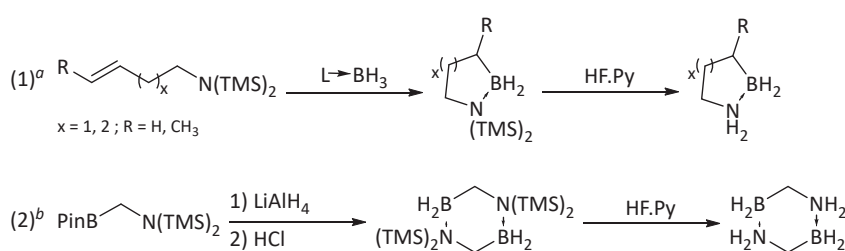
In summary, reactions of amine-borane formation introduced in this chapter are efficient to obtain a large range of amine-boranes even if some synthetic issues could be met. For

instance, tri/tetra-hydridoborate starting materials had to be synthesized prior to use from  $\text{LiAlH}_4$  and corresponding boronic acids/esters. The trihydridoborate salt is not easy to handle due to its medium to very low solubility<sup>34</sup> and because of its ability to form strongly associated structures<sup>37</sup> with polar solvents (THF,  $\text{Et}_2\text{O}$ ), thereby, rendering the molar quantification imprecise. Moreover, these methodologies were unsuccessful for synthesizing intracyclic C-BH-NH compounds.<sup>4c</sup>

### II.3.d. Multistep-synthesis of intracyclic amine-borane. Synthesis of CBN molecules for hydrogen release purposes (C-BH-NH).

A CBN molecule has been defined as a cyclic organic structure having one or two amine-borane functions in the ring. For the sake of brevity, we only focused our attention on the synthesis of CBNs bearing  $-\text{NH}_2\text{-BH}_2-$  amine-borane functions for hydrogen-storage applications (C-BH-NH).<sup>4c,23b,24a,38</sup>

The synthesis of intracyclic C-BH-NH required the synthesis of a precursor bearing both boron and nitrogen on the same carbon chain. Researchers had to design new synthetic pathways to insert hydrogen atoms on the amine-borane function. The intracyclic amine-borane was generated by complexation of the bis-N-protected allylamine or homoallylamine to  $\text{BH}_3$  and subsequent cyclisation by intramolecular amine-directed hydroboration<sup>23b,24a</sup> (Scheme 7, eq. 1).



**Scheme 7.** Synthetic pathway of CBNs for hydrogen release studies. (a) see ref. <sup>23b,24a</sup> ; (b) see ref. <sup>4c</sup>

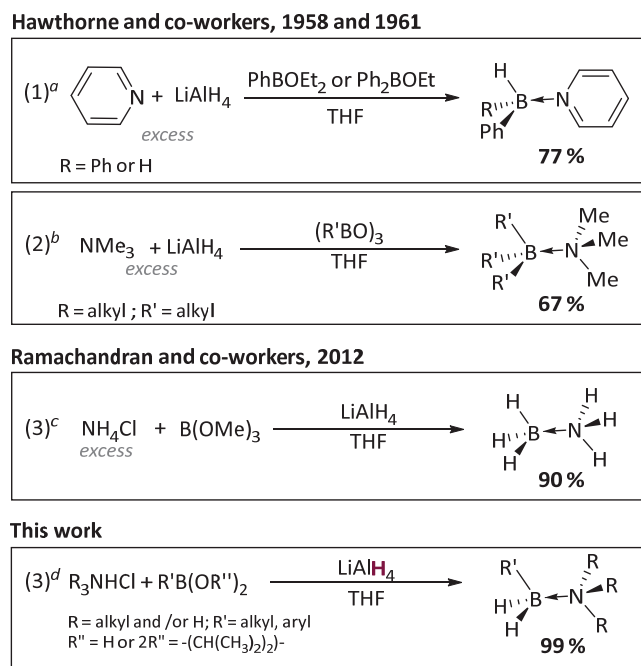
Thus, the B-N heterocycle was generated. Alternatively the borane function could be obtained starting from the pinacol boronate bearing a silyl protected amine, followed by  $\text{LiAlH}_4$  reduction and subsequent HCl treatment leading to a dimer of amine-borane. Then, for both strategies, removal of the N-TMS protecting group was accomplished using HF-pyridine. However, these procedures required numerous steps, several purifications

for a maximum overall yield of 69 %. But so far, it is the only way reported in the literature for synthesizing intracyclic C-BH-NH amine-boranes.

### II.3.e. One-pot synthesis of a large panel of CBN amine-boranes.

Previous works reported by Hawthorne and co-workers<sup>33c,39</sup> described the one-pot synthesis of amine-boranes by addition of a boronate, a borinate or a trialkylboroxine to a mixture of  $\text{LiAlH}_4$  and of a tertiary amine (such as trimethylamine or pyridine, Scheme 8, eq. 1, 2). Later, Ramachandran and co-workers<sup>40</sup> extended the procedure to the synthesis of the AB (Scheme 8, eq. 3). These procedures provided amine-boranes in moderate to good yield, but required large amounts of amine and further purification steps.

During the course of this work, we have reported a new procedure providing directly a wide range of amine-boranes from commercially available or easily available starting materials. The amine-borane has been synthesized by triggering the reduction of a boronic acid or pinacol ester with  $\text{LiAlH}_4$  in the presence of an ammonium chloride. The reaction had the advantage to be quantitative, fully selective and to proceed from 0 °C to room temperature in 10 min to 2 h maximum. In addition the reaction did not need any excess of amine or  $\text{LiAlH}_4$  and thus afforded directly the product in high purity (Scheme 8, eq. 4).



Scheme 8. Generalized one-pot methodology. (a) see ref.<sup>39</sup> (b) see ref.<sup>33c</sup> (c) see ref.<sup>33b,40</sup> (d) see ref.<sup>17</sup>.

Thus, this reaction permitted to access amine-boranes bearing sensitive vinyl groups as well as amine-borane containing polymers in the main-chain (see Section 2) and in side-chains (see Section 3).

A wide range of amine-borane derivatives have been synthesized with this procedure (Figure 9) such as BN-hydrocarbons (**1a**), di-functional amine-boranes involving primary or tertiary amines (**1b**, **1d**) and amines having ether groups on their chain (**1c**) as well as involving alkyls (**1a**) or aryls boronic species (**1b-h**). As mentioned, the chemoselectivity of the reaction enabled the synthesis of sensitive monomers bearing vinyl functions and suitable for chain polymerization. For instance, the *n*-propylamine-(4-vinylbenzene)borane (**1g**) and the (4-vinylbenzyl)amine-(4-vinylbenzene)borane (**1h**) have been synthesized.

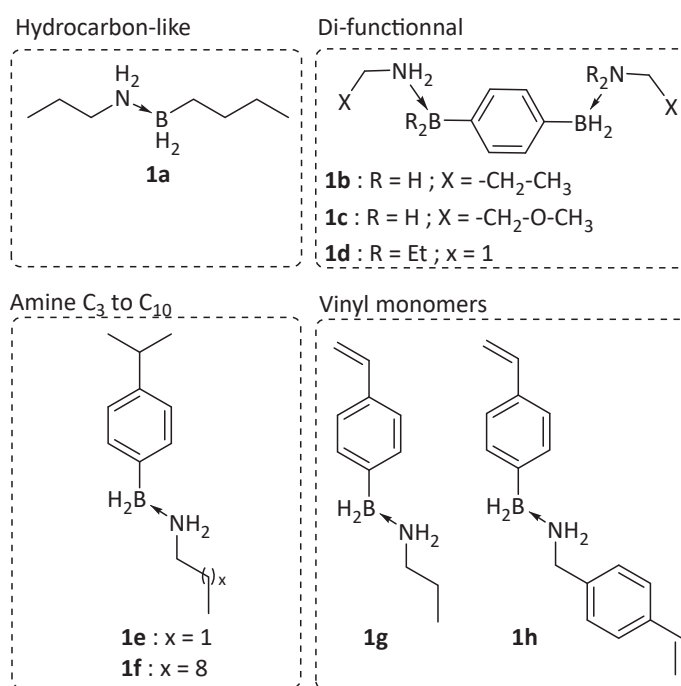


Figure 9. Amine-borane molecules synthesized with our one-pot condition.

Only one boron species turned out to be incompatible with our conditions. The unsubstituted phenylborane was found to be sensitive to disproportionation in presence of LiAlH<sub>4</sub> and to form several di- and tri-phenylborohydrides species as well as LiBH<sub>4</sub>.<sup>39b</sup> The instability of the B-phenyl bond has also been observed in our conditions. However,



as soon as the *para* position of the B-phenyl were substituted by alkyl functions, the disproportionation has not been observed anymore.

Nevertheless this one-pot methodology has offered many advantages in terms of efficiency but also in terms of handleability, particularly because it allowed the use of soluble boron starting materials (such as boronic acids/esters) in contrast to previous methods employing hydridoborate salts. For this reason, this method also appeared to be particularly user friendly for the synthesis of amine-borane containing polymers. Indeed, this reaction has been a mainstay of the work reported in this manuscript and has opened the door to polymers with high C-BH-NH amine-borane content.

Indeed, the AB and other C-BH-NH amine-borane analogues have been extensively studied for hydrogen storage applications.<sup>14</sup> The following section has highlighted issues accompanying the design of amine-borane hydrogen reservoirs.

## II.4. Ammonia-borane for hydrogen tanks

---

*“As we burn our way through petroleum resources”,<sup>41</sup>* generating massive quantities of greenhouse gas and toxic pollutants, the use of petrol resources as energetic supply has become less attractive. The ever growing demographic demand accompanied by progress in technology and transportation led us to carry out an important upgrade in the field of energy by improving efficiency and sustainability.

### II.4.a. The challenge of developing hydrogen fuel cells

Hydrogen has been presented as an ideal synthetic fuel, generating energy by reacting with oxygen to produce water efficiently.<sup>42</sup> The key scientific challenge consisted in finding safe and efficient solutions to store and release hydrogen for both stationary and mobile applications.

Elemental dihydrogen has been the focus of many studies but it appeared to require extreme temperature and pressure conditions to store it at a decent volumetric density.

Pure H<sub>2</sub> storage has been achieved by compression at 700 bar to achieve 40 H<sub>2</sub> g/L or by cryogenic liquefaction at 20 K to afford 70 g/L.<sup>43</sup> However, storing pure dihydrogen turned out to raise safety problems because of the flammability associated to difficulties to store it hermetically.

Thus, “solid state” hydrogen materials represent a safer solution due to their ability to store high H<sub>2</sub> volumetric and gravimetric capacities in normal conditions of temperature and pressure.<sup>43</sup> They concentrate Hydrogen through chemical bonding. A lot of “solid state” hydrogen materials have been reported in the literature. In fact, hydrogen can be stored on the surfaces of solids (by adsorption) or within solids (by absorption).<sup>44</sup> Hydrogen can be also strongly bound within molecular structures.<sup>42</sup> The latter contains generally the highest H<sub>2</sub> gravimetric capacities. Among them we can find amine-borane compounds that are among the most promising materials for automotive applications. Not only do they offer high volumetric hydrogen capacities (e.g. 100-140 g/L for AB, in normal conditions of temperature and pressure) but they also provide good kinetics of hydrogen delivery at middle temperatures.<sup>14</sup>

#### **II.4.b. Promising characteristics of ammonia-borane (AB) and scientific issues**

Among all the amine-boranes, the AB has received the most attention. This started as early as 1950 for military applications, because of its particularly high hydrogen content (19.4 wt%). AB is non-flammable, non-explosive under standard conditions and can release hydrogen by thermal activation. However only a maximum of 13.1 wt% of hydrogen content has been used using thermal activation.<sup>14</sup> AB decomposed in a stepwise process because all the three hydrogens are not equivalent, but the mechanisms of dehydrogenation were multiple and not yet fully understood (See chapter II.6).

The AB technology for transportations has to be improved on several critical points according to the criteria set by the U.S. Department of Energy (DOE) for transportations<sup>14</sup> that is an excellent guide-line for improving hydrogen technology in this field (Table 3).

Table 3. Critical U.S DOE targets for on board hydrogen storage<sup>14</sup>.

Storage parameters	2017	Target
Gravimetric capacity [wt%]	5.5	7.5
Operating stability [°C]	-40/60 (sun)	-40/60 (sun)
Min/max delivery temperature [°C]	-40/85	-40/85
System regeneration time [kg H <sub>2</sub> /min]	1.5	2.0
Toxicity and safety	Meets or exceeds applicable standards	

In fact, to meet hydrogen fuel cell requirements of DOE, AB must release 99.7 % pure hydrogen at ~ 80 °C. So far, AB fall outside this requirements, because the release of dihydrogen around 125 °C and is accompanied by numerous impurities in the gas phase such as ammonia, diborane, aminoborane (H<sub>2</sub>N=BH<sub>2</sub>), borazine, cycloborazane and other oligomers<sup>4a,11</sup> that are incompatible with a fuel cells.

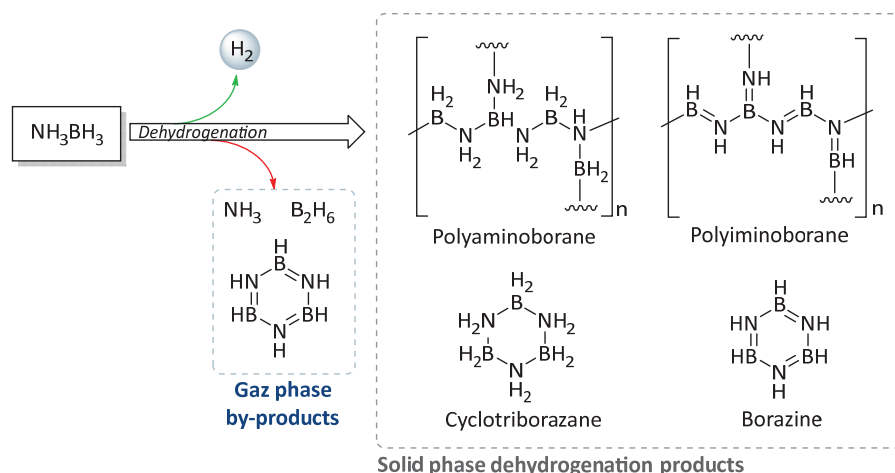


Figure 10. Examples of AB decomposition product recovered in the gas phase and in the solid residue

The efficient and energetically acceptable regeneration from spent fuel is critical because the decomposition of AB generates highly stable products, by oligomerization (for example borazine) and by polymerization giving a mixture of polyaminoborane (PAB) and polyiminoborane (PIB) (Figure 10). For example, the standard heat of formation of borazine in the gas phase is  $\Delta H_{f,298K}^0 = -124.1 \pm 3.2$  kcal/mol, too stable to be regenerated into AB at a reasonable energy cost.<sup>45</sup> Efforts in regeneration of the material have led to know that the matter is possible in quite harsh and energetically costly condition.<sup>33b,38,46</sup> Thus regeneration of AB spent fuel using molecular dihydrogen has not been realized so far but solution paths have been drawn by scientist in the past decades. Manners and co-workers<sup>47</sup> reported in a theoretical study that suitable modifications of the electronic

properties of both Nitrogen and Boron could lead to a system having a slightly endothermic hydrogen release, yielding the reaction step potentially reversible.<sup>47</sup> Moreover designing specific amine-borane based materials could decrease the experimental exothermicity by decreasing undesired covalent B-N bonds created subsequently to dehydrogenation and leading to the formation of highly stable BN-polymers. Finally, recent development of boron-nitrogen “frustrated-Lewis pair”<sup>1b,1d</sup> on dihydrogen splitting, suggested that the challenge of boron-nitrogen rehydrogenation is theoretically affordable.

Hydrogen production from the AB has been the focus of numerous experiments and a lot of methods to trigger hydrogen release have been reported both thermally and chemically induced (from metal to acid catalysis) in solid state or in liquids. In the next sections, both techniques will be discussed but we will put a particular emphasis on the thermal activation of AB in the solid state.

## **II.5. Thermal stepwise hydrogen release of ammonia-borane.**

---

The two main analytical technics that permitted to observe thermally induced hydrogen release from amine-boranes as well as associated phenomena have been the thermogravimetric analysis (TGA) and the differential scanning calorimetry (DSC).<sup>4a,48</sup> Moreover, a quantitative measure of hydrogen released was accurately obtained by temperature programmed desorption of dihydrogen (TPD or TPD-H<sub>2</sub>)<sup>25b</sup> which contained a thermal conductivity detector (TCD) (Figure 11). The sample was heated and flushed by a vector gas (as for example Argon). The gas released by the sample mixed with the vector gas and reached the TCD. TCD detected quantitatively the gas emitted by differentiating the thermal conductivity of the gas mixture from the reference (pure vector gas). TPD provided very good values of qualitative and quantitative dihydrogen emission specifically, thanks to the greater value of dihydrogen’s specific heat capacity ( $C_{p-H_2} = 14.32 \text{ KJ.Kg}^{-1}.\text{K}^{-1}$ ) with respect to the one of other gas and volatiles (helium excepted). It was particularly important to detect dihydrogen from AB using TPD as ammonia and

diborane had a significantly lower heat capacity than dihydrogen ( $C_p\text{-NH}_3 = 2.19 \text{ KJ.Kg}^{-1}.\text{K}^{-1}$  and  $C_p\text{-B}_2\text{H}_6 = 0.06 \text{ KJ.Kg}^{-1}.\text{K}^{-1}$ ). Consequently, dihydrogen was selectively quantified with this technique regardless of impurities (however a blank-experiment is always required). Solid-state *in-situ* spectroscopic measures such as IR<sup>49</sup> or <sup>11</sup>B MAS-NMR<sup>50</sup> heating experiments gave crucial mechanistic information on the structure of intermediates and products. Finally, coupling these apparatus to GC-MS gave access to the composition of the emitted gas phase.<sup>25b</sup> The temperature of dehydrogenation has depended dramatically on the temperature scanning program. Consequently, differences (1-5 K) could have been noticed between the different studies in the literature.

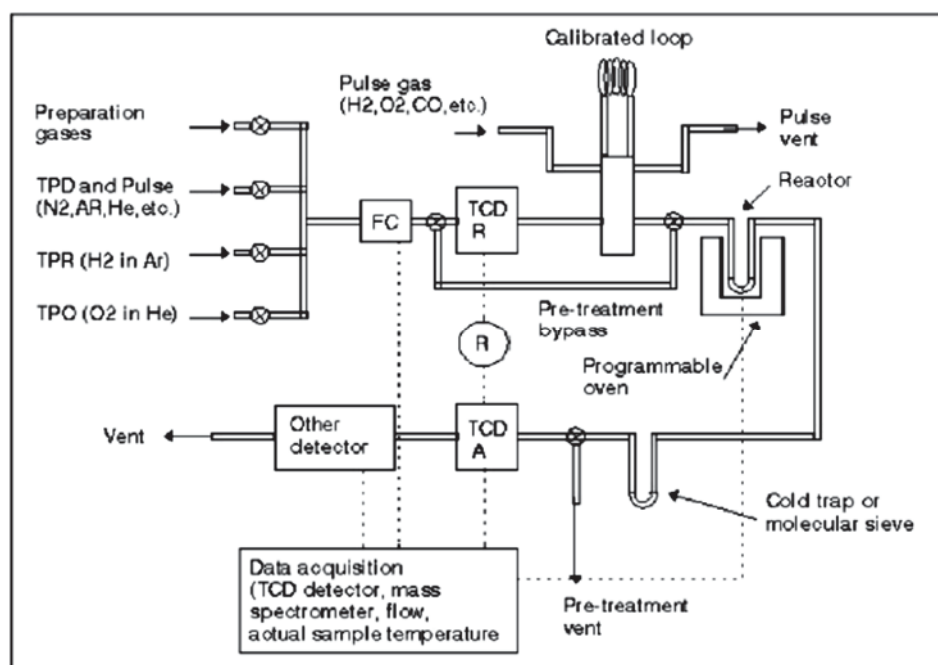


Figure 11. TPD apparatus

When heated, ammonia-borane released hydrogen in a two-step process preceded by a “melting” endotherm,<sup>51</sup> observed by DSC (Figure 12).

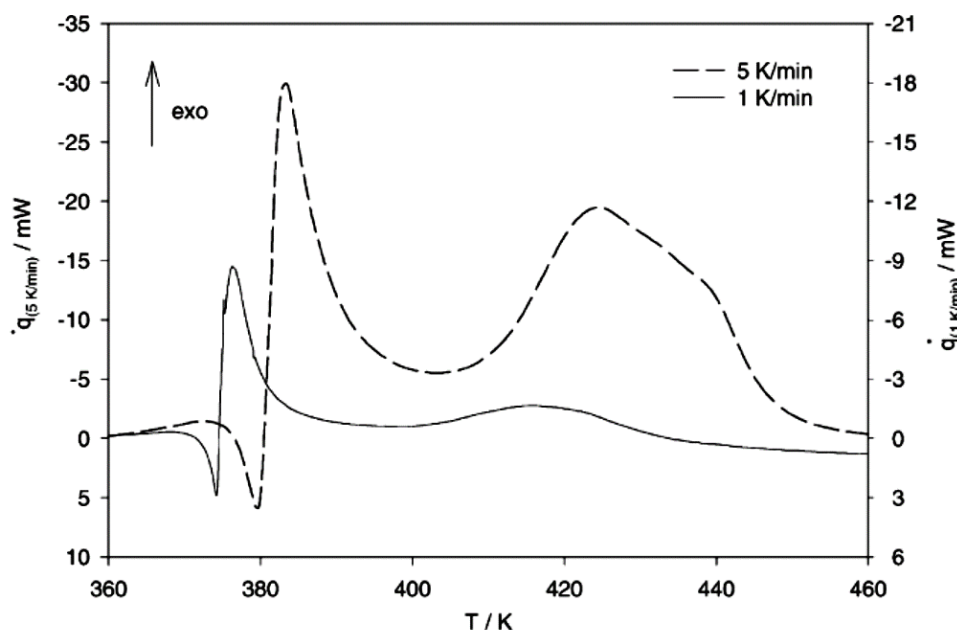


Figure 12. Thermal decomposition of AB followed by DSC with a temperature rate of 5 K/min (dots) and 1 K/min (line) reported by F. P. Hoffman and co-workers.<sup>48</sup>

According to experiments reported by F.P. Hoffman and co-workers,<sup>48</sup> with a temperature scanning rate of 5 K/min, the phase-change occurred at 110 °C (383 K) followed by an exothermic peak of dehydrogenation with a maximum at 117-125 °C (385-393 K), corresponding to the release of one equivalent of dihydrogen and followed by an important foaming of the sample. According to authors, during this step, oligomers and polyaminoboranes were formed. Then a second broad exothermic wave occurred between 140 and 180 °C (413-453 K), after which a total of 2.2 equivalents of H<sub>2</sub> were released.<sup>4a</sup> With a slower temperature scanning rate of 1 K/min, the same pattern has been observed but shifted by almost 10 °C earlier in temperature.<sup>48</sup> For a complete dehydrogenation, it has been necessary to heat above 1200 °C.<sup>11</sup> The incomplete release of hydrogen at “mild” temperatures (50-200 °C) has been confirmed by infra-red monitoring, by heating polyaminoborane at 200 °C during 18 h,<sup>52</sup> after which the characteristic B-H stretching was still visible ( $\nu = 2230\text{-}2420\text{ cm}^{-1}$ ).

Moreover, the first decomposition step corresponding to the liberation of 1 eq. of H<sub>2</sub> was studied by DSC in isothermal conditions at temperatures between 70 °C (343 K) and 90 °C (363 K)<sup>48</sup> (Figure 13).

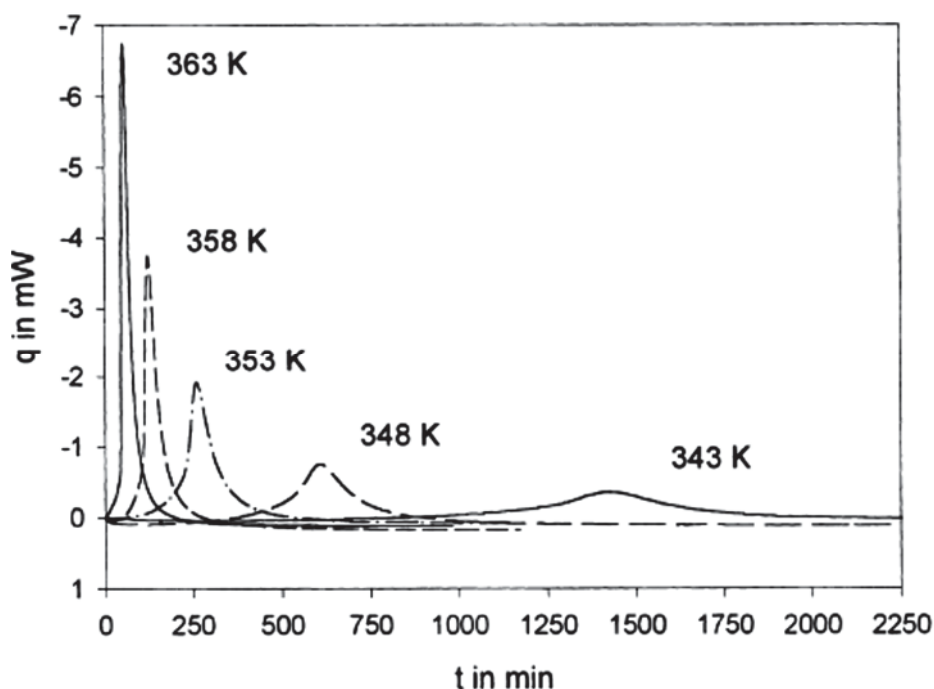


Figure 13. Isothermal decompositions of AB at temperatures from 343 and 363 K. Reported by F. P. Hoffman and co-workers<sup>48</sup>.

The study evidenced that dihydrogen release was triggered at temperature as low as 343 K (70 °C) and that the rate of decomposition strongly depended on the temperature ranging from 40 min at 363 K (90 °C) to more than 24 h at 343 K (70 °C). The experimental enthalpy determined from the different DSC patterns was equal to  $\Delta H = -21.7 \pm 1.2$  kJ/mol ( $-5.2 \pm 0.3$  kcal/mol) and was almost independent of the temperature. This value represented the release of about 1 eq. of dihydrogen as well as the formation of covalent B-N bonds, mainly to generate polyaminoborane. Calculated enthalpy for the formal release of 1 eq. of dihydrogen gives  $\Delta H = -5.1$  kcal/mol at 298 K,<sup>53</sup> i.e. identical to the experimental one.

However, this value did not take in account the formation of B-N bonds which were known to be significantly exothermic.<sup>54</sup> Consequently, the experimental enthalpy was expected to be even lower. Nevertheless, it seems likely that several reactions took place simultaneously during the first dehydrogenation step, including endothermic ones, leading to an overall modestly exothermic decomposition process. For instance, the release of the second equivalent of H<sub>2</sub> is known to be endothermic (the enthalpy of formation of BH-NH is  $\Delta H_f = 13.6$  kcal/mol<sup>53</sup>). Actually, it was consistent with the formation of minute amount of borazine during the first dehydrogenation step.<sup>4a</sup>

## II.6. Mechanistic insights on the thermal dehydrogenation of AB in the solid state.

Mechanisms of thermal decomposition of AB has been extensively studied both experimentally by using *in situ* analytical techniques such as  $^{11}\text{B}$  MAS-NMR,<sup>50,55</sup> and by theoretical investigations.<sup>3,15,47,53-54</sup> The thermal dehydrogenation of AB in the solid state displayed several possible pathways that were competitive and/or depended on the experimental conditions. Researchers particularly focused their attention on understanding the release of the first equivalent of dihydrogen that has revealed to be a key-step in understanding the chemistry of AB and derivatives. An excellent study was reported in 2007 by Dixon and co-workers.<sup>3</sup>

### II.6.a. Key mechanistic points

The transition state (TS) leading to hydrogen elimination could be intuitively seen as an intramolecular four membered TS (Figure 14) yielding to one equivalent of dihydrogen and to the corresponding aminoborane. This hypothesis did not hold because the TS energy barrier was very high (37 kcal/mol) and consequently very unlikely to occur. Moreover, the dissociation of the dative B-N bond was preferred by almost 10 kcal/mol, which excluded the possibility of a concerted four center TS (Figure 14).

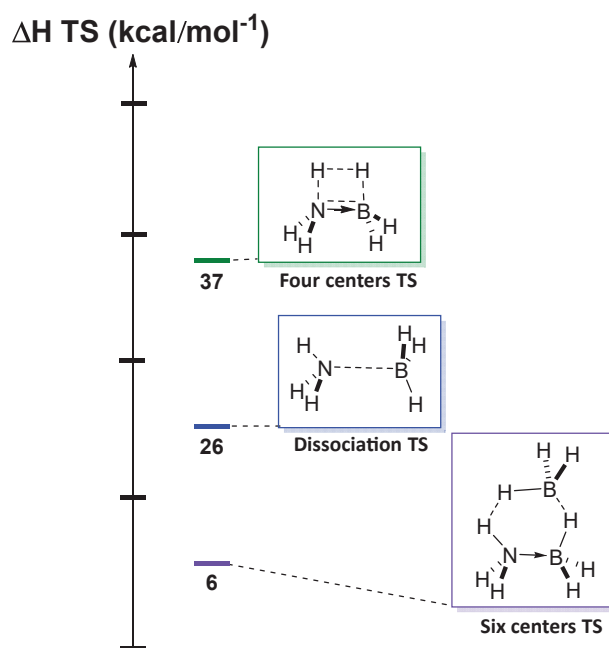


Figure 14. Scale of possible hydrogen release TS and comparison with dissociation TS



The addition of an external  $\text{BH}_3$  molecule to the system that may come from the dissociation of the BN bond of another AB molecule, allowed a six membered TS and a resulting drop of TS energy barrier to 6 kcal/mol. Indeed in AB dehydrogenation pathways, six membered TS have been particularly preferred, entailing bimolecular processes.

In the ground state, AB is stabilized by a network of DHB interactions. DHB and conventional hydrogen bonding (HB) appeared to be comparable in strength, ranging from 1.2 to 7.2 kcal/mol.<sup>16</sup> Indicatively, to appreciate the potential of DHB for stabilization AB has been compared with the estimated complexation energies at 298 K of a water dimer. Thus, the AB dimer demonstrated 14.0 kcal/mol<sup>3</sup> of stabilization (7.0 kcal/mol/DHB) whereas the water dimer showed only 3.2 kcal/mol of stabilization through hydrogen-bonding interactions.<sup>56</sup>

#### II.6.b. The two main mechanistic pathways of AB thermal dehydrogenation in the solid state.

The following pathways presented below, summarized and resumed mechanistic studies reported so far.<sup>3,54</sup> Additional information could be found in original papers.

In 2007, Dixon and co-workers<sup>3</sup> demonstrated by an extensive theoretical study, the possibility of two major competing pathways (Figure 15) that are governed by two types of intermediates able to generate dihydrogen directly with reasonable energetic barriers. First, starting from the dimer of AB, a  $\text{BH}_3$  molecule could be formed by dissociation of one B-N bond resulting in a 3-center-2 electrons intermediate (**3c-2e complex**, Figure 15) by formation of a B-H-B bond. This intermediate released 1 eq. of  $\text{H}_2$  leading to the formation of a  **$\text{sp}^2$ -monomer** of aminoborane. In the case of AB, the aminoborane  **$\text{sp}^2$ -monomer** was not stable and could further react, among other options, with an AB to give the aminoborane  **$\text{sp}^3$ -dimer**.<sup>54</sup> Alternatively, the AB dimer isomerized to an ion-pair diammoniate of diborane (**DADB**, Figure 15) and subsequently generated 1 eq. of dihydrogen accompanied by the straightforward formation of the  **$\text{sp}^3$ -dimer** of aminoborane.

Experimentally, the DADB has been selectively formed by kinetic control. It has been observed by *in situ*  $^{11}\text{B}$  MAS-NMR<sup>50</sup> as the major intermediate under isothermal heating at 88°C. Finally it has been important to stress that the rate of the single events can be influenced by the reaction conditions, particularly by the temperature rate, by the chemical environment and by the presence of a catalyst.

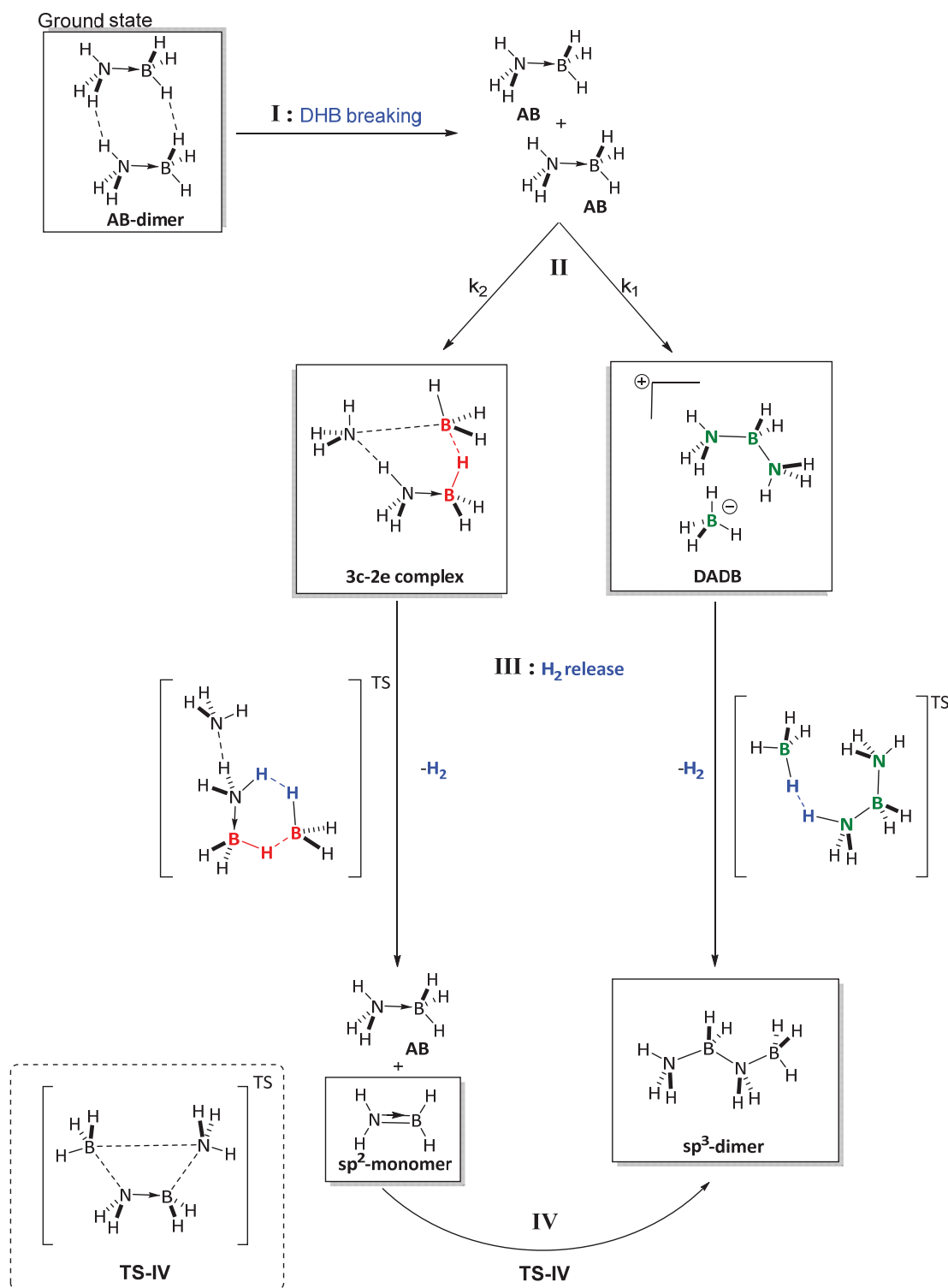


Figure 15. Schematic representation of the two competitive mechanistic pathway of AB decomposition

## II.7. AB dehydrogenation with other media

---

The decomposition pathways of AB showed differences in mechanisms and products by modifying the environment (solvents<sup>4b</sup>, ionic liquids<sup>57</sup>) as well as by the means of activation (thermal, metal catalyzed,<sup>30,58,59</sup> acid triggered,<sup>60</sup> solvolysis,<sup>59b,61</sup> etc.). Two examples have been given in this paragraph.

### II.7.a. Ammonia-borane dehydrogenation in solution

The thermal dehydrogenation of AB has been investigated in several organic solvents such as THF, or glyme.<sup>4b</sup> It has been shown that AB stability depended on its concentration, which turned out to be consistent with a second order decomposition pathway and a bimolecular mechanism. In organic solvents, AB did not exhibit neither DADB intermediate nor polymer decomposition products which contrasted with the derived observations in the solid state. Other <sup>11</sup>B and <sup>15</sup>N NMR studies have suggested that DADB was effectively formed but was very unstable and reacted immediately to form cyclic boron-nitrogen dehydrogenation products.

In contrast, very polar ionic liquids were reported to stabilize the DADB ionic pair and consequently to facilitate its formation from the AB dimer. Ionic liquids enhanced the kinetic of ammonia-borane decomposition.<sup>57a</sup> For example, at 85 °C the neat solid released 0.8 H<sub>2</sub> equivalent with an induction period of 2 h while in bmimCl (1 weight equivalent) 2.2 equivalents were produced with no induction period. The different polarity and nature of the environment with respect to the solid state has explained variations of kinetics and thermodynamics.

### II.7.b. Metal catalyzed amine-borane dehydrocoupling

The metal catalyzed dehydrogenation of AB and amine-borane derivatives has allowed to isolate key-intermediates and products by performing controlled dehydrogenation at room temperature or in mild conditions with AB and amine-boranes of formula RNH<sub>2</sub>-BH<sub>3</sub> or R<sub>2</sub>NH-BH<sub>3</sub>.

The first example was reported by Manners and co-workers in 2001. A Rh-based catalyst was used to form cyclic aminoboranes and borazines.<sup>58a</sup> The method was extended in 2003<sup>30</sup> to form several aminoborane dimers, borazines, and in particular the monomeric aminoborane (*i*Pr<sub>2</sub>N=BH<sub>2</sub>). Later, improvements were reported by Goldberg and Heinekey using the Brookhart's Ir catalysts.<sup>58b</sup> Notably, only the first equivalent of H<sub>2</sub> was released selectively. Then, very active Ru catalysts were reported by Fagnou and co-workers<sup>58c</sup> and subsequently Schneider and co-workers.<sup>58d</sup> Of note, Ru catalyst is able to release precisely 1 or 2 equivalents of H<sub>2</sub>, depending on the experimental conditions. The method has also been investigated on non-precious metal catalysts such as Ni,<sup>58e</sup> Fe,<sup>58g,58h</sup> Co,<sup>58f</sup> Ti and Zr,<sup>58i</sup> as well as nanoparticles.<sup>59</sup>

So far, Rh and Ir catalysts remained of great importance as they permitted to catch key intermediates of AB dehydrocoupling<sup>62</sup> and led to well defined complex structures such as high molecular weight polyaminoboranes.<sup>63</sup>

---

### III. Nitrogen and/or boron substituted amines-borane – electronic effects and reactivity in hydrogen release

---

Modifying substituents at both nitrogen and boron has been a promising strategy to improve the dehydrogenation profile of amine-borane materials. Actually, in a computational study, Manners, Harvey and co-workers pointed out the relevance of electronic effects induced by substituents.<sup>47</sup> Noticeably, calculations revealed that the thermal dehydrogenation could be made more thermoneutral by increasing the B-N  $\sigma$ -bond strength of the amine-borane adduct.

#### III.1. N and/or B-methyl-substituted amine-boranes

---

The methylation of the nitrogen atom, to give mono- and dimethyl N-substituted amine-boranes modified significantly the physical properties and the dehydrogenation profile of amine-boranes with respect to their AB analogue (Table 4). In fact, additional methyl

groups decreased the melting point as well as the exothermicity of the reaction. The dimethylamine-borane dehydrogenation was found to be almost thermoneutral. In contrast, the addition of methyl substituents on the boron atom increased the exothermicity of dehydrogenation. These observations correlated with the relationship established between amine-borane B-N  $\sigma$ -bond strength.

*Table 4. Effect of N-methyl substitution on amine-borane. Comparison with calculated enthalpies*

Amine-borane $R_2HN-BHR'_2$	Melting point (°C)	Dehydrogenation peak (°C)	$\Delta H$ (kcal/mol) <sup>c</sup>
$H_3N-BH_3^a$	118-120	120-130	-5.1
$MeH_2N-BH_3^b$	58-59	100-130	-3.5
$Me_2HN-BH_3^b$	36	130	-1.8
$H_3N-BH_3/MeH_2N-BH_3$ 35:75 <sup>b</sup>	35-37	-	-
$H_3N-BH_2Me^b$	-	-	-9.4
$H_3N-BHMe_2^b$	-	-	-11.7

<sup>a</sup> See ref. <sup>51</sup>, <sup>b</sup> See ref. <sup>64</sup>  
<sup>c</sup>  $\Delta H$  calculated for the reaction :  $R_2HN-BHR'_2 \longrightarrow R_2N=BR'_2 + H_2$  at 298 K

Mixtures of AB and  $MeNH_2BH_3$  (from 20 % to 50 %  $NH_3BH_3$ ) have shown very surprising physical properties. The melting temperature range was significantly lower than the melting point of pure materials. An example has been reported in the Table 4, on which a mixture of  $MeNH_2BH_3$  and 35 %  $NH_3BH_3$  had a melting temperature range of 35-37 °C, that was 22 °C and 83 °C lower than that of  $MeH_2N-BH_3$  and  $NH_3BH_3$  respectively. We assumed that apparently, the mixture of the two amine-boranes behaved like a single compound having one physical constant and probably one averaged DHB network. We have supposed that this network was less organized than in separate single species and it could be the reason of a lower melting point. Later, the same trend has been observed on alkylamine-borane/AB mixtures (from 33 % to 100 %  $NH_3BH_3$ ) that yielded a liquid product before and after dehydrogenation.<sup>65</sup> However, to the best of our knowledges, the effect of  $H_3N-BH_3/(alkyl)H_2N-BH_3$  mixture on the thermal dehydrogenation pattern has not been reported so far. A similar behavior has been observed in this work and will be discussed in Section 3, chapter III.4.

### **III.2. Amine-boranes inserted in linear or cyclic organic scaffolds. Effects on the decomposition.**

---

The insertion of amine-boranes into organic scaffolds has been extensively studied in order to get rid of several dehydrogenation drawbacks observed with AB. By modifying the structure of AB, researchers aimed at a better control of kinetics and thermodynamics<sup>4c</sup> of the reaction of H<sub>2</sub> release as well as improved properties of the material before and after consumption.<sup>23b</sup> Moreover, the design of organic amine-boranes has permitted to improve the purity of dihydrogen gas while keeping a good H<sub>2</sub> gravimetric capacity.

Researchers developed several boron-nitrogen containing alkanes (BN-alkanes) and cycloalkanes (BN-cycloalkanes) having between 9.6 wt.% and 4.7 wt.% available dihydrogen. Experimental characteristics have been summarized in tables below, in order to highlight a structure / activity relationship.

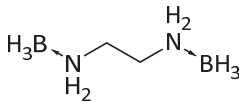
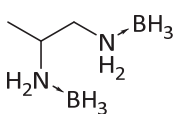
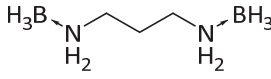
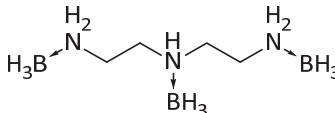
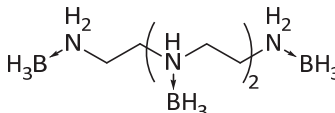
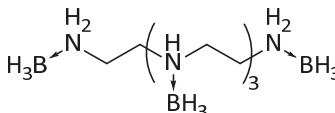
#### **III.2.a.C-BH-NH: hydrogen containing amine-boranes inserted in linear organic scaffolds**

At first, BN-alkanes have been extensively studied as promising hydrogen storage candidates due to their ability to enhance the stability of the NH<sub>2</sub>-BH<sub>2</sub> moieties under 80 °C and to get rid of undesired gas impurities emissions such as B<sub>2</sub>H<sub>6</sub>, NH<sub>3</sub> and borazine. However, the absence of NH<sub>3</sub> and borazine has not been a surprise considering the structure of the starting materials. Instead, other analogues such as alkylamines or alkylcycloborazanes could be expected. In Table 5, we attempted to collect comparable data although it has to be kept in mind that the results could vary with the experimental conditions and that no really standardized set of tests has been established.

It appeared that 1,2-TMDAB was the most efficient compound as it gave the best hydrogen yield and the highest rate of dihydrogen release at 110 °C (27 min/eq.). At comparable electronic environments, the alkane scaffold showed a significant influence on the dehydrogenation profile. A branched isomer (1,2-TMAB) appeared to be more

efficient and to have a less exothermic decomposition than its linear analogue (1,3-TMAB).

**Table 5. Thermal dihydrogen release of BN-alkane. Experimental characteristics.**

Molecules Name (Ref.)	H <sub>2</sub> availability [wt.%] (yield [%])	Temperature of H <sub>2</sub> release [°C]	Enthalpy [Kcal/mol] <sup>c</sup>	Rate at 110 °C [min/1equiv. H <sub>2</sub> ]
 EDAB (ref. <sup>25a</sup> )	11.3 (88)	125 <sup>a</sup>  170 <sup>a</sup>	Exothermic -2.41 Exothermic -0.91	50
 1,2-TMDAB (ref. <sup>66</sup> )	7.8 (95)	100 <sup>b</sup> 155 <sup>b</sup>	Exothermic -2.62 (total)	27
 1,3-TMDAB (ref. <sup>66</sup> )	7.8 (81)	103 <sup>b</sup> 145 <sup>b</sup>	Exothermic -1.69 (total)	50
 DETAB (ref. <sup>25b</sup> )	9.6 (79)	100-190 <sup>b</sup> 190-220 <sup>b</sup>	Exothermic (-3.20) Endothermic (+0.09)	50
 TETAB (ref. <sup>25b</sup> )	8.9 (76)	90-150 <sup>b</sup> 170-230 <sup>b</sup>	n.r. <sup>d</sup>	“sluggish”
 TEPAB (ref. <sup>25b</sup> )	8.5 (69)	90-150 <sup>b</sup> 170-230 <sup>b</sup>	n.r. <sup>d</sup>	“sluggish”

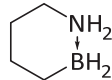
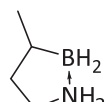
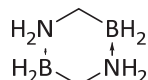
<sup>a</sup> 1 °C/min ; <sup>b</sup> 5 °C/min ; <sup>c</sup> determined by DSC ; <sup>d</sup> not reported

This enhanced rate could be attributed to a lower crystallinity of 1,2-TMAB which allowed an easier diffusion of the molecules. Moreover it appeared that increasing the functionalization degree of the molecule tended to increase the temperature range of dehydrogenation.

### III.2.b.C-BH-NH: amine-boranes inserted in cyclic organic scaffolds

BN-cycloalkanes have been extensively studied by Liu and co-workers.<sup>4c,23b,24a,38</sup> Comparative experimental data were reported in the table below (Table 6) in order to highlight the influence of the different cyclic backbones.

**Table 6. Thermal dihydrogen release of BN-cycloalkane. Experimental characteristics.**

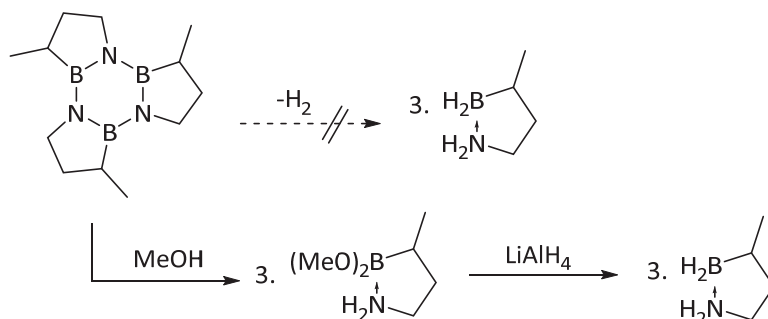
Molecules Name (ref.)	H <sub>2</sub> availability [wt.%]	yield [%]	Temperature of H <sub>2</sub> release [°C]	Catalyst	Experimental rates
 1,2-BN cyclohexane (ref. <sup>24a</sup> )	4.7	> 99 %	150 <sup>a</sup>	-	2 equiv. H <sub>2</sub> in 2 h at 150 °C
 1,2-BN methyl- cyclopentane (ref. <sup>23b</sup> )	4.7	> 99 %	80 <sup>a</sup>	FeCl <sub>2</sub> , FeCl <sub>3</sub> , CoCl <sub>2</sub> , NiCl <sub>2</sub> , CuCl <sub>2</sub>	2 equiv. H <sub>2</sub> in 20 min at 80 °C with FeCl <sub>2</sub>
 Bis-BN cyclohexane (ref. <sup>4c</sup> )	9.4	< 50 %	150 <sup>a</sup>  85 <sup>a</sup>	Pd/c.  [Ru] cat	1 equiv. H <sub>2</sub> in 1 h at 85 °C with Pd/c

<sup>a</sup> Isotherm.

By designing BN-cycloalkanes, Liu and co-workers aimed at developing stable and readily usable materials for transport applications. One compound of particular interest was the 1,2-BN-methylcyclopentane which was a liquid under standard conditions and consequently has been identified as a potential candidate for usage in our current distribution channels. The cyclic alkane scaffold have brought a substantial stability to the amine-borane molecule toward dihydrogen release. The major part of these cyclic C-BH-NH required a metal catalysis to trigger the decomposition. In addition, the cyclic scaffold of BN-cycloalkane permitted to obtain well-defined dehydrogenated trimers or tetramers (see example on Scheme 9). However, none of these species were regenerated with



dihydrogen so far, due to their strong stability. However, treating 1,2-BN-methylcyclopentane spent fuel with methanol led to the recovery of a boronate function which, treated by  $\text{LiAlH}_4$  has yielded to the “loaded” starting material (Scheme 9).



*Scheme 9. Re-synthesis of 1,2-BN-methylcyclopentane from the spent fuel.*

To modify AB dehydrogenation parameters, other possibilities have been reported in the literature. Among the direct modification of amine-borane substituents, the use of AB embedded on 3D material templates was investigated in the past decades. In this section, we reviewed different materials which have been impregnated with AB and we attempted to highlight advantages and limitations of their hydrogen release properties.

#### IV. Amine-borane embedded in an external matrix: modification of the dehydrogenation profile

The use of nano-porous templates allowed a facilitated dehydrogenation of ammonia-borane while keeping a reasonable dihydrogen gravimetric capacity (Table 7). Among the most efficient materials in terms of dehydrogenation activation, the mesoporous silica MCM41<sup>67</sup> and the  $[\text{Y}^{3+}][1,3,5\text{-benzenetricarboxylate}]$  metal-organic framework (JUC-32-Y)<sup>68</sup> scaffolds have showed the best results by decreasing the temperature of infinite stability ( $T_{\text{max}}$  stability) of AB down to 50 °C. This was 35 °C lower than that of neat AB. Also, the dehydrogenation peak occurred 20 °C and 34 °C earlier for AB/silica and AB/MOF respectively.

*Table 7. Ammonia-borane embedded on nanoporous scaffolds. Hydrogen release characteristics.<sup>a</sup>*

Amine-borane	Scaffold	Grav. Cap. H <sub>2</sub> [wt%]	T <sub>max</sub> [°C] stability	T <sub>p</sub> [°C] peak H <sub>2</sub>	Enthalpy [kcal/mol]	Ref.
NH <sub>3</sub> -BH <sub>3</sub>	None	19.6	85	118	-5.1	11
	Mesoporous silica	9.8	50	98	-0.2	67
	Metal-organic framework	8.8	50	84	n.r	68
	Carbon cryogel	14.9	< 80	109	-27.8	69
	Nanocrystalline boron-nitride	9.8	< 90	100 <sup>b</sup>	-3.9	70
	Mesoporous graphitic carbon-nitride	9.2	75	94	n.r	71
MeNH <sub>2</sub> -BH <sub>3</sub>	None	9.8	< 100	141	-3.5	72
	PMA	5.55	< 90	121	n.r	

Temperature rate 5°C/min

<sup>a</sup> Variation in desorption temperatures can be observed depending on the setup experiment. Please refer to the specific experimental conditions.<sup>b</sup> 1°C/min

Moreover the formation of undesired gas such as borazine was also significantly suppressed. In case of AB/silica, the authors demonstrated by DSC studies that the presence of the silica scaffold eliminated the AB melting. They supposed that the dihydrogen bonding network was disrupted by the silica surface, leading to an activation of the AB. However the chemical involvement of the silica surface has not been excluded. In case of AB/MOF, a catalytic effect of the metal sites as well as a nanoconfinement effect was reported to be the best explanation. Incorporating AB on carbon cryogel enabled a boost in gravimetric capacity<sup>69</sup> with respect to other materials. The high exothermicity of the decomposition process was due to the formation of undesired -O-B containing products at the surface.

Nanocrystalline boron-nitride (nano-BN) materials were able to decrease the dehydrogenation temperature of AB as well.<sup>70</sup> The material was obtained by ball milling with AB. The nano-BN surface was expected to disrupt the DHB network explaining the slight decrease of dehydrogenation temperatures. However, higher amounts of borazine were generated. Authors reported that the nano-BN surface probably facilitated the cyclisation pathway leading to borazines. Last but not least, mesoporous graphitic carbon-nitride (MGCN) were loaded with AB by impregnation.<sup>71</sup> As predicted by DFT calculations, the material was expected to display strong interactions between the basic nitrogen site of MGCN and protonic hydrogens of AB leading not only to a disruption of DHB, but also to an enhanced polarization of AB. The material released up to 86 % of its hydrogen content at ~94 °C.

Embedding of MeAB has been also investigated by elaboration of a poly(methyl acrylate) and MeAB composite (PMA/MeAB).<sup>72</sup> Not only does the material showed enhanced dehydrogenation properties, but it also permitted to get rid of MeAB gas phase pollution due to a sublimation of the latter during the decomposition process. Still, a chemical reaction of the surface has been observed through identification of B-O bond formed during the decomposition process.

Embedding AB and derivatives on nanoporous scaffolds have significantly improved hydrogen release properties of amine-boranes. Long range disruption of the DHB network appeared to have an important effect on AB stability as it decreased significantly dehydrogenation temperatures. Interactions with the surface functions leading to covalently associated products were likely to affect the mechanism by modifying intermediates and products. However, to the best of our knowledge, no investigation on this matter have been reported so far.

---

## V. Conclusion

---

AB and several derivatives have been reported in the literature as promising candidates for solid or liquid hydrogen reservoirs. Even if mechanisms of dehydrogenation are not

yet fully understood, the effect of DHB appeared to be crucial. The effect of amine-borane environment (solvent, N and B substituents and external matrix) has been particularly interesting because it has provided key information for understanding the following works.

During our researches on polymers containing boron Lewis-pairs, we have been interested in the chemistry of amine-borane for hydrogen release. We first designed polymer having amine-borane moieties in the main-chain. We foresaw the influence of the macromolecular structure on the thermal dehydrogenation in the solid state. For this reason, our aim was focused in understanding the interplay between molecular and macromolecular effects, employing both experimental and theoretical approach. The matter has been as discussed in the following **Section 2**

.

## **Section 2**

**Polyboramines: main-chain amine-borane  
polymers as hydrogen reservoirs.**

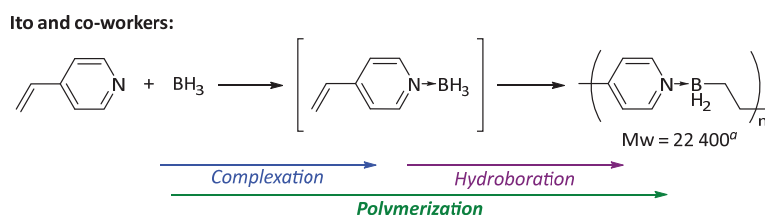
## I. Introduction

We designed polymers displaying  $\text{NH}_2\text{-BH}_2$  type amine-boranes in the main-chain that we called "polyboramines". Only scattered examples have been reported in the literature about polymers having boron-nitrogen Lewis-pairs in their network. This was probably due to their intrinsic lack of solubility/stability in common solvents. The first chapter of this section have overviewed polymers containing amine-borane bonds in the main-chain reported in the literature with a particular emphasis on the different ways of polymerization and the dynamic behavior of these compounds.

## II. Literature precedents: polymers containing amine-boranes bonds in the main-chain

### II.1. Amine-boranes in the main-chain of organic polymers

The first preparation of polymers containing amine-boranes in the main-chain has been reported by Ito and co-workers in 1994.<sup>73</sup> Polymers were prepared from bifunctional monomers by a two-step polyaddition method, e.g. amine-borane complexation and subsequent hydroboration (Scheme 10). The selectivity of the reaction was particularly substrate-dependent.

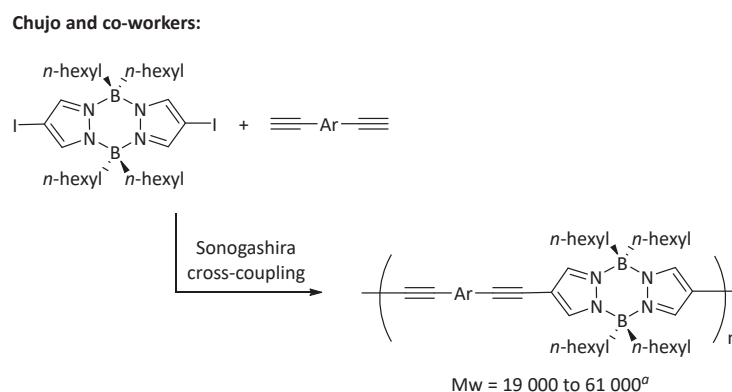


**Scheme 10.** Two-steps polymerization pathway by formation of the amine-borane adduct in situ and subsequent hydroboration<sup>73</sup>, (a) GPC (THF).

Actually, the para-vinylpyridine was reported to be the only type of vinylamine able to yield polymers. Primary and secondary amines underwent dehydrogenation. Moreover,

tertiary aliphatic amines provided too stable borane adducts that were unreactive for hydroboration.

Later, Chujo and co-workers<sup>74</sup> have reported the synthesis of a pyrazabole polymers. The polymerization was driven by Sonogashira cross-couplings between a diyne monomer and a previously synthesized pyrazabole difunctional monomer (Scheme 11). This polymerization method displayed a good tolerance to chemical groups and permitted to synthesize several derivatives in relatively high yields. However, the authors mentioned that the yield of Sonogashira reaction depended importantly of the purity of the starting monomers.

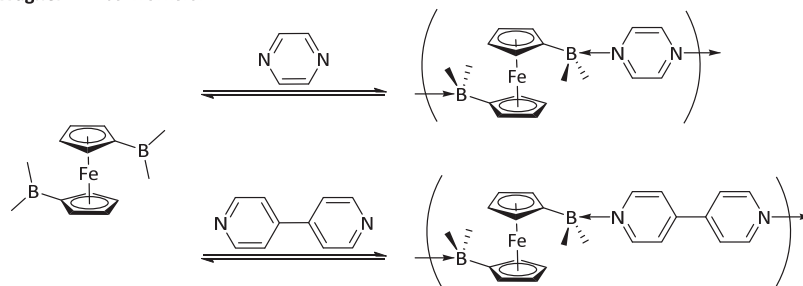


**Scheme 11.** Synthesis of N-B coordinated polymers by double Sonogashira cross-coupling on the previously synthesized adduct. (a) GPC (THF), PS standart.

In 1999, Wagner and co-workers reported the synthesis of a reversibly assembled amine-borane polymer by mixing ditopic ferrocenylborane and 4,4'-bipyridine<sup>75</sup> or pyrazine<sup>76</sup> (Scheme 12). The strong dark color of these polymers observed in the solid-state is the result of a charge-transfer process. The characterization of the resulting polymer has turned out to be problematical due to their instability in solution. In fact, their dissolution in polar solvents such as CH<sub>2</sub>Cl<sub>2</sub> or DMF led to a partial or full dissociation of the network. The authors observed also that stability in solution was dependent both on concentration and temperature. Stable materials were recovered in the solid state in which they possess a high thermal stability. DSC and TGA analyses confirmed the stability of these materials up to 140 °C and 245 °C, respectively for the pyrazine and the 4,4'-bipyridine based polymer.



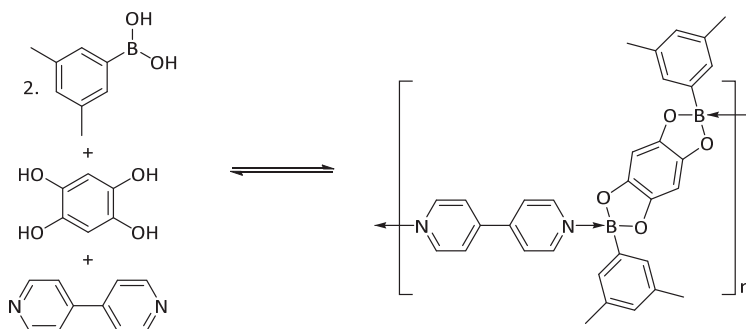
Wagner and co-workers:



Scheme 12. Reversible assembly of polymers by amine-borane formation

Targeting the design of new dynamic molecular networks, Severin and co-workers<sup>77</sup> published a method of three-component self-assembly. It consisted in generating *in situ* a bisboronic monomer by esterification of a boronic acids and concomitantly forming the dative boron-nitrogen bond upon reaction with 4,4'-bipyridine. This method led to polymers containing boron-nitrogen dative bonds in the main-chain. The bisboronic section was formed by condensation from 1,2,4,5-tetrahydroxybenzene and arylboronic acids. The resulting polymer was recovered by precipitation as a deep purple material, similarly to the ferrocene-based coordination polymer described above, as a result of a charge-transfer transition phenomenon. As the boronate is known to stabilize the boron atom in its trigonal form, molecular networks were very weakly associated according to the long B-N bond measured from X-ray crystal structures.

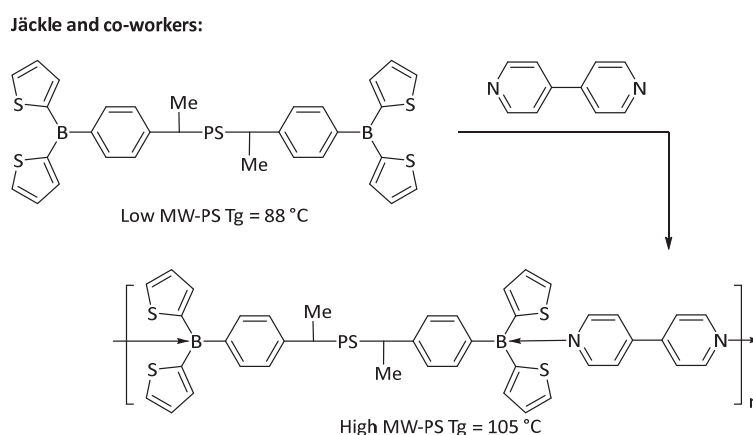
Severin and co-workers:



Scheme 13. Example of polymer containing B-N dative bonds in the main chain as well as B-O bonds and synthesized by a three component reaction.

Indeed, when put in solution, the polymer completely dissociates, changing the color from dark purple to yellow. The versatility of this approach opened the access to a large panel of linear and 2D networks.<sup>78</sup>

Supramolecular interactions can also be useful tools to modify the properties of more classical structures such as polystyrenes. In this manner, Jäkle and co-workers<sup>79</sup> reported the preparation of borane-end functionalized telechelic polystyrenes. The size of polymer chains has been increased by introducing a 4,4'-bipyridine linker. The formation of amine-borane bonding between low molecular weight polymer chains, gave high molecular weight polymers as evidenced by the increase of glass transition temperatures (Scheme 14).



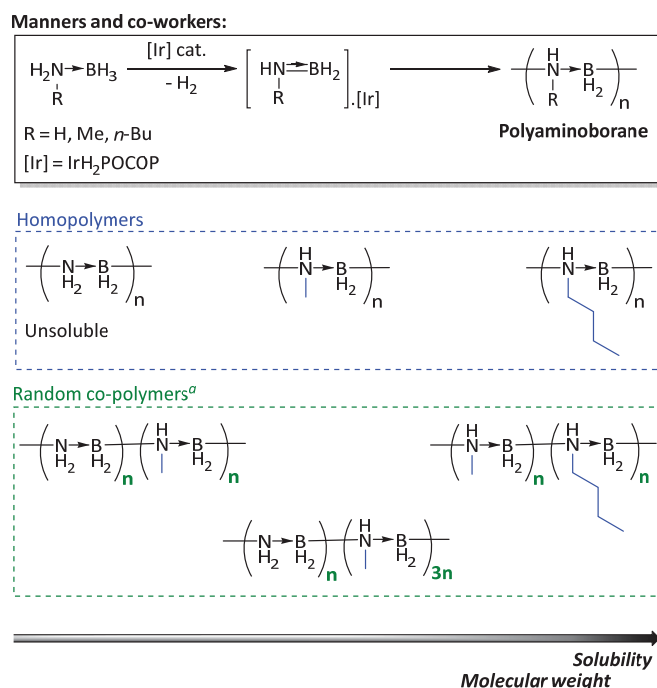
**Scheme 14.** Enhancement of the molecular weight of polystyrenes through amine-borane bond assembly of Bisborane-ditelechelic polystyrenes with 4,4'-bipyridines.

In fact, DSC studies revealed a shift in glass transition temperature from 88 °C for the starting material, to 105 °C for the bipyridine associated polymer. The authors reported that these temperatures roughly corresponded to a change from a low to a high molecular weight polystyrene.

## II.2. Polyaminoboranes: boron-nitrogen isosters of polyolefins and key-intermediates in hydrogen release from amine-borane materials.

In 2008, Manners and co-workers found a method affording high molecular weight boron-nitrogen macromolecules of formula  $-[(R)NH-BH_2]_n-$ , isosters of polyolefins and commonly called polyaminoboranes.<sup>63,80</sup> The polymerization was realized by Iridium-catalysed dehydrocoupling of AB or N-alkyl amine-boranes analogues, using the Brookhart's Ir(III)

pincer complex IrH<sub>2</sub>POCOP as a precursor. The proposed mechanism<sup>81</sup> suggested that Iridium catalyst triggered the release of one equivalent of dihydrogen generating the aminoborane monomer as an intermediate and subsequently promoted the insertion of this "monomer" into the polymer chain (Scheme 15). This mechanism was also in agreement with recently published mechanistic investigations.<sup>62a</sup>



**Scheme 15. Synthesis of polyaminoboranes from amine-boranes by Iridium catalysis.**

Engaging AB to make the polyaminoborane  $-\text{[NH}_2\text{-BH}_2\text{]}_n-$ , isoster of polyethylene, was unsuccessful because of the rapid precipitation of the formed oligomers. However, it has been possible to build high molecular weight polyaminoborane analogues of formula  $-\text{[(alkyl)NH-BH}_2\text{]}_n-$  from methylamine-borane and *n*-butylamine-borane starting materials. The insertion of an alkyl substituent allowed to increase the solubility of the macromolecules. Random copolymers were also prepared from mixtures of two amine-boranes being either N-alkyl amine-boranes or AB. Besides, a clear relationship between the relative amount of N-alkyl "solubilizer" and the averaged sized of polyaminoboranes could be established (Scheme 15). This study highlighted solubility issues encountered by polymers containing NH<sub>2</sub>-BH<sub>2</sub> amine-borane functions, probably due to DHB interactions between chains. Thus, it have demonstrated the importance of substituents on the material properties.

### III. This work: polyboramines for hydrogen release - Effects of the polymer scaffold

During our studies of boron Lewis-pairs containing polymers,<sup>82</sup> we have been interested in designing macromolecules containing amine-borane functions, analogues of AB, in the main-chain (Figure 16). We have been interested in studying their behavior as hydrogen reservoirs, particularly regarding the influence of the polymer backbone on the reactivity.

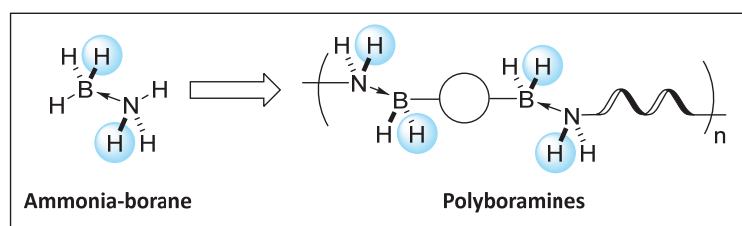
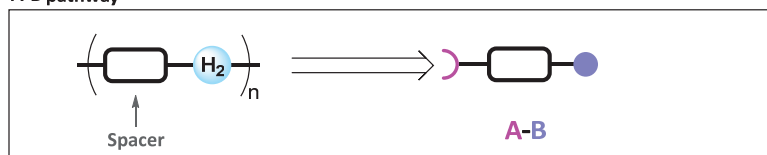
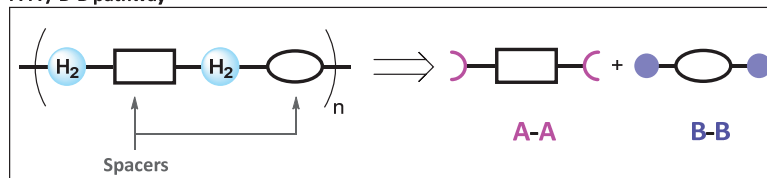


Figure 16. Concept of Polyboramines. Integration of AB into a polymer backbone.

The development of a methodology providing the direct formation of macromolecular structures has been the first key-step of this work. It has been discussed in chapter III.2. of this section. After an introduction of polyboramines (chapter III.4), their reactivity in hydrogen transfer reaction on carbonyls has been presented (chapter III.5) as well as their behavior in thermal hydrogen release (chapter III.6). Comparative studies have been realized with the aim of determining the effect of both substituents and macromolecular scaffold. Finally, computational and mechanistic investigations emphasized some key parameters involved in hydrogen release processes (chapter III.7).

#### III.1. Structural and synthetic requirements

To access polyboramines, we first selected an A-A / B-B type polycondensation strategy (Figure 17). Even though this method requires a strict stoichiometry to afford high molecular weight polymers, the synthesis of bifunctional diamines and bisboron monomers appeared to be more accessible in order to validate the proof of concept. It also offered a greater structural variability.

Two approaches of polycondensation :**A-B pathway****A-A / B-B pathway**

**Figure 17. Structural and synthetic design of polyboramines. A-A / B-B type polycondensation. Trade-off between rigidity and amine-borane strength.**

The nature of the spacers was expected to have an influence on the solubility and the rigidity of resulting polymers. We thus, chose aliphatic primary diamines based on electronic considerations and widespread availability. As good Lewis-bases, they featured reasonably strong amine–borane bonds. Bisboron species were chosen either with an aryl or with saturated or unsaturated alkyl spacers. In particular, the study of chemical and physical properties of polyboramines was performed mainly using the aryl-bisboron block (Figure 18). We expected that the aryl moieties to provide stability and desired material properties such as a reasonably high glass transition temperature.

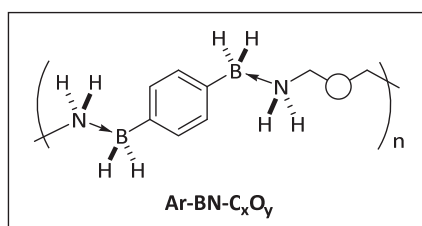


**Figure 18. Selected polymer for reactivity studies. Cycle = alkyl or ether chain**

The polymerization was induced by the formation of the  $\text{BH}_2\text{-NH}_2$  amine-borane bond. Consequently, we needed to set up a reaction providing directly the amine-borane bond in quantitative yield and selectively, in order to generate macromolecular assemblies. Moreover, the range of possible temperature conditions was rather limited. At low temperature the polymer was likely to exhibit solubility limitations while at “high” temperature the latter may initiate dehydrogenation. Last but not least, the control of the stoichiometry was crucial to reach high molecular weights. To those ends, we first studied

the reaction on monofunctional molecules before implementing it for the synthesis of macromolecules.

### III.2. Development of a methodology for the straightforward access to $\text{NH}_2\text{-BH}_2$ amine-boranes

The development of the coupling method has been first optimized at the molecular level using molecular model **1a**, as well as representative molecular brick **1b** (Figure 19). **1b** was designed to possess an aryl-bisborane core linked to monoamines similarly to polyboramines.

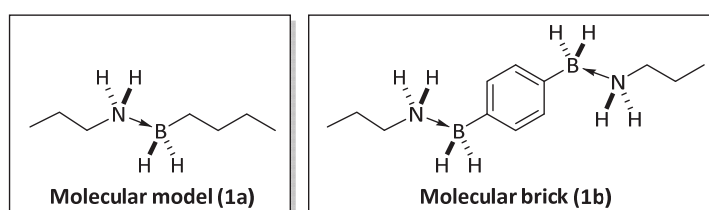
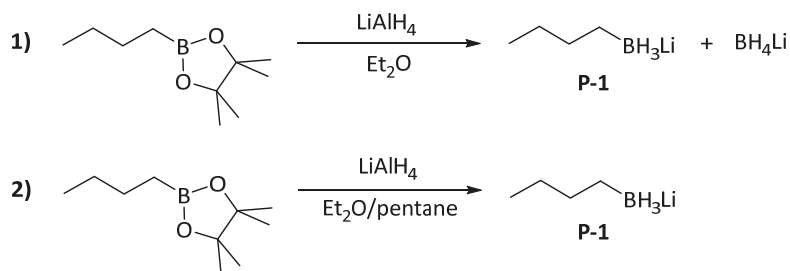
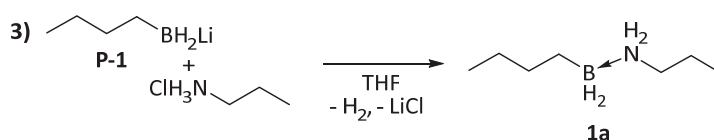


Figure 19. Chosen molecular model (1a) and molecular brick (1b) for developing the conditions of amine-borane bond formation / polymerization

The  $^{11}\text{B}$  NMR signal of B-aryl substituted amine-boranes such as **1b** often appeared to be broadened. The determination of  $J$  couplings required advanced NMR setup (higher fields, tuning of the sequence parameters). Whereas, B-alkyl substituted amine-boranes such as **1a** exhibited well-defined triplets. Thus, the two molecules have been complementary to optimize the reaction of polymerization.

#### III.2.a. The two-step strategy

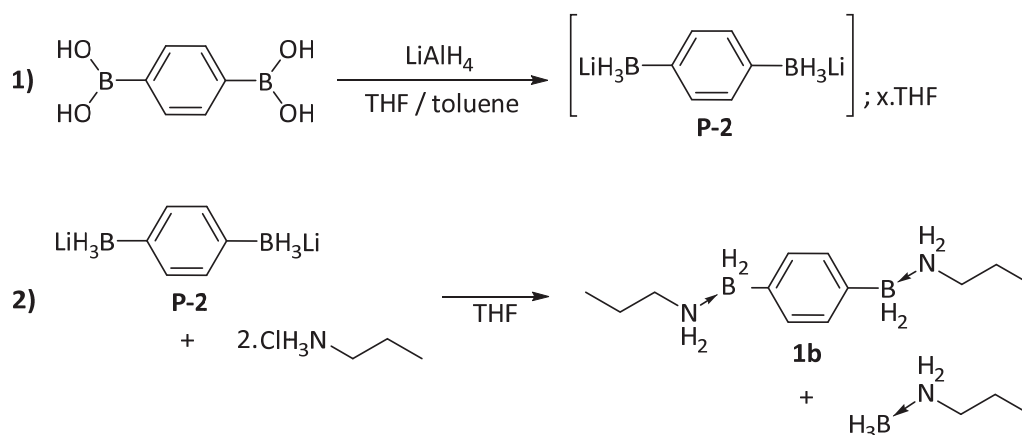
We started by investigating the reaction of salt metathesis /  $\text{H}_2$  release which was known to deliver quantitatively and selectively the desired amine-borane under mild conditions. This reaction required the preliminary preparation of the trihydridoborate compound that was synthesized from the boronic acid or ester precursor, using  $\text{LiAlH}_4$ , as reported in the literature.<sup>33d</sup> (Scheme 16, eq. 1 and 2). For this step to be efficient, the use of a precise solvent mixture was important. A polar aprotic solvent such as  $\text{Et}_2\text{O}$  or THF was necessary but not sufficient because it also favors side-reactions such as deborylation (Scheme 16, eq. 1).

**Step one: reduction of boronate****Step two: salt metathesis / H<sub>2</sub> release**

*Scheme 16. Two steps reaction pathway: synthesis of the trihydridoborate precursor and subsequent salt metathesis and H<sub>2</sub> release reaction with an ammonium chloride.*

The addition of pentane in the solvent mixture afforded the selective formation of the desired butyl-trihydridoborate precursor **P-1** in 99% yield after simple filtration of insoluble aluminum salts (Scheme 16, eq. 2). Once isolated, lithium trihydridoborates strongly coordinated to ethers. Additional <sup>1</sup>H NMR quantification was required to determine the exact amount of Et<sub>2</sub>O per trihydridoborate molecule (Scheme 16, eq. 3).

The second step was the reaction of salt metathesis / H<sub>2</sub> release, involving **P-1** and *n*-propyl ammonium chloride at room temperature in THF. The emission of H<sub>2</sub> gas was visible. Meanwhile the initially insoluble ammonium starting material disappeared gradually. This reaction has been optimized to access molecular brick **1b** (Scheme 17). The first step led to precursor **P-2**, which formed strongly associated coordination polymers with THF (Scheme 17, eq.1). Our first attempts to remove THF by high-vacuum during several days led to a completely insoluble and unreactive colorless material due to the formation of a strongly associated network which has been already mentioned by Wagner and co-workers.<sup>34</sup> Consequently, we decided to keep the product in its THF-solvated form. Engaging **P-2** in the second step afforded **1b** as well as 33 % of deborylated by-product (Scheme 17, eq. 2 and Figure 20). The variation of the reaction parameters such as temperature, dilution, solvents, did not increase the selectivity.



Scheme 17. Two steps synthesis of molecular brick **1b**. Formation of by-products.

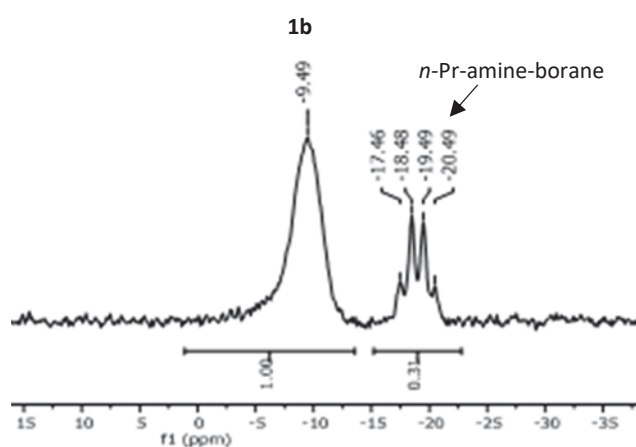


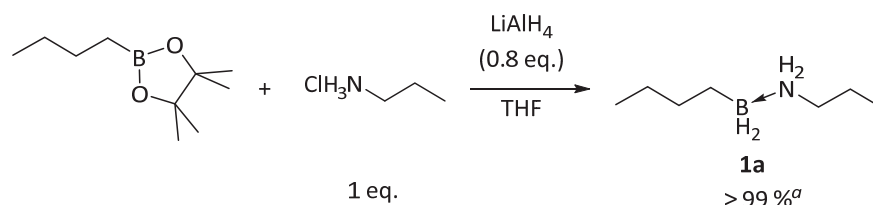
Figure 20.  $^{11}\text{B}$  NMR spectrum in THF of the synthesis of **1b** from **P-2** and **SM-1**

### III.2.b. One-pot reaction allowing the straightforward access to amine-boranes

As discussed in the bibliographical section, Hawthorne and co-workers<sup>33c</sup> and more recently Ramachandran and co-workers<sup>40</sup> reported the formation of amine-borane structures in one step. Although the reported procedures did not provide quantitative yields and were limited to easily purifyable amine-boranes (distillation or sublimation), the straightforward one-pot access to amine-borane moieties was very promising for polymer synthesis purposes. We developed a general one-pot method to prepare our amine-boranes, from boronic acids or pinacol boronates. It used stoichiometric amounts of starting materials and 1.1 equivalent of  $\text{LiAlH}_4$ . The reaction delivered **1a** and **1b** selectively and in quantitative yields, as indicated by  $^{11}\text{B}$  NMR. For the synthesis of **1a**,  $^{11}\text{B}$  NMR monitoring displayed the apparition of a triplet at -10.8 ppm corresponding to the



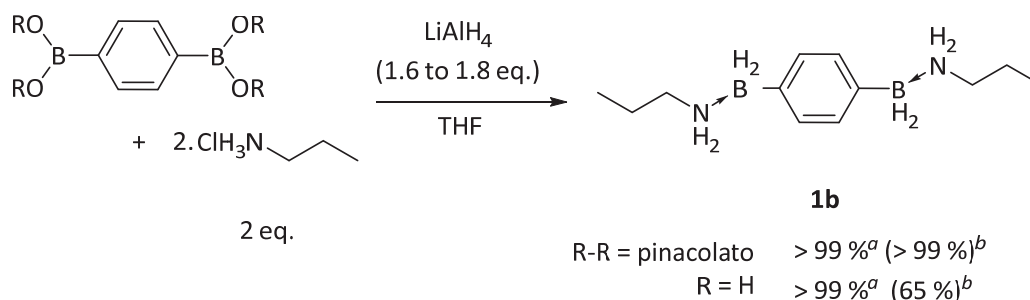
product, as well as the complete disappearance of pinacol *n*-butylboronate starting material signal (singlet at 31 ppm).



*Scheme 18. One-pot methodology for the synthesis of molecular model 1a. (a) <sup>11</sup>B NMR yield.*

Bis(amine-borane) **1b** has been synthesized from two different boron starting materials (Scheme 19). From pinacol *p*-phenylenebisboronate, the product was easily recovered after filtration from insoluble salts. It however it still contained important amounts of pinacol aluminum soluble impurities. Purifications by selective precipitation were unsuccessful.

In contrast, the synthesis of **1b** from *p*-phenylenebisboronic acid provided directly a pure compound, due to the insolubility of aluminum-oxide products. Although the NMR yield was quantitative, the isolated yield was only moderate (65 %) because part of the product remained trapped in the filter cake. **1b** has been isolated as a white crystalline solid (see Figure 22, below). Traces of THF were still present in the solid even after high vacuum treatment (10<sup>-5</sup> mbar).



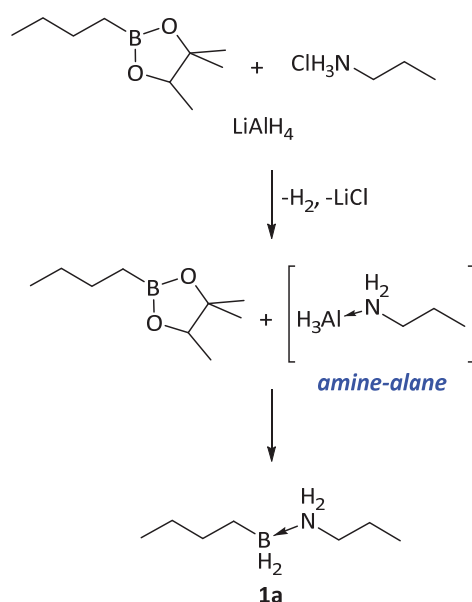
*Scheme 19. One-pot methodology for the synthesis of molecular brick 1b (a) <sup>11</sup>B NMR yield. (b) Isolated yield*

There are two key-points to address for the success of this methodology: 1) the amount of LiAlH<sub>4</sub> is very close to the stoichiometric ratio (1.07 eq.), because we found that excess

of  $\text{LiAlH}_4$  generated Lithium trihydridoborate by-product (**P-2**). 2)  $\text{LiAlH}_4$  had to be added into a mixture of ammonium hydrochloride and boronate starting materials.

Swapping the order of addition by first mixing  $\text{LiAlH}_4$  and the ammonium led to a mixture of unidentified products. It has been reported that the reaction of  $\text{LiAlH}_4$  with an ammonium formed an amine-alane that rapidly loose  $\text{H}_2$  to produce aluminum-nitrogen species.<sup>83</sup> Moreover, the one-pot reaction time leading to the amine-borane was faster (2 min – 1 h) than the formation of the trihydridoborate (2 – 6 h). This observation suggested that the latter was not likely to be an intermediate in the mechanism of the one-pot formation of amine-borane.

To account for the formation of the product, we surmised an initial acid-base reaction between the ammonium hydrochloride and the tetrahydroaluminum, generating the amine-alane intermediate *in situ* (Scheme 20) which leads to the amine-borane by subsequent oxygen/hydrogen exchange. Experimental and computational investigations are ongoing in our lab.



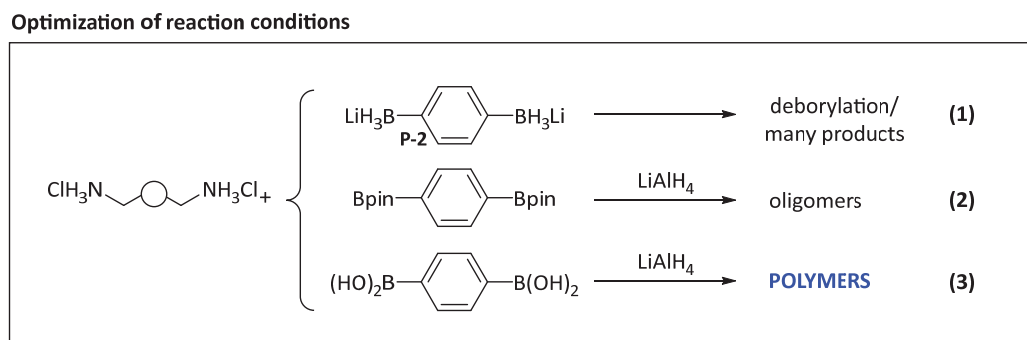
**Scheme 20.** Postulated mechanism on the one-pot synthesis of amine-borane. Amine-alane is likely to be a key-intermediate

The setup of a highly efficient three-component one-pot reaction led to the straightforward access to pure amine-boranes and permitted to synthesize polyboramines.

### III.3. Application of the procedure to the polymerization

We screened the different methods selected with the molecular model **1a** and the molecular brick **1b** to synthesize polyboramines (Scheme 21). First we tried the two-step method by generating the bisborohydride **P-2** in a separate flask from the boronic acid. The former was subsequently added to the diammonium salt. This procedure led to various side-reactions along with significant deborylation (Scheme 21, eq 1). When using the one-pot procedure, the deborylation was completely avoided, but bisboronic pinacol ester gave only short chain oligomers (Scheme 21, eq. 2)

We successfully accessed polymers by applying the one-pot methodology with the *p*-phenylene-bisboronic acid and diammonium chlorides (Scheme 21, eq. 3).



*Scheme 21. Determination of the best procedure for the synthesis of polyboramine*

The polymer fraction soluble in THF was recovered by filtration followed by several washing of the filter cake. However, part of the product remained trapped in the aluminum oxide filter cake, thus decreasing the yield of the isolated material. TGA calcinations were realized in a temperature range of 30 – 900 °C in order to quantify the amount of LiCl and alumina residual salts ( $T_{\text{eb}}(\text{LiCl}) = 1382\text{ °C}$ ,  $T_{\text{eb}}(\text{Al}_2\text{O}_3) = 2\,977\text{ °C}$ ). They indicated that the vast majority of the lithium chloride and aluminum salts remained in

the insoluble fraction with less than 4 wt.% residue in the isolated polymer (Figure 21). In contrast, when pinacol *p*-phenylene bisboronate was used as a precursor, about 30 wt.% of residual salts were detected in the polymer (Figure 22).

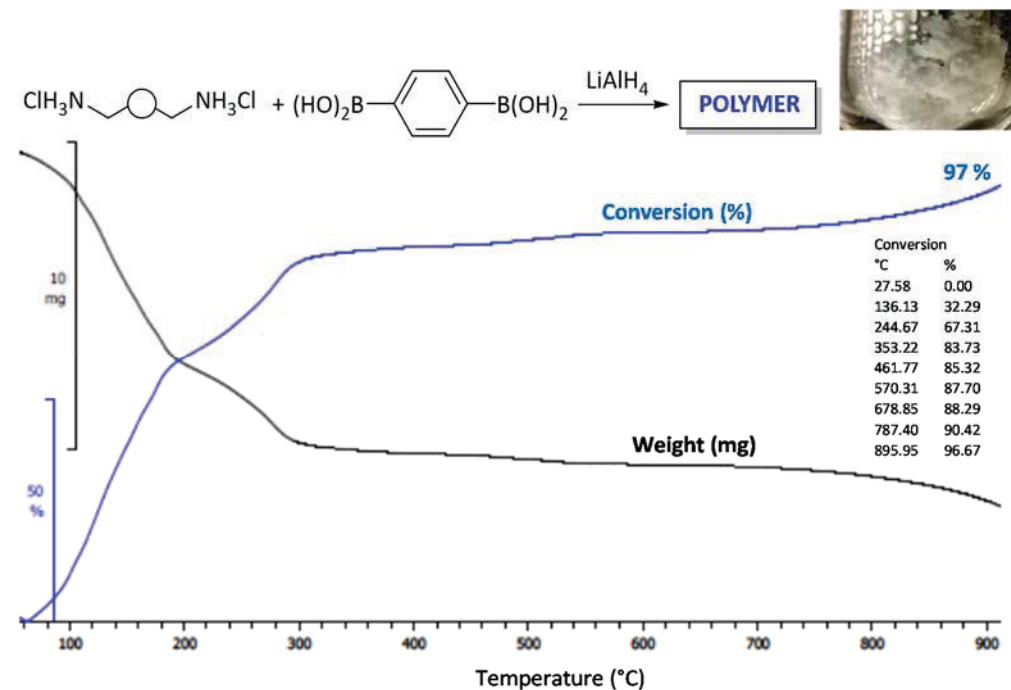


Figure 21. Gravimetric determination of residual salts present in Ar-BN-C4O polymer synthesized from boronic acid precursor.

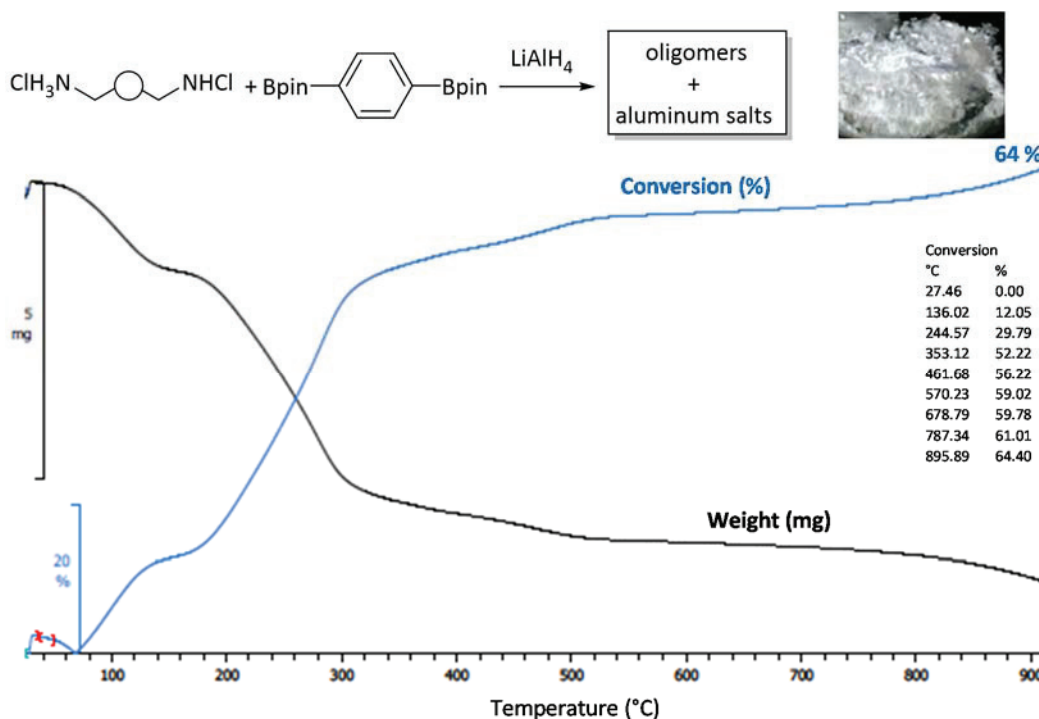


Figure 22. Gravimetric determination of residual salts present in oligomers of Ar-BN-C4O synthesized from pinacol boronate precursor.

The polymer was isolated as a white powder after evaporation of volatiles (see picture on Figure 21). However, as observed on **1b**, even after two days under high vacuum ( $10^{-5}$  mbar), the material still retained some THF. By precipitating the polymer in pentane, the major part of THF could be removed.

We synthesized six polyboramines using the selected method. Several primary diamines were screened by changing the aliphatic spacer. We varied the chain length and / or the nature (alkane or ether) (Figure 23). Aliphatic diammonium chloride precursors were commercially available or were easily prepared from commercially available diamines (**SM-2** to **SM-5**) by treatment with anhydrous hydrogen chloride in THF to yield white solids (Figure 23, eq. 1). A careful wash until neutral pH was crucial for the polymerization step.

Polymers **Ar-BN-C2**, **Ar-BN-C4** and **Ar-BN-C8** displaying respectively an ethylene, diethylene and tetraethylene spacer between the two nitrogen, were isolated as white solids. **Ar-BN-C4** and **Ar-BN-C8** were synthesized selectively but in moderate yields (65 % and 48 % respectively) due to partial retention of the product in the filter cake. Whereas **Ar-BN-C2** displaying a significantly lower solubility in THF was isolated in only 31 % yield. In addition, after thorough removal of the solvent **Ar-BN-C2** and **Ar-BN-C4** polymers became poorly soluble in THF upon re-solubilization. We attributed this behavior to the establishment of DHB interactions in the solid state.

The addition of extra oxygens in the aliphatic chains of **Ar-BN-C4O** and **Ar-BN-C8O2** significantly enhanced the solubility of polymers in THF which turned out to be perfectly reversible. However, they were synthesized in moderate yield (52 % and 48 % respectively) due to partial retention of the product in the filter cake. The absence of residual salts was confirmed by TGA calcination.

These polyboramines generally called **Ar-BN-C<sub>x</sub>O<sub>y</sub>** displayed H<sub>2</sub> capacity between 3.2 and 4.9 wt.% which appeared to be modest compared to AB (19.6 wt.%), but still very promising according to the 2017 objective of the US DOE department (5.5 wt.%). This study aimed at demonstrating the influence of a polymer scaffold on physical and

chemical properties, in order to control kinetics and thermodynamics of amine-borane dehydrogenation for possibly reloading it with dihydrogen. For that, the hydrogen gravimetric capacity parameter was not crucial in this study but still has to be improved.

#### Synthesis of Polyboramines

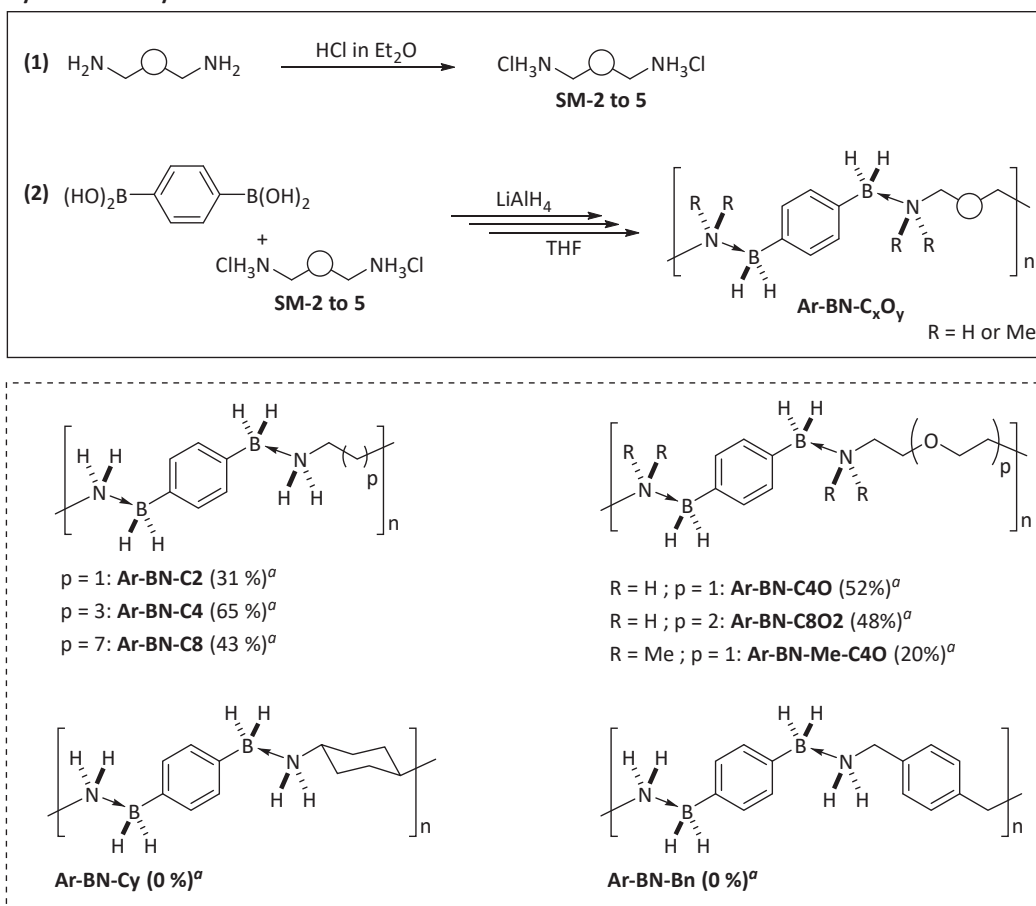


Figure 23. Synthesis of a scope of 6 polyboramines using the straight forward procedure from bisboronic acid monomer.

Starting from a tertiary diammonium salt, polymer **Ar-BN-Me-C4O** was isolated in 20 % yield only. This was likely due to the increased steric hindrance on the nitrogen atom, which lowered the stability of the Lewis-pair and thus of the polymer. SEC analyses (Experimental section 4) suggested that this polymer had very short chains (DPI = 10) albeit a decomposition within SEC is not excluded and one must remain cautious.

Finally we attempted to synthesize other polyboramines by using conformationally more constrained diamine spacers. Unfortunately, during their synthesis, **Ar-BN-Cy** and **Ar-BN-Bn** precipitated massively rendering impossible their isolation from aluminum salts. IR

analyses of the mixture revealed that these polymers decomposed at room temperature in the crude, probably by dihydrogen loss. The synthesis of those two polymers has not been further investigated.

### III.4. Characteristics of polyboramines / oligomers and molecular bricks.

---

The **Ar-BN-C<sub>x</sub>O<sub>y</sub>** family of polyboramines exhibited similar spectroscopic characteristics. In particular the polymer **Ar-BN-C4O** has served as a representative example in this chapter. In addition, polymers have been compared with their oligomer and molecular-brick analogues. For additional spectroscopic data see the experimental section 4.

#### III.4.a. NMR and IR footprints

<sup>11</sup>B NMR spectra of polymers **Ar-BN-C<sub>x</sub>O<sub>y</sub>** showed a large signal at  $\delta = -10$  ppm (Figure 24). The <sup>1</sup>H NMR spectra displayed broadened massifs, typical of polymers. B-H bonds and N-H bonds were visible in <sup>1</sup>H NMR as a broad singlet around  $\delta = 2.36$  ppm and  $\delta = 4.71$  ppm respectively. The two signals were discriminated by addition of D<sub>2</sub>O in the mixture. The N-H chemical shift disappeared by deuterium / proton exchanges while the signal attributed to B-H remained unchanged (Figure 25). IR spectroscopy exhibited a clear band for B-H stretching at  $\nu = 2313$  cm<sup>-1</sup> (Figure 26).

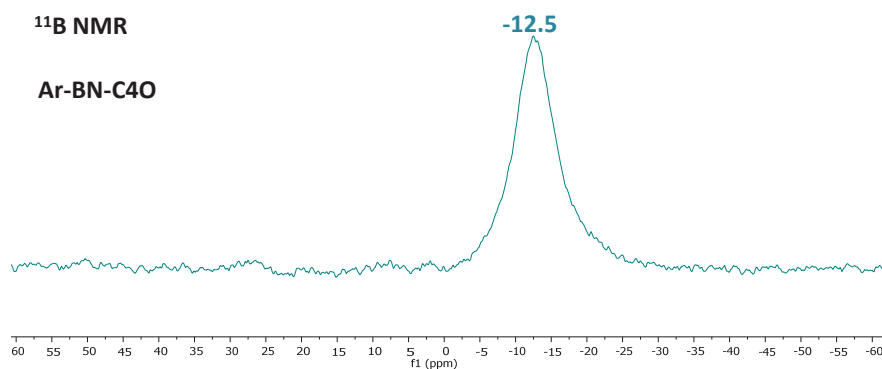


Figure 24. <sup>11</sup>B NMR spectrum of polymer Ar-BN-C4O displaying a broad singlet at -12.5 ppm

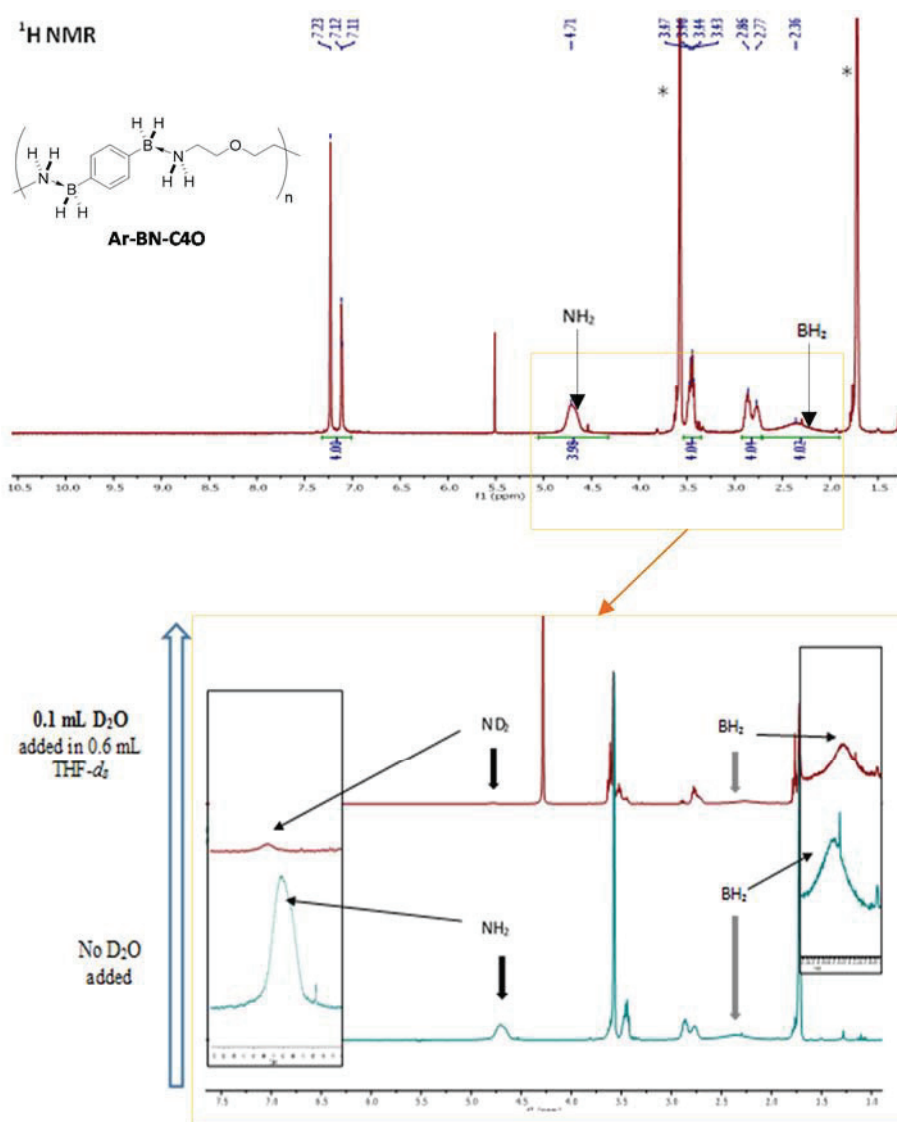


Figure 25. <sup>1</sup>H NMR spectrum of Ar-BN-C4O (up), addition of D<sub>2</sub>O showing protic hydrogens of NH<sub>2</sub> by proton deuterium exchange (down).

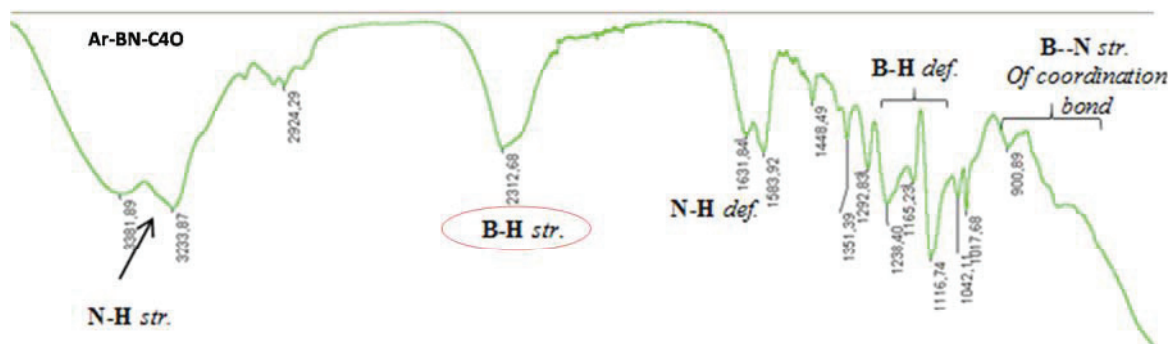


Figure 26. IR-ATR spectrum of Ar-BN-C4O. Well visible B-H stretching at 2312 cm<sup>-1</sup>.



Polymer **Ar-BN-Me-C4O** containing tertiary diamines displayed a downfield chemical shift at -3 ppm (see experimental section 4). This value tended toward the chemical shift of a trigonal boron. It has confirmed the weaker Lewis-pair bonding of the tertiary amine-borane linkage of the main-chain in THF, due to steric hindrance.

### III.4.b. Steric exclusion chromatography (SEC)

As polyboramines tend to establish DHB interactions leading to modest solubility properties in THF, we had to choose specific conditions for SEC characterization. We used a mixture of THF / 1wt.%. TBAB as eluent at a column temperature of 30 °C. TBAB allowed the breaking of DHBs in solution, enabling the total elution of the polymer. Polymer **Ar-BN-C4O** has been analyzed due to its good solubility properties. The molar mass has been estimated as  $> 10^5$  Da (based on polystyrene standard). It corresponded to a polymerization degree of about 1000 units. The polydispersity index was 2.9, consistent with an A-A / B-B pathway of polycondensation.

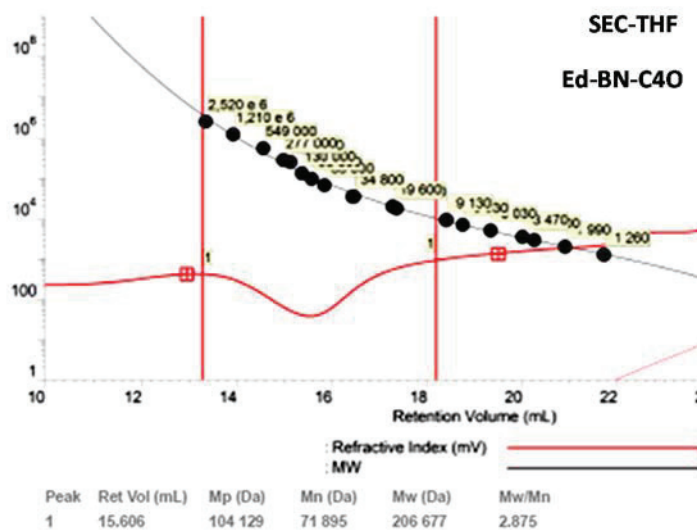


Figure 27. Steric exclusion chromatography of **Ar-BN-C4O** in our conditions. Calibration polystyrene. Reversed polarity.

The synthesis of **Ar-BN-C4O** from pinacol *p*-phenylenebisboronate led only to the formation of oligomers (**Ar-BN-C4O-oligo**). SEC analyses indicated mainly the existence of trimers or tetramers.

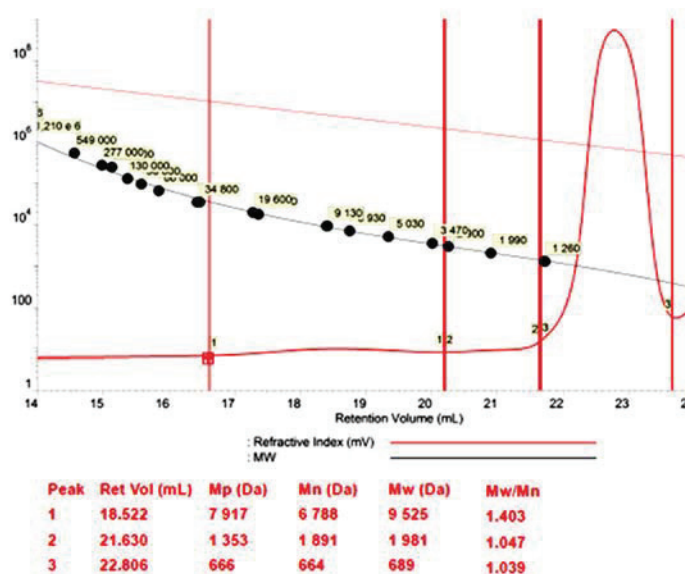


Figure 28. SEC of a polymer synthesized from pinacol *p*-phenylene bisboronate Ar-BN-C4O-oligo. The peak n°3 is in majority and represent tri- tetramers.

As expected, **Ar-BN-Me-C4O** which featured weakly associated tertiary amine-borane bonds due to steric hindrance on the nitrogen exhibited only short chains. (Figure 29). Normal conditions using pure THF as eluent with a temperature column of 40 °C was sufficient to obtain a chromatogram. This behavior correlated with the fact that **Ar-BN-Me-C4O** does not exhibit DHBs.

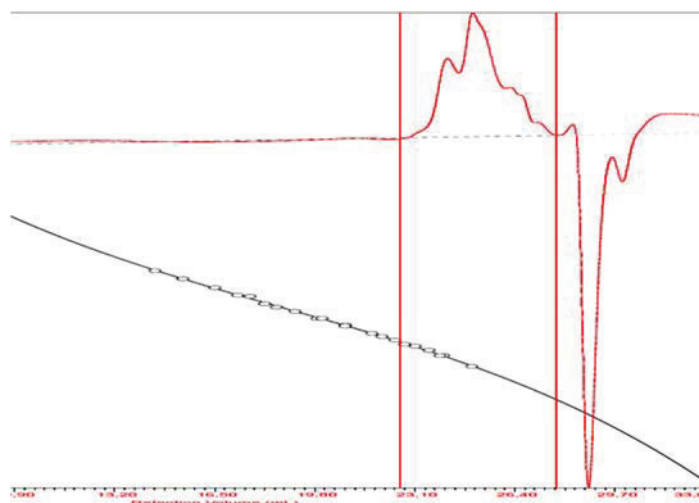


Figure 29. SEC chromatogram of Ar-BN-Me-C4O showing several indiscernible families of oligomers. Polystyrene calibration: Mw = 557 g/mol.

### III.4.c. Glass transitions and fusion temperatures

The glass transition ( $T_g$ ) of polyboramines has been determined on polymers **Ar-BN-C4**, **Ar-BN-C8** and **Ar-BN-C40** to be about 60 °C (see also experimental section 4). The nature of the diamine spacer did not significantly influence the  $T_g$  value itself but the heat capacity ( $\Delta C_{p_{T_g}}$ ) parameter of the transition.<sup>84</sup> In fact, with a temperature range of 5 °C/min, **Ar-BN-C8** (tetraethylene spacer) presented the highest  $\Delta C_{p_{T_g}}$  (0.825 J.g<sup>-1</sup>.K<sup>-1</sup>), while the  $\Delta C_{p_{T_g}}$  of **Ar-BN-C2** was null, meaning there was no detectable  $T_g$  for this polymer. Reported in the literature<sup>84</sup> have shown that the  $\Delta C_{p_{T_g}}$  value was proportional to the amorphous content of the polymer. Based on our results, it appeared that the amorphous content was mainly induced by the aliphatic component even though this affirmation cannot be assumed with certainty as any other phenomenon taking place among 90 °C has been hidden by the decomposition process (Figure 30).

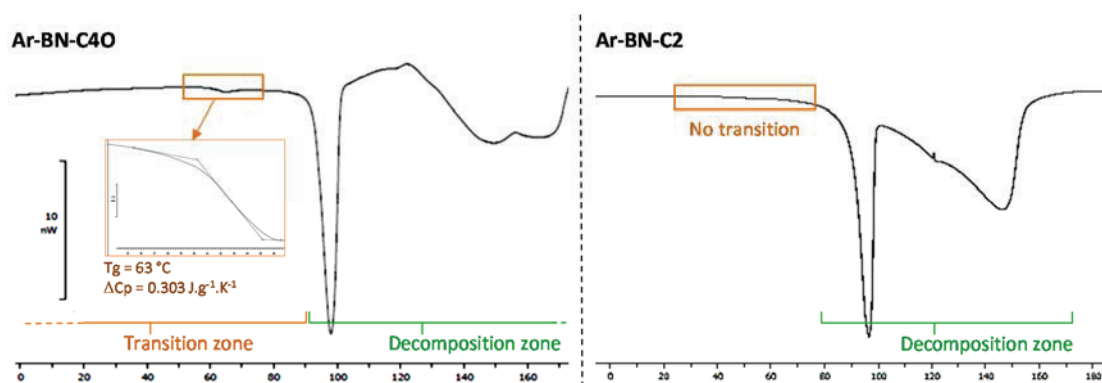


Figure 30. DSC of Ar-BN-C40 from 0 °C to 170 °C, evidence of a  $T_g$  taking place in the “transition zone”. Following by a decomposition zone e.g. dehydrogenation..

Instead, the molecular analogue **1b** exhibited a melting endotherm at 88 °C. This was 20 °C lower than the AB melting (Figure 31). Analogue **1c** containing an extra oxygen atom in aliphatic chains was liquid at 25 °C. Thus, the nature of the aliphatic substituents has played a significant role on the melting temperature.

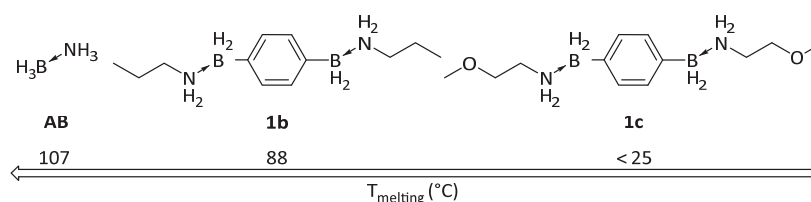


Figure 31. Melting temperature of molecular models compared to  $NH_3-BH_3$ .

#### III.4.d. Fluorescence properties

We noticed that the presence of diborylaryl chromophores gave fluorescent properties in THF to the materials (under 365 nm UV light). Concerning the polymer it appeared that the fluorescent color change depended on the size and the nature of the aliphatic chain within polymers (Figure 32). This parameter has not been further studied yet.

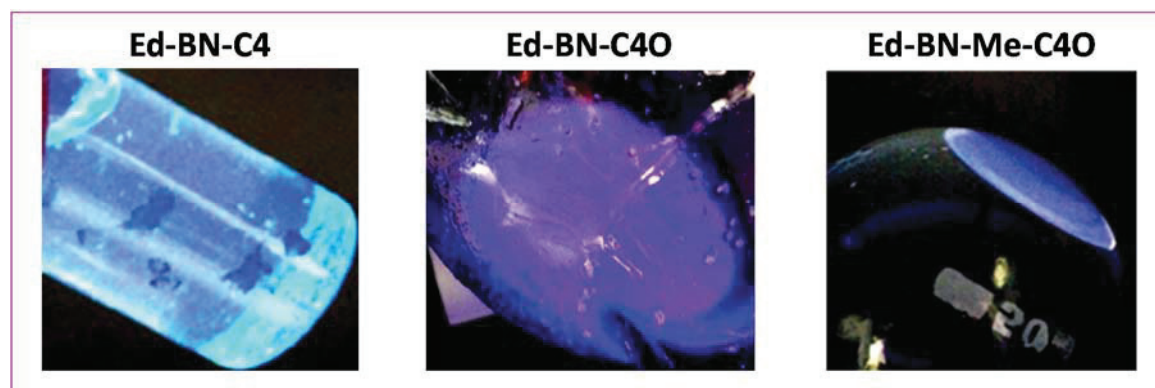


Figure 32. Example of polyboramines under U.V. light. Changes in the color from azure to violet.

Interestingly, after decomposition by dehydrogenation the fluorescence turned off. We suppose that this property could be used as a good indicator of the dehydrogenation state for transport applications.

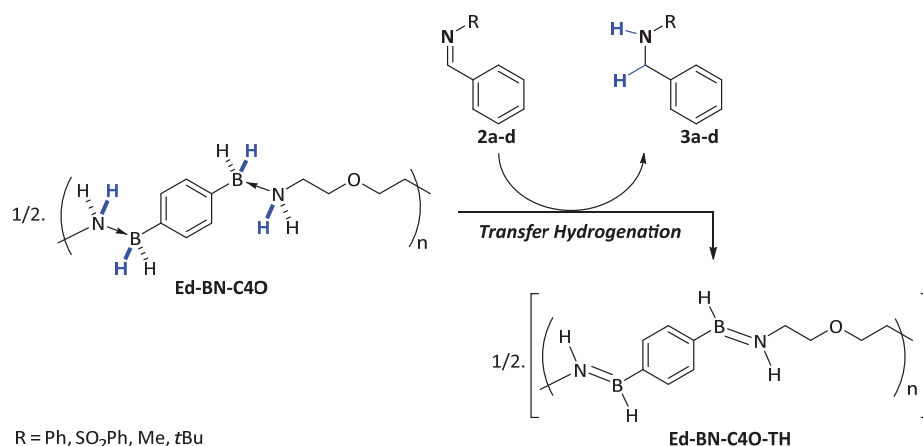
#### III.5. Transfer hydrogenation reaction: indicator of electronic effects of substituents

---

##### III.5.a. Introduction

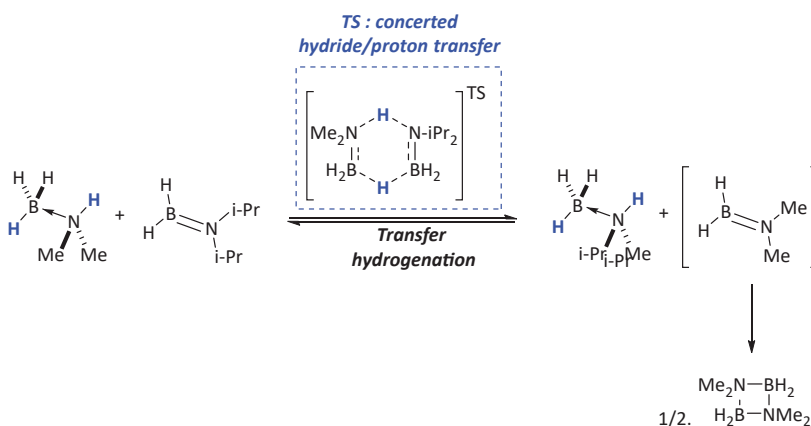
The AB can be used as an *in situ* hydrogen source for the reduction of polar unsaturated compounds.<sup>9b,9c,85</sup> In particular, the transfer hydrogenation reaction of aromatic imines took place through a concerted hydride/proton transfer processes<sup>9c,85b</sup> (Scheme 22). The reaction, reported in 2010, provided the corresponding amine and aminoborane products. The latter reacted rapidly to form cyclic cycloborazanes that could react with another equivalent of imine to yield borazine and polyborazylene. At 60 °C, AB reacted in 7 h. At 40 °C, the reaction time increased to 2 days. The second equivalent reacted in 24

h at 60 °C in good yields. Of note, the mechanism allowing the transfer of a second equivalent of dihydrogen has not been studied.



**Scheme 22.** Transfer hydrogenation of imines with AB. A concerted hydride/proton transfer transition state.

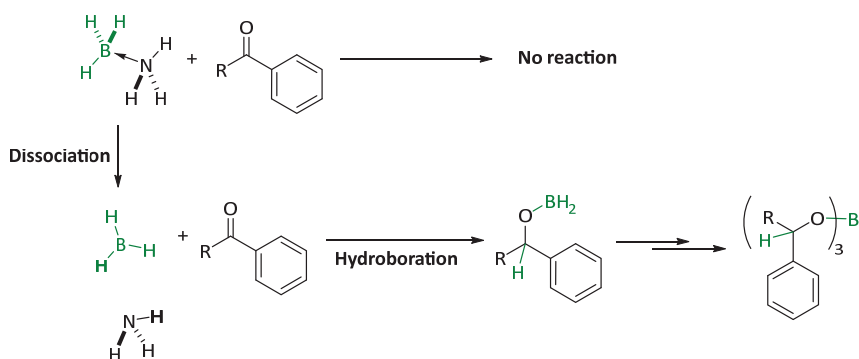
Interestingly, it has been recently reported that amine-borane underwent hydrogen transfer reaction on a sp<sup>2</sup>-aminoborane in a very similar concerted transition state.<sup>86</sup> The reaction formed a reversible equilibrium but the latter was displaced by subsequent formation of very stable dicycloborazane (Scheme 23). This analogy has confirmed the good “polarity match” between C-N and B-N compounds.



**Scheme 23.** Transfer hydrogenation between amine-boranes and aminoboranes through a similar concerted transition state.

In contrast, as described in the literature,<sup>10,87</sup> the reaction between AB and aldehydes or ketones yielded only hydroborated products.<sup>10,87</sup> In the absence of an external source of proton, the reaction of AB with aldehydes or ketones generated the tri-alkoxyborates rather than the alcohol, as well as free ammonia. Mechanistic investigations suggested

that AB itself was not reactive toward carbonyls but after dissociation of AB in  $\text{NH}_3$  and  $\text{BH}_3$ , hydroboration took place (Scheme 24). The alcohol can be recovered by addition of a protic solvent.



*Scheme 24. Reaction of AB with aldehydes and ketones. R = H, alkyl, aryl.*

### III.5.b. This work: effect of substituent and polymer backbone on the hydrogenation of carbonyls

In order to measure the change in reactivity between AB, molecular bricks and their polyboramine we examined the transfer hydrogenation reaction on imines, ketones and aldehydes. We investigated both the influence of substituents on the amine-borane and the influence of the polymer backbone (Figure 33).

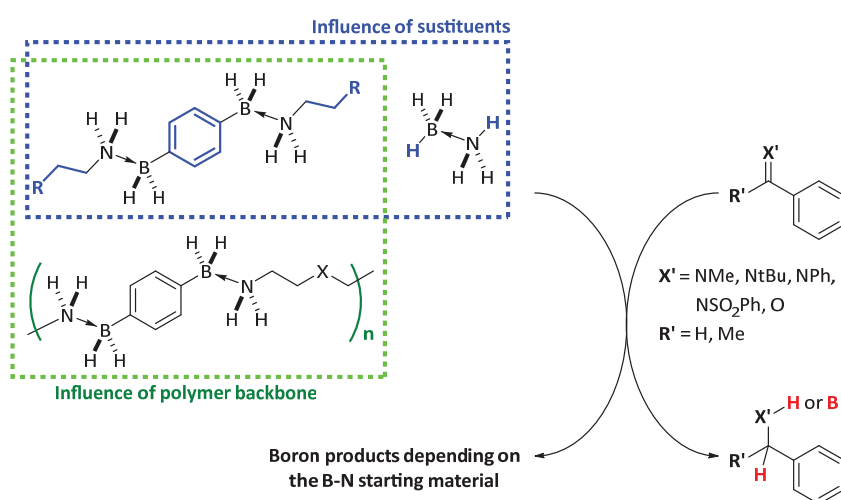


*Figure 33. Global approach for measuring the change in reactivity provided by substituents of amine borane and its polymer backbone.*

In the following section, different amine-borane compounds have been screened using *N*-benzylideneaniline as a reference. Then using **Ar-BN-C4O** polymer, a short scope of imines has underlined the reactivity of polyboramines. Finally the transfer hydrogenation on ketones and aldehyde has been presented.

### III.5.c. Transfer hydrogenation of *N*-benzylidene aniline: a comparative study

We chose a mildly reactive imine to highlight the reactivity of different amine-boranes. Most of the amine-borane reacted at room temperature (25 °C). Increasing the temperature to 40 °C led to small improvements in the conversion. The reaction was monitored by  $^1\text{H}$  NMR using tetrachloroethane as an internal standard (see experimental section 4). Polymer **Ar-BN-C4O**, molecular brick **1b** and **AB** have been subjected to these conditions. We used a 1 : 1 molar ratio between the amine-borane function and the imine one (Table 8).

**Table 8.** Transfer hydrogenation on *N*-benzylidene aniline. A comparative study between different amine-boranes

Amine-Borane compound + *N*-benzylideneaniline  $\xrightarrow[\text{r.t. to } 40\text{ }^\circ\text{C}]{\text{THF-d8}}$  *N*-benzylaniline + Dehydrogenated Boron-Nitrogen compound(s)

Entry	amine-borane	Identity	Conv. <sup>a</sup> (%)	Yield <sup>a</sup> (%)	Selectivity <sup>b</sup> (%)
1		<b>Ar-BN-C4O</b>	52	52	100
2		<b>1b</b>	79	39	49
3		<b>AB</b>	9	9	100
4 <sup>c</sup>		<b>AB</b>	9	9	100
5 <sup>d</sup>		<b>Ar-BN-C4O</b>	82	82	100
6 <sup>d</sup>		<b>1c</b>	89	78	88

General conditions: amine-borane (0.04 mmol or 0.04 mmol/unit), *N*-benzylideneaniline (0.08 mmol), THF-d8 (0.6 mL), r.t, 2.5 h then 40 °C, 3.5 h. (a) Determined by  $^1\text{H}$  NMR with  $\text{C}_2\text{H}_2\text{Cl}_4$  as internal standard (4.7  $\mu\text{L}$ , 0.045 mmol). (b) Calculated as the ratio yield/conv.\*100 (c) With 1 equivalent of LiCl. (d) Modified experimental conditions: amine-borane compound is used directly from the crude in THF (without never being dried).

The molecular brick **1b** showed better conversion than the polymer analogue **Ar-BN-C4O**, however the yield of benzylphenylamine was significantly lower (Table 8, entry 1 and 2). Indeed, the selectivity of transfer hydrogenation by the molecular brick was found to vary from 49 % to 88 % while the polymer showed a full selectivity, suggesting that no side-reaction occurred in presence of the latter.

We think that the difference of selectivity between the amine-borane polymer and the amine-borane molecule could be correlated to solubility parameters. As supported by the visual comparison of the two mixtures after reaction, the polyboramine after transfer hydrogenation (**Ar-BN-C4O-TH**) is an insoluble material (Figure 34) whereas the molecular analogue (**1b-TH**) remained partly soluble. We assumed that molecular transfer hydrogenation products that we called **1b-TH**, were partially or fully solubilized and consequently more available for further reacting with benzylphenylamine, thus decreasing the yield of amine product. However, the selectivity differences could also be the result of different reaction pathways taken by the molecular and the polymer species.

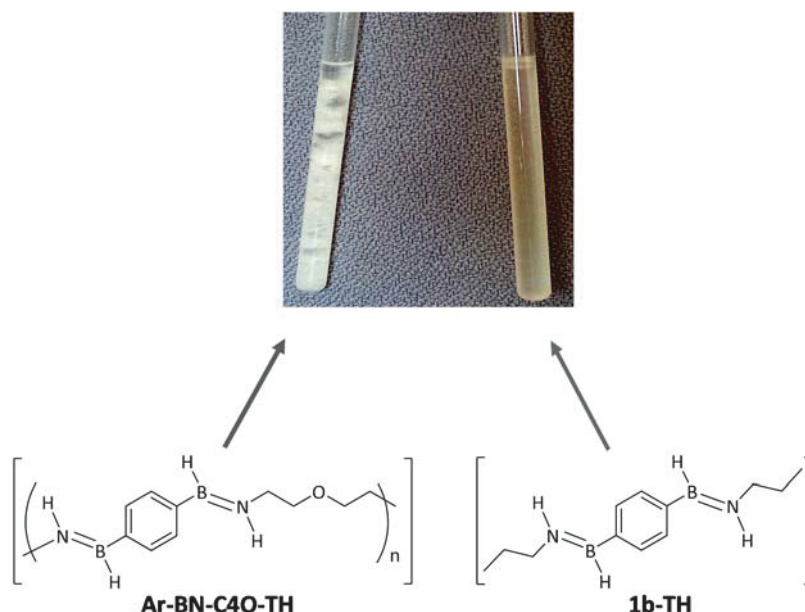


Figure 34. Visual comparison between the polyboramine after Hydrogen Transfer (**Ar-BN-C4O**) on the left, and the molecular brick counterpart (**1b-TH**), on the right. Structures between brackets indicates not isolated compounds.

Less than 10 % of imine conversion has been observed when using AB (Table 8, entry 3), that was consistent with the literature report. It means that the presence of N and B substituents on **1b**, enhanced the reactivity of the amine-borane function, probably due



to electronic effects induced by substituents that enhanced the polarity of the B-N bond. To exclude any possible catalytic effect of traces of LiCl, we engaged AB with amounts of LiCl salts increasing from traces to stoichiometric amount. No positive effect on the reaction rate has been observed (Table 8, entry 4).

Bis(amine-borane) **1c** featuring one extra oxygen atom in the alkyl chain of the nitrogen substituent has been used in transfer hydrogenation as well. **1c** gave good conversions and yields with a moderate selectivity, similarly to what has been observed for the molecular amine-borane **1b**. (Table 8, entry 5). **1c** has been engaged directly into the THF solution without having been dried (after a precise  $^1\text{H}$  NMR quantification). It was due to difficulties to handle it (viscous oil). Under the same conditions **Ar-BN-C4O** showed an improved conversion of **2a** as well (Table 8, entry 5).

In fact, as mentioned above, we observed that the solubility of some polymers was not fully reversible because, after removal of the reaction solvent, the establishment of strong DHB interactions in the solid state have not been reversibly broken in THF and thus avoided their complete re-solubilization. This interpretation has been supported by the difference in  $^{11}\text{B}$  NMR signal, before and after removal of the reaction solvent (Figure 35).

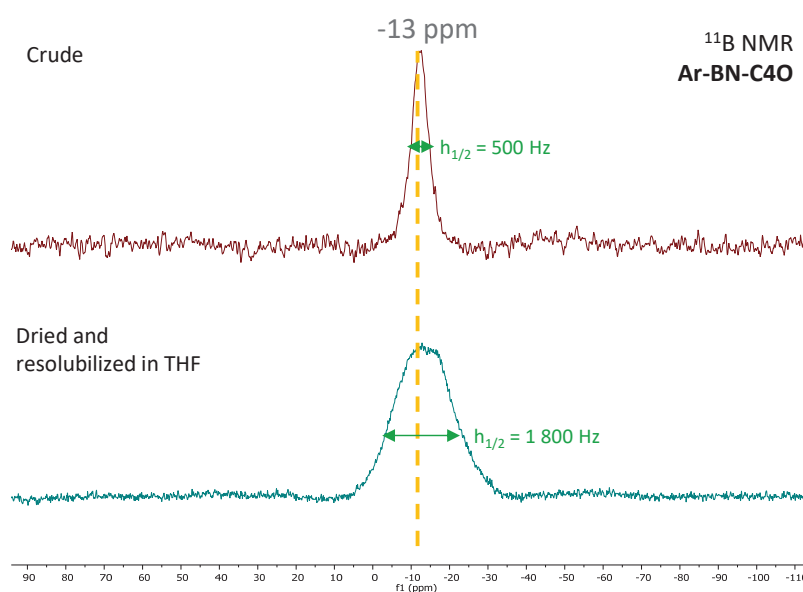


**Figure 35.** Differences of  $^{11}\text{B}$  NMR spectra signals between the crude and the re-solubilized polyboramine, measured trough the half-height width.

Re-solubilization of the polyboramine was characterized by an enlargement on the signal, consistent with an increased distribution of chemical environments. In summary, the "pre-treatment" of the polyboramine influence its reactivity in the reaction of transfer hydrogenation.

In conclusion, comparative studies have put in evidence that amine-boranes **1b** and **Ar-BN-C4O** have realized transfer hydrogenation in mild condition and displayed a better reactivity than **AB**. Moreover the amine-borane polymer showed an improved selectivity with respect to their molecular analogue. Finally, intermolecular interactions could play a significant role on the reactivity of amine-borane.

### III.5.d.Scope of the hydrogen transfer reduction of imines

We screened the reactivity of polyboramines, especially **Ar-BN-C4O** with different N-substituted arylimines **2a-d** to form corresponding amines **3a-d** by transfer hydrogenation reaction. Our results have been presented in the table below (Table 9).

Imine **2a** reacted relatively slowly at 40 °C with one equivalent of amine-borane function (see experimental section 4) to reach a plateau at around 60 % of **3a** yield. N-benzylidene benzenesulfonamide **2b**, instead, reacted quantitatively in less than 6 min (Figure 36 and Table 9, entry 1 and 2).

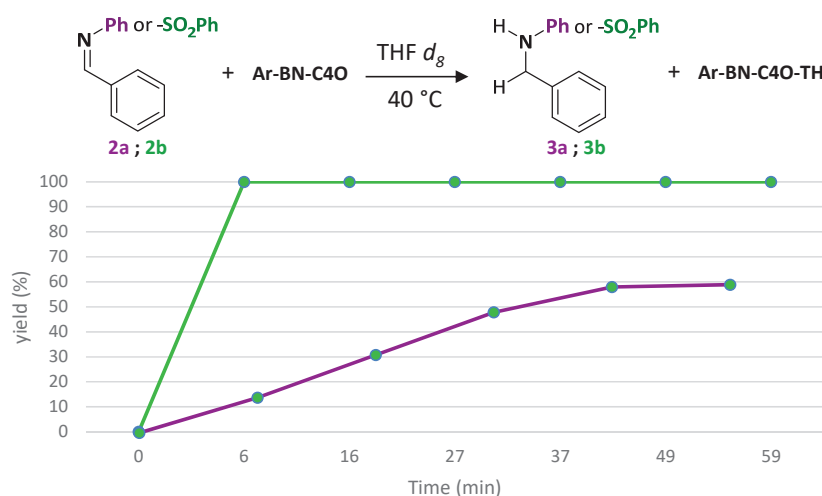
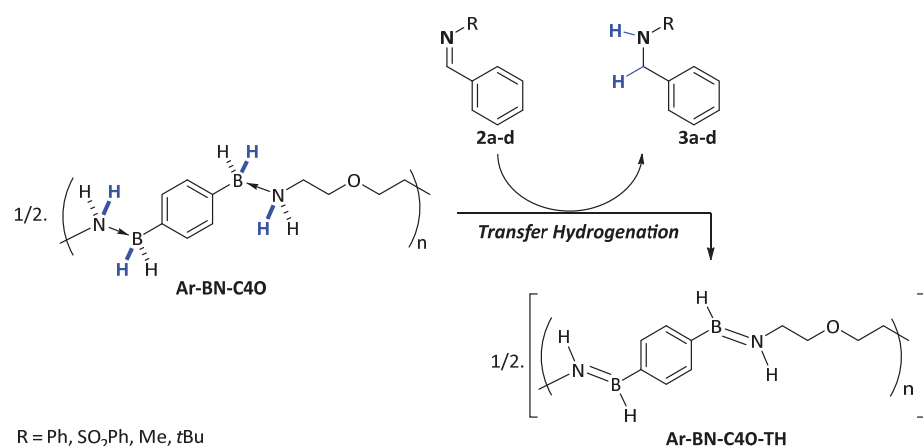


**Figure 36.** *<sup>1</sup>H NMR monitoring of the synthesis of 3a and 3b. For 3a, the reaction has been completed after 6 min. Conditions Ar-BN-C4O 1 B-N unit equivalent, 40 °C, anhydrous THF-*d*<sub>8</sub>, <sup>1</sup>H NMR monitoring.*

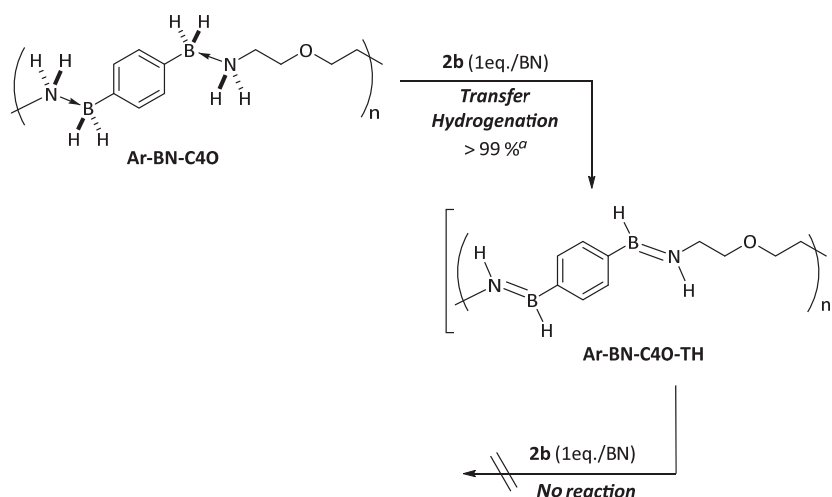
Table 9. Screening of aryl-imines in transfer hydrogenation reaction



Entry	Id.	R	Temperature (°C)	Conversion <sup>a</sup> (%)	Yield <sup>a</sup> (%)
1	<b>2b</b>	-SO <sub>2</sub> Ph	r.t.	> 99	> 99
2	<b>2b</b>	-SO <sub>2</sub> Ph	40	> 99	> 99
3 <sup>b</sup>	<b>2b</b>	-SO <sub>2</sub> Ph	r.t.	43	43
4	<b>2c</b>	-Me	40	77	77
5	<b>2c</b>	-Me	r.t.	51	51
6 <sup>d</sup>	<b>2c</b>	-Me	r.t.	53	53
7 <sup>c</sup>	<b>2c</b>	-Me	40	> 99	> 99
8	<b>2d</b>	-t-Bu	40	65	63
9 <sup>c</sup>	<b>2d</b>	-t-Bu	40	> 99	> 99
10	<b>2a</b>	-Ph	40	60	60
11 <sup>c</sup>	<b>2a</b>	-Ph	r.t.	> 99	> 99

General conditions: **1b** (0.04 mmol/unit), imine (0.08 mmol), Anhydrous THF-*d*<sub>8</sub> (0.6 mL), 12 h (no evolution beyond). (a) determined by <sup>1</sup>H NMR with C<sub>2</sub>H<sub>2</sub>Cl<sub>4</sub> as internal standard (4.7 μL, 0.045 mmol). (b) imine (0.16 mmol). (c) **1b** (0.08 mmol/unit). (d) **1a** (0.04 mmol/unit).

We used the very reactive substrate **2b** to determine whether the second equivalent of hydrogen of amine-boranes was also available. The reaction was repeated with 2 equivalents of **2b** per amine-borane function and gave only a 43 % yield (Table 9, entry 3). It suggested that the second equivalent of polyboramine **Ar-BN-C4O** was not consumed (Scheme 25).



**Scheme 25.** Substoichiometric experiment to determine the reactivity of the second equivalent of dihydrogen from Ar-BN-C4O.

N-benzylidene methylamine **2c** was converted to **3c** in 12 h at 40 °C with a 77 % conversion and at room temperature with a 51 % conversion (Table 9, entry 4 and 5). Increasing the reaction time to 24 h or even several days had any effect on conversions meaning that after 12 h, the reaction reached a *plateau*.

Reacting **2c** with Ar-BN-C4 polymer which did not feature any oxygen atom in the aliphatic chain, gave very similar results (Table 9, entry 6). Apparently, the presence of the oxygen atom did not influence the reaction. Adding two equivalents of amine-borane led to the full hydrogenation of the imine (Table 9, entry 7). Substrate N-benzylidene *t*-butylamine **2d** exhibited slightly lower reactivity than **2c**, due to additional electron donating effects that decreased the polarity of the imine. Still, the addition of another equivalent of amine-borane led to full conversion of **2d** (Table 9, entry 8 and 9). Transfer hydrogen of **2a** exhibited the lowest reactivity even if the N-phenyl substituent is electron attractor. The origin of this result has not yet fully understood. However, complete conversion has been reached at room temperature by doubling the amount of amine-borane (Table 9, entry 10 and 11).

To summarize, polyboramines have been able to undergo transfer hydrogenation quantitatively and under mild conditions. Electronic substituents on imines played an important role on the reactivity toward polyboramines. The oxygen atom into the aliphatic chain did not influence the reaction. From recently established similarities of

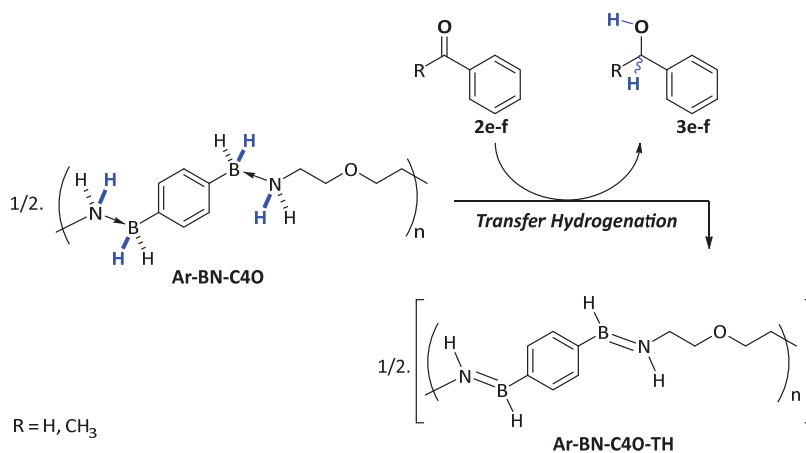
imines with  $sp_2$ -aminoboranes in transfer hydrogenation,<sup>86a</sup> reversible transfer hydrogenation phenomena are not to be excluded.

### III.5.e. Hydrogen transfer reduction of aldehyde and ketones

We reported the very efficient transfer hydrogenation of aldehydes and ketones realized by polyboramine **Ar-BN-C4O** and a molecular brick **1b** in THF. To the best of our knowledge it is the first report of direct transfer hydrogen reaction on aldehydes and ketones realized by amine-borane species. Actually, AB exclusively promoted hydroboration.

The reaction was performed in anhydrous THF, repeated twice, with and without previous addition of activated molecular sieves *in situ*. Benzaldehyde **2e** and acetophenone **2f** were reacted with stoichiometric amounts of **Ar-BN-C4O** amine-borane units, and converted quantitatively from room temperature to 40 °C in less than 2.5h.

**Table 10. Transfer hydrogenation of benzaldehyde and acetophenone realized by polyboramine Ar-BN-C4O.**



Entry	R	Temperature (°C)	Conversion <sup>a</sup> (%)	Yield <sup>a</sup> (%)
1	H	r.t.	> 99	> 99
2	-CH <sub>3</sub>	40	> 99	> 99
3	-CH <sub>3</sub>	r.t.	92	92

General conditions: **Ar-BN-C4O** (0.04 mmol/unit), **2e-f** (0.08 mmol), Anhydrous THF-d<sub>8</sub> (0.6 mL), 2.5 h. (a) determined by <sup>1</sup>H NMR with C<sub>2</sub>H<sub>2</sub>Cl<sub>4</sub> as internal standard (4.7 μL, 0.045 mmol). (b) 12 h. Reaction repeated several times, with and without *in situ* activated molecular sieves.

Similarly to hydrogen transfer on imines, molecular brick **1b** converted **2e** and **2f** delivering directly corresponding alcohols in good yields with a lower selectivity (Table 11). As expected, reaction of **AB** with benzaldehyde **2e** only resulted in hydroboration reactions.

**Table 11.** Transfer hydrogenation on benzaldehyde and acetophenone. A comparative study between different amine-boranes

Entry	Amine-Borane	Identity	R	Conversion <sup>a</sup> (%)	Yield <sup>a</sup> (%)
1		<b>1b</b>	H	99	<b>99</b>
2		<b>2b</b>	H	99	<b>81</b>
3		<b>1b</b>	CH <sub>3</sub>	99	<b>99</b>
4		<b>2b</b>	CH <sub>3</sub>	77	<b>75</b>
5	<b>AB</b>	<b>AB</b>	H	80	<b>0</b>

General conditions: amine-borane (0.04 mmol or 0.04 mmol/unit), **2e-f** (0.08 mmol), THF-d<sub>8</sub> (0.6 mL), r.t., 2.5 h then 40 °C, 3.5 h (no evolution beyond).

The transfer hydrogenation reaction of benzaldehyde **2e** and acetophenone **2f** gave the <sup>1</sup>H NMR spectra of **3e** and **3f** respectively (see example on **2e**, Figure 37, up and experimental section 4). Products were doubtless identified by GCMS and compared with commercially available products and literature data. In contrast, the hydroboration of **2e** and **2f** by **AB** gave a mixture of alkoxybenzyl boron species in agreement with literature data<sup>87</sup> (Figure 37, down).

Reaction mixtures:

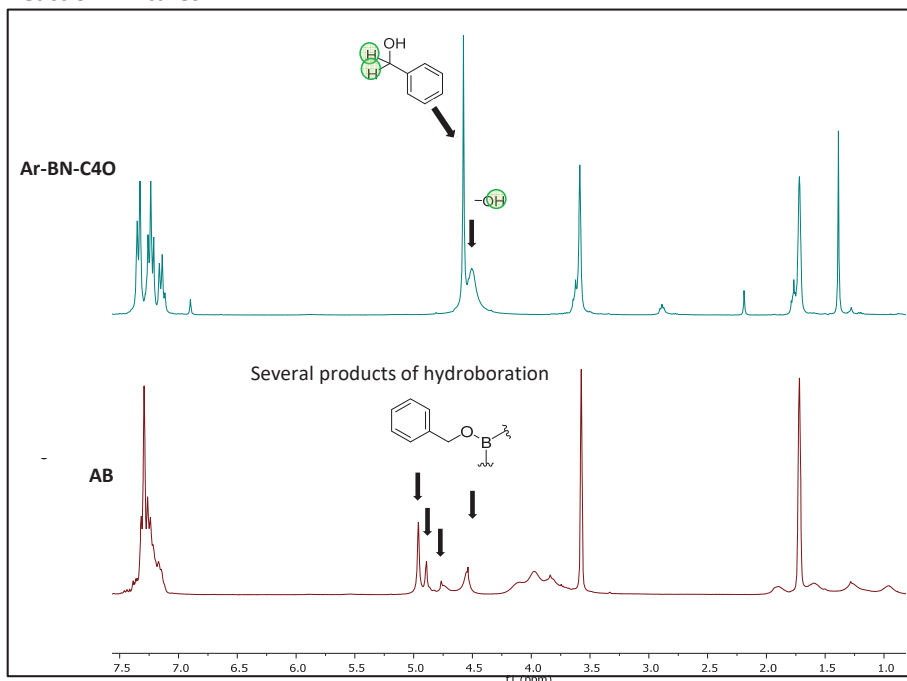


Figure 37. Reaction mixtures of transfer hydrogenation reaction performed by Ar-BN-C4O in THF- $d_8$  on benzaldehyde yielding benzylalcohol (c.f., e.g.,  $\delta$  ( $\text{CH}_2$ ) = 4.56 ppm (d,  $J$  = 6 Hz, 2H) (up), and hydroboration done by ammonia-borane yielding boron-bounded alcoholates as tribenzylborate (c.f., e.g.,  $\delta$  ( $\text{CH}_2$ ) = 4.99 ppm s, br).

The mechanistic pathway of transfer hydrogenation of aldehydes and ketones could be established by analogy with the BINAP/diamine-Ru Noyori's catalyst,<sup>88</sup> which involved a concerted six-membered transition state in the asymmetric transfer hydrogenation of ketones. (Figure 38). This concerted pathway is also analogue to the transition state determined for the amine-borane transfer hydrogenation of imines.

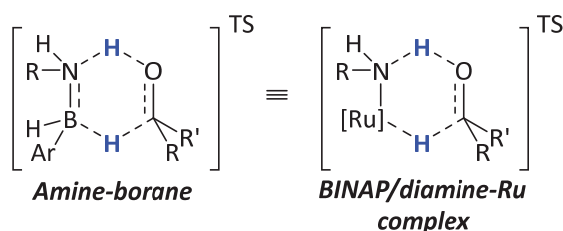


Figure 38. Analogy of transition states between amine-borane and diamine-Ru Noyori's catalyst in the transfer hydrogenation of aldehydes and ketones.

In this section we demonstrated that N-alkyl, B-aryl substituted amine-boranes had enhanced properties with respect to AB and even gave access to the transfer hydrogenation of a new category of polarized double bond that were aldehydes and

ketones. Moreover we demonstrated also that the polymer backbone brought additional advantages to the reactivity especially in terms of selectivity.

### III.5.f. Hypotheses on the polymer structure after transfer hydrogenation

During the hydrogen transfer reaction involving **Ar-BN-C4O** and **1b**, the THF solution got saturated with a new polymer that we called **Ar-BN-C4O-TH**, less soluble than the starting material. An  $^{11}\text{B}$  NMR monitoring revealed the formation of a single species in solution, having a chemical shift of 27 ppm. According to substoichiometric experiments suggesting that only the first equivalent of dihydrogen was transferred during the reaction, **Ar-BN-C4O-TH** should still contain one equivalent of dihydrogen into amine-borane functions. The  $^{11}\text{B}$  NMR signal could corresponds to the linear  $\text{sp}^2$  aminoborane structure, according to previously reported chemical shifts (i.e., e.g.,  $[\text{iPr}_2\text{N}=\text{BH}_2]$   $\delta = 34.6$  ppm,  $[\text{Me}_2\text{N}=\text{BH}_2]$   $\delta = 37.9$  ppm,  $[\text{Me}_2\text{N}=\text{BCl}_2]$   $\delta = 30.8$  ppm,  $[\text{Me}_2\text{N}=\text{BF}_2]$   $\delta = 17.0$  ppm).<sup>86b,89</sup> In contrast,  $^{11}\text{B}$  NMR chemical shifts corresponding to oligomers of aminoborane fall out of this range (i.e., e.g.,  $[\text{Me}_2\text{N}-\text{BH}_2]_2$   $\delta = 4.7$  ppm,  $[\text{Me}_2\text{N}-\text{BCl}_2]_2$   $\delta = 10.4$  ppm,  $[\text{Me}_2\text{N}-\text{BF}_2]_2$   $\delta = 0.9$  ppm,  $\text{Me}_3\text{N}-\text{BH}_2-\text{NMe}_2-\text{BH}_3$   $\delta = 3.2$  ppm).<sup>86b,89</sup> However the formation of some borazines (i.e., e.g.,  $[\text{HN}-\text{BH}]_3$   $\delta = 32.0$  ppm,  $[\text{MeN}-\text{BH}]_3$   $\delta = 33.0$  ppm),<sup>90</sup> cannot be excluded even if it would suppose that both hydrogen equivalent of amine-borane were consumed.

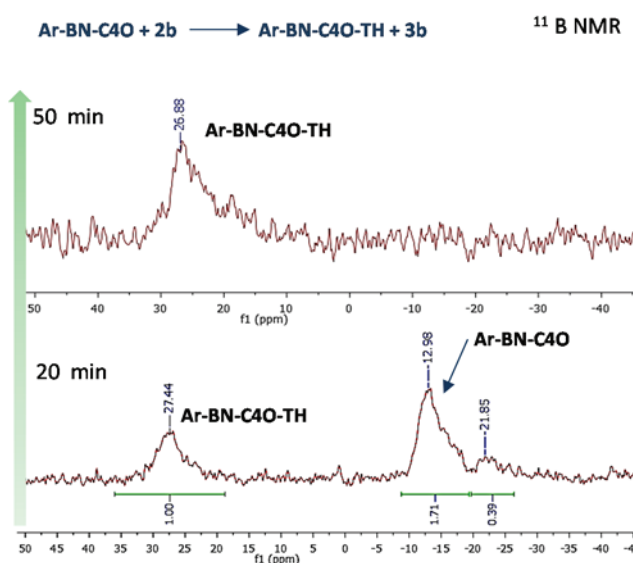


Figure 39.  $^{11}\text{B}$  NMR monitoring of polymer **Ar-BN-C4O** during transfer hydrogenation on **2b**.



We demonstrated the reactivity of polyboramines in solution and showed noticeable differences resulting from electronic effects and polymer backbone effects. The following chapter has reported the investigation of polyboramines in the field of hydrogen release for energetic purposes.

### III.6. Polyboramines involved in thermal hydrogen release

---

AB and analogues have undergone, for the major part, thermal induced dehydrogenation, in the solid state. Amine-borane thermal dehydrogenation was found to be bimolecular<sup>3</sup> and autocatalytic<sup>54,91</sup> (i.e. dehydrogenated species facilitated the process). The hydrogen-release profile was influenced by the temperature/time of heating. In other words, dehydrogenation profiles depended of the temperature rate or of the isothermal temperature heating.

#### III.6.a. Temperature of hydrogen-release and enthalpy of reaction.

When molecules AB and **1b** were heated at 5 °C/min, their DCS (differential scanning calorimetry) profiles exhibited a melting endotherm at 110 °C and 88 °C respectively (Figure 40). MeNH<sub>2</sub>-BH<sub>3</sub> heated at 2 °C/min<sup>92</sup> melted at 55 °C. This temperature of melting depended largely on DHB intermolecular interactions as well as on boron/nitrogen substituents. The three compounds exhibited a subsequent exothermic dehydrogenation peak at 120 °C, 125 °C and 140 °C for AB, **1b** and MeNH<sub>2</sub>-BH<sub>3</sub> respectively. These DSC patterns were similar and typical of an amine-borane dehydrogenation (Figure 40).

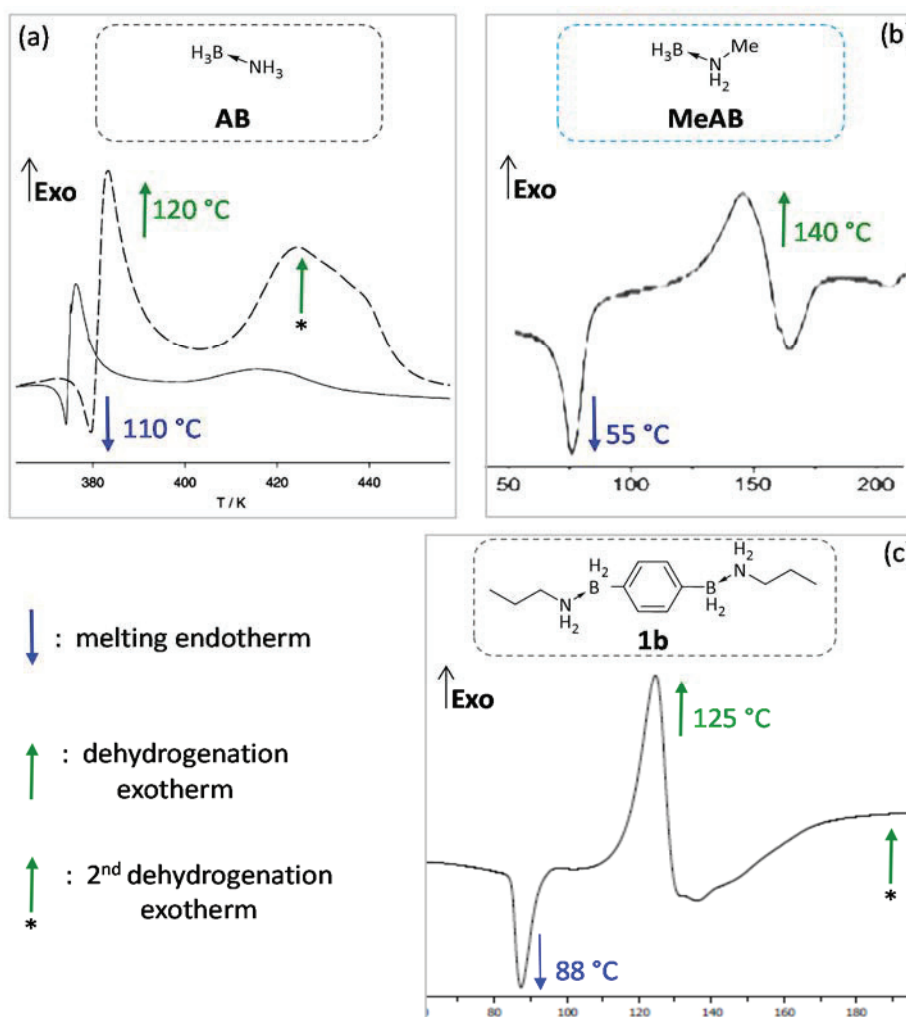


Figure 40. DSC profiles in the thermal dehydrogenation of (a) AB, 1 °C/min (line), 5 °C/min (dashed) ; (b) N-methylamineborane, 2 °C/min ; (c) 1b, 5 °C/min

We next investigated dehydrogenation profile of polyboramines by DSC and TPD. As observed, for instance on **Ar-BN-C4O** (Figure 41), dehydrogenation happened under 100 °C (95 °C) (Figure 41a) which differed from the molecular counterpart **1b** that released hydrogen at 125-130 °C (Figure 41b). This feature was evidently caused by the polymer scaffold. The second peak of dehydrogenation has also been downshifted at a maximum of 195 °C for **1b** to 175 °C for polyboramine **Ar-BN-C4O**. This second peak has been attributed to the release of a second equivalent of dihydrogen by analogy to AB studies.<sup>11</sup> In addition, polyboramine **Ar-BN-C4O** displayed endothermic dehydrogenation processes for both steps (Figure 41c), in stark contrast with the molecular brick, that exhibited exclusively exothermic steps (Figure 41d). We carried out computational studies to explain these particular observations (see chapter III.7).

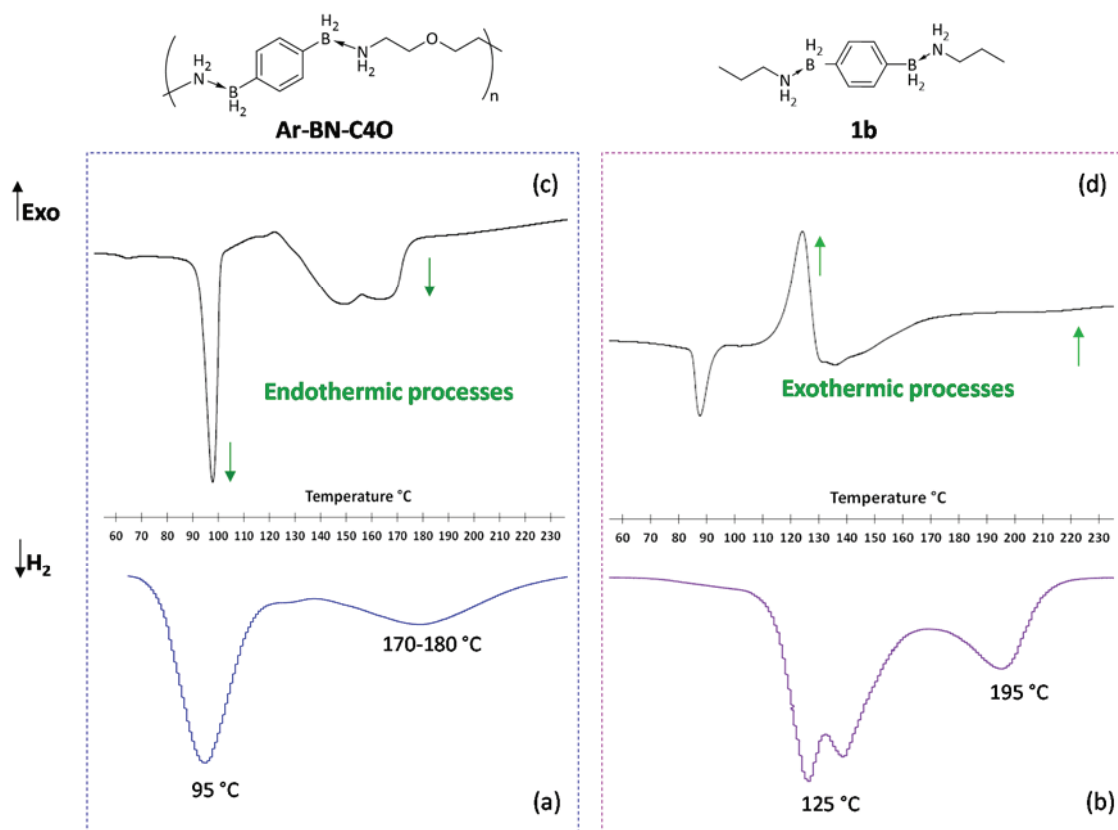


Figure 41. Dehydrogenation profiles. Temperature rate: 5 °C/min. (a) DSC of polyboramine Ar-BN-C4O, (b) DSC of molecular brick 1b, (c) TPD of polyboramine Ar-BN-C4O, (d) TPD of molecular brick 1b.

Our results have been also supported by *in situ* IR spectroscopy monitoring. In particular, the B-H bond of amine-borane, aminoboranes and analogues displayed visible IR stretching in the range of 2200-2400 cm<sup>-1</sup>.<sup>52</sup> When heated at a temperature rate of 5 °C/min, the characteristic B-H stretching of **Ar-BN-C4O**, averaged at 2313 cm<sup>-1</sup>, started to decrease visibly from 90 °C (Figure 42a). After 160 °C the amine-borane stretching at 2313 cm<sup>-1</sup> has completely disappeared (Figure 42b, c). Qualitatively, these observations have been in agreement with DSC results.

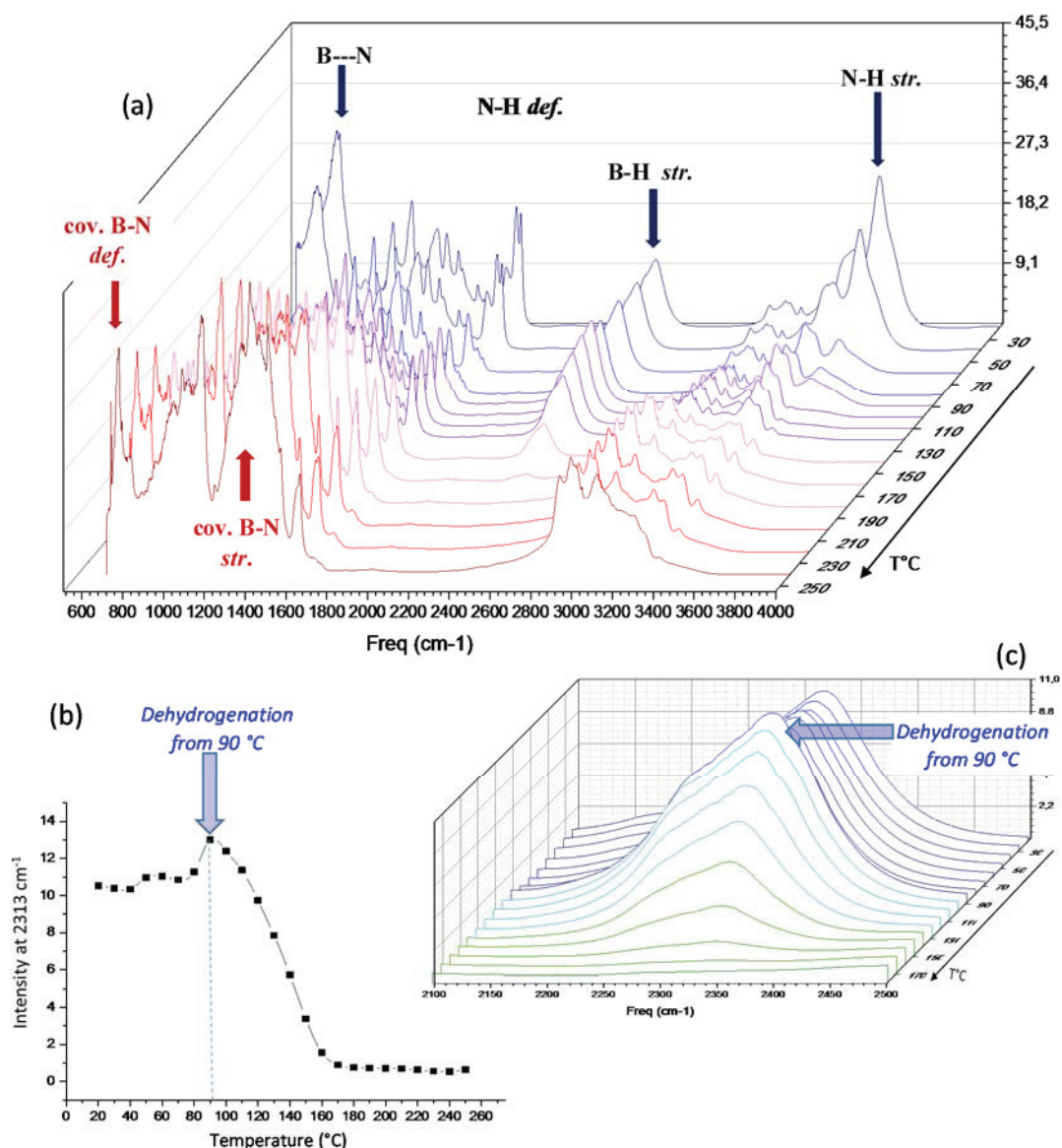


Figure 42. Dehydrogenation process of polyboramine Ar-BN-C4O followed by *in situ* IR spectroscopy. Complete disappearance of B-H stretches ( $\nu = 2200 - 2400 \text{ cm}^{-1}$ ).

By zooming in the baseline in the  $2200 - 2400 \text{ cm}^{-1}$  region (Figure 43), we identified some elongation bands that were 50 to 100 times lower in intensity with respect to original B-H stretching. They likely corresponded to new B-H containing species but nevertheless, were only present in very minute amounts. According to IR spectroscopy, it appeared that the polymer has delivered quantitatively the two equivalents of  $\text{H}_2$  per amine-borane functions between 30 and 230 °C.

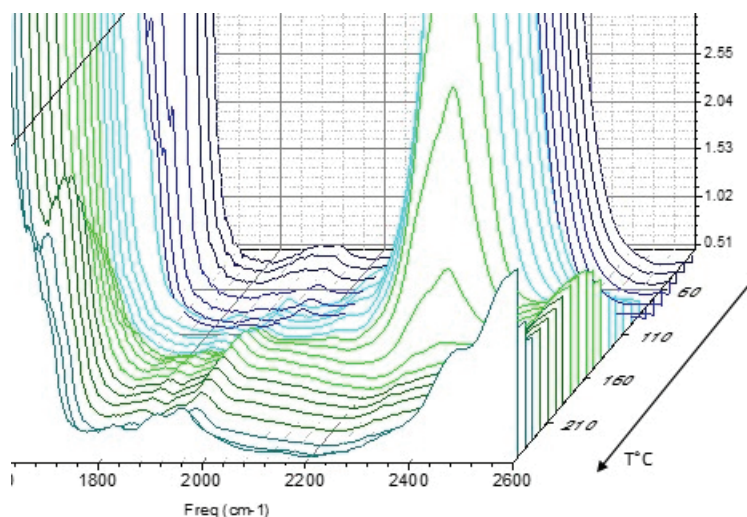


Figure 43. Zooming in the baseline between 1600 and 2600  $\text{cm}^{-1}$  to see B-H stretching residues

Results have been supported by TGA monitoring, using the same temperature program (Figure 44). A mass loss was observed between 70 °C and 230 °C (Figure 44, up) with a maximum rate at  $\sim 90$  °C according to the second order derivative (Figure 44, down). Moreover the integration indicates that 3.9 % of the polymer weight has been lost in this range of temperature. It corresponded to the total dihydrogen content of the polyboramine **Ar-BN-C40**. A GC-MS monitoring confirmed that no gas impurities were generated during the dehydrogenation process. We used the TPD  $\text{H}_2$  quantification to determine accurately the yield of the polyboramine's dihydrogen release.

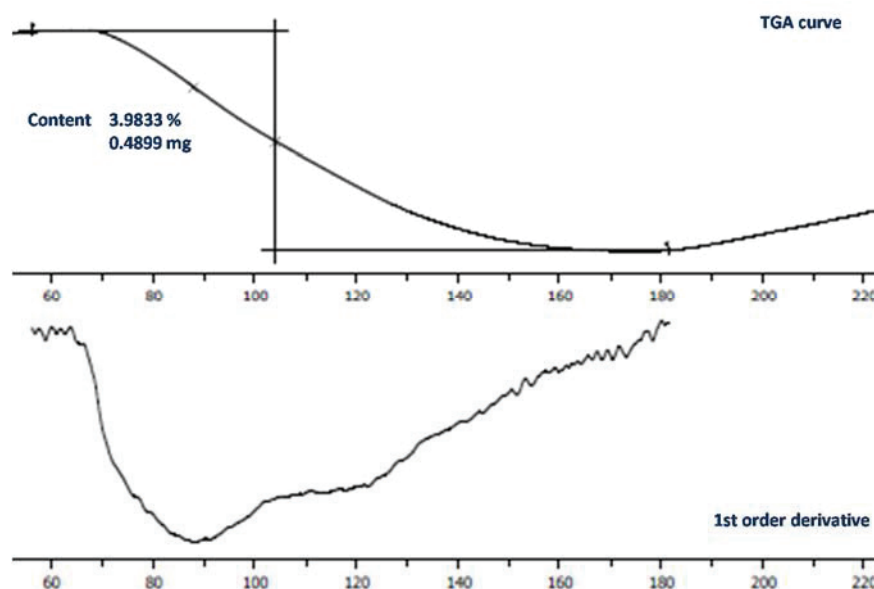


Figure 44. TGA analysis of the polymer **Ar-BN-C40**. Temperature rate: 5 °C/min, (a) Gravimetric mass loss (%), (b) second order derivative.

### III.6.b. Quantitative analysis of dihydrogen delivery

The TPD apparatus permitted to integrate the area corresponding to the gaseous H<sub>2</sub> gas emitted by the amine-borane compound (for more details, see experimental section 4). The quantity of hydrogen released could depend of the temperature program. Isothermal conditions ranging from 120 to 160 °C gave the best H<sub>2</sub> yields. We found that polyboramines emitted up to 86 % of their H<sub>2</sub> content at 160 °C (Figure 45). Similarly, the molecular brick analogue delivered up to 97 % of the total H<sub>2</sub> in the same conditions (see experimental section 4)

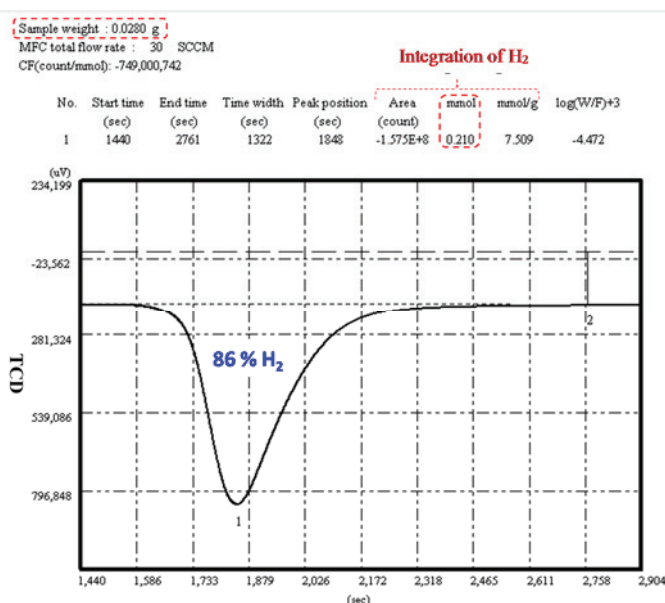


Figure 45. Integration of the TPD curve after isothermal experiment on polyboramine Ar-BN-C4O. Conditions: 160 °C 1h. Yield 86 % H<sub>2</sub> content. For details and calculation methods, please refer to the experimental section 4.

To confirm our observation, we further tried to establish a relationship between the endothermic process observed by DSC and the dehydrogenation of polyboramines. Particularly, our aim was to check if the dehydrogenation process was not superimposed with a melting endotherm.

### III.6.c. Evidences for a dehydrogenation peak

We varied the temperature rate to check whether some other phenomenon could appear on the DSC chart (endotherm splitting, exothermic peak, etc.), by modifying the temperature rate from 0.1 to 15 °C/min (Figure 46). The two endothermic steps remained visible throughout the heating rate reduction from 15 °C/min to 1 °C/min (Figure 46c-e)

and the first endotherm peak temperature at  $\sim 100$  °C was almost independent from the temperature rate in this range. At 1 °C/min, the endotherm became more widespread. The onset temperature was located around 50 °C, and the two decomposition steps were slightly superimposed. The formation of structures facilitating the dehydrogenation such as DADB<sup>50</sup> as well as auto-catalytic phenomena could explain the earlier hydrogen release observed. These hypotheses were supported by further decreasing the temperature rate. Upon, heating at 0.5 °C/min (Figure 46b), only one endotherm peak was observed, and the temperature peak dropped from  $\sim 100$  °C to 85 °C. Even more, at 0.1 °C/min (Figure 46e) an identical single endothermic peak was identified with a stark decrease of the temperature peak to 65 °C. The temperature rate dependence of the dehydrogenation peak was observed similarly on AB,<sup>48</sup> but it involved exothermic peaks and was attributed to the formation of kinetically favored DADB as well as auto-catalytic effects.<sup>50</sup> The discussion of possible DADB-like structures during polyboramine dehydrogenation on a mechanistic point of view has been further discussed in chapter II.6 of this section.



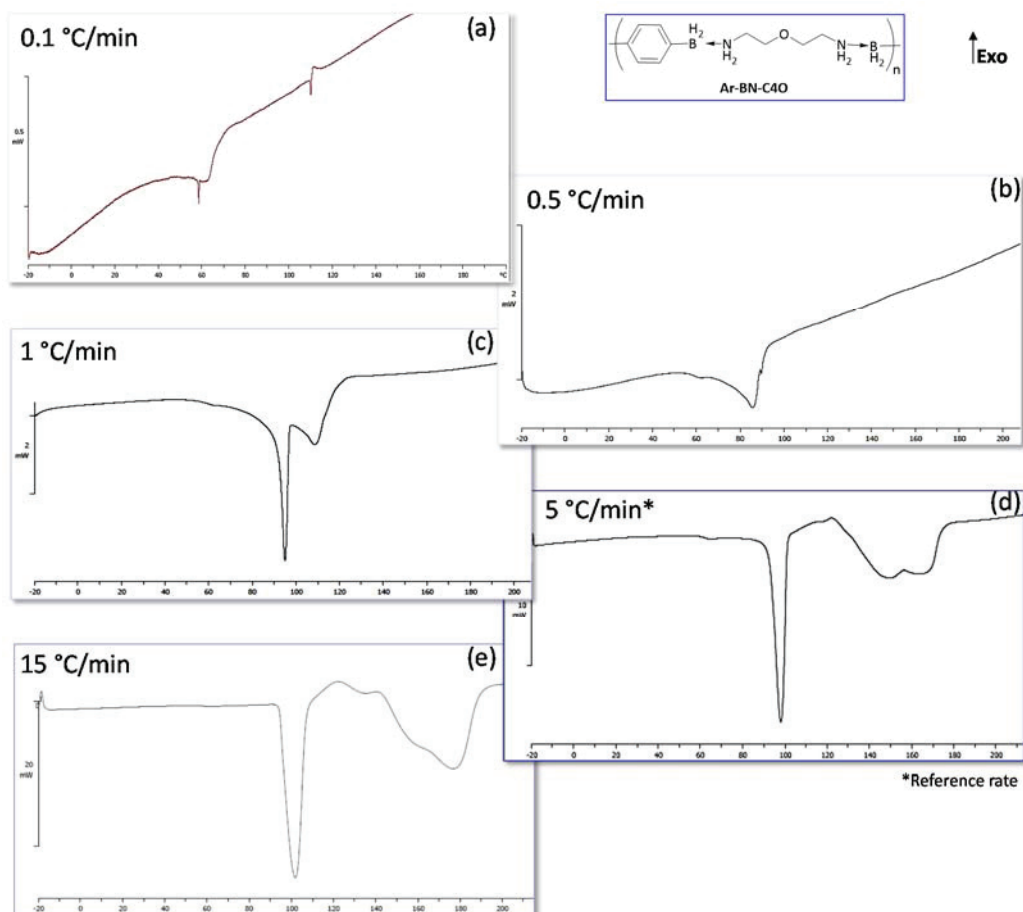


Figure 46. Dehydrogenation of Ar-BN-C4O at different temperature rates. (a) 0.1 °C/min, (b) 0.5 °C/min, (c) 1 °C/min, (d) 5 °C/min, (e) 15 °C/min. Reference conditions: 5 °C/min.

To further evidence the link between dehydrogenation and endothermicity observed in DSC, we studied the influence of the aliphatic chain length. As mentioned in chapter III.4 above, the aliphatic nitrogen substituent of molecules **1b** and **1c** has a significant influence on the melting temperature. Thus, by varying the aliphatic spacer within polyboramines we expected to separate a hypothetical melting phenomena from the dehydrogenation one.

#### III.6.d.Variation of the aliphatic chain within polyboramines

Several polyboramines with different size and nature of aliphatic chains, have been screened by DSC with a temperature rate of 5 °C/min. At first observation, all DSC profiles yielded a two-step endotherm (Figure 47).



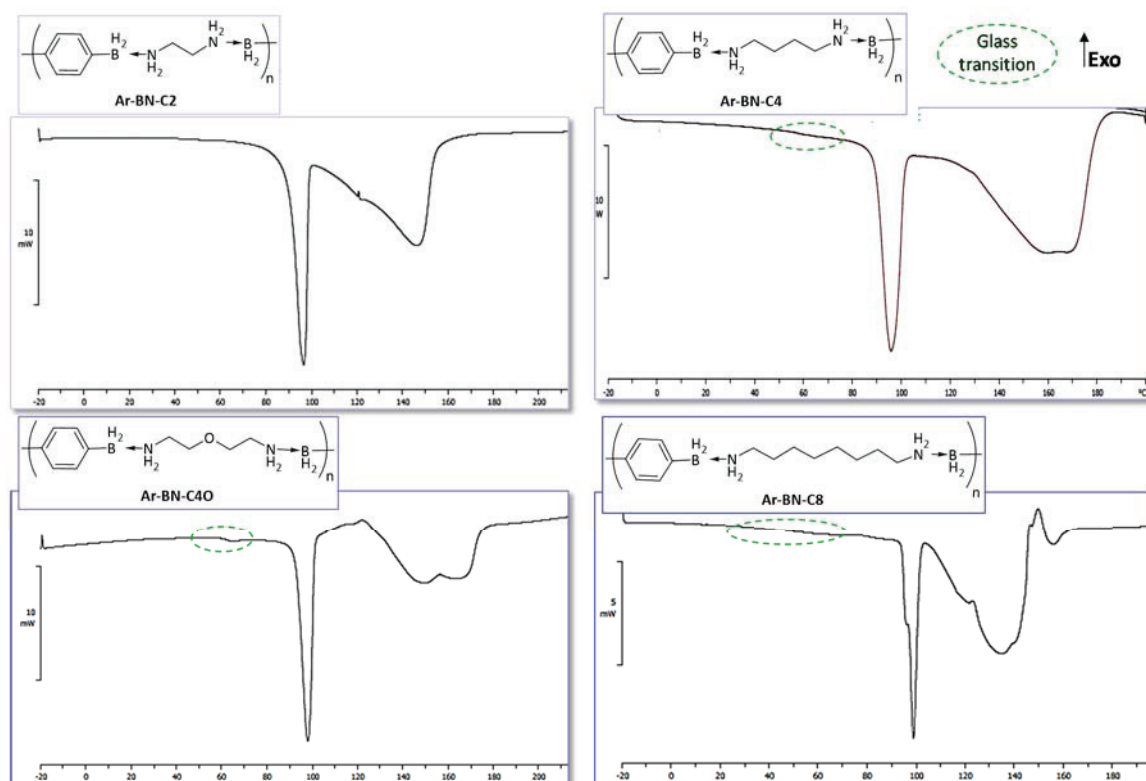
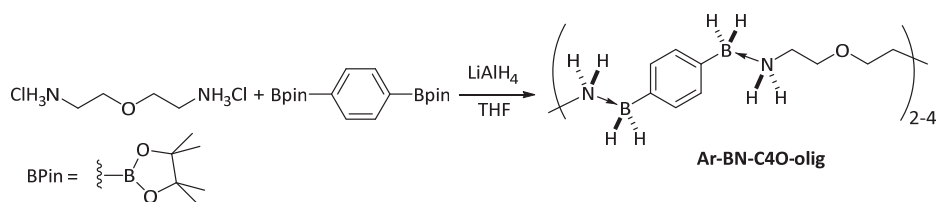


Figure 47. DSC profiles of polyboramines containing variable aliphatic chains, at a temperature rate of 5 °C/min.

Actually, the four polyboramines exhibited similar DSC patterns, even though they had variable backbones from a very short (two carbon) to a very long (eight carbons) spacer with or without additional heteroatoms. Dehydrogenation peaks corresponding to the first dehydrogenation step were independent of the temperature rate and were all located in the temperature range of 95 °C - 100 °C. However, it had to be pointed out that the dehydrogenation peak of polymer **Ar-BN-C8**, appeared to be slightly split in two. It could be either due to a multi-step dehydrogenation pattern or to a superimposition between a melting endotherm and a decomposition process. In any case it confirmed that the dehydrogenation of polyboramines **Ar-BN-C<sub>x</sub>O<sub>y</sub>** are apparently endothermic. The second dehydrogenation varied much more widely in a temperature range of 140-170 °C but was still an endothermic process.

### III.6.e. Dehydrogenation of oligomers

Oligomers **Ar-BN-C4O-olig**, have been identified by SEC as a mixture of di-, tri- or tetramers (Scheme 26). We submitted these species to dehydrogenation treatments to see whether their behavior looked like molecular bricks or polyboramines.



*Scheme 26. Reaction pathway for the synthesis of oligomers Ar-BN-C4O-olig from pinacol p-phenylenebisboronate*

In fact the TPD experiment showed that **Ar-BN-C4O-olig** featured the same dehydrogenation profile than **1b** molecule, with two maxima at 125 °C and 140 °C (Figure 48a, b).

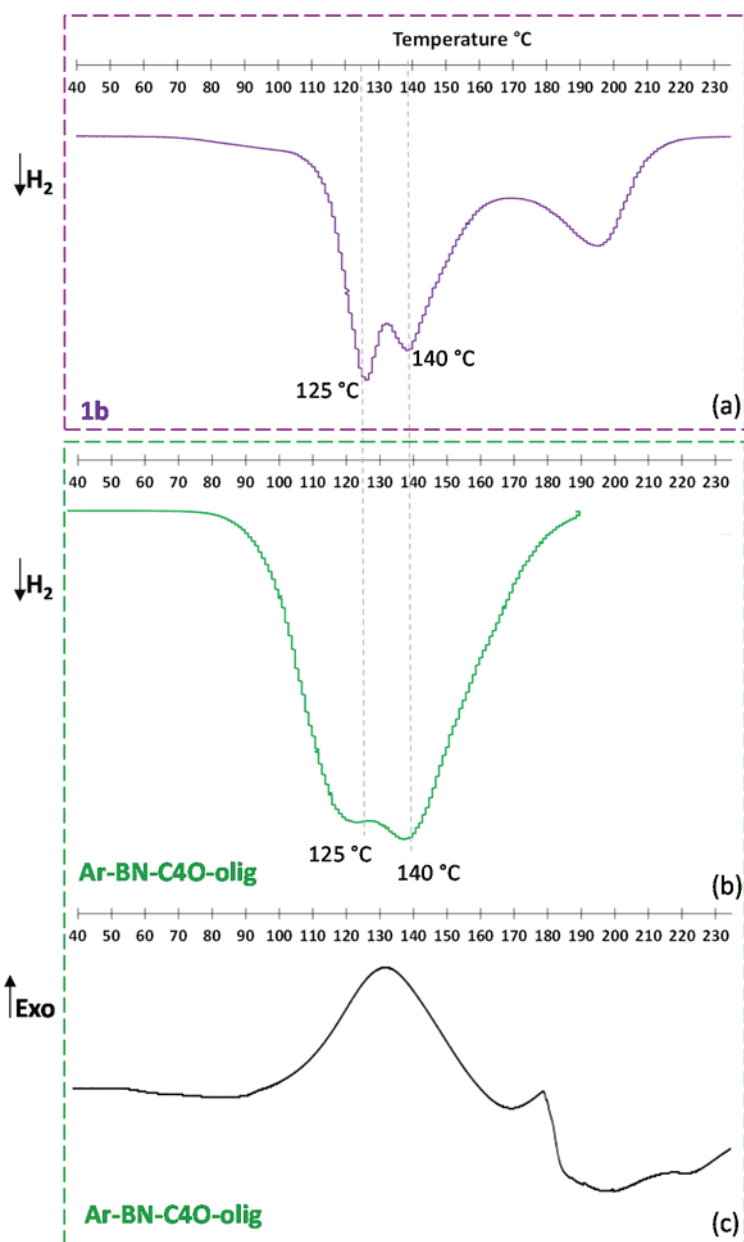


*Figure 48. Engaging Ed-BN-C4O-olig in dehydrogenation studies showed a strong analogy with molecular brick 1b. Temperature rate: 5 °C/min. (a) TPD of 1b, (b) TPD of Ed-BN-C4O-olig, (c) DSC of Ed-BN-C4O-olig.*

The peaks were broadened with respect to **1b**, which was consistent with a distribution of oligomers between 2, 3 and 4 units. The DSC curve followed the same trend and indicated a widespread exothermic wave centered at 130 °C (Figure 48c). According to previous results, the absence of endothermic phenomena confirmed that **Ar-BN-C4O-olig** was closer to a molecular structure rather than a polymer. Importantly, no melting peak has been observed on the DSC chart. We supposed that the latter was expected at higher temperature with respect to molecular brick **1b** but the dehydrogenation happened first. This last observation suggested that in the case of polyboramines, a melting endotherm was very unlikely to exist and that consequently, endothermic waves observed corresponded exclusively with a dehydrogenation process.

Additional *in situ* IR monitoring confirmed the qualitative result observed for **Ar-BN-C4O-olig** showing that the B-H stretching ( $\nu = 2313 \text{ cm}^{-1}$ ) started to decrease from 110 °C until its complete disappearance at 180 °C (Figure 49).

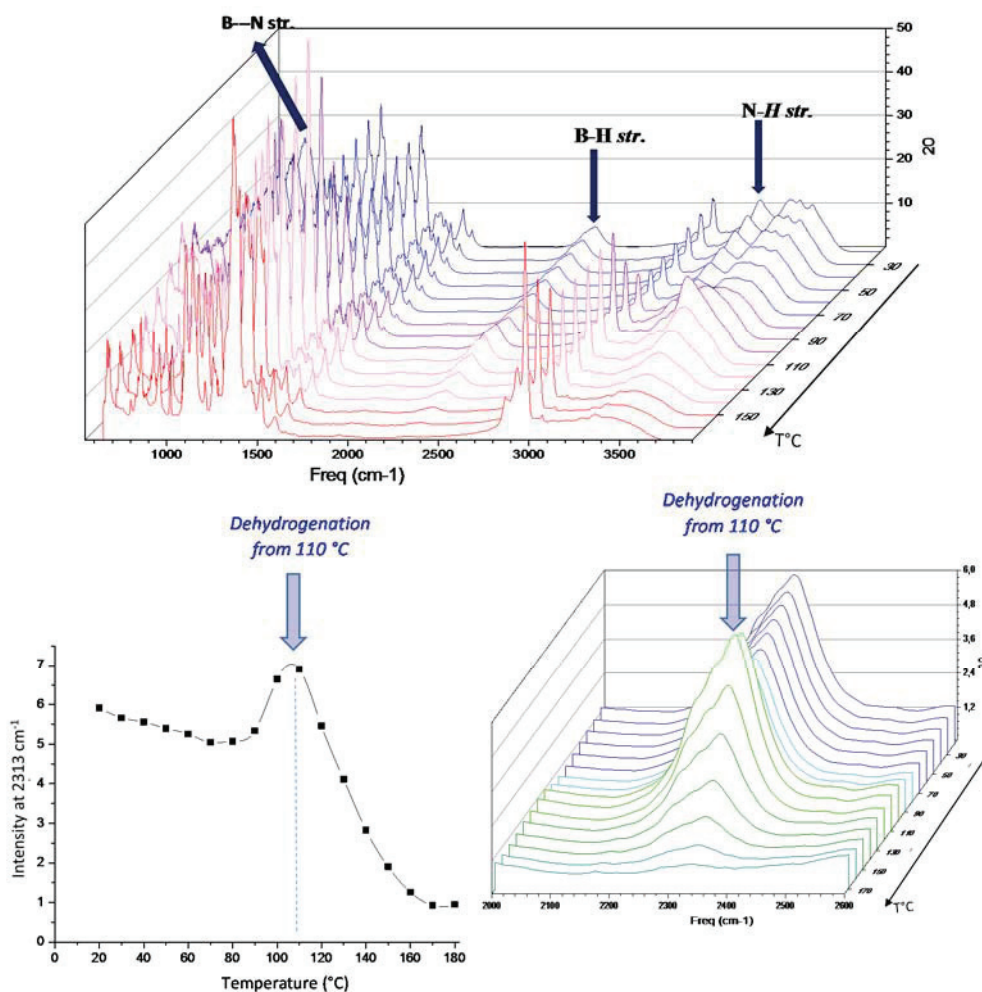


Figure 49. Thermal dehydrogenation of **Ar-BN-C4O-olig**. IR-In situ monitoring.

### III.6.f. Characterization of dehydrogenated structures and hypotheses

We aimed at analyzing the polyboramine **Ar-BN-C4O** after thermal dehydrogenation. The dehydrogenated polymer has been called **Ar-BN-C4O-Dh**. **Ar-BN-C4O-Dh** was recovered as a white solid, similar to the starting material, in contrast with AB that led to important foaming during the process (Figure 50).

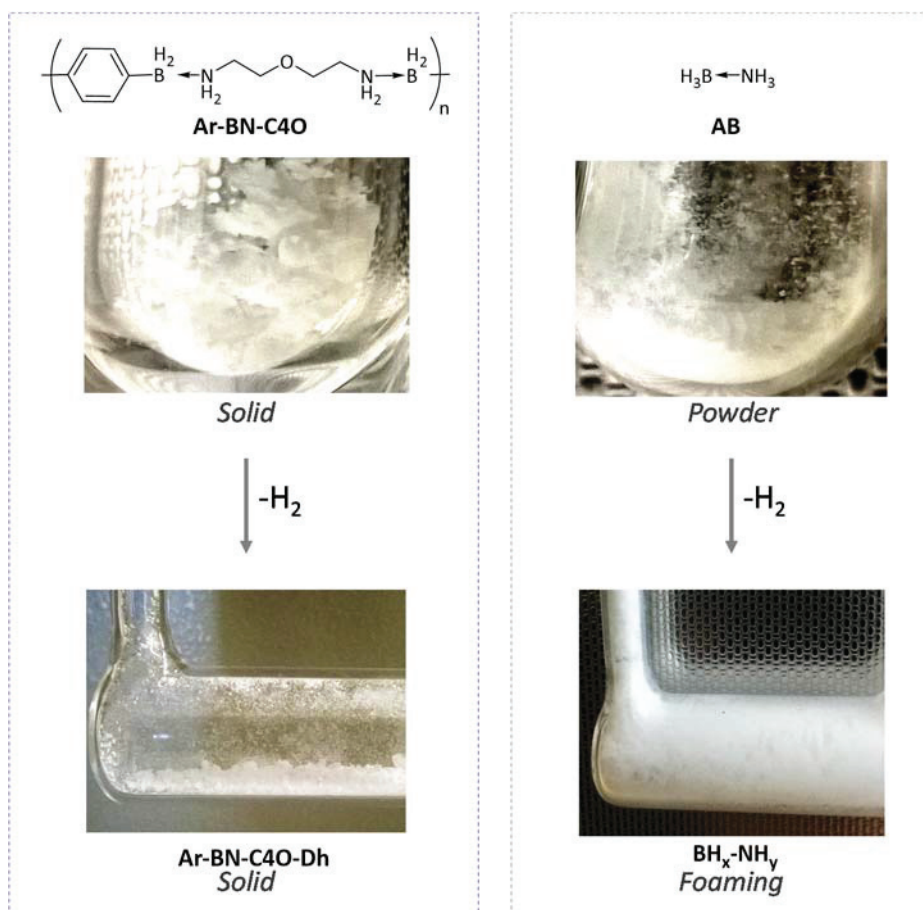


Figure 50. Visuals of polymer (left) and AB (right) before and after thermal treatment.

The new polymer **Ar-BN-C4O-Dh** obtained after isothermal dehydrogenation of **Ar-BN-C4O** at 160 °C has been analyzed. The white solid was poorly soluble in most organic solvents, except in a DMF / 0.5 wt% LiBr solution. We used this mixture as an eluent for DMF-SEC analysis at 60 °C to maximize the solubility (Figure 51). The chromatogram showed higher molar masses with respect to the original polyboramine ( $> 5.10^5$  g/mol). The dehydrogenation appeared to increase the masses rather than to induce chain scissions. This behavior came from the formation of boron-nitrogen bonds between the chains. The formation of covalent B-N bonds are well known to occur during the

dehydrogenation of AB and to be responsible of the formation of highly stable and almost inert products. Nevertheless, due to steric and mobility limitations induced by the polymer chains, we expected the formation of B-N bond to be less important than with molecular counterparts.

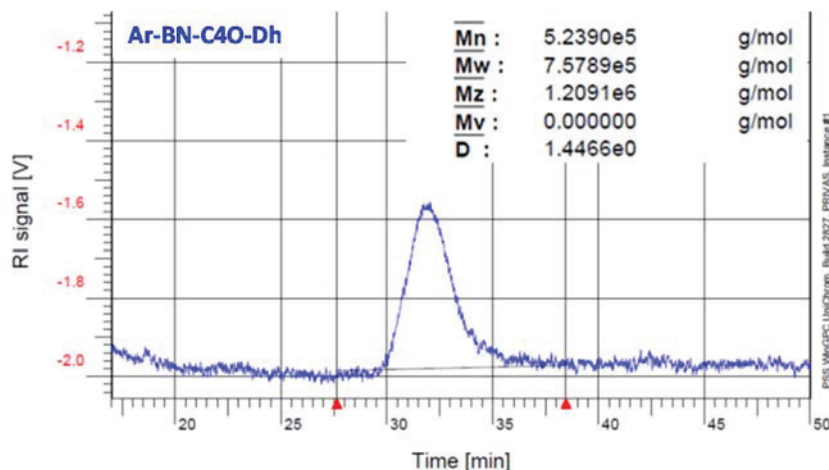


Figure 51. SEC of polymer Ar-BN-C4O after thermal treatment. Eluent: DMF + 0.5 w% LiBr. Temperature of column 60°C.

Both the dehydrogenated polyboramine **Ar-BN-C4O-Dh** and molecular analogue **1b-Dh** were subjected to solid state  $^{11}\text{B}$  MAS-NMR analysis. Due to the quadrupolar nature of the boron nucleus, chemical shifts could not be determined accurately in the solid state. Nevertheless, a qualitative comparative approach has been possible as the two NMR spectra were found to be similar. In both cases the NMR spectra showed the presence of two large peaks at  $\sim 0$  ppm (Figure 52, I and I') and  $\sim 16$ -23 ppm (Figure 52, II and II') indicating the presence of two types of structures. Based on literature data, chemical shifts I and I' could be attributed either to the aminoborane dimer (c.f., e.g.,  $[\text{Me}_2\text{N-BH}_2]_2$   $\delta = 4$  ppm,<sup>62a</sup>  $[\text{MeNH-BMe}_2]_2$   $\delta = 1$  ppm,  $[\text{Me}_2\text{N-BF}_2]_2$   $\delta = 0.9$  ppm<sup>89</sup> or to the linear iminoborane (c.f., e.g.,  $\text{Me}_2\text{HCN}\equiv\text{BMes}$   $\delta = 4.3$  ppm,  $\text{Me}_3\text{CN}\equiv\text{BMes}$   $\delta = 4.3$  ppm,  $\text{Me}_3\text{SiN}\equiv\text{BMes}$   $\delta = 20.5$  ppm<sup>89</sup>) (Figure 52 and Figure 53). According to experimental data reported above indicating that the large majority of hydrogen content has been released during the thermal treatment of the material, the second hypothesis appeared to be the most probable.

It is important to stress out that the formation of B-N bonds during the thermal treatment is prone to increase the molecular weight both for the polymer and for the molecular model. Particularly, since the latter had a bifunctional structure, it could behave during

dehydrogenation as a bifunctional monomer and form polymeric structures through the establishment of B-N bonds (Figure 53b).

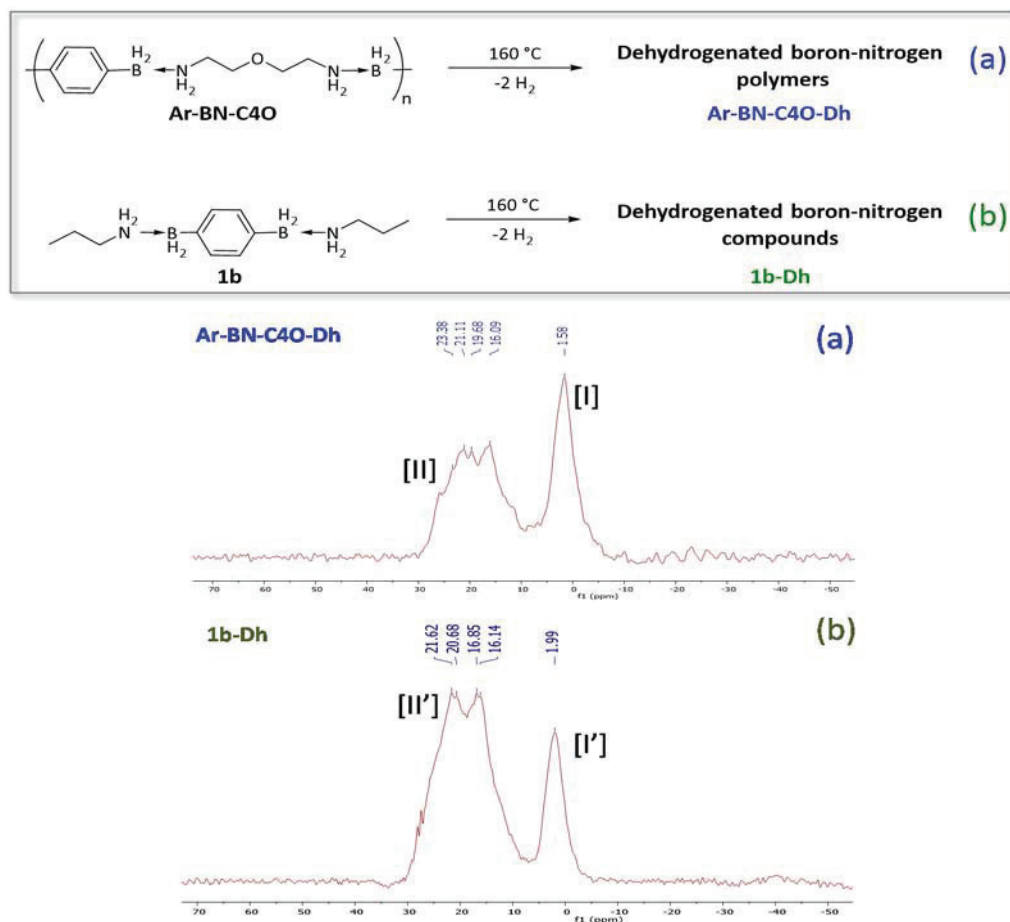


Figure 52.  $^{11}\text{B}$  MAS NMR spectra of thermally dehydrogenated Ar-BN-C4O and 1b to give (a) Ar-BN-C4O-Dh and (b) 1b-Dh

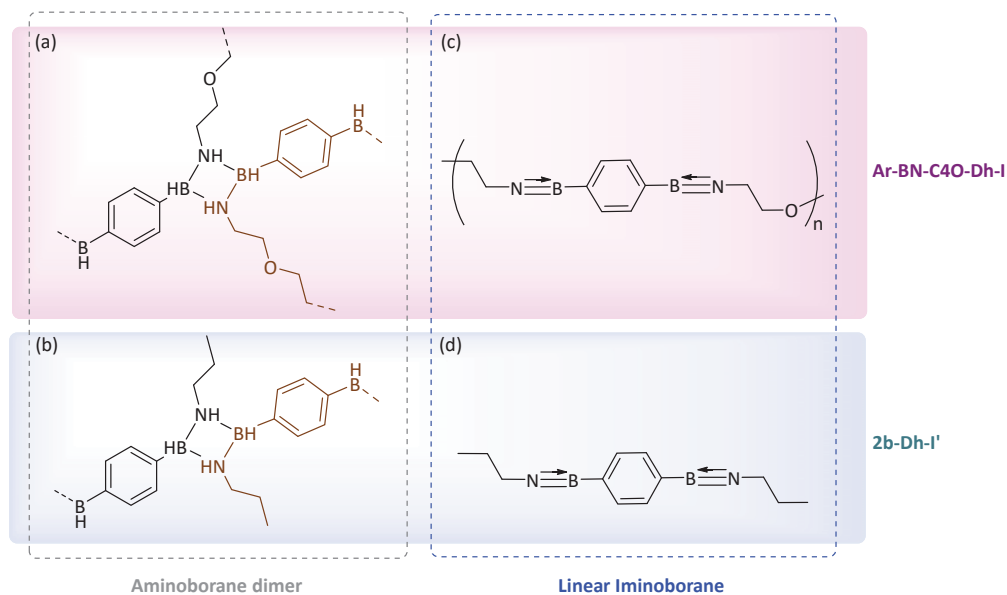
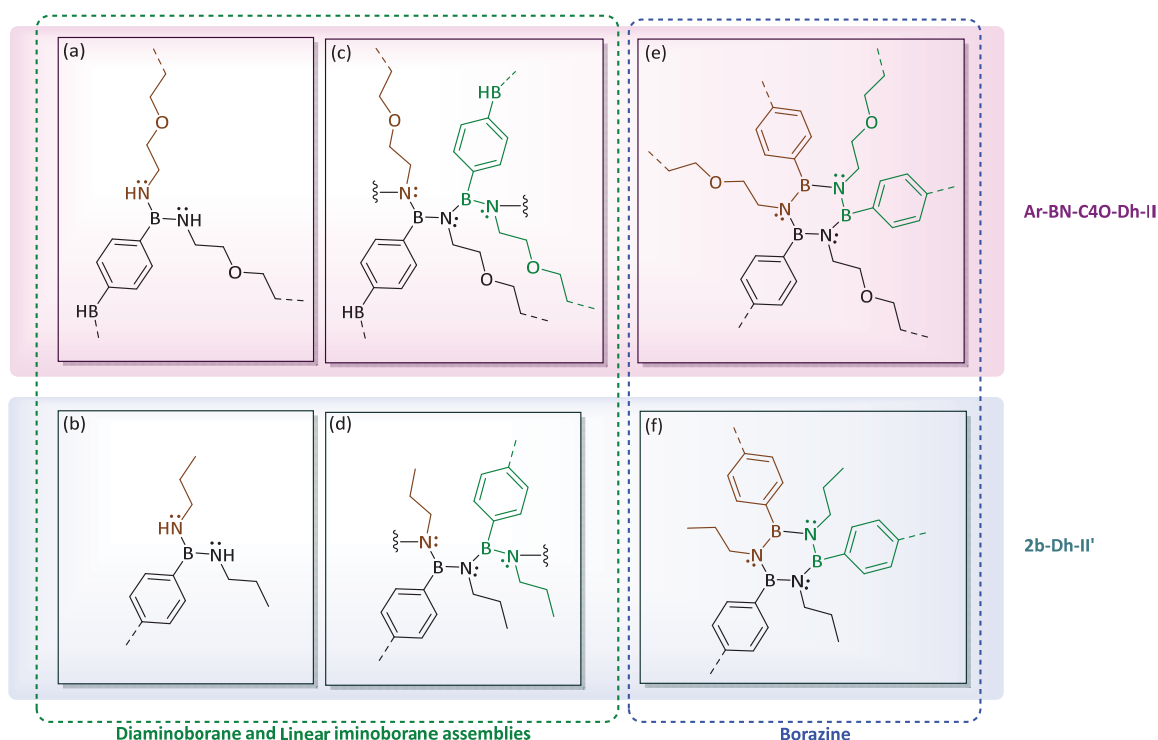


Figure 53. Hypothetical structures attributed to I and I' peaks: (a), (c) polymer Ar-BN-C4O-Dh-I and (b), (d) molecular brick 1b-I'.



The second  $^{11}\text{B}$  NMR peak mass **II** and **II'** showed a mixture of several species. They shifted to an unusual zone of chemical shifts ranging from 16 ppm to 24 ppm (Figure 52). Based on literature data, these structures could correspond to diamino-boranes (i.e., e.g.,  $\text{ArNH}[\text{BH}]\text{NHAr}$   $\delta = 26 \text{ ppm}^{93}$ ) (Figure 54a and b) and by extension of this hypothesis, to different oligomeric forms of linear iminoboranes (Figure 54c and d). Among other possibilities, the 13-26 ppm peak mass was likely to include some borazine units (i.e., e.g.,  $[\text{NAr}=\text{BH}]_3$   $\delta = 31.4\text{-}32.3 \text{ ppm}^{93}$ ) (Figure 54e and f).



**Figure 54.** Hypothetical structures attributed to **II** and **II'** peak masses. For polymer **Ar-BN-C4O-Dh-II**, and molecular brick **1b-Dh-II'**. Respectively: (a) and (b) diaminoborane, (c) and (d) linear iminoborane assemblies obtained by extension of the diaminoborane, (e) and (f) borazine.

Interestingly, the two  $^{11}\text{B}$  NMR spectra displayed differences. The relative intensity of the two peaks appeared to be different and suggested that the polyboramine and the molecular brick could have a different reactivity. For the polymer **Ar-BN-C4O-Dh**, the peak of major intensity was **I** (Figure 52a) and potentially corresponded to the linear iminoborane species (Figure 53c). Whereas, in the case of **1b-Dh**, the peak mass **II'** was the most abundant (Figure 52b), and could correspond to iminoborane oligomers and cyclic structures (Figure 54b, d, f).

Structural differences between the polyboramine and the molecular model were very likely due to mobility limitations brought by the polymer backbone. Thus, we supposed that the polymer backbone limited the formation of B-N bonds by adding substantial rigidity to the network. Further investigations are ongoing to determine more precisely the structure of the species formed and to further understand the role of the polymer backbone in the stabilization dehydrogenated species (Figure 55).

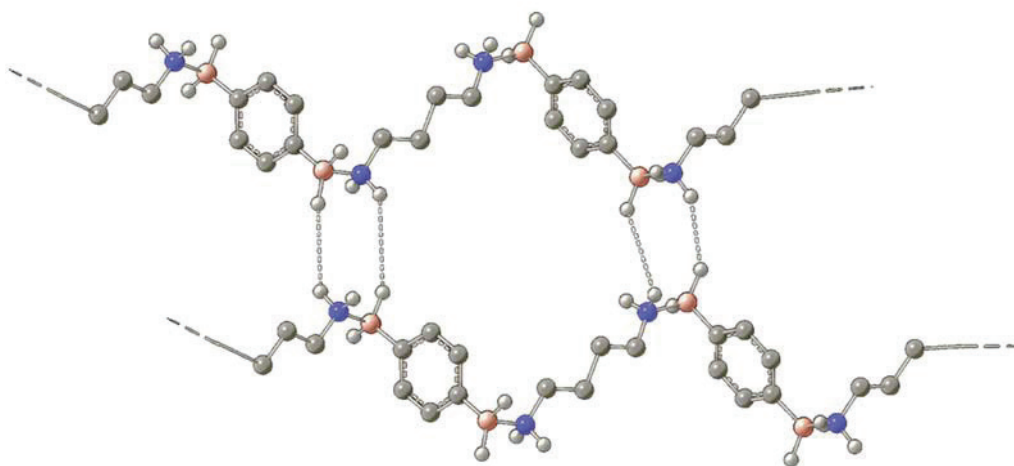


Figure 55. Artistic representation of the polyboramine Ar-BN-C4, helping to visualize the polymer backbone.

### III.7. Mechanistic investigation

---

We have demonstrated that polyboramines were more than the sum of their monomeric equivalents. The polymer chains have brought additional properties as evidenced in the thermal dehydrogenation process. To understand better the phenomena linked to  $H_2$  release, we carried out DFT computational studies, in collaboration with Dr. Paolo Larini. Our aim was focused on understanding the influence of substituents and backbone on the reactivity of both molecular surrogates and polyboramines. Insights on kinetics and thermodynamics of hydrogen storage have helped to orient our hypotheses. We used a fragment *n*-propylamine-4-phenylborane ( $nPrNH_2-BH_2Ph$ , **NBH<sub>2</sub>-mon**) (Figure 56) that was chosen as a good compromise between a good representation of the reality and computational demand.



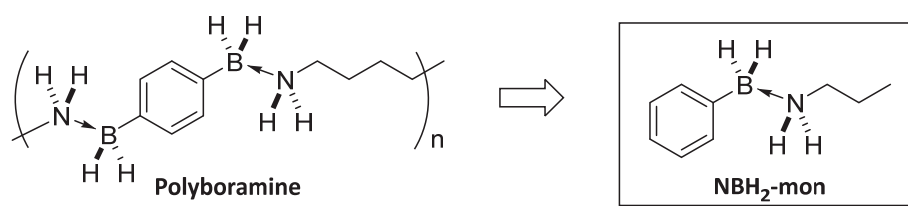


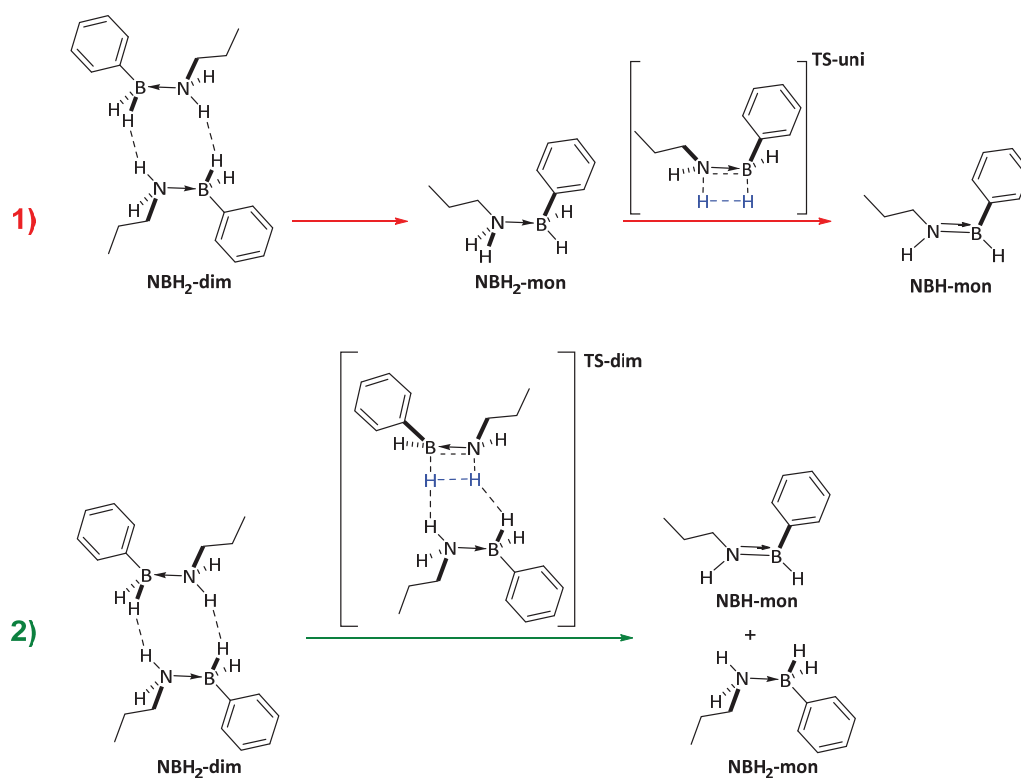
Figure S6. Choice of the molecular model for DFT calculation

The computational modelling of amine-borane bond was not straightforward since the latter was based on a Lewis-pair interaction. We aimed at finding alternative computational methods that were not too computationally demanding but still precise enough to evaluate the bond dissociation energy (BDE) of B-N bonds in amine-boranes, as well as energies of DHBs. Thus, a benchmark was carried out using the AB dissociation energy as a reference.<sup>94</sup> The B97D3 functional was selected, since it could give the best accordance with experimental BDE of AB. Of note, this functional has also been used by Grimme *et al.* to compute frustrated Lewis-pairs.<sup>95</sup>

The dehydrogenation mechanism of **NBH<sub>2</sub>-mon** involved several pathways.<sup>3,47,53-54,86a,96</sup> In this manuscript, the study has been restricted to the first dehydrogenation step. Further investigations are ongoing regarding the second dehydrogenation step<sup>54</sup> (aminoborane to iminoborane)

**NBH<sub>2</sub>-mon** dimer (that has been noted **NBH<sub>2</sub>-dim** hereafter) was found to be the most stable structure as it was stabilized by DHB interactions between the N-H and the B-H moieties. It was calculated that DHBs within **NBH<sub>2</sub>-dim** accounted for 6.25 kcal/mol/DHB (in comparison in **AB** they represented 7.0 kcal/mol/DHB<sup>3</sup>). **NBH<sub>2</sub>-dim** has been defined as the default energy reference of the molecular model.

Four pathways have been identified starting from **NBH<sub>2</sub>-dim**. Two of them involved intramolecular four-membered transition state (TS) (Scheme 27 and Figure S7) and were too high in energy to occur. In fact, starting from **NBH<sub>2</sub>-dim**, the four membered TS involved the previous break of DHBs to obtain the "single" amine-borane **NBH<sub>2</sub>-mon**. (Scheme 27, eq. 1, Figure S7, green path).



Scheme 27. Illustration of red and green pathways involving four membered transition states.

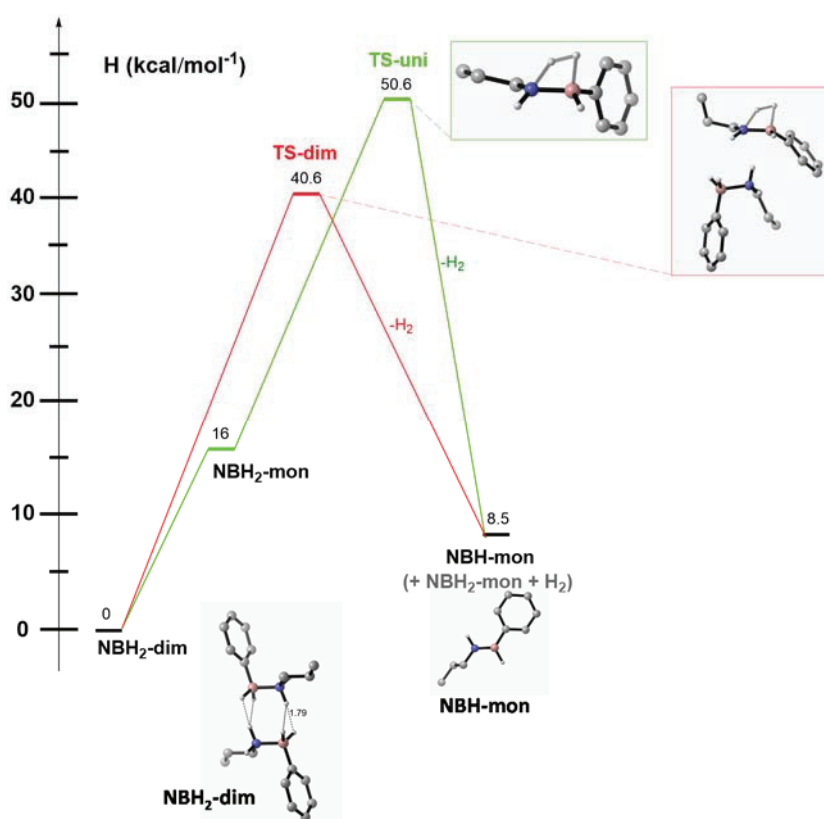
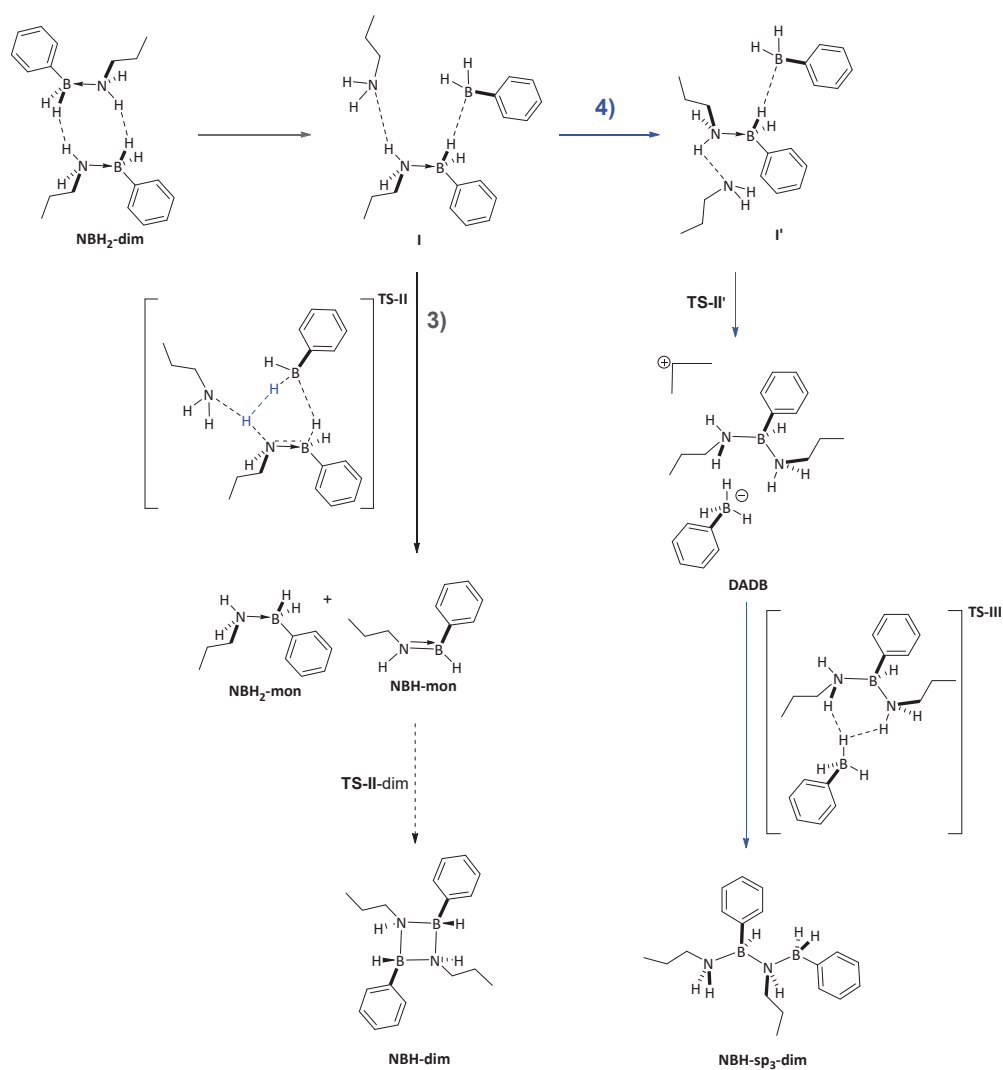


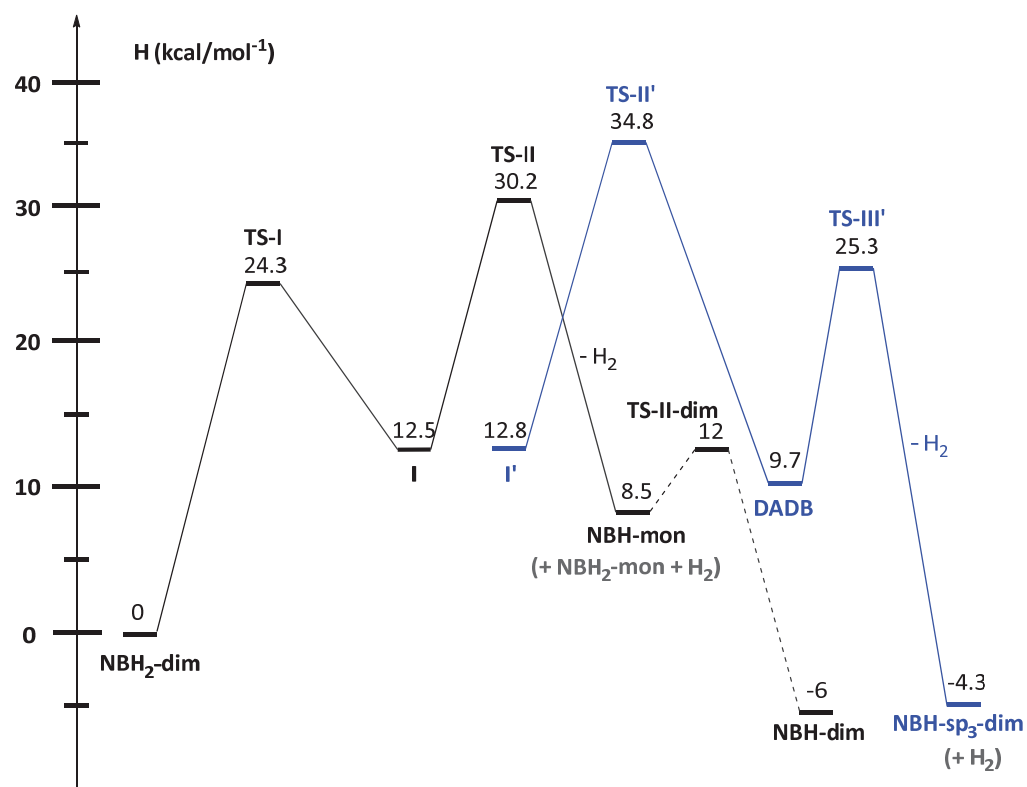
Figure 57. The two unfavorable pathways involving four-membered intramolecular TS.

From these, the release of  $H_2$  required 35 kcal/mol to reach **TS-uni**. Alternatively, starting directly from **NBH<sub>2</sub>-dim**, the **TS-dim** was much higher in energy (40.6 kcal/mol, Figure 57, red path, Scheme 27, eq. 2).

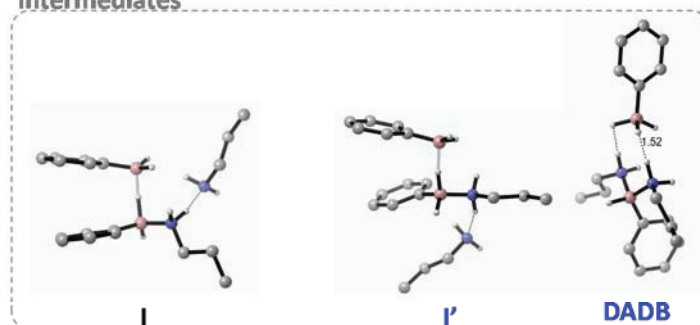
In summary, these two first pathways which represented a direct release of  $H_2$  through an intramolecular four membered TS, generated the aminoborane monomer **NBH-mon** (Figure 57, Scheme 27) in both cases. However, these mechanisms involved activation barriers that were too high in energy to fit with our experimental conditions (i.e. with the observed temperature range of  $H_2$  release). In other words, alternative pathways explaining the release of dihydrogen were very likely to exist at lower energy.



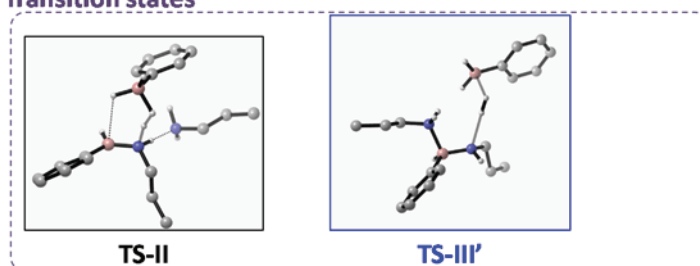
*Scheme 28. Illustration of black and blue pathways involving six-membered transition states*



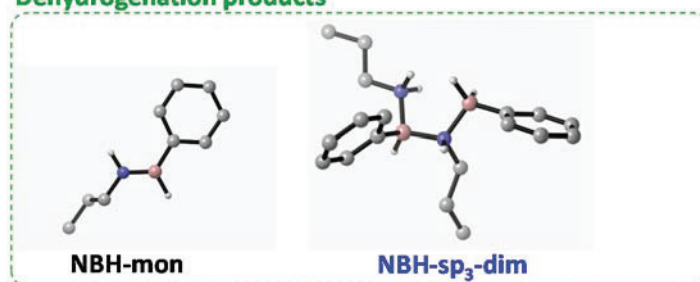
## Intermediates



## Transition states



## Dehydrogenation products



## Post dehydrogenation products

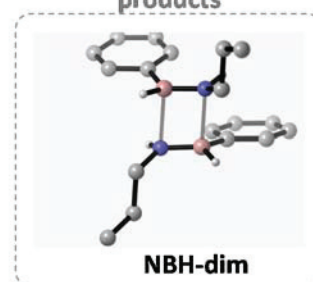


Figure 58. The two pathway involving bimolecular six-membered transition state

Actually the cleavage of a B-N bond in **NBH<sub>2</sub>-dim** structure (Scheme 28, Figure 58) giving the intermediate **I** (*via* **TS-I**), yielded two dehydrogenation pathways that were significantly more favorable. Intermediate **I** was prone to form a B-H-B, 3 centers-2 electrons bond that was observed in **TS-II** six-membered TS of 17.7 kcal/mol (from 12.5 to 30.2 kcal/mol, Scheme 28, eq. 3, Figure 58, black path). This pathway led to the formation of the aminoborane monomer **NBH-mon** accompanied by one equivalent of unreacted **NBH<sub>2</sub>-mon**. The aminoborane monomer **NBH-mon** underwent a subsequent side-reaction by formation of intermolecular covalent B-N bonds. This reaction appeared thermodynamically very favorable. In our system, the dimerization of two molecules of **NBH-mon** (**TS-II-dim**), gave the aminoborane dimer (**NBH-dim**) and was exothermic by 17 kcal/mol. It has been also reported that aminoborane monomers could also generate other species such as linear dimers and oligomers.<sup>54</sup>

The last pathway involved the formation of the **DADB** ionic pair (Scheme 28, eq. 4, Figure 58, blue path). In this pathway, **I'** was obtained from **I** by the rotation along the B-N and underwent the rearrangement *via* **TS-II'** to give **DADB** as product with an energy barrier of 21.8 kcal/mol (from 12.8 to 34.8 kcal/mol). From **DADB**, molecular dihydrogen was generated through transition state **TS-III'** (15.6 kcal/mol from 9.7 to 25.3 kcal/mol), yielding the dehydrogenation product **NBH-sp<sub>3</sub>-dim**. This type of structure has been called in the literature “sp<sub>3</sub> dimer” of aminoboranes.<sup>54</sup>

These two pathways appeared to be globally exothermic (and particularly very exoergique)<sup>17</sup> with moderately high TS. Consequently, the selectivity was governed by kinetic control. By comparing the determining rate-limiting steps of the black and blue pathways, the formation of **DADB** was less favorable than the direct dehydrogenation from **I** because **TS-II'** leading to **DADB** was 4.6 kcal/mol higher than **TS-II** leading to the dehydrogenated **NBH-mon** (Figure 59, left). This result differed from the dehydrogenation profile of **AB** reported by Dixon and co-workers, in which the rate limiting step TS leading to **AB-DADB** was only 2.0 kcal/mol higher than the TS leading to the dehydrogenated **AB-NBH-mon** (Figure 59, right). Consequently, the experimental observation of the **DADB** compound could be less expected within our N-*n*-propyl, B-aryl substituted amine-borane system.

Theoretical investigations gave us information at a molecular level about the effects of the B-aryl and N-propyl amine-borane substituents with respect to AB, on competitive dehydrogenation pathways. It appeared that the presence of these substituents did not favor the formation of DADB but favored the dehydrogenation directly from the 2electrons-3centers complex. By extension we assumed that it was unlikely that the formation of DADB occurred within the polymer since it would require substantial, energetically unfavorable chain rearrangements. Thus, we supposed that **TS-II** to be substantially lower in energy in the dehydrogenation mechanism of polymers.

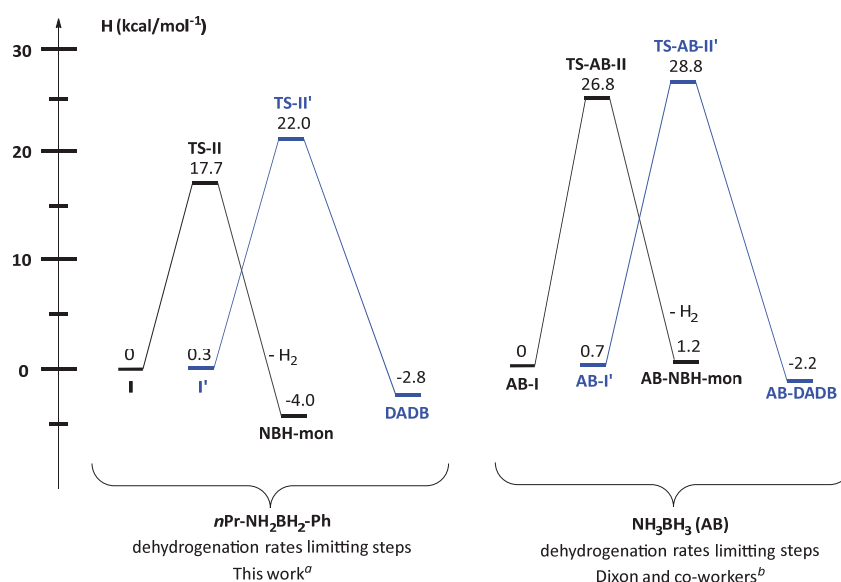


**Figure 59. Comparison of rate limiting steps transition states between  $n\text{Pr-NH}_2\text{BH}_2\text{-Ph}$  calculated in this work and  $\text{AB}$  calculated by Dixon and co-workers. Respectively, **I** and **AB-I** were chosen as the default energy reference. <sup>a</sup> *ref.*<sup>17</sup>, <sup>b</sup>*ref.*<sup>3</sup>**

### III.8. Hypotheses related to the influence of polymer backbone in polyboramines supported by computational data.

#### III.8.a. Entropic effects

The presence of a polymer scaffold within amine-borane functions brought significant rigidity to the system and was expected to modify energies in intermediates and transition states. We compared in particular the steps of  $H_2$ -release for the black and blue dehydrogenation pathways.

In the blue pathway, the formation of aminoborane  $sp_3$ -dimer (**NBH- $sp_3$ -dim**), was likely to be strongly limited by mobility limitations induced by the polymer backbone (Figure 60) because it would lead to the formation of highly reticulated three-dimensional networks and would require considerable entropy to be lost.

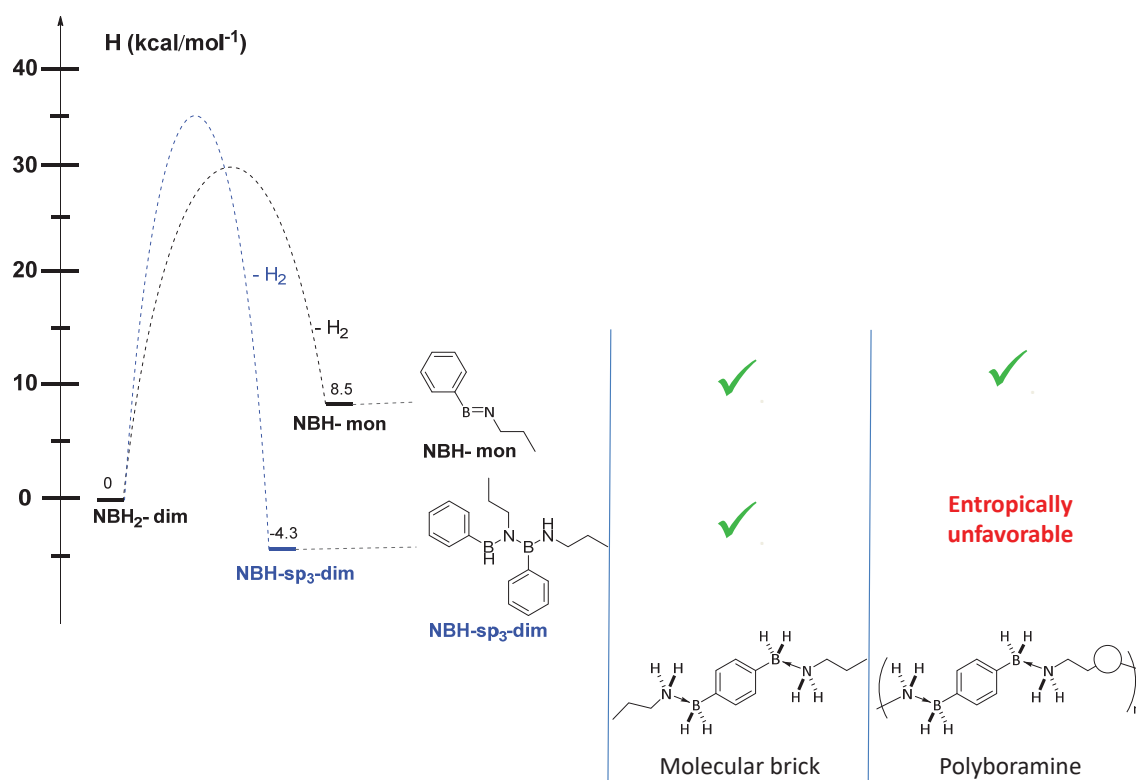


Figure 60. Comparison of the two dehydrogenation steps leading to aminoborane monomer (**NBH-mon**) or  $sp_3$  dimer (**NBH- $sp_3$ -dim**) and envisioned effects of the polymer backbone

In contrast, the macromolecular environment having less conformational mobility than single molecules, could be more prone to stabilize aminoboranes species in their

monomeric form, that likely led to decrease the proportion of dimerization leading to **NBH-dim**. The potential discrimination of the polymer in favor of the black pathway could therefore explain the difference observed in  $^{11}\text{B}$  NMR between the dehydrogenated polymer and its molecular counterpart (see chapter III.6.f of this section)

The theoretical mechanistic pathway showed that the formation of the aminoborane "monomer" was globally an endothermic reaction, in contrast with the formation of covalent B-N bonds, either to form **NBH-dim** or **NBH-sp<sub>3</sub>-dim**, that were instead very exothermic. In fact, we assumed that the endotherm observed for the polyboramine dehydrogenation (chapter III.6) has been the result of a reduced mobility induced by the macromolecular structure that limited the formation of exothermic covalent B-N bonds between dehydrogenated species.

### III.8.b.End-of-chains and dissociation bond-energy

DSC and TPD analyses showed that the polyboramine had a propensity to dehydrogenate at lower temperature than its molecular analogue (chapter III.6). In contrast with molecular species, polymer chains do have isolated amine or dihydroborane chain-ends functions. Meanwhile, it has been proposed (in black and blue pathway) that the dissociation of an amine-borane bond initiated the dehydrogenation and that the isolated borane was involved in the dehydrogenation TS. From these facts, we think that polyboramine end-of-chains act as pre-activated nuclei to trigger the dehydrogenation.

Moreover, the study reported in the literature of bipyridine-bisborane<sup>75</sup> and pyrazine-bisborane<sup>76</sup> in the main-chain of polymers and as single model molecules suggested that polymers had more propensity to dissociate in solution than the molecular analogue and that concentration effects have an influence on the BN bond chemical shift that is linked to the strength of the adduct. In our case, we believe that the polymer structure favored the cleavage of the amine-borane dative bonds due to reduced degrees of mobility within the system that increased strains onto amine-borane bond.



Secondly, recent studies highlighted the catalytic effect of monomeric aminoboranes monomer in the dehydrogenation pathway,<sup>54</sup> which likely explained the suspected autocatalysis pattern observed on AB dehydrogenation. The polymer backbone was thought to stabilize part of aminoborane monomers and consequently could catalyze the dehydrogenation. These assumptions proposed an explanation to answer why polyboramines dehydrogenate 30 °C lower than their molecular counterparts.

### III.8.c. Pre-organised backbone oriented structure

Conversely, a cooperative zip-like behavior arising from the secondary structure adopted by the polymer chains might be also at play. A preorganization could have a templating effect *via* the establishment of amine-borane DHB dimers by analogy with peptides which adopted a helicoidally conformation through conventional hydrogen bonding along the polymer chain. In that case, direct H<sub>2</sub> release via a neutral intermediate would be again favored.

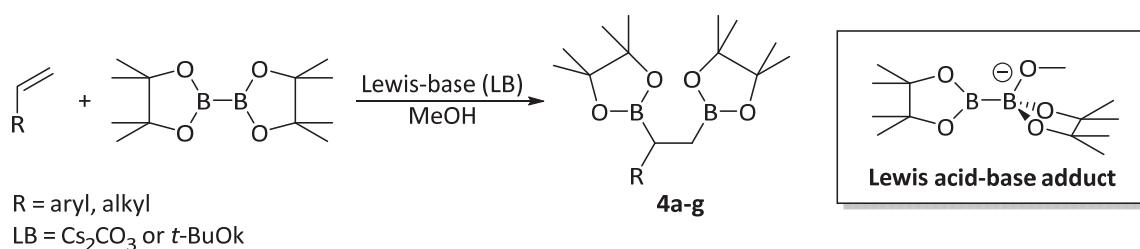
We are currently investigating advanced simulations and characterization technics to figure out the exact role of the polymer backbone. First, in collaboration with David Gajan (CRMN, Lyon) and Jasmine Viger-Gravel (Prof Emsley group, EPFL, Switzerland), MAS-NMR studies are ongoing to determine with accuracy the nature of species formed during and after hydrogen release. Moreover we are performing a comparative kinetical study by MAS-NMR monitoring, between a polyboramine and a molecular brick. We wish to observe the relative amount of intermediates (DADB, 3 centers-2 electrons complex, etc.) and to observe eventually differences in reaction pathways. Second, in collaboration with Paolo Larini (ITEMM, ICBMS, Lyon) and Fabrice Brunel (C2P2, Lyon), we are investigating polymer structure modeling by using MM technics in order to identify the most favorable conformations adopted by the polyboramines.

### III.9. Extension of the family of polyboramines, synthesis of bisboronic monomers and applications in polymerization.

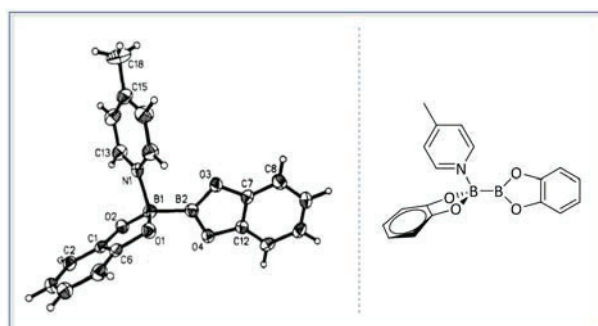
We aimed at extending the family of polyboramines by varying the bisboronic monomer. Only a few bisboronic acids or esters are commercially available. To synthesize new bisboronic monomers, we sought efficient methodologies affording gram quantities of either aliphatic or unsaturated bisboronic acid or esters monomers at reasonable costs. The first part of this work has been achieved during my student visiting to Todd Marder's group (university of Würzburg, Germany) in which I spent six weeks.

#### III.9.a. Metal-free diboration of alkenes.

We synthesized a range of ethylene bisboronic pinacol esters **4a-g** using a metal-free diboration procedure reported by H. Fernandez and co-workers.<sup>97</sup> The reaction employed pinacol diboronate ( $B_2Pin_2$ ) as the boron-source. The authors proposed that the latter was activated in presence of a Lewis-base to form a Lewis acid-base adduct being the reactive species (Scheme 29). A diboronate Lewis-acid/base adduct was actually previously isolated by T. Marder and co-workers<sup>98</sup> by crystallization. (Figure 61).



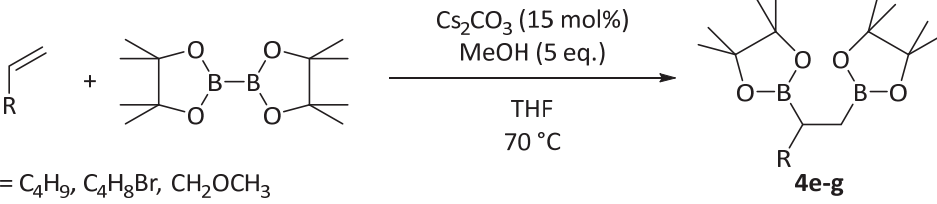
*Scheme 29. Metal-free diboration of alkenes through the formation of a postulated Lewis acid-base adduct as a key-intermediate.*



*Figure 61. Crystal structure of the 4-methylpyridine adduct of bis(dithiocatecholato)-diboron.<sup>98a</sup>*

The reaction was performed on aliphatic alkenes, using cesium carbonate as the activating agent following the reported procedure<sup>97</sup> (Table 12). Pinacol ethylene bisboronates derivatives were recovered in good yields and full selectivity. Isolation by column chromatography turned out to be difficult due to their important polarity.

**Table 12. Metal-free diboration of aliphatic alkenes.**

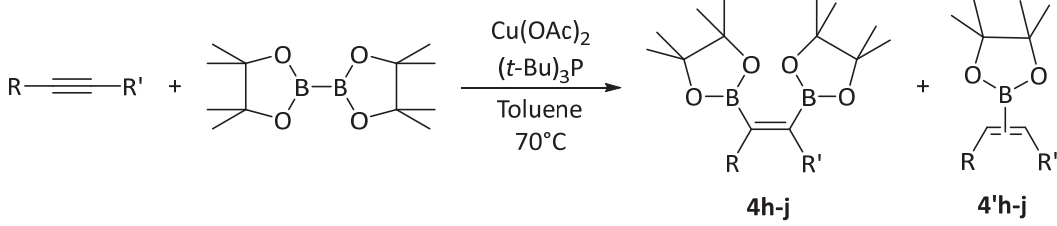
 <p>R = C<sub>4</sub>H<sub>9</sub>, C<sub>4</sub>H<sub>8</sub>Br, CH<sub>2</sub>OCH<sub>3</sub></p> <p>4e-g</p>				
Entry	R =	Product	Conversion [%] <sup>a,b</sup>	Selectivity [%] <sup>a,b</sup>
1	C <sub>4</sub> H <sub>9</sub>	<b>4e</b>	> 99	> 99
2	C <sub>4</sub> H <sub>9</sub> Br	<b>4f</b>	94	> 99
3	CH <sub>2</sub> OCH <sub>3</sub>	<b>4g</b>	86	> 99

<sup>a</sup>Determined by GCMS <sup>b</sup>Conversion and selectivity relative to of **4e-g**

### III.9.b. Copper-catalysed diboration of non-terminal alkynes

We adapted the methodology of copper-catalyzed diboration of alkynes from a publication reported by Yoshida and co-workers.<sup>99</sup> Product **4h** was obtained quantitatively and selectively in toluene, using t-Bu<sub>3</sub>P/Cu(OAc)<sub>2</sub> as the precatalyst (Table 13, entry 1).

**Table 13. Copper catalyzed diboration of alkynes.**

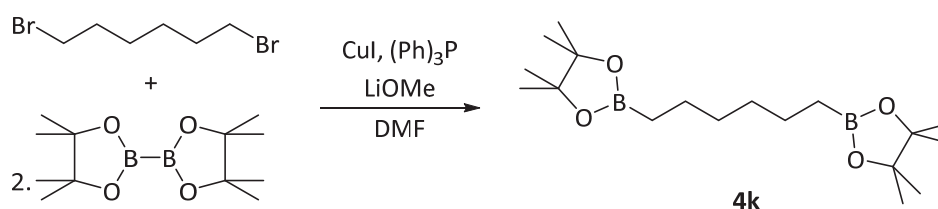
 <p>4h-j      4'h-j</p>					
Entry	R =	R' =	Product	Conversion [%] <sup>a,b</sup>	Selectivity [%] <sup>a,b</sup>
1	C <sub>3</sub> H <sub>7</sub>	C <sub>3</sub> H <sub>7</sub>	<b>4h</b>	> 99	> 99
2	Ph	Ph	<b>4i</b>	40	70
3	4-Me-Ph	SiMe <sub>3</sub>	<b>4j</b>	5	-

<sup>a</sup>Determined by GCMS <sup>b</sup>Conversion and selectivity relative to of **4e-g**

The presence of small amounts of methanol or water within the reaction mixture yielded hydroborated products. Phenyl substituted alkynes displayed low conversions and generated mainly hydroborated products (70 %) (Table 13, entry 2). Finally electron-rich silyl-substituted alkynes did not react (Table 13, entry 3).

### III.9.c. Copper catalyzed C-Br boration

The C-Br boration catalyzed by copper with triphenylphosphine ligand, reported by Marder and co-workers<sup>100</sup> was particularly versatile, as it allowed to afford a wide range of bisboronic monomers. We applied the procedure to the synthesis of pinacol hexylenebisboronate **4k**. The reaction was very selective and the product has been isolated in good yield (83%) after column chromatography purification.



*Scheme 30. Copper catalyzed diboration of the 1,6-dibromohexane*

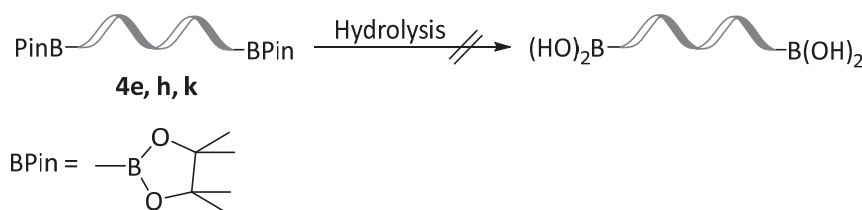
Finally, compounds **4e**, **4h** and **4k** have been selected for a scale-up on gram-scale, for polymerization applications.

### III.9.d. Use of bisboron monomers in polymerization

This project has been carried out with the help of Xavier Ingouf and Sebastien Lasalle, whom I have supervised for 3 months.

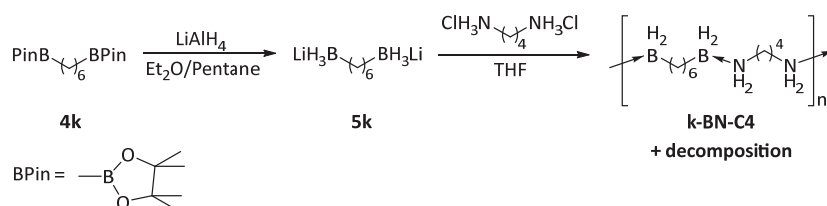
We engaged bisboron monomers **4e**, **4h** and **4k** in the synthesis of new polyboramines. We first aimed at applying the one-pot methodology developed previously (see chapter III.2 in this section) to access the new polyboramines. Our previous results suggested that engaging pinacol bisboronate species as the diboron monomer led only to the formation of oligomers and to the presence of pinacol and aluminum residues within the product. Actually, the methodology required the use of boronic acids to generate aluminum oxides side-products that were insoluble in THF and thus easily removable. Our attempts to

hydrolyze quantitatively pinacol bisboronate monomers to bisboronic acids have failed. Mixtures of inseparable products were formed. (Scheme 31). Only monomer **4k** has been hydrolyzed in moderate yields following a procedure reported in the literature.<sup>100</sup>



*Scheme 31. Mainly unsuccessful hydrolysis of pinacol bisboronate species.*

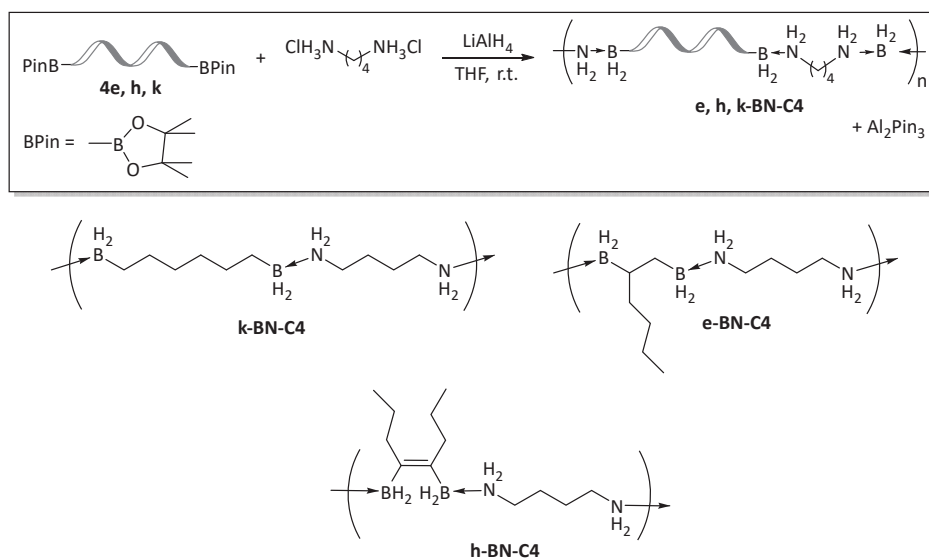
Consequently we looked for alternative ways to afford cleanly polyboramines directly from the bisboronate monomers **4e**, **4h** and **4k** displaying pinacol boronate functions. We thus re-investigated the two-step procedure (discussed in chapter III.2.a). The synthesis of bistris(hydrido)borate **5k** from **4k** was readily synthesized quantitatively (Scheme 32). After isolation, **5k** was used in the second step to react with butylene diammonium chloride in THF affording the amine-borane accompanied by the release of gas. Analyses in <sup>11</sup>B NMR spectroscopy indicated the presence of two triplets at  $\delta = -7.33$  and  $-8.35$  ppm characteristic of the amine-borane function. In addition, the reaction was accompanied by significant precipitation. In fact, analysis of the crude in IR spectroscopy indicated only minute B-H amine-borane elongation band suggesting a partial decomposition of the polymer by dehydrogenation.



*Scheme 32. Two-steps synthesis of polyboramine k-BN-C4 led to partial decomposition.*

The one-pot reaction developed in our laboratory and discussed in chapter III.2.b, was finally applied directly to the pinacol bisboronate monomers instead of bisboronic acids. The three-component reaction consisting in adding LiAlH<sub>4</sub> to a suspension mixture of the two monomers bisboron and diamino were performed in THF at room temperature. Previously synthesized monomers **4e**, **4h**, **4k** were utilized (Scheme 33) yielding

polyboramines **e**, **h**, **k-BN-C4** quantitatively accompanied by amount of pinacol aluminate that we have not yet managed in separating.



**Scheme 33.** One-pot synthesis of polyboramines **e**, **h**, **k-BN-C4** from pinacol bisboronate precursor in THF.

We selected  $n\text{PrNH}_2$ - $n\text{BuBH}_2$  **1a** as a representative molecular brick to compare the spectroscopic data. The  $^{11}\text{B}$  NMR signal of **1a** was a thin triplet at  $\delta = -10.6$  ppm (Figure 62). Polymer **k-BN-C4** displayed a substantially broader signal centered at  $\delta = -13.0$  ppm (Figure 63) as well as another peak at  $\delta = 32.0$  ppm. The latter indicated a partial degradation of the amine-borane bond. We knew from our previous studies that engaging a pinacol boronate monomer into the reaction leads to the solvation of important amounts of aluminum in the mixture. The latter has been suspected to induced degradation of the material in solution probably by dehydrogenation.

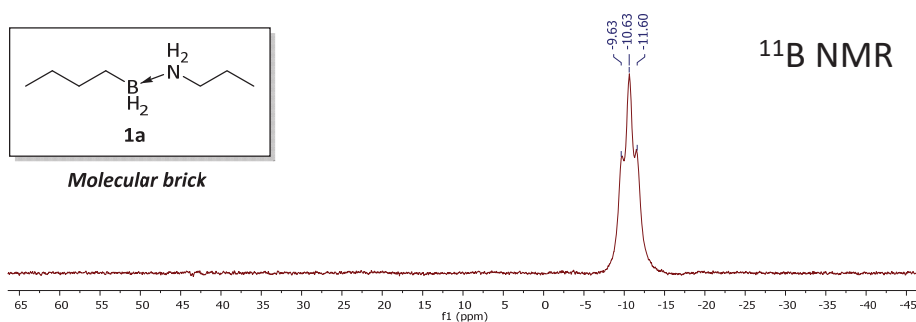


**Figure 62.**  $^{11}\text{B}$  NMR spectra of **1a** chosen as the reference molecular brick. The product is a triplet at  $\delta = -10.4$  ppm

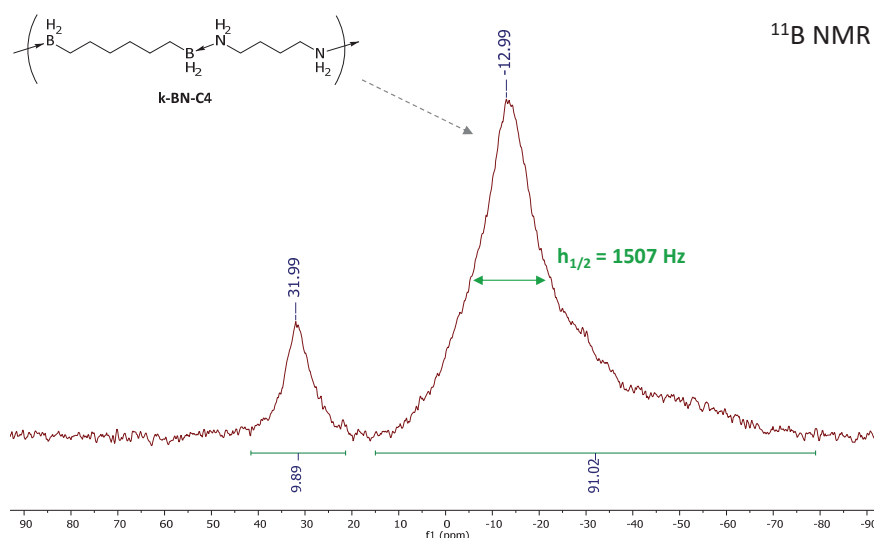


Figure 63.  $^{11}\text{B}$  NMR spectra of polyboramine k-BN-C4. The peak at  $\delta = -13.0$  ppm corresponds to the amine-borane functions. The peak at  $\delta = 32.0$  ppm corresponds to partial decomposition of the polymer.

The formation of the amine-borane function has been confirmed by IR ( $\nu(\text{B-H}) = 2300\text{ cm}^{-1}$ ,  $\nu(\text{N-H}) = 3398\text{ cm}^{-1}$ , Figure 64) and by  $^1\text{H}$  NMR spectroscopy (Figure 65) on which  $\text{NH}_2$  and  $\text{BH}_2$  hydrogens are clearly visible at  $\delta = 4.40$  ppm and  $\delta = 2.61$  ppm respectively. The broad multiplet centered at  $\delta = 1.25$  ppm corresponded to the aliphatic polymer backbone. The intense singlets at  $\delta = 1.18 - 1.14$  ppm belong to residual methyls of the pinacol byproducts.

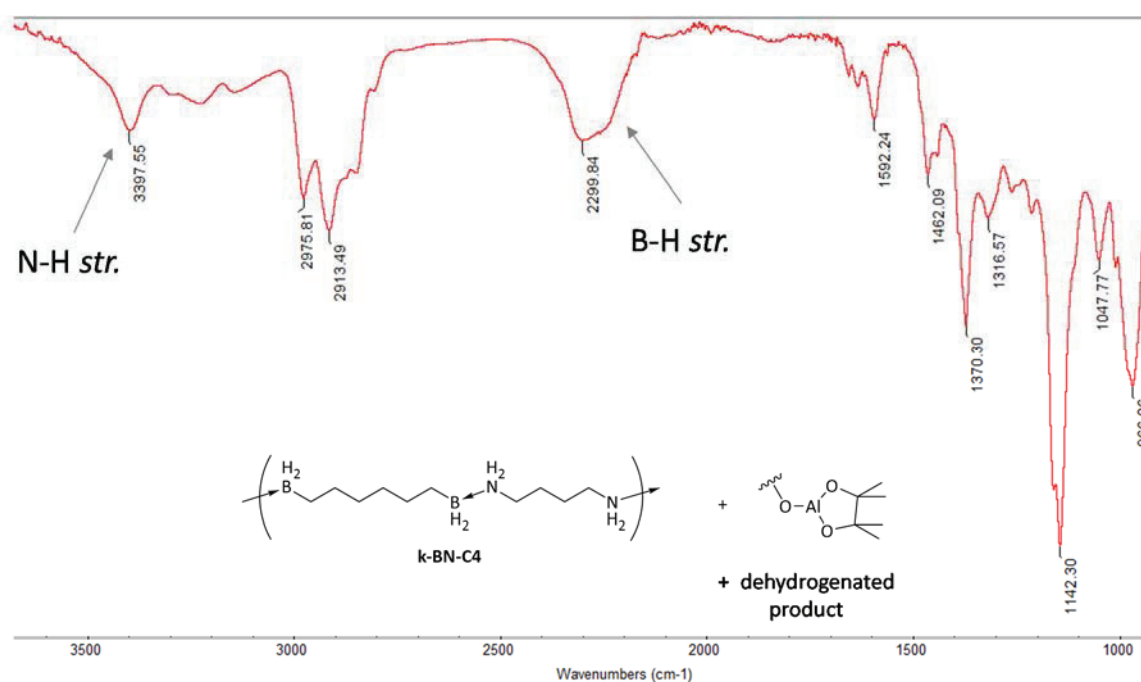


Figure 64. ATR-IR spectra (transmittance) of k-BN-C4O exhibit the characteristic stretches of N-H and B-H bonds within an amine-borane.

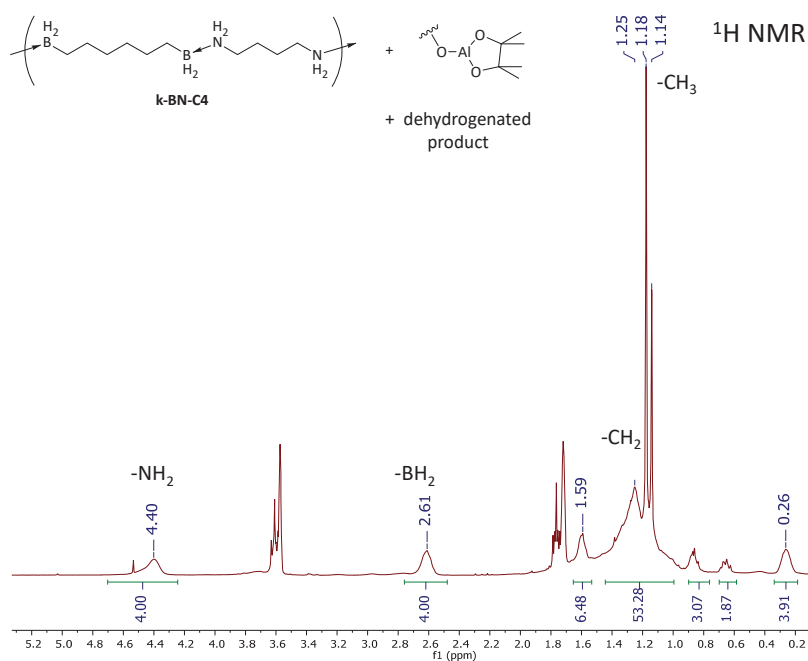


Figure 65.  $^1\text{H}$  NMR spectra of polymer *k*-BN-C4. We can see typical broad singlets of amine-borane NH and BH at  $\delta = 4.40$  ppm and  $\delta = 2.61$  ppm respectively.

Gratifyingly, the polymer **e-BN-C4** containing a dissymmetric bisboronic monomer has been formed quantitatively. The  $^{11}\text{B}$  NMR revealed a broad peak centered at  $-7.5$  ppm and no other decomposition peak (Figure 66). A small quadruplet was visible at  $-43.3$  ppm, typical of  $\text{LiBH}_4$ . The presence of this impurity can be attributed to minute amounts of deborylation side-reactions.

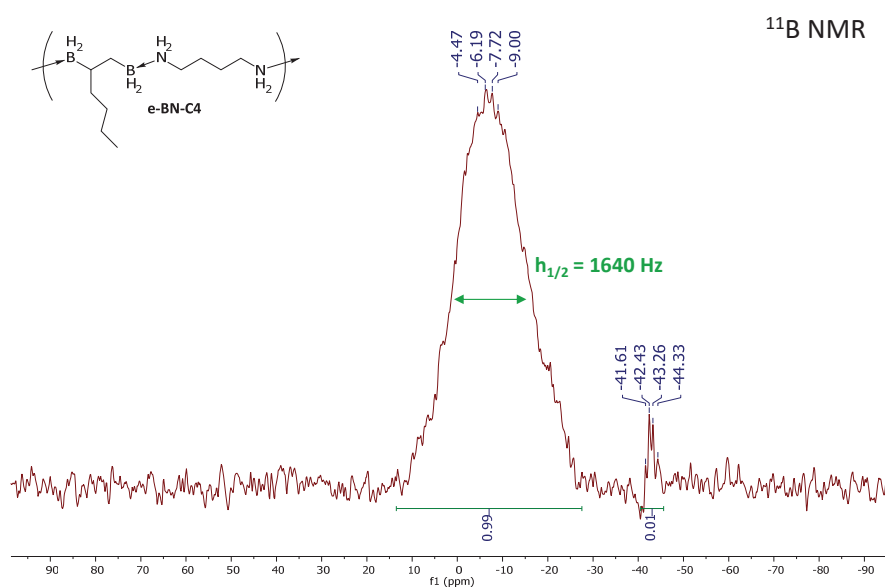
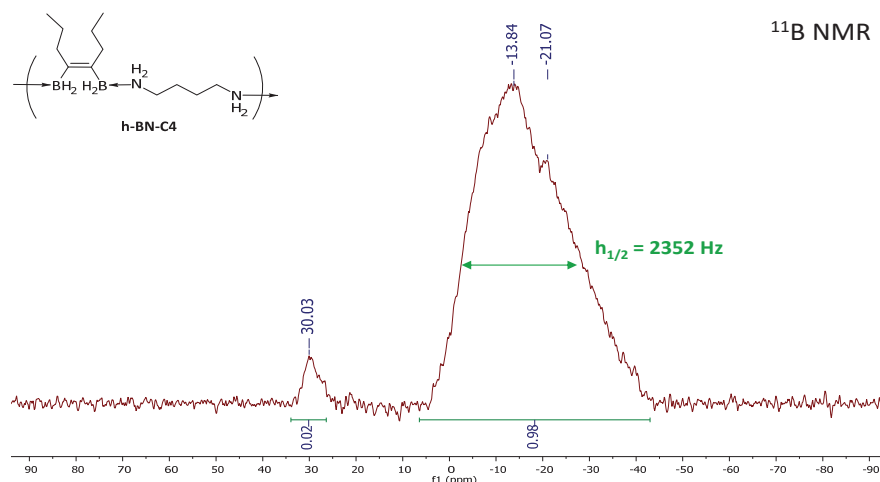


Figure 66.  $^{11}\text{B}$  NMR spectra of polyboramine *e*-BN-C4. The peak at  $\delta = -7.7$  ppm corresponds to amine-borane functions. The peak at  $\delta = -43.3$  ppm corresponds to  $\text{LiBH}_4$ .



Finally we obtained also the polymer **h-BN-C4** which featured a cis-bisboron alkene functions. The characteristic  $^{11}\text{B}$  chemical shift was averaged at  $\delta = -13.8$  ppm (Figure 67) and some degradation (2 %) was still visible at  $\delta = 30$  ppm. Interestingly, the small peak at  $-20.1$  ppm characteristic of  $\text{R-BH}_3\text{Li}$  ( $\text{R} = \text{alkyl, aryl}$ ) probably indicated chain-ends functions.



**Figure 67.**  $^{11}\text{B}$  NMR spectra of polyboramine **h-BN-C4**. The peak at  $\delta = -13.8$  ppm corresponds to amine-borane functions. The peak at  $\delta = -30.3$  ppm corresponds to partial decomposition of the polymer. The small peak identified at  $\delta = -21.2$  ppm is consistent with boron chain-end.

Polymers **e,h,k-BN-C4** displayed particularly broadened  $^{11}\text{B}$  NMR signals, with a half-value width ranging from  $h_{1/2} = 1507$  Hz to  $2352$  Hz which was higher than for the previously described **Ar-BN-C<sub>x</sub>O<sub>y</sub>** family of polyboramines that are made from the rigid aryl bisboron fragment. In fact, these exclusively aliphatic polymers had likely an enhanced mobility leading to a wider distribution of environments within the polymer.

In summary, our first results on the family of aliphatic polyboramines **e,h,k-BN-C4** appeared very promising. Their synthesis has been achieved using a one-pot three component reaction in development in our laboratory.

To achieve this study, it will be crucial to optimize this procedure in order to get rid of the aluminum species and thereby avoid partial decomposition. Since this study, our researches have suggested that the solubility of amine-borane containing polymers was not limited to THF and depended largely of the polymer backbone. Consequently, as demonstrated for the synthesis of pendant-chain amine-borane polymers (introduced in

section 3 hereafter), the pinacol aluminum impurities can be precipitated selectively in a more apolar solvent mixture during the polymer synthesis. This approach has offered significantly more perspective than the initial method we developed.

---

## IV. Conclusion and perspectives

---

We have synthesized polyboramine polymers by simple treatment of bisboronic building blocks and diammonium salts with  $\text{LiAlH}_4$ . We accessed several types of main-chain amine-borane assembled  $\text{H}_2$ -storing polymers. The family of polyboramines containing a rigid aromatic core between borons (**Ar-BN-C<sub>x</sub>O<sub>y</sub>**), displayed a glass transition temperature that could potentially enable their processability. They hydrogenate imines, aldehydes and ketones under mild conditions, more selectively than their molecular analogues. Furthermore, polyboramines displayed a unique thermal behavior. The thermal dehydrogenation occurs below 100 °C and was endothermic, in stark contrast to regular amine-boranes used for this purpose. This was a direct consequence of the incorporation of the amine-borane into polymeric chains. We believe that backbone effects on polymer reactivity could be of interest for other areas in boron, polymer, and dihydrogen-storage chemistry. We started the study of new polyboramines containing shorter and/or less rigid spacers. First results suggested that they could bring about important information on the role and the behavior of polymer backbones involved in chemical dehydrogenation processes.

Mechanistic and conformational computational studies are currently ongoing in collaboration with Dr. Paolo Larini (ITEMM, ICBMS, Lyon) and Dr. Fabrice Brunel (C2P2, Lyon), as well as advanced NMR characterizations in collaboration with Dr. David Gajan (CRMN, Lyon) and Dr. Jasmine Viger-Gravel (Prof Emsley group, EPFL, Switzerland). Our goal is to isolate key intermediates and products as well as supramolecular conformations to collect information about dehydrogenation pathways taken by both polyboramines and molecular analogues. We aimed also at realizing a mapping of structure/properties/reactivity of a wide range of polyboramines, using either A-A / B-B or A-B type polycondensation (see the concept in chapter III.1, section 2), primary and secondary diamines or triamines as well as very rigid to very soft polymer backbone. This

study in correlation with theoretical and analytical studies could lead to a material having the desired properties of dehydrogenation and allow the re-loading of dihydrogen in the network.

### **Section 3**

**Integration of pendant-chain amine-boranes within (co)polymers. Effect of the intrinsic structure.**

---

## I. Introduction

---

This section addresses the design of homopolymers or random copolymers that possess pendant amine-borane moieties with various degrees of functionalities. These materials have been tested for solid state thermal dehydrogenation. In particular, we anticipated that changes in dehydrogenation kinetics would be observed depending on the amine-borane to polymer matrix ratio. Thus, we decided to quantify structural effects of the matrix architecture on the dehydrogenation profile.

First, an overview of the literature background regarding amine-borane moieties inserted in a polystyrene scaffold will be presented, with a particular interest in the different synthetic methods to access those materials. Then, the syntheses of our polymers will be introduced. The behavior of several (co)polymers and molecular analogues under thermal dehydrogenation will thus be compared. A study of polymer structures before and after dehydrogenation will bring about tentative explanations to the observed results. Finally the effect of AB doping on the dehydrogenation pattern of amine-borane containing polymers will be addressed.

---

## II. Literature precedents: Amine-Borane containing polystyrenes

---

Boron containing polymers were investigated in recent years, particularly for their optical and electronic properties for applications in electronics and sensors materials.<sup>101</sup> Among the family of side-chain functionalized organoboron polymers we can find conjugated organoboranes that display useful optical or electronical characteristics (Figure 68).

A second family regroups functionalized polyolefins and other chain-growth polymers that offer the advantage of a versatile polymer backbone for boron functionalization. They represent a straightforward access to soluble high molecular-weight polymers displaying variable degrees of functionalization. A review published in 2010 by Jäkle and co-

workers,<sup>101</sup> summarized very well the different type of organoboron polymers reported up to that date.

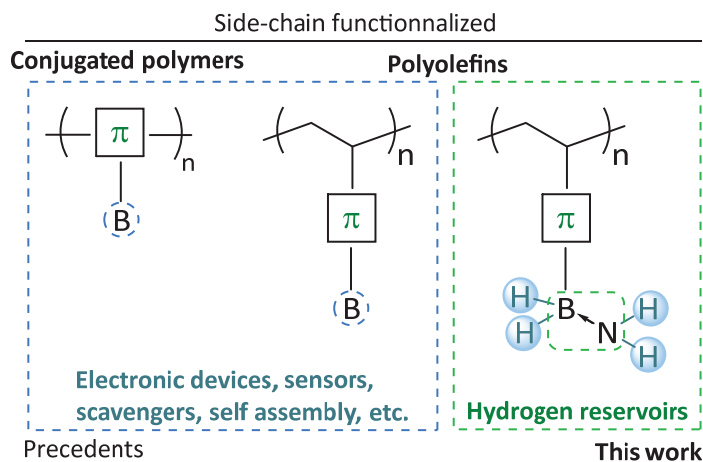


Figure 68. Overall view of polymers having boron function as a pendant chain.

Boron grafted polystyrenes have been studied extensively for their luminescence properties<sup>102</sup> (Figure 69a). They were studied as anion sensors<sup>103</sup> (Figure 69b). They have also been implemented as diol catchers for medical applications thanks to the quantitative formation of boronates from the boronic acid function<sup>104</sup> (Figure 69c).

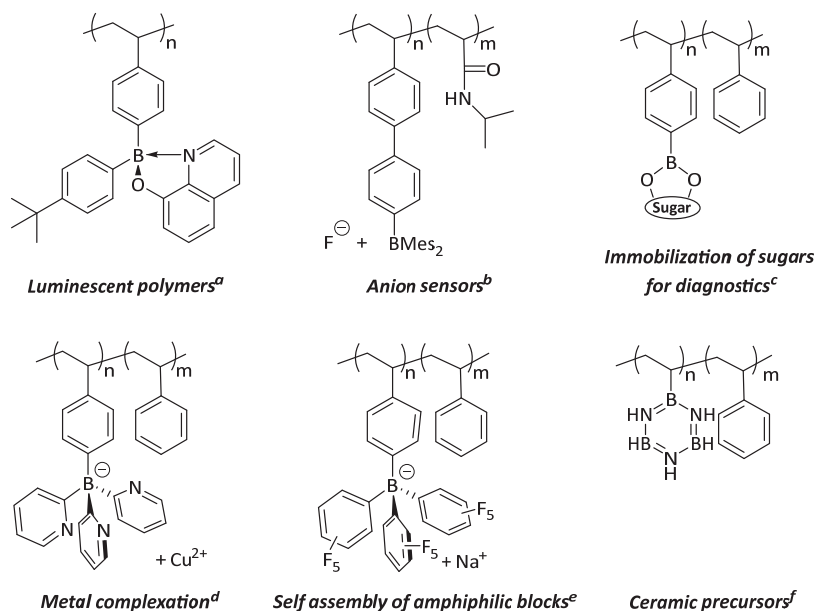


Figure 69. Examples of functionalized polystyrenes and applications. (a) Organoboron quinolate homopolymer. Ref.<sup>102,105</sup> (b) Luminescent triarylborate homo and block co-polymer. Ref.<sup>103</sup> (c) Boronic acid block co-polymer for glucose detection. Ref.<sup>104,106</sup> (d) Boron-based scorpionate ligand chelate block co-polymer. Ref.<sup>107</sup> (e) Amphiphilic organoborate block-copolymers. Ref.<sup>108</sup> (f) Hybrid organic inorganic statistic co-polymers. Ref.<sup>109</sup>

In addition, triarylborates are negatively charged species consequently they allowed the complexation of metals. Actually chelating boron-substituted polymers were reported for the synthesis of metallo-polymers after complexation with metals<sup>107</sup> (Figure 69d). Alternatively boron-containing amphiphilic block copolymers were investigated for the capacity to give micelles<sup>108</sup> (Figure 69e). Interestingly, borazine-functionalized polystyrenes were synthesized for their physical characteristics as hybrid organic/inorganic polymers for the elaboration of ceramics<sup>109</sup> (Figure 69f).

## II.1. Polymerization of 4-vinylphenylboronic acid/ester

### II.1.a. Free radical polymerization

The 4-vinylphenylboronic acid (VBA) and esters such as pinacol 4-vinylphenylboronate (PVB) are readily polymerized by free radical polymerization using an initiator in mild conditions (Figure 70). The most common initiators are AIBN (azobisisobutyronitrile) and diazo compounds, BPO (benzoylperoxide) or potassium persulfate.<sup>110</sup> A lot of random copolymers involving VBA or PVB and usual comonomers such as styrene, vinylpyrrolidone, acrylonitrile, maleic anhydride, and others, have been reported in the literature.<sup>111</sup>

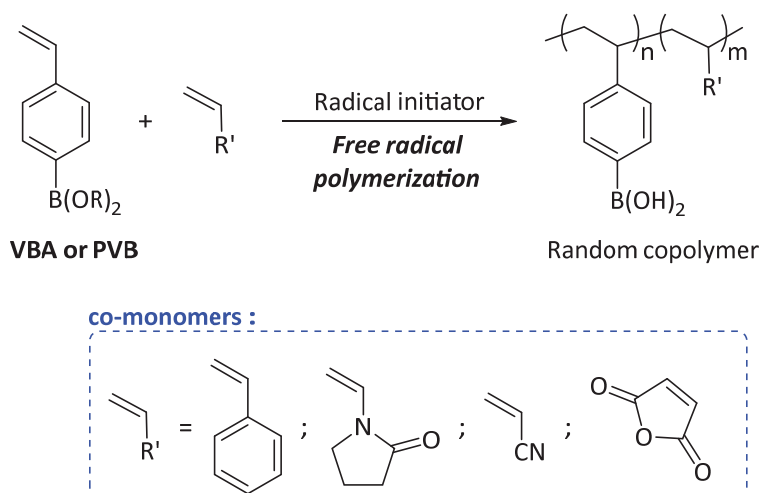
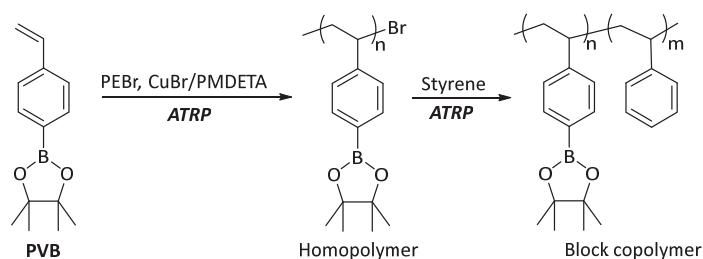


Figure 70. Free radical polymerization. Examples of random copolymers

### II.1.b. Atom transfer radical polymerization (ATRP)

Radical polymerization by atom transfer (ATRP) has been used by Jäkle and co-workers, for the synthesis of well-defined boron functionalized polymers.<sup>112</sup> This technique gives access to polymers featuring controlled molar masses and narrow dispersities ( $D < 1.1$ ) and thus to precise block-copolymer architectures.<sup>113</sup> The reaction is usually initiated with 1-phenylethyl bromide (PEBr) and catalyzed by CuBr/pentamethyldiethylenetriamine (PMDETA). In the ATRP process, the bromo-functionalized polymeric dormant species is activated by the copper complex to generate radicals via one electron transfer process. This reversible process rapidly establishes an equilibrium that is predominately shifted to the bromopolymer species with very low radical concentrations. It thus inhibits terminations by bimolecular coupling. Consequently the good dispersity of polymer molar masses arises from the fact that each growing chain has the same probability to propagate with each monomer insertion. In addition, when the propagation is finished, dormant chains can be re-initiated by adding a new portion of monomer (Scheme 34)



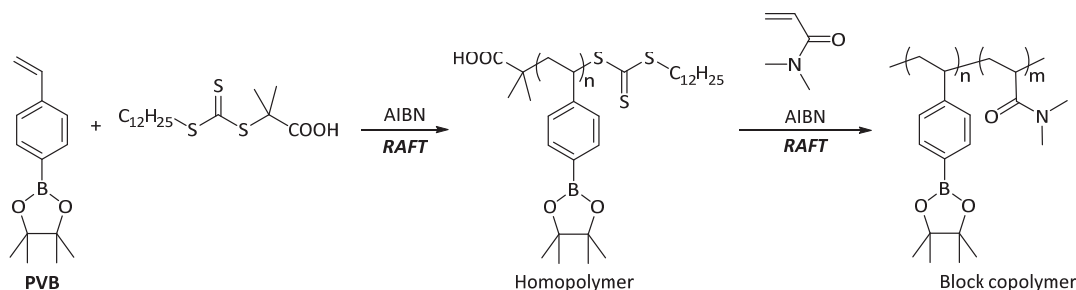
*Scheme 34. Example of ATRP for the synthesis of boron containing copolymers.*

### II.1.c. Reversible addition-fragmentation chain transfer (RAFT)

The RAFT polymerization makes use of a chain transfer agent in the form of a thiocarbonylthio compound that mediates the polymerization via a reversible chain-transfer process. As for ATRP, it permits the control of the molar masses and dispersities thanks to a degenerative chain-transfer process.<sup>114</sup> The first example of boron containing polymers being prepared by RAFT polymerization has been reported in 2007 by Summerlin and co-workers.<sup>115</sup> Block copolymers with PVB and acrylamido- segments were prepared in the presence of 2-dodecylsulfanylthiocarbonylsulfanyl-2-methylpropionic acid as the chain transfer agent and 2,2'-azobisisobutyronitrile (AIBN) as the initiator



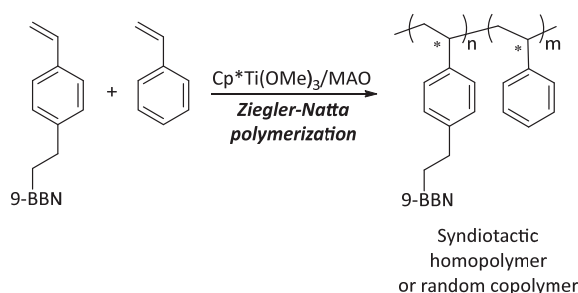
(Scheme 35). These polymers readily self-assembled forming polymeric micelles in water. This method has given access to new families of boron-containing block copolymers. RAFT and ATRP are complementary because they tolerate different sets of monomers.



*Scheme 35. Example of RAFT for the synthesis of boron containing copolymers.*

#### II.1.d. Ziegler-Natta polymerization

Syndiotactic homopolymerization and random copolymerization of boron-functionalized styrenic monomers has been studied by Chung and co-workers.<sup>116</sup> Copolymerization of styrene and 9-BBN boron-functionalized styrene has been performed using Ziegler-Natta polymerization with the syndiospecific titanium catalyst  $\text{Cp}^*\text{Ti(OMe)}_3$  in the presence of methylaluminoxane (MAO) (Scheme 36). The procedure afforded syndiotactic polymers featuring molar masses of  $M_n=28,000$  to  $83,000$  and dispersities between 2.0 and 2.9.



*Scheme 36. Example of Ziegler-Natta polymerization for the synthesis of syndiotactic boron containing copolymers*

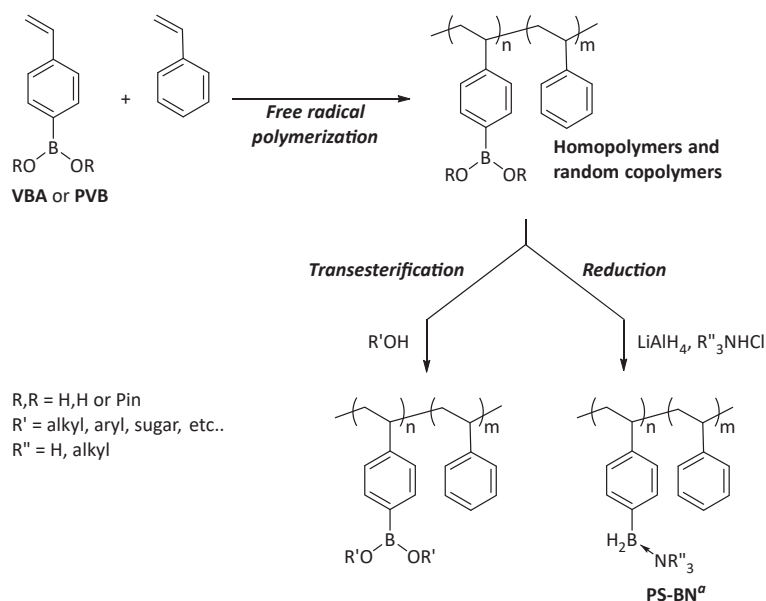
Several methodologies for the (co)polymerization of boron-functionalized styrenics can be found in the literature and are complementary. The Ziegler-Natta strategy is a radical-free reaction and affords boron-functionalized syndiotactic copolymers with high molar

masses. ATRP and RAFT allow for the control of the macromolecular architectures yielding well-defined boron-containing polymers. Finally, for the synthesis of random copolymers, conventional free-radical polymerizations are the most successful due to a facile experimental setup and ease of purification while warranting the absence of potential undesired reactions as for instance deborylation.

## II.2. Strategies of functionalization

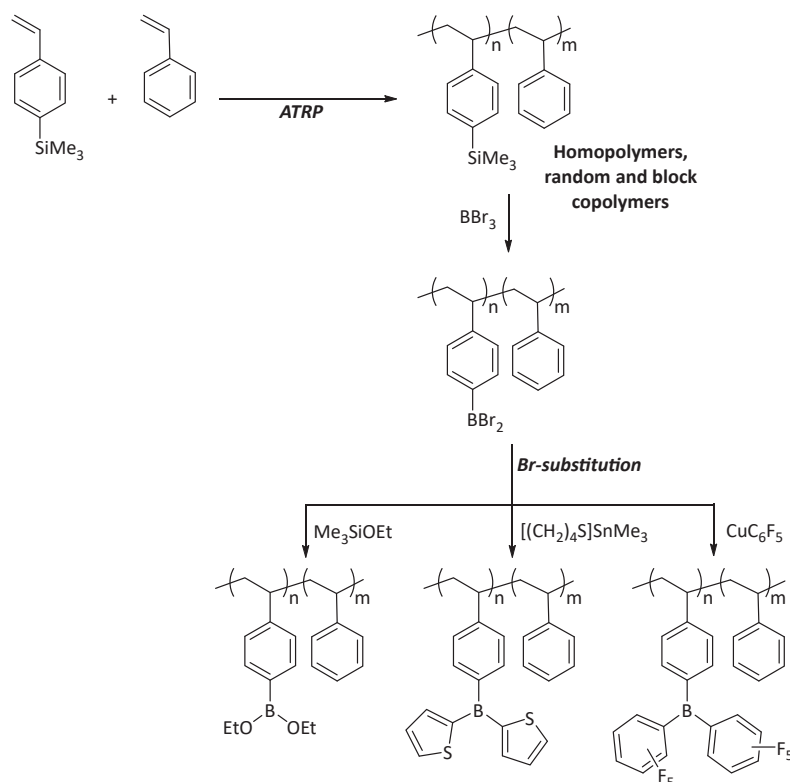
---

To synthesize boron-containing polymers, the boron moieties can be inserted prior or after the polymerization step. The choice of the functionalization strategy depends of many parameters such as the sensitivity of the boron function, the solubility parameters of the polymer, etc. An alternative consists in the utilization of a boron precursor that is adapted to the polymerization conditions and can be post-functionalized (deprotected, reduced...) into the desired boron moiety. VBA and PVB are particularly useful and readily available precursors for post-polymerization functionalization (Scheme 37). A lot of compounds can be accordingly modified by transesterification reaction for example. They give also access to amine-borane functionalized polystyrenes-*g*-boramines as we will demonstrate in this work.<sup>117</sup>



**Scheme 37.** Free-radical polymerization strategy affording readily available organoborane polymer and post-functionalization by transesterification and hydrogenation to obtain B-H substituted amine-boranes. (a) This work.

It is important to mention the highly versatile multi-step strategy reported by Jäkle and co-workers that provided access to a wide-range of boron-functionalized polymers and co-polymers.<sup>113</sup> It consists in the (co)polymerization by ATRP using 4-trimethylsilylstyrene as monomer, to incorporate the silyl functionality along the polymer backbone (Scheme 38). Then, the silyl group is readily exchanged by a dibromoboryl one, using BBr<sub>3</sub> to yield the dibromoborane-functionalized copolymer that constitutes a particularly versatile platform for post-functionalization treatments. Indeed, it offers the possibility of grafting various functions at the boron atom, e.g. pentafluorophenyl, thiophenyl, and esters.



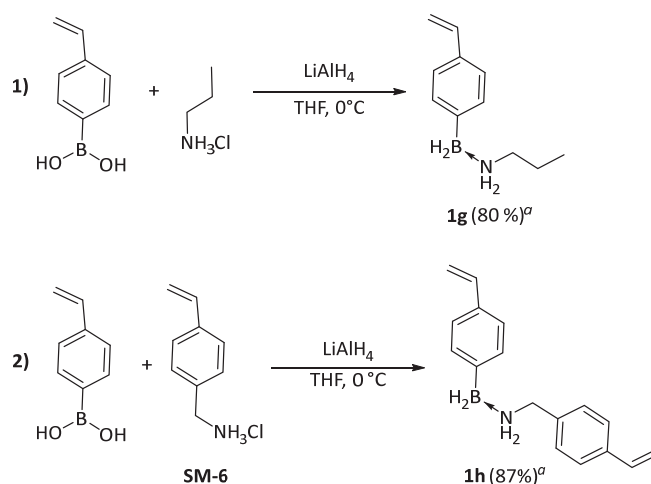
**Scheme 38.** Atom transfer free-radical polymerization (ATRP) with 4-trimethylsilylstyrene and post-polymerization Si-B exchange and access to several borane functionalized (co)polymers through facile bromine substitution.

In the following chapter, we report our findings on the potential of side-chain functionalized amine-borane copolymer as reactive materials for hydrogen release. A range of  $-\text{NH}_2\text{-BH}_2-$  amine-borane functionalized (co)polymers were synthesized by using the strategy of free-radical polymerization / post-functionalization developed in our laboratory, in order to obtain random structures with tunable amine-borane content.

### III. This work: Design of pendant-chain amine-borane polymers: dynamic structure / activity relationship

#### III.1. Establishment of a synthetic pathway

At first, we tried to copolymerize 4-[amine-borane]-styrenic monomers with styrene. To synthesize monomers, we employed the one-pot three-component procedure previously developed in our laboratory starting from **VBA** and *n*-propylammonium chloride. The reaction was carried out under strict control of the reaction temperature (maintained below 0 °C), to prevent any undesired polymerization at this stage. The monomer 4-vinylphenyldihydroborane-(*n*-propyl)amine **1g** was recovered in good yield and high purity (Scheme 39, eq. 1). The bifunctional monomer 4-vinylphenyldihydroborane-(4-vinylbenzyl)amine **1h** has been obtained in the same conditions from **VBA** and 4-vinylbenzylammonium chloride (Scheme 39, eq. 2) that was previously prepared from 4-vinylbenzylbromide using by the Gabriel reaction and a subsequent HCl treatment. In our conditions, the vinyl function remained untouched, as confirmed by <sup>1</sup>H NMR spectroscopy (see experimental section 4)

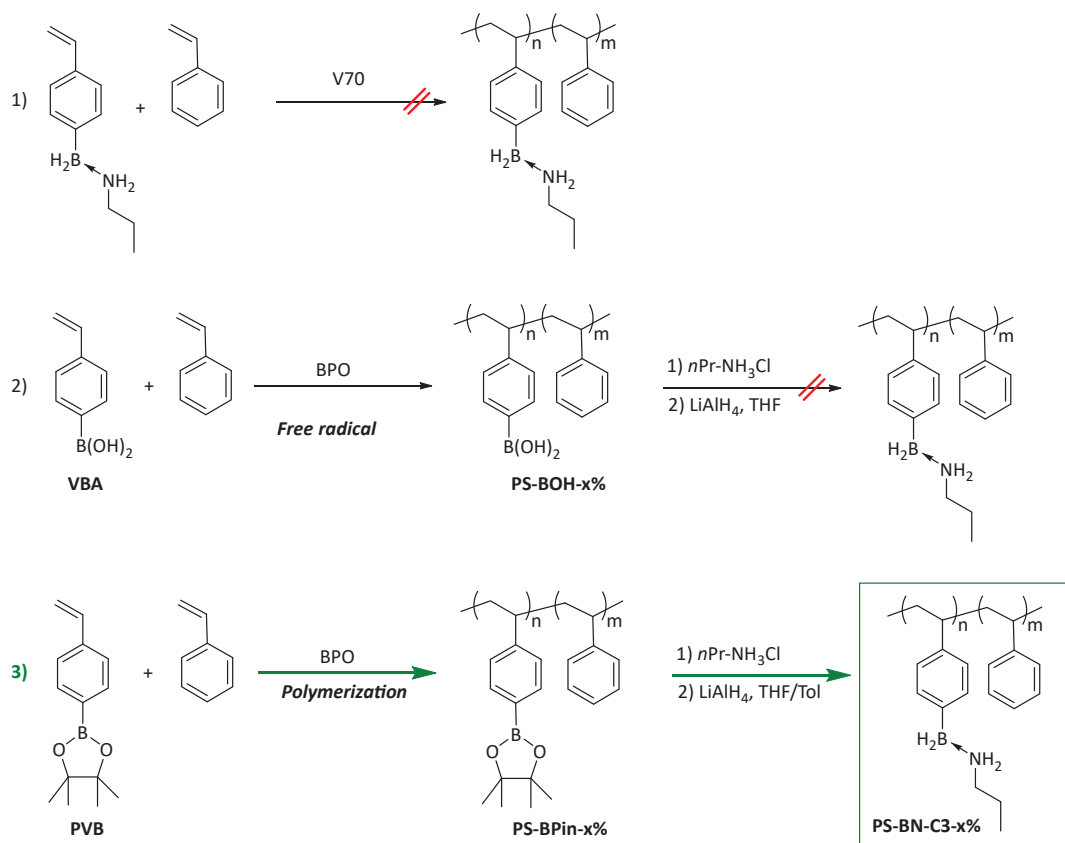


Scheme 39. Synthesis of  $\text{NH}_2\text{-BH}_2$  amine-borane monomers. (a) Isolated yields.

Monomer **1g** was then copolymerized with styrene under free-radical conditions. It was important to keep the temperature below 40 °C due to the propensity of the  $\text{NH}_2\text{-BH}_2$  moieties to release dihydrogen molecules under thermal activation. We employed the

V70 (2,2'-azobis(4-methoxy-2,4-dimethyl valeronitrile) initiator that decomposes at 30 °C (10-hour half-life) (Scheme 40, eq. 1). However, our attempts to access polymers soluble in THF were unsuccessful. The polymerization led only to insoluble materials and IR spectroscopy suggested that the B-H bond was present only in minute amounts. It appeared that the radical polymerization induces the decomposition of B-H bonds, either by radical hydrogen atom abstraction or by initiating dehydrogenation.

We decided to adopt the polymerization/post-functionalization strategy by synthesizing a precursor polymer containing more stable boron moieties, such as poly(styrene-*ran*-VBA) (Scheme 40, eq. 2). The polymerization was carried out in THF or in THF/methanol at 60 °C, using BPO as initiator (10-hour half-life; decomposition temperature 72 °C).

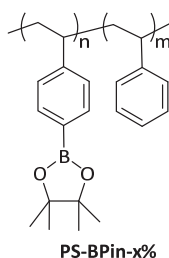


**Scheme 40.** The three different strategies envisaged. The polymerization and post-functionalization from VBA led to amine-borane functionalized copolymers.  $x = n/(m+n)$

The solubility of polymer in THF decreased with increasing VBA content due to the presence of many B-OH polar groups. The use of small amounts of methanol (or water) was then required to reach high molar masses. A range of (co)polymers [poly(styrene-*ran*-

In contrast, the use of PVB boron monomer for the (co)polymerization reaction with styrene gave access to a range of very soluble [poly(styrene-*ran*-PVB)] ; [x PVB%] (called **PS-BPin-x%** Scheme 40, eq. 3) where **x** is the PVB rate (Table 14). PVB was readily obtained from VBA in presence of pinacol and magnesium sulfate.<sup>118</sup> The reaction was performed in THF at 60 °C during 18 h, using BPO as initiator. The crude material was precipitated in cold pentane and the polymer was recovered by centrifugations as a white powder. The pinacol boronate content was controlled by <sup>1</sup>H NMR spectroscopy and corresponded to the proportion of PVB and styrene starting materials.

**Table 14. Calorimetric and chromatographic properties of [poly(styrene-ran-PVB)] ; x PVB%**



x [%] <sup>a</sup>	3	10	20	40	70	100
Yield [%] <sup>c</sup>	90	85	83	87	92	87
Mw [Da]	15 989	-	25 145	31 546	32 567	40 211
Đ <sub>M</sub> <sup>d</sup>	1.81	-	2.05	2.31	2.19	2.83

(a) Rate of phenyl groups functionalized with amine-boranes [x = n/(m+n)\*100] (b) After isolation and purification: (c) Molar mass dispersity (Đ<sub>M</sub> = Mw/Mn).

Polymers **PS-BPin-3%** to **PS-BPin-100%** have a weight average molar mass of  $10^5$  Da. The molar mass dispersity is around 2 which is characteristic of a free radical polymerization process (Table 14 ).

### III.2. Synthesis characterization of PS-BN-C3 and PS-BN-C10 (co)polymers

Pinacol-boronate functions were readily converted into *n*-propylamine-dihydroborane moieties by using stoichiometric amount of *n*-propylammonium chloride and 0.8 equivalent of  $\text{LiAlH}_4$ . Pinacol aluminate ( $\text{Al}_x\text{Pin}_y$ ) and lithium chloride side-products precipitated during the reaction by using a 1:2 THF/Toluene solvent mixture and were eliminated by centrifugations. The absence of any residual salts was confirmed by TGA (Figure 71).

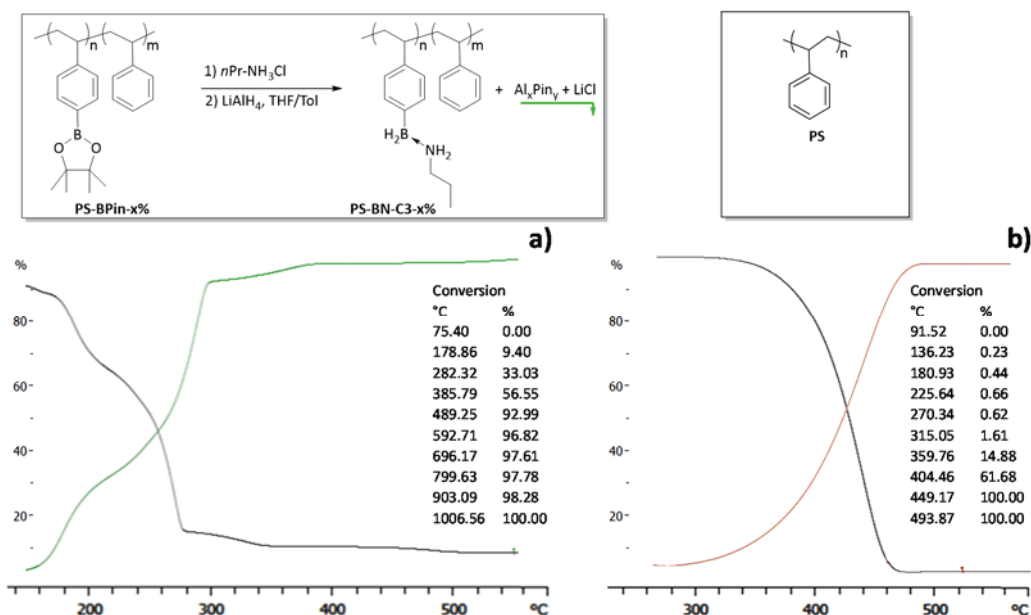


Figure 71. TGA of (a) polymer PSBN-C3 and (b) polystyrene. On chart (a), the absence of mass residue under 900 °C confirms the absence of residual salts.

#### III.2.a. Synthesis of PS-BN-C3-x% and effects of DHB

This approach allowed for the post-functionalization of **PS-BPin-x%** yielding a range of poly[styrene-*ran*-((4-vinylphenyldihydro)borane-(*n*-propyl)amine)] displaying a content



from  $x = 3 \%$  to  $100 \%$  of 4-vinylphenyldihydro)borane-(*n*-propyl)amine unit. They were generally called **PS-BN-C3-*x*%**.

When *x* increased, the solubility of the resulting polymer **PS-BN-C3-*x*%** dramatically decreased. In fact, **PS-BN-C3-3%** containing the lowest rate of amine-borane functionalized units (3 %) was the only polymer to stay perfectly soluble in THF similarly to **PS** and to the **PS-BPin-3%** precursor. Besides, the formation of **PS-BN-C3-10%** was accompanied by a visible increase of the mixture/dispersion viscosity (Figure 72).

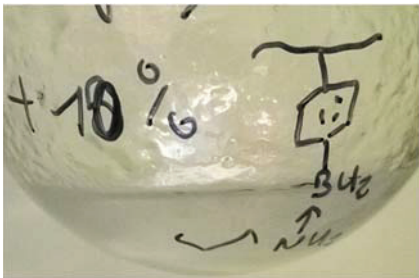
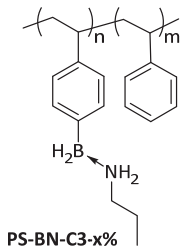


Figure 72. Synthesis of **PS-BN-C3-10%** in THF, increase of the viscosity.

Once isolated, the required THF solvation time jumped from 1 hour to 1 day for **PS-BN-C3-3%** and **PS-BN-C3-10%** respectively (Table 15). Other polymers (**PS-BN-C3-30%**, **PS-BN-C3-40%**, **PS-BN-C3-70%**, **PS-BN-C3-100%**) partly precipitated in the reaction mixture, decreasing the overall yield of the isolated material despite our efforts to adapt the procedure.

Table 15. Synthesis of **PS-BN-C3-*x*%**. Experimental results.



x [%]	3	10	40	70	100
Name	PS-BN-C3-3%	PS-BN-C3-10%	PS-BN-C3-40%	PS-BN-C3-70%	PS-BN-C3-100%
Yield [%]	98	97	67	28	15
Solubility <sup>a</sup>	1 h	1 day	Not soluble		
<sup>a</sup> Solubility in THF after isolation of the polymer from reaction mixture and from volatiles					

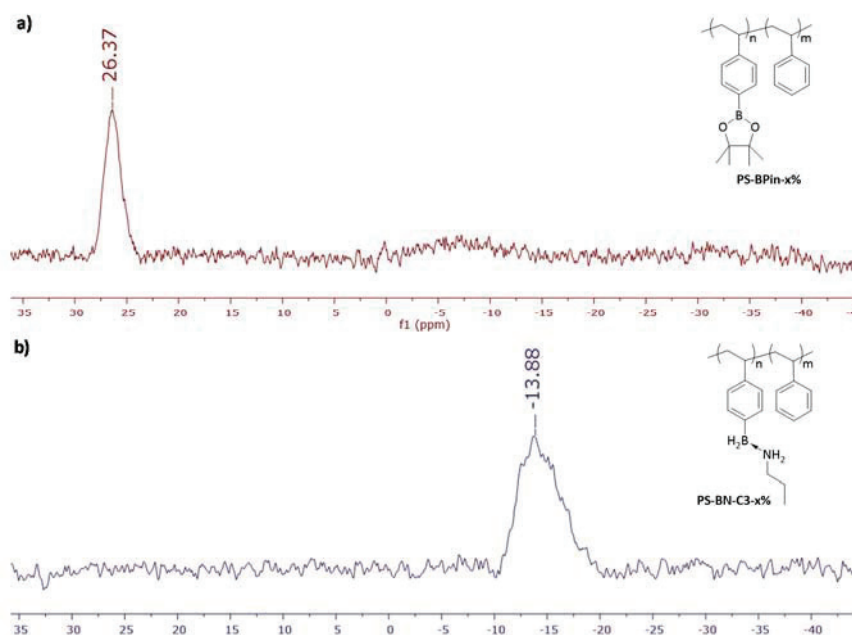


Figure 73.  $^{11}\text{B}$  NMR spectra during the post functionalization of polymers PS-BPin-x% to form PS-BN-C3-x%. (a) before reaction, (b) after 2h at room temperature.

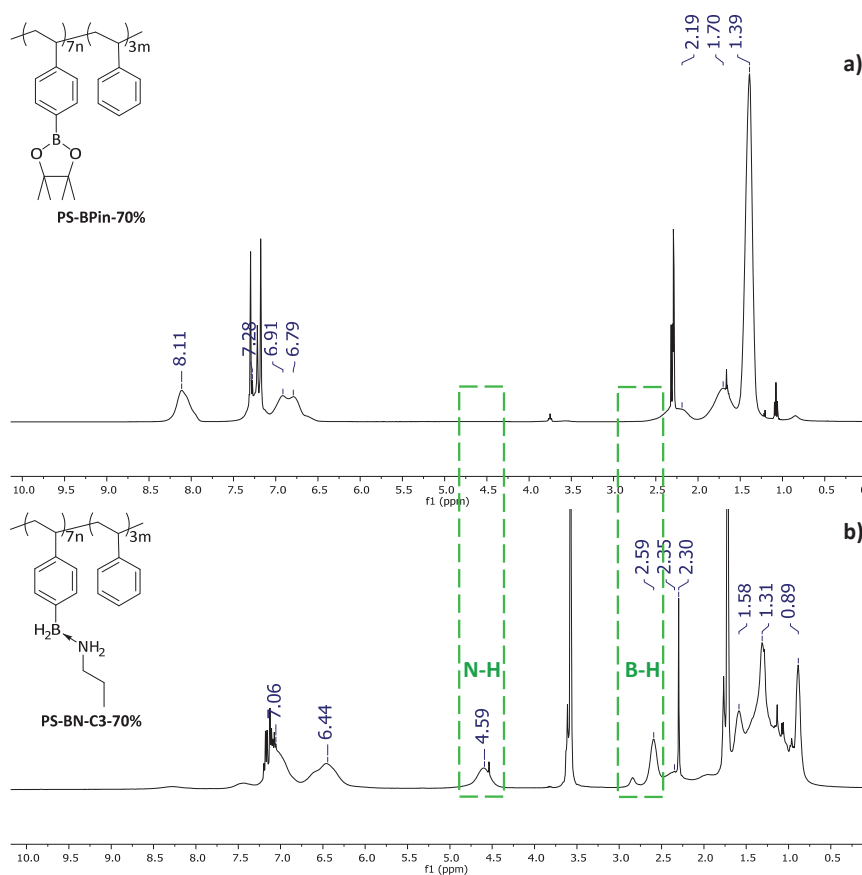


Figure 74. Example of  $^1\text{H}$  NMR changes for the post-functionalization step. Starting material (a) PS-BPin-70% and product (b) PS-BN-C3-70%.

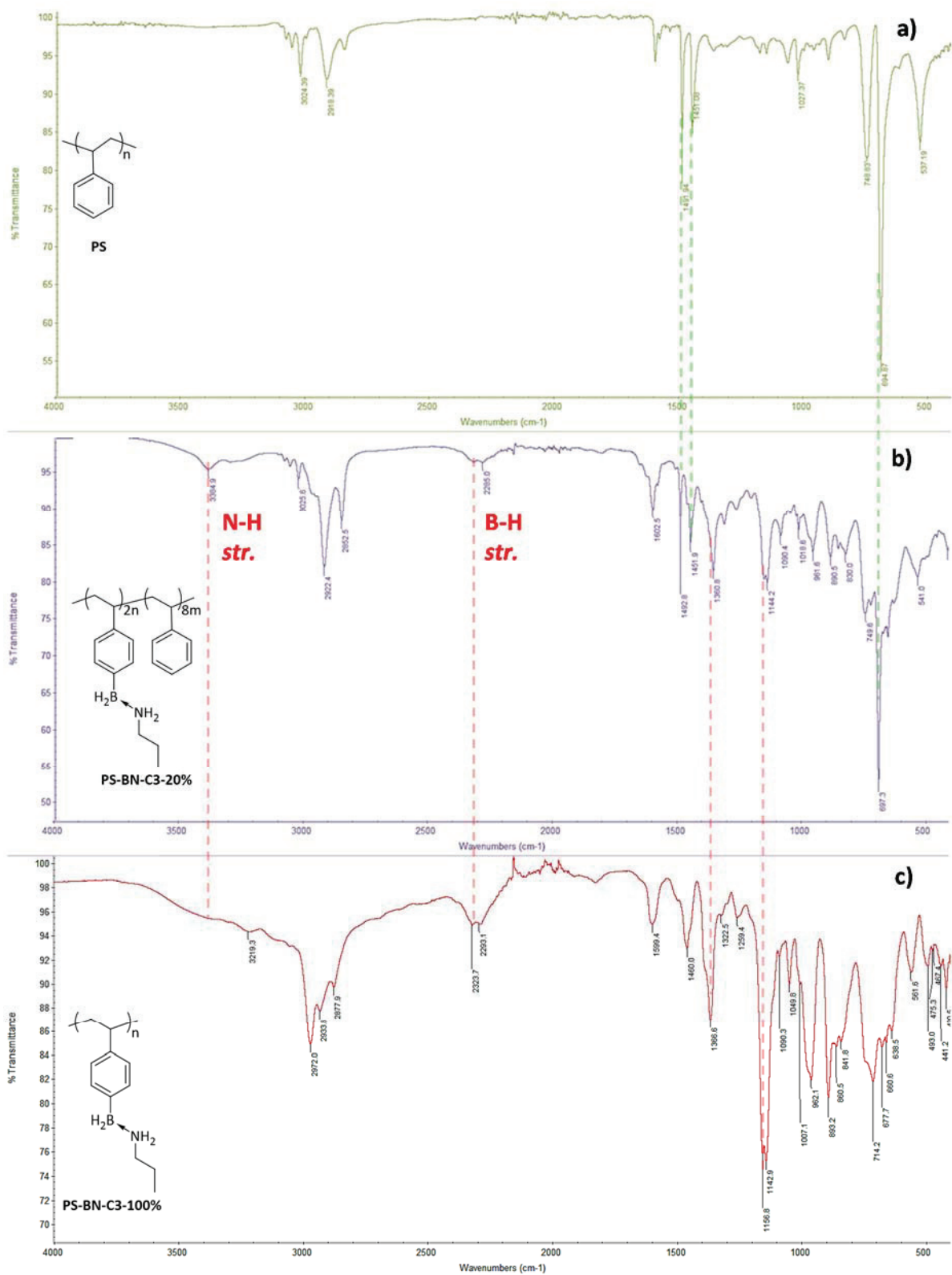
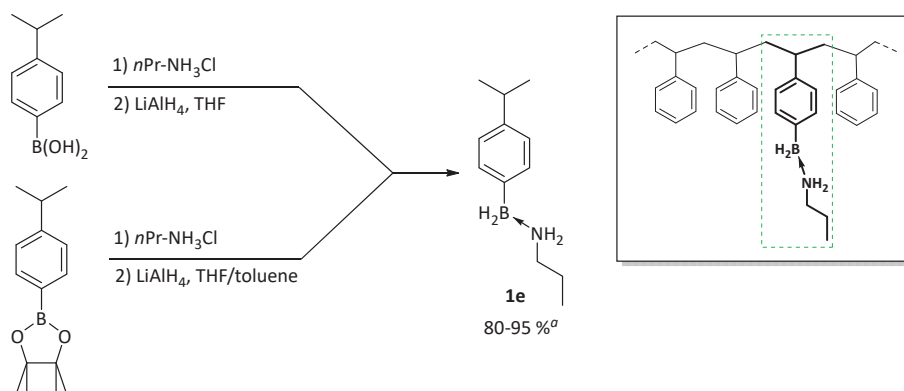


Figure 75. ATR-IR spectra of polymer containing different rate of amine-borane. (a) Polystyrene (0% amine-borane), (b) PS-BN-C3-10%, (c) PS-BN-C3-100%

The transformation of pinacol boronate functions to amine-dihydroborane moieties into the polymer is characterized by a shift of the  $^{11}\text{B}$  NMR signal from 26 ppm to -14 ppm (Figure 73), by the appearance of B-H and N-H  $^1\text{H}$  NMR chemical shifts at 4.6 ppm and 2.6 ppm respectively (Figure 74) and by a signal characteristic of the typical B-H stretching in ATR-IR spectroscopy that is proportional to the amine-borane content (Figure 75). IR and  $^{11}\text{B}$  liquid and/or solid-state NMR monitoring have been particularly useful for identifying high amine-borane containing **PS-BN-C3-x%** polymers because of their lack of solubility (see also experimental section 4)

As an element of comparison, we synthesized the representative boron-containing molecular analogue of the above-mentioned polymers: *n*-propylamine-(4-*i*-propylphenyldihydro)borane **1e** (Scheme 41). **1e** has an isopropyl group to mimic the polymer chain. It can be synthesized either from the boronic acid or pinacol-boronate starting material using the three-component procedure.



**Scheme 41.** Synthesis of the molecular brick **1e** representing the amine-borane function

**1e** is highly soluble in THF, toluene and chloroform. Consequently the insolubility observed with polymers having high amine-borane content is not exclusively due to the presence of amine-borane functions. We supposed that inter-chain DHB interactions are responsible for strongly coordinated supramolecular assemblies which consequently lower the solubility of the materials. Polymers displaying hydrogen-type interactions are already known in the field of polymer/supramolecular chemistry. As a good representative example, polyamides display hydrogen bonding between chains (Figure

76a) and their concentration determines the melting point and the semi-crystalline nature and physical properties of the material. By analogy, the drop in solubility observed when the amine-borane content increases could be explained by the larger number of DHBs established between polymer chains (Figure 76b).

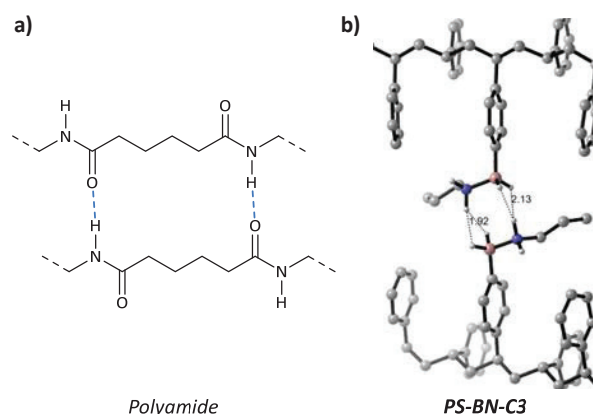


*Figure 76. Hydrogen-type interaction between polymer chains. Analogy between (a) a polyamide displaying hydrogen bonding and (b) PS-BN-C3 displaying dihydrogen bonding.*

To mitigate the undesired effects of DHBs, we synthesized a new family of (co)polymers having amine-borane functions featuring longer aliphatic chains.

### III.2.b.Synthesis of PS-BN-C10-x%

Using the same procedure, polymers **PS-BN-C10-x%** were synthesized from **PS-BPin-x%** in THF/Toluene 1:2 at room temperature. Compounds **PS-BN-C10-3%** to **PS-BN-C10-100%** were obtained readily and quantitatively without any undesired precipitation (Table 16). After isolation, polymers also remained perfectly soluble in THF. All polymers **PS-BN-C10-x%** as well as the corresponding molecular brick **1f**, were characterized by  $^{11}\text{B}$  NMR,  $^1\text{H}$  NMR,  $^{13}\text{C}$  NMR and IR.

Table 16. Synthesis of PS-BN-C10-x%. Experimental results.

<b>x [%]</b>	3	10	20	40	70	100	Molecular brick
<b>Name</b>	<b>PS-BN-C10-3%</b>	<b>PS-BN-C10-10%</b>	<b>PS-BN-C10-20%</b>	<b>PS-BN-C10-40%</b>	<b>PS-BN-C10-70%</b>	<b>PS-BN-C10-100%</b>	<b>1f</b>
<b>Yield [%]</b>	89	95	99	89	88	92	98
<b>Solubility<sup>a</sup></b>	Soluble						
<sup>a</sup> Solubility in THF after isolation of the polymer from reaction mixture and from volatiles							

### III.3. Thermally induced dehydrogenation: Impact of the polymer scaffold.

We engaged the two families of polymers **PS-BN-C3** and **PS-BN-C10** in thermal dehydrogenation. We found that in both cases the amine-borane content has a significant influence on the temperature of hydrogen release. We tried to rationalize the precise role of the polymer scaffold in this phenomenon by investigating the macrostructure changes during the hydrogen loss and by carrying out comparative studies on molecular analogues.

#### III.3.a. Thermally induced dehydrogenation of the molecular bricks

At first, we employed several molecular analogues of general formula: [*n*-alkyl-NH<sub>2</sub>-BH<sub>2</sub>-aryl] with similar substituents on the nitrogen and the boron. The hydrogen emission has been monitored with a TPD apparatus. The peak of hydrogen release has been identified for each species, **AB**, **1b**, **1e** and **1f** and reported on the chart below (Figure 77).

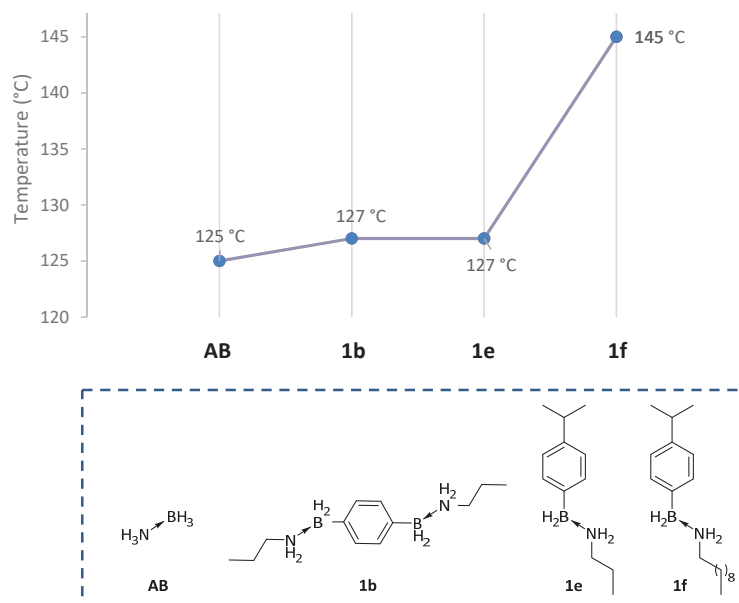


**Figure 77.** Influence of the electronic and steric environment on the thermal dehydrogenation temperature peak. Temperature program: 30 to 250 °C, 5°C/min.

When heated at 5°C/min, **AB**, **1b** and **1e** exhibited almost the same temperature of dehydrogenation (125-127°C). This observation is consistent with theoretical calculations that have demonstrated that the three compounds having very similar substituents and therefore electronic environment should dehydrogenate with almost identical energetic profiles. The same trend was expected for **1f** since it has similar substituents as well. Instead the temperature of dehydrogenation of **1f** was measured 20 °C higher, at 145 °C (Figure 77).). We believe that this different behavior is induced by the N-substituted decyl hydrocarbon chain on the amine-borane moiety. We suppose that the latter brings a more important apolar environment (and some bulkiness) with respect to **AB**, **1b** and **1e** substituents that increases the energy of polarized species involved in transition states and intermediates by analogy with the behavior of amine-boranes in solution<sup>4b</sup> (see chapter II.7.a in section 1). Moreover the presence of a longer alkyl-chain is also likely to decrease the number of DHB interactions that is an energetically favorable requirement for initiating the dehydrogenation pathway. Globally, these results suggest that electronic effects aren't the only determinant parameters of amine-borane thermal dehydrogenation. The amine-borane's environment is likely to play an important role, particularly in the establishment of the supramolecular structure.

### III.3.b. Thermally induced dehydrogenation: Impact of the polymer environment

Several polymers of the family **PS-BN-C3-x%** and **PS-BN-C10-x%**, in which **x** is the content of amine-borane functionalized styrene moieties, have undergone a thermal treatment of 5 °C/min to reach 250 °C and hydrogen has been detected in the same manner. All polymers **PS-BN-C3-x%**, **PS-BN-C10-x%** release dihydrogen in a single step with a maximum centered approximately at the median of the distribution. As illustrated, the hydrogen TPD-pattern of **PS-BN-C10-100%**, showcases a peak centered at 154 °C (Figure 78 and see also experimental section 4).

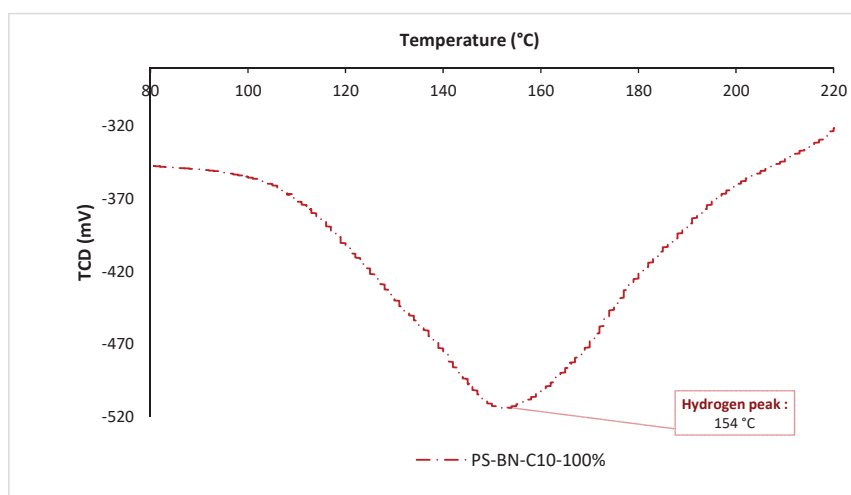


Figure 78. TPD. Measurement of hydrogen generated by thermal treatment of PS-BN-C10-100%. Temperature program: 5 °C/min

For the other polymers, the hydrogen release peak ranged from 127 °C to 173 °C. It depended on both the amine-borane content as well as the nature (C3 or C10) of the alkyl chain. These values have been reported in the chart below (Figure 79).

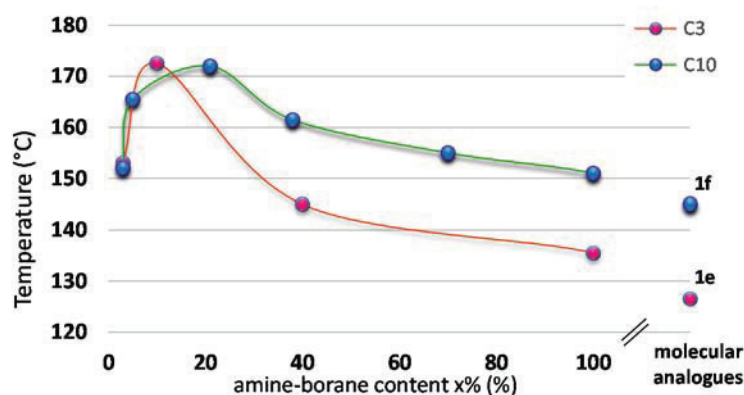


Figure 79. Thermal treatment of polymers PS-BN-C3-x% (green line) and PS-BN-C10-x% (red line) in which  $x = [n/(n+m)] \cdot 100$  is the ratio of amine-borane functionalized styrene moieties, ranging from 3 % to 100 %. Detection of the hydrogen peak with TPD apparatus. The hydrogen peak temperature is reported on the chart



For both polymers **PS-BN-C3-x%** (green curve) and polymers **PS-BN-C10-x%** (red curve) a maximum was reached at 165-173°C for polymers displaying 10 % of amine-borane content. With an amine-borane above 10 %, the temperature of hydrogen release gradually decreased both for **PS-BN-C3-x%** and **PS-BN-C10-x%** until they reach a minimum at 100 % of amine-borane ratio. This value is 8-10 °C higher than their respective molecular bricks **1e** and **1f**.

The fact that the temperature of hydrogen release increased when the amine-borane content decreased is consistent with a bimolecular mechanism. In fact, it can be assumed that the probability of meeting for two amine-borane moieties is dependent of the amine-borane concentration along the polystyrene chain. Thus, if the content of amine-borane is low, the bimolecular dehydrogenation process will be more difficult and will require more energy. The importance of amine-borane concentration has been demonstrated in the literature<sup>4b</sup> by studying amine-borane dehydrogenation in solution (see chapter II.7.a in section1).

However, the behavior of **PS-BN-C3-x%** and **PS-BN-C10-x%** -[under 10% amine-borane]- was surprising as they exhibited a sharp drop in hydrogen-release temperature, which is not consistent with the previous theory. We chose to investigate the structure of polymers by DSC measurements, in particular, to determine the influence of the amine-borane function on the supramolecular structure at low content.

As exemplified on **PS-BN-C10-3%** (Figure 80) the first heat is marked by the dehydrogenation process that can be considered as thermoneutral as the enthalpy of the overall process never exceeds 25 J.g<sup>-1</sup> (see experimental section 4). In comparison, Polyboramine dehydrogenation is endothermic by 300 J.g<sup>-1</sup> and **AB** dehydrogenation is exothermic by 650 000 J.g<sup>-1</sup> (complete dehydrogenation). However, the hydrogen release decomposition step prevents us from seeing structural changes within the polymer (Figure 80).

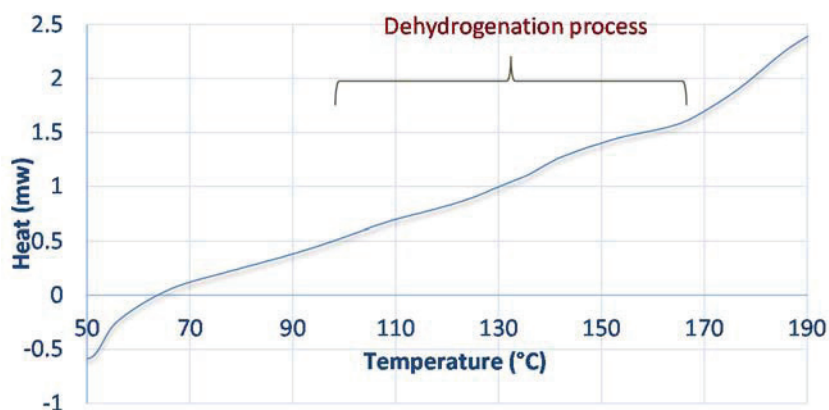


Figure 80. Polymer PS-BN-C10-3% engaged in TPD experiment. First heat. Temperature program: 30-250 °C, 5°C/min.

Consequently we decided to focus our attention on post-dehydrogenation DSC curves (Figure 81). The cooling step (blue arrow) and the second heating step (red arrow) of the dehydrogenated **PS-BN-C10-3%-Dh** material exhibit a glass transition around 113 °C.

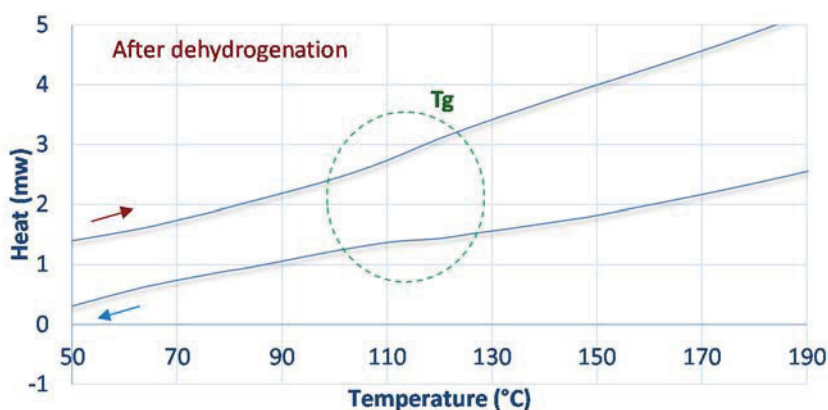


Figure 81. Polymer PS-BN-C10-3%-Dh engaged in TPD experiment. Cooling (blue arrow), temperature program: 250-30 °C, -5°C/min, and second heating (red arrow), temperature program: 30-250 °C, 5°C/min.

The glass transition of a polymer is the physical indication of an amorphous arrangement between macromolecules and is related to their mobility. It is known that the amorphous content of a polymer can dramatically affect the product stability.<sup>84</sup> Below the glass transition temperature ( $T_g$ ) there is limited molecular mobility whereas above  $T_g$  there is high mobility. It results in much lower viscosity and potentially much greater chemical interactions between the components. The value of the heat capacity or  $\Delta C_{p,T_g}$  that occurs at the glass transition is a quantity indicative of the proportion of amorphous material.<sup>84</sup>

We determined the heat capacity of the glass transition for each dehydrogenated functional polymer. Their values were reported on the dehydrogenation temperatures charts of **PS-BN-C3-x%** (Figure 82) and **PS-BN-C10-x%** (Figure 83). The glass transition temperatures of dehydrogenated materials are between 95 °C and 125 °C.

The value of the glass transition heat capacity of **PS-BN-C3-3%** is close to polystyrene, with  $\Delta C_p \sim 0.2 \text{ J.g}^{-1}.\text{K}^{-1}$  and thus, has a similar high amorphous content. Beyond this value, the glass transition temperature increased while the corresponding  $\Delta C_p$  rapidly decreased until the glass-transition phenomenon disappeared completely above 40 % of amine-borane content (see experimental section 4 for DSC). Indeed, it is well established that during the dehydrogenation step, the boron-nitrogen functions are very likely to establish covalent bonds and dipolar interactions that results in the bridging of macromolecular chains. The higher the amine-borane content, the more the polymer is prone to crosslink and form a three-dimensional material. According to DSC studies, dehydrogenated polymers **PS-BN-C3-40%-Dh** and **PS-BN-C3-100%-Dh** are highly rigid materials which exhibit no glass transition temperature.

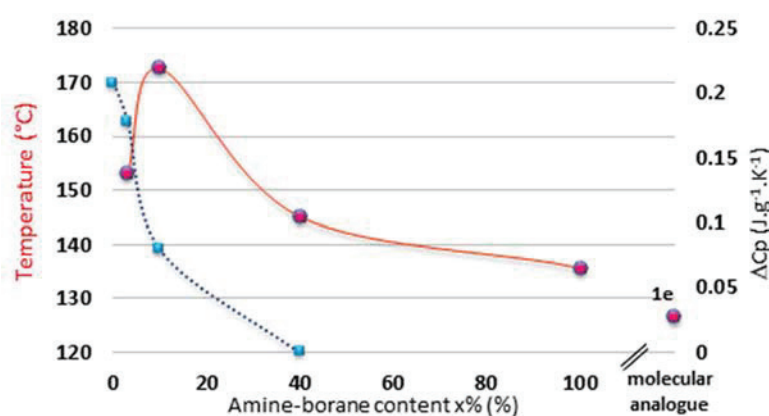


Figure 82. Hydrogen release temperature of polymers **PS-BN-C3-x%** (green line) and heat capacity of the glass transition determined on the dehydrogenated temperature (blue dots).

Glass transitions have been identified in **PS-BN-C10-x%** polymers, until 70 % of amine-borane functionalized content. This means that they globally present a higher amorphous content with respect to their C3 analogues (Figure 83). In contrast with **PS-BN-C3-x%** polymers, the heat capacity of **PS-BN-C10-x%** glass transitions increased from polymer containing 0 to 10% decylamine-borane functionalized unit. It appears that the plasticizing

effect of the C10 aliphatic chains influences the glass state, lowering the  $T_g$ , and prevails regardless of any potential crosslinking arising from DHB in amine-boranes and subsequent covalent bonds after dehydrogenation. Beyond 10 %, the heat capacity of glass transitions dramatically decreased and correlated with observations done on the category of **PS-BN-C3-x%** polymers.

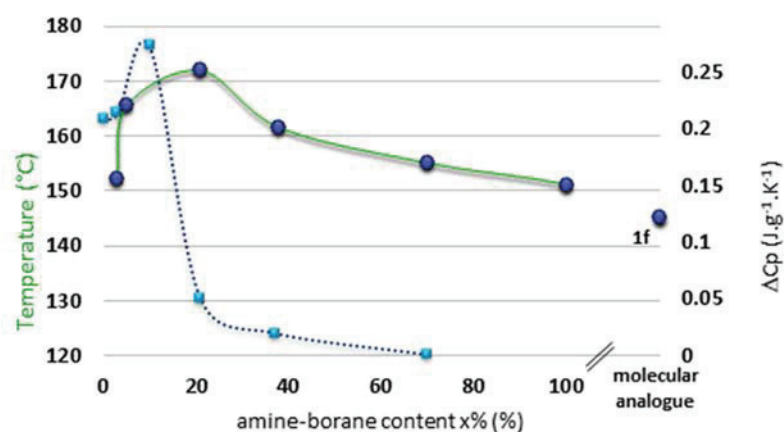


Figure 83. Hydrogen release temperature of polymers **PS-BN-C10-x%** (red line) and heat capacity of the glass transition determined on the dehydrogenated temperature (blue dots).

In essence, the measure of the glass transition heat capacities demonstrated that under 10 % of amine-borane functionality, polymers **PS-BN-C3** and **PS-BN-C10** have an amorphous content that is close to that of polystyrene: the amorphous state is thermodynamically unstable due to increased potential chemical interactions between amine-boranes required for dehydrogenation (fluid state above  $T_g$ ). This could explain the higher reactivity of low-ratio **PS-BN-C3** and **PS-BN-C10** polymers. When increasing the amine-borane content, the glass transition fades away (DHB crosslinking) and statistics take over. The amine-borane content becomes the determining factor: the higher the probability of favorable dimerized structures for dehydrogenation, the lower the temperature of dihydrogen release. The two dehydrogenated polymers at 25 °C, **PS-BN-C10-3%-Dh** (Figure 84, left) and **PS-BN-C10-100%-Dh** (Figure 84, right) having initially low and high amine-borane content respectively, are visually very different. This confirmed the existence of different states of matter during the thermal dehydrogenation.



*Figure 84. Comparative visuals of dehydrogenated polymers exhibiting different macroscopic aspect at 25°C demonstrating different phase states during the dehydrogenation process. PS-BN-C10-3%-Dh, left, transparent aspect and PS-BN-C10-100%, right, white solid.*

We showed that the post-functionalization of a polystyrene matrix with  $\text{-NH}_2\text{-BH}_2\text{-}$  “hydrogen containing” amine-boranes opens the possibility of tuning the kinetics of hydrogen release, in the solid state, without catalysts and with no modification of the electronic environment. By means of simple measurement methods, a structure/reactivity relationship has been established, emphasizing the importance of the material secondary structure in the dehydrogenation process of polymers **PS-BN-C3-x%** and **PS-BN-C10-x%**, and more generally for amine-borane dehydrogenation processes.

We are aware, however, that amine-borane functionalized polystyrenes contain only moderate dihydrogen in weight ratio. In the best cases, polymers **PS-BN-C3-100%** and **PS-BN-C10-100%** are 2.1 wt%  $\text{H}_2$  and 1.4 wt%  $\text{H}_2$  respectively. We aimed at improving this issue by investigating the doping of polymer **PS-BN-C10-100%** (easily processable) with **AB**.

#### III.4. PS-BN-C10-100%/AB hybrid polymers. A new type of high content solid hydrogen material

---

First, the comparison of hydrogen release curves of the polymer **PS-BN-C10-100%** and of **AB** revealed notable differences (Figure 85). The polymer releases dihydrogen in one step centered at 153 °C while **AB** loses dihydrogen in two steps centered at 125 °C and 167 °C.

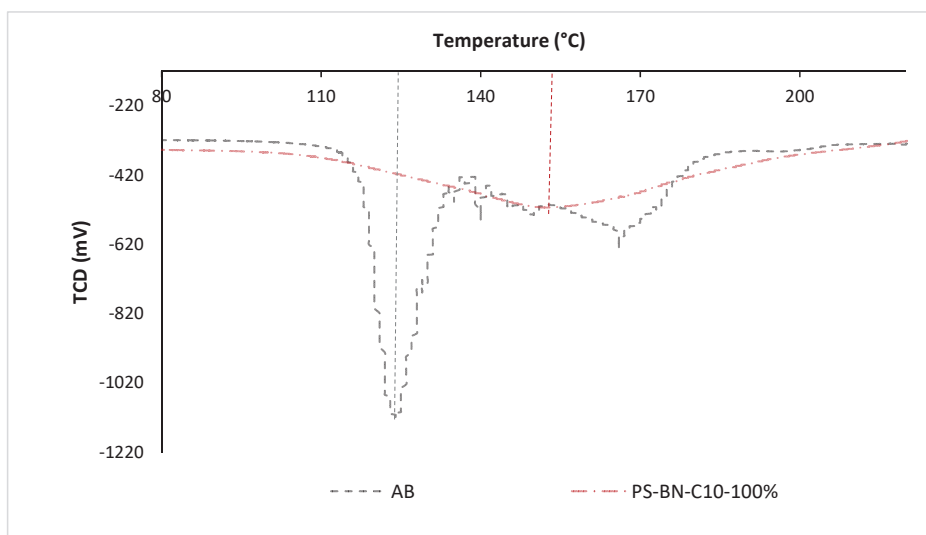
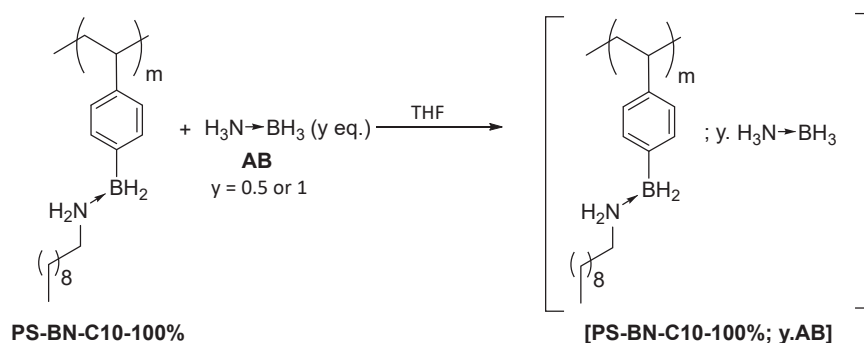


Figure 85. Dehydrogenation TPD curves of AB (grey dots) and PS-BN-C10-100% (red dots)

We synthesized hybrid organic/inorganic materials called **[PS-BN-C10-100%;  $\gamma$ .AB]** that have been obtained by impregnation of  $\gamma$  equivalents of **AB** into polymer **PS-BN-C10-100%** in THF (Scheme 42). The resulting clear solutions were then dried under vacuum to yield a colorless solid. In this manner we synthesized **[PS-BN-C10-100%; 0.5.AB]** and **[PS-BN-C10-100%; 1.AB]** materials containing respectively 0.5 and 1 equivalent of AB with respect to 4-vinylphenyldihydro)borane-(*n*-propyl)amine units. The presence of **AB** has been confirmed by IR spectroscopy (Figure 86 and experimental section 4). The spectrum of **[PS-BN-C10-100%; 1.AB]** for example showed the increase in the IR-evidenced elongation characteristics of amine-borane functions with respect to **PS-BN-C10-100%**. It was particularly evident for the visible B-H stretching at  $\sim 2320\text{ cm}^{-1}$ , typical of the amine-borane moiety.



Scheme 42. Synthesis of organic/inorganic hybrid material by doping polymer PS-BN-C10-100% with AB.

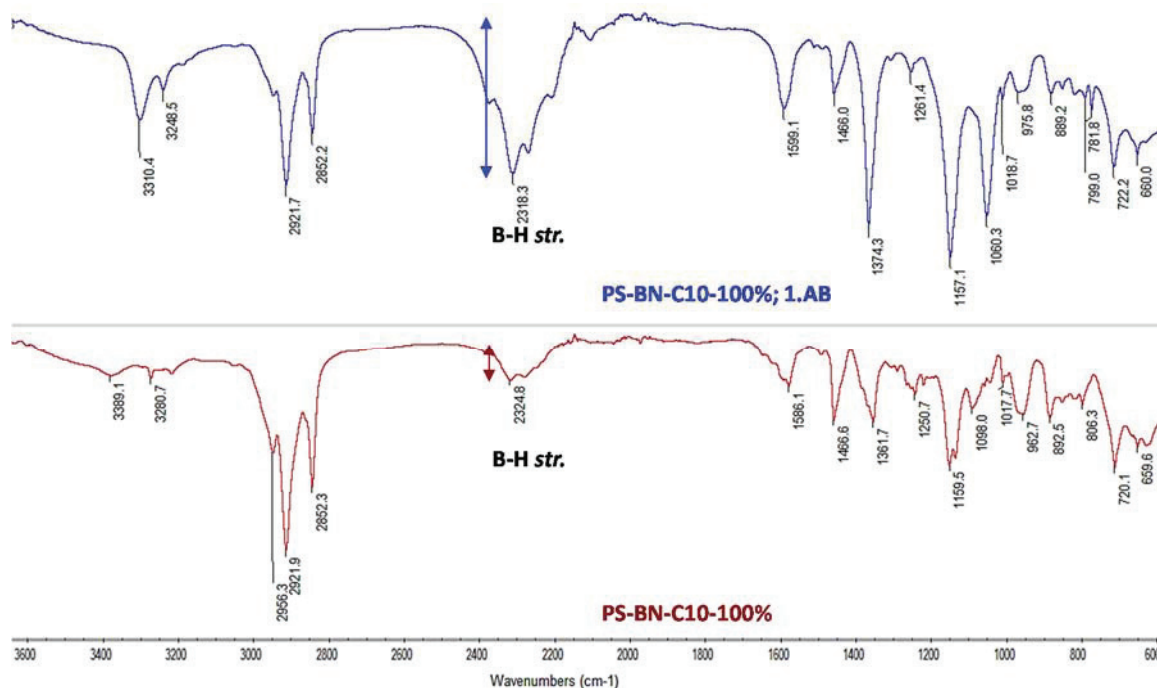


Figure 86. IR spectra of PS-BN-C10-100% (down) and [PS-BN-C10-100%; 1.AB] (up)

TPD experiments were performed on the two hybrid materials **[PS-BN-C10-100%; 0.5.AB]** (Figure 87) and **[PS-BN-C10-100%; 1.AB]** (Figure 88). The TPD trace of the dehydrogenation of **[PS-BN-C10-100%; 0.5.AB]** is not the superimposition of the traces of both starting materials. The dehydrogenation process apparently happens in one step taking place on a very large range of temperature (80 °C to 220 °C). The curve of the hybrid material (green line) is roughly more similar to the polymer curve (red dots). However the outset temperature is lower than that for the polymer and even earlier than **AB** itself. This suggests that a synergistic effect might take place into the hybrid material.

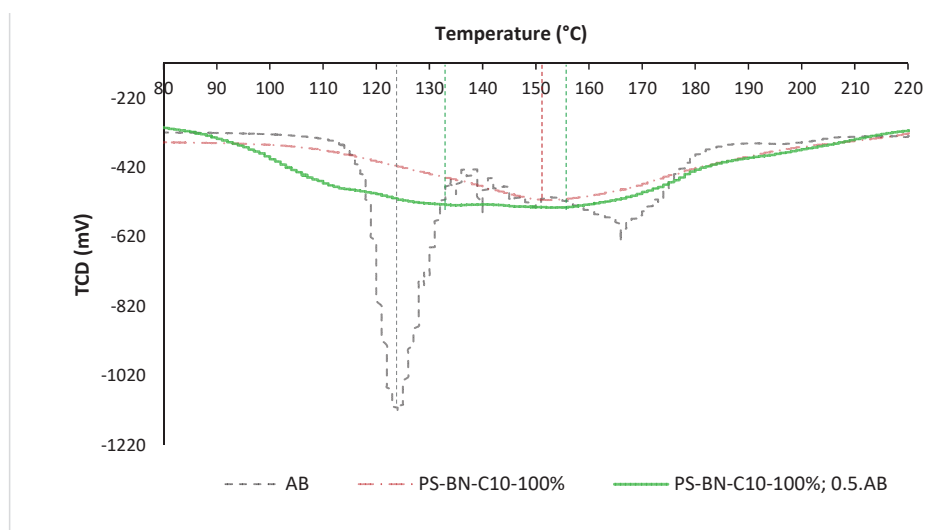


Figure 87. Dehydrogenation TPD curves of AB (grey dots), PS-BN-C10-100% (red dots) and [PS-BN-C10-100%; 0.5.AB] (green line)



The TPD hydrogen curve obtained for **[PS-BN-C10-100%; 1.AB]** (Figure 87) confirmed the existence of a strong synergistic system. The dehydrogenation peak is located at 116 °C much earlier than the starting materials that displayed their maxima at 125 °C and 167 °C respectively. Moreover, the dehydrogenation curves of material **[PS-BN-C10-100%; 1.AB]** repeatedly exhibited narrow peaks and which are, this time, more similar to the **AB** first dehydrogenation peak.

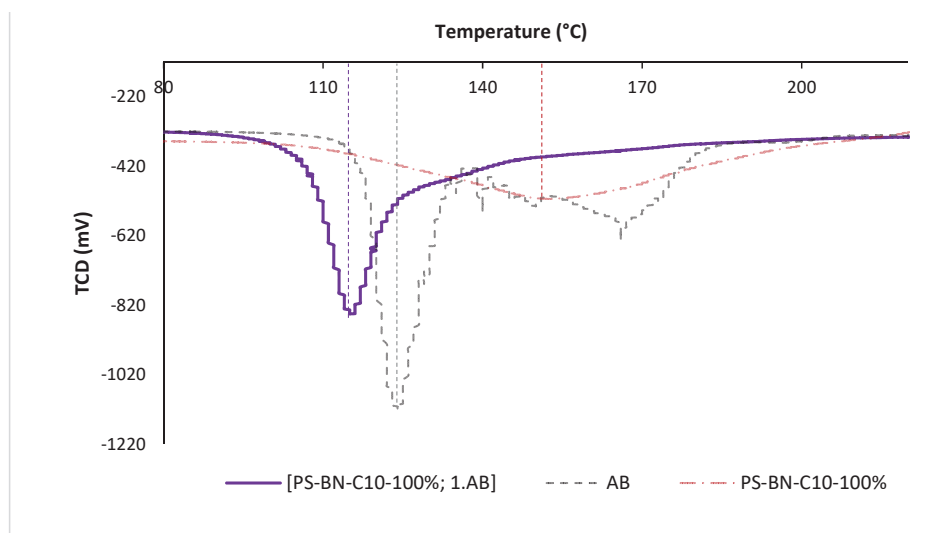


Figure 88. Dehydrogenation TPD curves of AB (grey dots), PS-BN-C10-100% (red dots) and [PS-BN-C10-100%; 1.AB] (violet line)

It seems clear that the two different types of amine-boranes present into the material do not dehydrogenate independently, and that interactions between the two species yield in a single behavior. The narrowness of the peak, similarly to AB, is evidently the result of an improved interaction between amine-borane functions into the material and by an enhanced mobility brought by **AB** molecules accommodating multi-molecular structures required along the dehydrogenation pathway. Finally, it is likely that the **AB** DHB network within the polymer is substantially disrupted and has a lower degree of crystallinity than in pure **AB**.<sup>64-65</sup> We envision the DHB disruption as being induced by the presence of substituents on amine-borane moieties and by the polymer backbone itself. In other words, and according to our conclusions and observations on the set of functionalized polystyrenes, the organic fraction is likely to provide a substantial degree of amorphicity to **AB** network. In essence we think that **AB** within **PS-BN-C10-100%** is thermodynamically



less stable than pure **AB**, which results in a decreased temperature of dehydrogenation for the mixture.

---

## IV. Conclusion and perspectives

---

We have synthesized two families of polymers: poly[styrene-*ran*-((4-vinylphenyldihydro)borane-(*n*-propyl)amine)] and poly[styrene-*ran*-((4-vinylphenyldihydro)borane-(*n*-decyl)amine)] by free radical polymerization and post-functionalization, using the one-pot methodology developed in our lab. We established the influence of structural parameters, such as the chain mobility or the hydrogen-bonding, on the dehydrogenation of these unique polymers. Moreover, doping these functionalized polymers with AB not only permitted to create a new hybrid organic/inorganic material with an increased H<sub>2</sub> gravimetric capacity from 1.5 wt.% to 3.3 wt.%, but resulted surprisingly in a substantial modification of the dehydrogenation pattern. These promising materials are thus characterized by a synergistic effect between the amine-borane bounded polymer and AB. Ongoing researches are focused on increasing even more the H<sub>2</sub> % weight content. Moreover we are currently investigating the possible structural or chemical modifications associated to a doping of the amine-borane polymer, and their influence on the dehydrogenation pattern that we observed (<sup>1</sup>H, <sup>11</sup>B and <sup>10</sup>B solid-state NMR studies in particular).

## General conclusion and perspectives

During our researches assessing new reactivity at boron, in particular embedded in Lewis-pair –containing materials, we synthesized innovative polymers bearing amine-borane moieties in their backbone. We have been interested in their potential as hydrogen reservoirs and in the structure/reactivity relationship involved in dehydrogenation pathways. Two principal families of polymer architectures have been designed. The first family was constituted of polymers having amine-borane bonds in the main-chain and the second one of polymers featuring pendant amine-borane motifs in a polystyrene backbone.

Both polymers were obtained *via* a simple, one-step, treatment of both boronic acids/esters and ammonium chlorides with  $\text{LiAlH}_4$ . The choice of the solvent mixture appeared to be a crucial parameter to isolate selectively the amine-borane material. We obtained polymers having molar masses in the range of  $10^5$  Da and both polyboramines and polystyrene-*g*-boramines showed interesting glass transition temperatures, potentially enabling their processability.

We observed important differences between polyboramines and molecular amine-boranes, notably concerning the thermal dehydrogenation pattern in the solid state. The thermal dehydrogenation of polyboramines occurred below  $100^\circ\text{C}$  and was endothermic, in stark contrast to molecular amine-boranes that dehydrogenate over  $100^\circ\text{C}$  in an exothermic fashion. We evidenced that these modifications were the direct consequence of the incorporation of the amine-borane moieties into polymeric chains. With the help of DFT calculations, we evidenced that a dimerization took place to allow for the dehydrogenation of amine-boranes and therefore that entropy likely played a major role in the peculiar behavior of our polymers. Our main hypotheses were leaning toward: 1) the increased concentration of borane chain-ends (due to ease of dissociation of amine-borane dative bonds in the mechanically stressed polyboramines) catalyzing the dehydrogenation and explaining the lowering of dehydrogenation temperature; and 2) the reduced mobility induced by the polymer matrix hampering the accumulation of

thermodynamically stabilized multi-molecular assemblies similar to DADB structures justifying the endothermic process. Moreover, we demonstrated that polyboramines and their molecular analogues had a better reactivity than AB for the reduction of carbonyls by transfer hydrogenation in solution. For the latter, polyboramines and molecular counterparts exhibited similar reactivities which contrasted to the observations made during solid state dehydrogenation.

By inserting amine-boranes as side-chains of a polystyrene backbone, we observed a non-linear effect of the amine-borane content on the thermal dehydrogenation profile in the solid state. The bell-shaped dependency of the dehydrogenation temperature vs. the amine-borane content could be explained by two separate and opposed phenomena. At low amine-borane content, the polystyrene-*g*-boramines displayed a  $T_g$  and a dehydrogenation temperature higher than said  $T_g$ . The increased mobility of chains allowed for the necessary reorganization (dimerization, as evidenced by DFT) and explained the rather low dehydrogenation temperature, comparable to the molecular analogues. On the other hand, at higher amine-borane content, the polystyrene-*g*-boramines behaved as crosslinked materials (due mainly to dihydrogen bonding), no longer exhibiting a  $T_g$ . In that case, statistics took over and the highest the amine-borane content the lowest the dehydrogenation temperature, due to increases in the dimerized structures necessary for dehydrogenation. We thus demonstrated the influence of structural properties such as the amorphous content as well as the amine-borane content, on the reactivity. Furthermore, doping the 100 % amine-borane functionalized polymer with 1 equivalent of AB, resulted in a significant modification of the solid-state thermal dehydrogenation process. We observed the AB-doped polymer behaving as a new, single entity. The thermal dehydrogenation temperature of this new material occurred below that of either AB or amine-borane polymer taken separately. These results suggested a synergistic effect between the amine-borane grafted polymer and AB. Ongoing research are focused on increasing the  $H_2$  % weight content of these systems using a higher AB doping percentage.

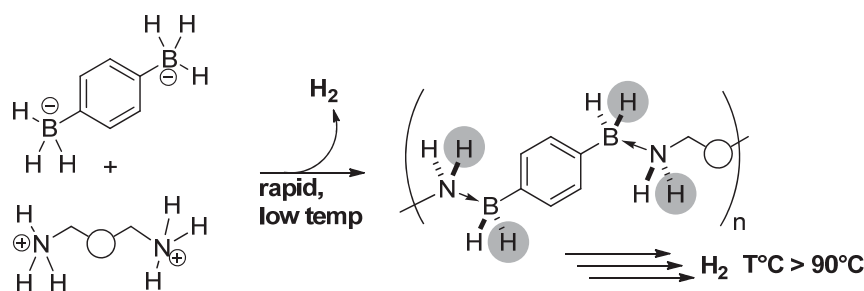
In order to establish rational correlations between the material structure and the amine-borane reactivity, we are currently assessing experimental results with advanced solid-

state NMR characterization ( $^1\text{H}$ ,  $^{11}\text{B}$  and  $^{10}\text{B}$  mainly) and computational studies at both molecular and macromolecular level (QMMM for instance). We want to determine the modifications brought about by the polymer backbone on the amine-borane environment and the influence of the secondary structure adopted by the macromolecules.

With this approach, we expect to design materials featuring finely tuned dehydrogenation properties and energetically favorable profiles in order to consider putative rehydrogenation pathways.

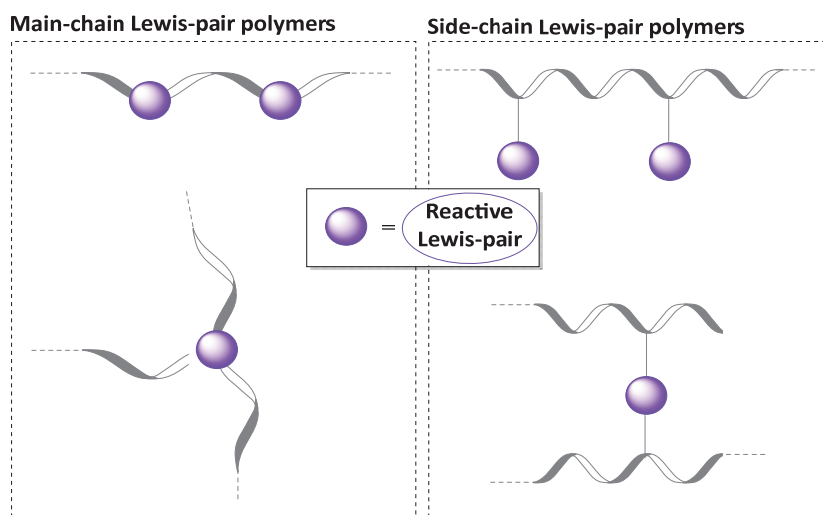
From a wider perspective, the study of Lewis pair-containing polymers is related a new trend in supramolecular chemistry. Conventional supramolecular chemistry is based on selective pair-interactions between a host and a guest (*e.g.* protein-protein interactions, single or multiple hydrogen bonding between donors and acceptors, metal-ligand interactions, pi-pi stacking between aromatic cycles). The affinity of such interactions can be varied by different stimuli such as temperature, ionic force, pH or solvation. As a consequence, integrating such supramolecular units into polymeric backbones leads to stimuli-responsive materials with tunable structures and physical properties, with growing fields of application. The introduction of Lewis pairing instead of H-bonds would provide an opportunity to study new supramolecular materials with a wide variability of the interaction energy as well as the exchange kinetics.

This thesis represents a proof of concept, since the integration of either conventional Lewis pairs or FLPs could be undergone following the same methodologies, with variations around the nature and structures of both acid and base partners. For instance, the lack of frustration in our polyboramines explains the strong displacement of the equilibrium towards the amine-borane bond from the hypothetical borohydride/ammonium mixture with expulsion of dihydrogen. Working on both sterics and electronics could help develop new reactive/responsive materials (supports for heterogeneous catalysis, storage materials, purification monoliths, chemically/mechanically adaptable materials, perm-selective membranes, organic transistors...).



This work would in particular necessitate the study of dative-bond strengths in various Lewis pair systems. Both reversibility and reactivity depend strongly on this parameter. A tentative ranking of Lewis pairing could also allow for evolutive materials with potential substitution or a first Lewis base with a stronger one (similarly for Lewis acids). This synthetic toolbox would yield almost limitless variability on accessible structures and reactivities/functions for these new supramolecular materials. One could also access simply 3D materials in which one might stabilize boron-centered reactive intermediates for a variety of new applications, from electronics to catalysis.

Eventually, an obvious reactivity, beyond Lewis pairs' and FLPs' intrinsic reactivities, that could be harnessed at this stage is the rich and ever developing Boron chemistry. Most notably, Borinium, Borenium, and Boronium cations; Diborenes and Diborynes: Borylenes and last but not least Boron-centered radicals. During the course of this PhD work, we have developed strategies to introduce stabilized Boron atoms in materials and these methodologies could prove useful to develop new B-containing polymers featuring the above-mentioned reactive Boron species.





## References

1. (a) Staubitz, A.; Robertson, A. P. M.; Sloan, M. E.; Manners, I., *Chem. Rev.* **2010**, *110*, 4023-4078; (b) Stephan, D. W.; Erker, G., *Angew. Chem. Int. Ed.* **2010**, *49*, 46-76; (c) Chernichenko, K.; Madarász, Á.; Pápai, I.; Nieger, M.; Leskelä, M.; Repo, T., *Nature Chemistry* **2013**, *5*, 718-723; (d) Sumerin, V.; Schulz, F.; Atsumi, M.; Wang, C.; Nieger, M.; Leskelä, M.; Repo, T.; Pyykkö, P.; Rieger, B., *J. Am. Chem. Soc.* **2008**, *130*, 14117-14119.
2. Hamilton, C. W.; Baker, R. T.; Staubitz, A.; Manners, I., *Chem. Soc. Rev.* **2009**, *38*, 279.
3. Nguyen, V. S.; Matus, M. H.; Grant, D. J.; Nguyen, M. T.; Dixon, D. A., *The Journal of Physical Chemistry A* **2007**, *111*, 8844-8856.
4. (a) Baitalow, F.; Baumann, J.; Wolf, G.; Jaenicke-Rößler, K.; Leitner, G., *Thermochim. Acta* **2002**, *391*, 159-168; (b) Shaw, W. J.; Linehan, J. C.; Szymczak, N. K.; Heldebrant, D. J.; Yonker, C.; Camaioni, D. M.; Baker, R. T.; Autrey, T., *Angew. Chem. Int. Ed.* **2008**, *47*, 7493-7496; (c) Chen, G.; Zakharov, L. N.; Bowden, M. E.; Karkamkar, A. J.; Whittemore, S. M.; Garner, E. B.; Mikulas, T. C.; Dixon, D. A.; Autrey, T.; Liu, S.-Y., *J. Am. Chem. Soc.* **2015**, *137*, 134-137.
5. Carboni, B.; Monier, L., *Tetrahedron* **1999**, *55*, 1197-1248.
6. Curran, D. P.; Solov'yev, A.; Makhoulouf Brahm, M.; Fensterbank, L.; Malacria, M.; Lacôte, E., *Angew. Chem. Int. Ed.* **2011**, *50*, 10294-10317.
7. Corey, E. J.; Shibata, S.; Bakshi, R. K., *The Journal of Organic Chemistry* **1988**, *53*, 2861-2863.
8. (a) Mummadi, S.; Unruh, D. K.; Zhao, J.; Li, S.; Krempner, C., *J. Am. Chem. Soc.* **2016**, *138*, 3286-3289; (b) Welch, G. C.; Juan, R. R. S.; Masuda, J. D.; Stephan, D. W., *Science* **2006**, *314*, 1124-1126.
9. (a) Chong, C. C.; Hirao, H.; Kinjo, R., *Angew. Chem. Int. Ed.* **2014**, *53*, 3342-3346; (b) Yang, X.; Fox, T.; Berke, H., *Chem. Commun.* **2011**, *47*, 2053; (c) Yang, X.; Zhao, L.; Fox, T.; Wang, Z.-X.; Berke, H., *Angew. Chem. Int. Ed.* **2010**, *49*, 2058-2062.
10. Shi, L.; Liu, Y.; Liu, Q.; Wei, B.; Zhang, G., *Green Chemistry* **2012**, *14*, 1372-1375.
11. Staubitz, A.; Robertson, A. P. M.; Manners, I., *Chem. Rev.* **2010**, *110*, 4079-4124.
12. Haaland, *Angew. Chem. Int. Ed.* **1989**, *28*, 992-1007.
13. Liu, Z.; Marder, T. B., *Angew. Chem. Int. Ed.* **2008**, *47*, 242-244.
14. Huang, Z.; Autrey, T., *Energy & Environmental Science* **2012**, *5*, 9257-9268.
15. Yan, S.; Zou, H.; Kang, W.; Sun, L., *J. Mol. Model.* **2016**, *22*, 17.
16. Chen, X.; Zhao, J.-C.; Shore, S. G., *Acc. Chem. Res.* **2013**, *46*, 2666-2675.
17. Ledoux, A.; Larini, P.; Boisson, C.; Monteil, V.; Raynaud, J.; Lacôte, E., *Angew. Chem. Int. Ed.* **2015**, *54*, 15744-15749.
18. Bessac, F.; Frenking, G., *Inorg. Chem.* **2006**, *45*, 6956-6964.
19. Campbell, P. G.; Marwitz, A. J. V.; Liu, S.-Y., *Angew. Chem. Int. Ed.* **2012**, *51*, 6074-6092.
20. Stock, A.; Pohland, E., *Berichte der deutschen chemischen Gesellschaft (A and B Series)* **1926**, *59*, 2215-2223.
21. Paine, R. T.; Narula, C. K., *Chem. Rev.* **1990**, *90*, 73-91.
22. Sundaram, R.; Scheiner, S.; Roy, A. K.; Kar, T., *The Journal of Physical Chemistry C* **2015**, *119*, 3253-3259.
23. (a) Bettinger, H. F.; Müller, M., *J. Phys. Org. Chem.* **2015**, *28*, 97-103; (b) Luo, W.; Campbell, P. G.; Zakharov, L. N.; Liu, S.-Y., *J. Am. Chem. Soc.* **2011**, *133*, 19326-19329.
24. (a) Luo, W.; Zakharov, L. N.; Liu, S.-Y., *J. Am. Chem. Soc.* **2011**, *133*, 13006-13009; (b) Abbey, E. R.; Zakharov, L. N.; Liu, S.-Y., *J. Am. Chem. Soc.* **2011**, *133*, 11508-11511; (c) Braunschweig, H.; Celik, M. A.; Hupp, F.; Krummenacher, I.; Mailänder, L., *Angew. Chem. Int. Ed.* **2015**, n/a-n/a.
25. (a) Neiner, D.; Karkamkar, A.; Bowden, M.; Joon Choi, Y.; Luedtke, A.; Holladay, J.; Fisher, A.; Szymczak, N.; Autrey, T., *Energy & Environmental Science* **2011**, *4*, 4187; (b) Zhang, L.; Li, S.; Tan, Y.; Tang, Z.; Guo, Z.; Yu, X., *Journal of Materials Chemistry A* **2014**, *2*, 10682.
26. Burg, A. B.; Schlesinger, H. I., *J. Am. Chem. Soc.* **1937**, *59*, 780-787.
27. (a) Paz-Sandoval, M. A.; Camacho, C.; Contreras, R.; Wrackmeyer, B., *Spectrochimica Acta Part A: Molecular Spectroscopy* **1987**, *43*, 1331-1335; (b) Burg, A. B.; Randolph, C. L., *J. Am. Chem. Soc.* **1949**, *71*, 3451-3455; (c) Narayana, C.; Periasamy, M., *J. Chem. Soc., Chem. Commun.* **1987**, 1857-1859.
28. Parry, R. W.; Edwards, L. J., *J. Am. Chem. Soc.* **1959**, *81*, 3554-3560.
29. Shore, S. G.; Boddeker, K. W., *Inorg. Chem.* **1964**, *3*, 914-915.

30. Jaska, C. A.; Temple, K.; Lough, A. J.; Manners, I., *J. Am. Chem. Soc.* **2003**, *125*, 9424-9434.
31. Baldwin, R.; Washburn, R., *The Journal of Organic Chemistry* **1961**, *26*, 3549-3550.
32. Brown, H. C.; Schlesinger, H. I.; Cardon, S. Z., *J. Am. Chem. Soc.* **1942**, *64*, 325-329.
33. (a) Sheldong, S.; Ann Arbor, M. I. R.; Parry, Journal of American Chemical Society: **1955**; Vol. 77, p 6084; (b) Ramachandran, P. V.; Gagare, P. D., *Inorg. Chem.* **2007**, *46*, 7810-7817; (c) Hawthorne, M. F., *J. Am. Chem. Soc.* **1961**, *83*, 831-833; (d) Singaram, B.; Cole, T. E.; Brown, H. C., *Organometallics* **1984**, *3*, 774-777; (e) Schaeffer, G. W.; Anderson, E. R., *J. Am. Chem. Soc.* **1949**, *71*, 2143-2145; (f) Brown, H. C.; Srebnik, M.; Cole, T. E., *Organometallics* **1986**, *5*, 2300-2303; (g) Heldebrant, D. J.; Karkamkar, A.; Linehan, J. C.; Autrey, T., *Energy & Environmental Science* **2008**, *1*, 156.
34. Franz, D.; Bolte, M.; Lerner, H.-W.; Wagner, M., *Dalton Trans.* **2011**, *40*, 2433-2440.
35. Nainan, K. C.; Ryschkewitsch, G. E., *Inorgannic Chemistry* **1969**, *8*, 2671-2674.
36. Brahmi, M. M.; Monot, J.; Desage-El Murr, M.; Curran, D. P.; Fensterbank, L.; Lacôte, E.; Malacria, M., *The Journal of Organic Chemistry* **2010**, *75*, 6983-6985.
37. (a) Seven, Ö.; Qu, Z.-W.; Zhu, H.; Bolte, M.; Lerner, H.-W.; Holthausen, M. C.; Wagner, M., *Chemistry - A European Journal* **2012**, *18*, 11284-11295; (b) Scheibitz, M.; Li, H.; Schnorr, J.; Sánchez Perucha, A.; Bolte, M.; Lerner, H.-W.; Jäkle, F.; Wagner, M., *J. Am. Chem. Soc.* **2009**, *131*, 16319-16329.
38. Campbell, P. G.; Zakharov, L. N.; Grant, D. J.; Dixon, D. A.; Liu, S.-Y., *J. Am. Chem. Soc.* **2010**, *132*, 3289-3291.
39. (a) Hawthorne, M. F., *J. Am. Chem. Soc.* **1958**, *80*, 4293-4296; (b) Hawthorne, M. F., *J. Am. Chem. Soc.* **1958**, *80*, 4291-4293.
40. Veeraraghavan Ramachandran, P.; Raju, B. C.; Gagare, P. D., *Org. Lett.* **2012**, *14*, 6119-6121.
41. Marder, T. B., *Angew. Chem. Int. Ed.* **2007**, *46*, 8116-8118.
42. Crabtree, G. W.; Dresselhaus, M. S.; Buchanan, M. V., *Physics Today* **2004**, *57*, 39-44.
43. von Helmolt, R.; Eberle, U., *J. Power Sources* **2007**, *165*, 833-843.
44. be Stored, H.
45. Johnson, W. H.; Kilday, M. V.; Prosen, E. J., *JOURNAL OF RESEARCH of the National Bureau of Standards-A. Physics and Chemistry* **1961**, *65A*, 101-104.
46. (a) Weng, B.; Wu, Z.; Li, Z.; Yang, H., *Int. J. Hydrogen Energy* **2012**, *37*, 5152-5160; (b) Davis, B. L.; Dixon, D. A.; Garner, E. B.; Gordon, J. C.; Matus, M. H.; Scott, B.; Stephens, F. H., *Angew. Chem. Int. Ed.* **2009**, *48*, 6812-6816; (c) Sutton, A. D.; Burrell, A. K.; Dixon, D. A.; Garner, E. B.; Gordon, J. C.; Nakagawa, T.; Ott, K. C.; Robinson, J. P.; Vasiliu, M., *Science* **2011**, *331*, 1426-1429.
47. Staubitz, A.; Besora, M.; Harvey, J. N.; Manners, I., *Inorg. Chem.* **2008**, *47*, 5910-5918.
48. Wolf, G.; Baumann, J.; Baitalow, F.; Hoffmann, F. P., *Thermochim. Acta* **2000**, *343*, 19-25.
49. Paolone, A.; Teocoli, F.; Sanna, S.; Palumbo, O.; Autrey, T., *The Journal of Physical Chemistry C* **2013**, *117*, 729-734.
50. Stowe, A. C.; Shaw, W. J.; Linehan, J. C.; Schmid, B.; Autrey, T., *PCCP* **2007**, *9*, 1831.
51. Demirci, U. B.; Bernard, S.; Chiriac, R.; Toche, F.; Miele, P., *J. Power Sources* **2011**, *196*, 279-286.
52. Baumann, J.; Baitalow, F.; Wolf, G., *Thermochim. Acta* **2005**, *430*, 9-14.
53. Dixon, D. A.; Gutowski, M., *The Journal of Physical Chemistry A* **2005**, *109*, 5129-5135.
54. Zimmerman, P. M.; Paul, A.; Zhang, Z.; Musgrave, C. B., *Inorg. Chem.* **2009**, *48*, 1069-1081.
55. .
56. Feyereisen, M. W.; Feller, D.; Dixon, D. A., *The Journal of Physical Chemistry* **1996**, *100*, 2993-2997.
57. (a) Himmelberger, D. W.; Alden, L. R.; Bluhm, M. E.; Sneddon, L. G., *Inorg. Chem.* **2009**, *48*, 9883-9889; (b) Bluhm, M. E.; Bradley, M. G.; Butterick, R.; Kusari, U.; Sneddon, L. G., *J. Am. Chem. Soc.* **2006**, *128*, 7748-7749.
58. (a) Jaska, C. A.; Temple, K.; Lough, A. J.; Manners, I., *Chem. Commun.* **2001**, 962-963; (b) Denney, M. C.; Pons, V.; Hebden, T. J.; Heinekey, D. M.; Goldberg, K. I., *J. Am. Chem. Soc.* **2006**, *128*, 12048-12049; (c) Blaquiere, N.; Diallo-Garcia, S.; Gorelsky, S. I.; Black, D. A.; Fagnou, K., *J. Am. Chem. Soc.* **2008**, *130*, 14034-14035; (d) Käß, M.; Friedrich, A.; Drees, M.; Schneider, S., *Angew. Chem. Int. Ed.* **2009**, *48*, 905-907; (e) Keaton, R. J.; Blacquiere, J. M.; Baker, R. T., *J. Am. Chem. Soc.* **2007**, *129*, 1844-1845; (f) Kakizawa, T.; Kawano, Y.; Naganeyama, K.; Shimoi, M., *Chem. Lett.* **2011**, *40*, 171-173; (g) Pons, V.; Baker, R. T.; Szymczak, N. K.; Heldebrant, D. J.; Linehan, J. C.; Matus, M. H.; Grant, D. J.; Dixon, D. A., *Chem. Commun.* **2008**, 6597; (h) Vance, J. R.; Schäfer, A.; Robertson, A. P. M.; Lee, K.; Turner, J.; Whittell, G. R.; Manners, I., *J. Am. Chem. Soc.* **2014**, *136*, 3048-3064; (i) Helten, H.; Dutta, B.; Vance, J. R.; Sloan, M. E.; Haddow, M. F.; Sproules, S.; Collison, D.; Whittell, G. R.; Lloyd-Jones, G. C.; Manners, I., *Angew. Chem. Int. Ed.* **2013**, *52*, 437-440.



59. (a) Li, P.-Z.; Aranishi, K.; Xu, Q., *Chem. Commun.* **2012**, 48, 3173; (b) Sun, D.; Mazumder, V.; Metin, Ö.; Sun, S., *ACS Nano* **2011**, 5, 6458-6464; (c) Mori, K.; Miyawaki, K.; Yamashita, H., *ACS Catalysis* **2016**, 6, 3128-3135; (d) Zahmakiran, M.; Ayvali, T.; Philippot, K., *Langmuir* **2012**, 28, 4908-4914.
60. Stephens, F. H.; Baker, R. T.; Matus, M. H.; Grant, D. J.; Dixon, D. A., *Angew. Chem. Int. Ed.* **2007**, 46, 746-749.
61. Basu, S.; Brockman, A.; Gagare, P.; Zheng, Y.; Ramachandran, P. V.; Delgass, W. N.; Gore, J. P., *J. Power Sources* **2009**, 188, 238-243.
62. (a) Johnson, H. C.; Robertson, A. P. M.; Chaplin, A. B.; Sewell, L. J.; Thompson, A. L.; Haddow, M. F.; Manners, I.; Weller, A. S., *J. Am. Chem. Soc.* **2011**, 133, 11076-11079; (b) Kumar, A.; Beattie, N. A.; Pike, S. D.; Macgregor, S. A.; Weller, A. S., *Angew. Chem. Int. Ed.* **2016**, n/a-n/a.
63. Staubitz, A.; Presa Soto, A.; Manners, I., *Angew. Chem. Int. Ed.* **2008**, 47, 6212-6215.
64. Grant, D. J.; Matus, M. H.; Anderson, K. D.; Camaioni, D. M.; Neufeldt, S. R.; Lane, C. F.; Dixon, D. A., *The Journal of Physical Chemistry A* **2009**, 113, 6121-6132.
65. Carre-Burritt, A. E.; Davis, B. L.; Rekken, B. D.; Mack, N.; Semelsberger, T. A., *Energy & Environmental Science* **2014**, 7, 1653.
66. Li, L.; Gu, Q.; Tang, Z.; Chen, X.; Tan, Y.; Li, Q.; Yu, X., *Journal of Materials Chemistry A* **2013**, 1, 12263.
67. (a) Dündar-Tekkaya, E.; Yürüm, Y., *Int. J. Hydrogen Energy* **2016**, 41, 9789-9795; (b) Kim, H.; Karkamkar, A.; Autrey, T.; Chupas, P.; Proffen, T., *J. Am. Chem. Soc.* **2009**, 131, 13749-13755.
68. Li, Z.; Zhu, G.; Lu, G.; Qiu, S.; Yao, X., *J. Am. Chem. Soc.* **2010**, 132, 1490-1491.
69. (a) Sepehri, S.; García, B. B.; Cao, G., *Eur. J. Inorg. Chem.* **2009**, 2009, 599-603; (b) Sepehri, S.; Feaver, A.; Shaw, W. J.; Howard, C. J.; Zhang, Q.; Autrey, T.; Cao, *The Journal of Physical Chemistry B* **2007**, 111, 14285-14289.
70. (a) Neiner, D.; Karkamkar, A.; Linehan, J. C.; Arey, B.; Autrey, T.; Kauzlarich, S. M., *The Journal of Physical Chemistry C* **2009**, 113, 1098-1103; (b) Kuang, A.; Zhou, T.; Wang, G.; Li, Y.; Wu, G.; Yuan, H.; Chen, H.; Yang, X., *Appl. Surf. Sci.* **2016**, 362, 562-571.
71. Tang, Z.; Chen, X.; Chen, H.; Wu, L.; Yu, X., *Angew. Chem. Int. Ed.* **2013**, 52, 5832-5835.
72. Yang, Z.; Cheng, F.; Tao, Z.; Liang, J.; Chen, J., *Int. J. Hydrogen Energy* **2012**, 37, 7638-7644.
73. Itsuno, S.; Sawada, T.; Hayashi, T.; Ito, K., *J. Inorg. Organomet. Polym.* **1994**, 4, 403-414.
74. Matsumoto, F.; Chujo, Y., *Macromolecules* **2003**, 36, 5516-5519.
75. Marco Fontani, F. P.; Wolfgang Scherera, Matthias Wagner, and Piero Zanello, *Eur. J. Inorg. Chem.* **1998**, 1453-1465.
76. Grosche, M.; Herdtweck, E.; Peters, F.; Wagner, M., *Organometallics* **1999**, 18, 4669-4672.
77. Christinat, N.; Croisier, E.; Scopelliti, R.; Cascella, M.; Röthlisberger, U.; Severin, K., *Eur. J. Inorg. Chem.* **2007**, 2007, 5177-5181.
78. Sheepwash, E.; Kramp, V.; Scopelliti, R.; Sereda, O.; Neels, A.; Severin, K., *Angew. Chem. Int. Ed.* **2011**, 50, 3034-3037.
79. Qin, Y.; Cui, C.; Jäkle, F., *Macromolecules* **2007**, 40, 1413-1420.
80. Pons, V.; Baker, R. T., *Angew. Chem. Int. Ed.* **2008**, 47, 9600-9602.
81. Staubitz, A.; Sloan, M. E.; Robertson, A. P. M.; Friedrich, A.; Schneider, S.; Gates, P. J.; Günne, J. S. a. d.; Manners, I., *J. Am. Chem. Soc.* **2010**, 132, 13332-13345.
82. (a) Ueng, S.-H.; Makhlof Brahmi, M.; Derat, É.; Fensterbank, L.; Lacôte, E.; Malacria, M.; Curran, D. P., *J. Am. Chem. Soc.* **2008**, 130, 10082-10083; (b) Telitel, S.; Vallet, A.-L.; Schweizer, S.; Delpech, B.; Blanchard, N.; Morlet-Savary, F.; Graff, B.; Curran, D. P.; Robert, M.; Lacôte, E.; Lalevée, J., *J. Am. Chem. Soc.* **2013**, 135, 16938-16947; (c) Lalevée, J.; Telitel, S.; Tehfe, M. A.; Fouassier, J. P.; Curran, D. P.; Lacôte, E., *Angew. Chem.* **2012**, 124, 6060-6063.
83. Ruff, J. K.; Hawthorne, M. F., *J. Am. Chem. Soc.* **1960**, 82, 2141-2144.
84. Thomas, S. R. A. L. C. *Detection and Quantification of Amorphous Content in Pharmaceutical Materials*; TA Instruments.
85. (a) Yang, X.; Fox, T.; Berke, H., *Org. Biomol. Chem.* **2012**, 10, 852-860; (b) Zhao, L.; Li, H.; Lu, G.; Wang, Z.-X., *Dalton Transactions* **2010**, 39, 4038.
86. (a) Leitao, E. M.; Stubbs, N. E.; Robertson, A. P. M.; Helten, H.; Cox, R. J.; Lloyd-Jones, G. C.; Manners, I., *J. Am. Chem. Soc.* **2012**, 134, 16805-16816; (b) Robertson, A. P. M.; Leitao, E. M.; Manners, I., *J. Am. Chem. Soc.* **2011**, 133, 19322-19325.
87. Yang, X.; Fox, T.; Berke, H., *Tetrahedron* **2011**, 67, 7121-7127.

88. (a) Noyori, R.; Ohkuma, T.; Kitamura, M.; Takaya, H.; Sayo, N.; Kumobayashi, H.; Akutagawa, S., *J. Am. Chem. Soc.* **1987**, *109*, 5856-5858; (b) Noyori, R.; Kitamura, M.; Ohkuma, T., *Proceedings of the National Academy of Sciences of the United States of America* **2004**, *101*, 5356-5362.
89. Nöth, H.; Vahrenkamp, H., *Chem. Ber.* **1967**, *100*, 3353-3362.
90. Mo, Z.; Rit, A.; Campos, J.; Kolychev, E. L.; Aldridge, S., *J. Am. Chem. Soc.* **2016**, *138*, 3306-3309.
91. Kalviri, H. A.; Gärtner, F.; Ye, G.; Korobkov, I.; Baker, R. T., *Chem. Sci.* **2015**, *6*, 618-624.
92. Bowden, M. E.; Brown, I. W. M.; Gainsford, G. J.; Wong, H., *Inorg. Chim. Acta* **2008**, *361*, 2147-2153.
93. Helten, H.; Robertson, A. P. M.; Staubitz, A.; Vance, J. R.; Haddow, M. F.; Manners, I., *Chemistry - A European Journal* **2012**, *18*, 4665-4680.
94. Submitted manuscript
95. Grimme, S.; Kruse, H.; Goerigk, L.; Erker, G., *Angew. Chem. Int. Ed.* **2010**, *49*, 1402-1405.
96. Sen, K.; Banu, T.; Debnath, T.; Ghosh, D.; Das, A. K., *RSC Advances* **2014**, *4*, 21924.
97. Bonet, A.; Pubill-Ulldemolins, C.; Bo, C.; Gulyás, H.; Fernández, E., *Angew. Chem. Int. Ed.* **2011**, *50*, 7158-7161.
98. (a) Nguyen, P.; Dai, C.; Taylor, N. J.; Power, W. P.; Marder, T. B.; Pickett, N. L.; Norman, N. C., *Inorg. Chem.* **1995**, *34*, 4290-4291; (b) Lawlor, F.; Marder, T.; Norman, N.; Pickett, N.; Power, W.; Scott, A.; others, *J. Chem. Soc., Dalton Trans.* **1997**, 839-846.
99. Yoshida, H.; Kawashima, S.; Takemoto, Y.; Okada, K.; Ohshita, J.; Takaki, K., *Angew. Chem.* **2012**, *124*, 239-242.
100. Yang, C.-T.; Zhang, Z.-Q.; Tajuddin, H.; Wu, C.-C.; Liang, J.; Liu, J.-H.; Fu, Y.; Czyzewska, M.; Steel, P. G.; Marder, T. B.; Liu, L., *Angew. Chem. Int. Ed.* **2012**, *51*, 528-532.
101. Jäkle, F., *Chem. Rev.* **2010**, *110*, 3985-4022.
102. Qin, Y.; Pagba, C.; Piotrowiak, P.; Jäkle, F., *J. Am. Chem. Soc.* **2004**, *126*, 7015-7018.
103. Cheng, F.; Bonder, E. M.; Jäkle, F., *J. Am. Chem. Soc.* **2013**, *135*, 17286-17289.
104. Cambre, J. N.; Sumerlin, B. S., *Polymer* **2011**, *52*, 4631-4643.
105. Qin, Y.; Kiburu, I.; Shah, S.; Jäkle, F., *Macromolecules* **2006**, *39*, 9041-9048.
106. Brooks, W. L. A.; Sumerlin, B. S., *Chem. Rev.* **2015**.
107. Shipman, P. O.; Cui, C.; Lupinska, P.; Lalancette, R. A.; Sheridan, J. B.; Jäkle, F., *ACS Macro Letters* **2013**, *2*, 1056-1060.
108. Cui, C.; Bonder, E. M.; Jäkle, F., *J. Am. Chem. Soc.* **2010**, *132*, 1810-1812.
109. Su, K.; Remsen, E. E.; Thompson, H. M.; Sneddon, L. G., *Macromolecules* **1991**, *24*, 3760-3766.
110. (a) Neureiter, N. P.; Bordwell, F. G., *J. Am. Chem. Soc.* **1959**, *81*, 578-580; (b) Pellon, J.; Schwind, L. H.; Guinard, M. J.; Thomas, W. M., *Journal of Polymer Science* **1961**, *55*, 161-167.
111. (a) Kamogawa, H.; Shiraki, S., *Macromolecules* **1991**, *24*, 4224-4226; (b) Letsinger, R. L.; Hamilton, S. B., *J. Am. Chem. Soc.* **1959**, *81*, 3009-3012; (c) Antonietti, M.; Förster, S.; Hartmann, J.; Oestreich, S., *Macromolecules* **1996**, *29*, 3800-3806; (d) Kahraman, G.; Beşkardeş, O.; Rzaev, Z. M. O.; Pişkin, E., *Polymer* **2004**, *45*, 5813-5828; (e) Giffels, G.; Beliczey, J.; Felder, M.; Kragl, U., *Tetrahedron: Asymmetry* **1998**, *9*, 691-696.
112. Qin, Y.; Cheng, G.; Sundararaman, A.; Jäkle, F., *J. Am. Chem. Soc.* **2002**, *124*, 12672-12673.
113. Jäkle, F., *Journal of Inorganic and Organometallic Polymers and Materials* **2005**, *15*, 293-307.
114. (a) Moad, G.; Rizzardo, E.; Thang, S. H., *Polymer* **2008**, *49*, 1079-1131; (b) Chiefari, J.; Chong, Y. K.; Ercole, F.; Krstina, J.; Jeffery, J.; Le, T. P. T.; Mayadunne, R. T. A.; Meijs, G. F.; Moad, C. L.; Moad, G.; others, *Macromolecules* **1998**, *31*, 5559-5562.
115. Cambre, J. N.; Roy, D.; Gondi, S. R.; Sumerlin, B. S., *J. Am. Chem. Soc.* **2007**, *129*, 10348-10349.
116. Dong, J. Y.; Manias, E.; Chung, T. C., *Macromolecules* **2002**, *35*, 3439-3447.
117. Unpublished results
118. Zhao, W.; Li, Y.; Yang, S.; Chen, Y.; Zheng, J.; Liu, C.; Qing, Z.; Li, J.; Yang, R., *Anal. Chem.* **2016**, *88*, 4833-4840.

## **Section 4:**

### **Experimental data**

---

## I. Material and methods

---

Unless otherwise stated, all reactions were carried out under an inert atmosphere (argon) using standard techniques for manipulating air-sensitive compounds.<sup>i</sup> All glassware was stored in an oven or was flame-dried prior to use under an inert atmosphere of argon as stated. Anhydrous solvents were obtained either by filtration through drying columns<sup>ii</sup> (CH<sub>2</sub>Cl<sub>2</sub>, Et<sub>2</sub>O, toluene, pentane) or by distillation over sodium/benzophenone (THF). Analytical thin-layer chromatography (TLC) was performed on TLC plates pre-coated with 250 µm thickness silica gel 60 F254 plates visualized by fluorescence quenching under UV light and stained using acidic solution of ninhydrin or p-anisaldehyde stain. Yields refer to spectroscopically pure compounds (for amine-borane compounds synthesis) or if mentioned, quantified by NMR spectroscopy with an internal standard (C<sub>2</sub>H<sub>4</sub>Cl<sub>2</sub>). NMR spectra were recorded on a Bruker AC 300 spectrometer operating at 300 MHz for <sup>1</sup>H NMR, 96 MHz for <sup>11</sup>B NMR and 75 MHz for <sup>13</sup>C NMR. Solid state NMR spectra were recorded on a Bruker Advance 300 and 500 MHz spectrometer with a conventional double resonance 4 mm CP-MAS probe. The MAS frequency was set to 10 kHz for all the <sup>1</sup>H and <sup>13</sup>C experiments reported here. Prior to use, C<sub>6</sub>D<sub>6</sub>, THF-*d*<sub>8</sub>, (CD<sub>3</sub>)<sub>2</sub>SO and CD<sub>3</sub>OD were dried over 4 Å molecular sieves. DMF-*d*<sub>7</sub> was used directly from dry commercially available vials. For <sup>1</sup>H NMR: THF-*d*<sub>8</sub> = 1.72 and 3.58 ppm, CD<sub>3</sub>OD = 3.31 ppm, (CD<sub>3</sub>)<sub>2</sub>SO = 2.50 ppm, DMF-*d*<sub>7</sub> = 2.74, 2.91 and 8.02 ppm, C<sub>6</sub>D<sub>6</sub> = 7.16 ppm. Data are reported as follows: chemical shift, multiplicity (s = singlet, d = doublet, t = triplet, q = quartet, m = multiplet and br = broad), coupling constant in Hz, and integration. In <sup>11</sup>B NMR, carbon attached to the boron may not be observed because the peak is strongly broadened by quadrupolar couplings. GC-MS were performed on Agilent Technologies apparatus. DSC and TGA experiments were performed on Mettler DSC 2 StarSyst and Mettler TGA/DSC StarSyst respectively. SEC THF and SEC DMF analyses were performed on Viskotek GPCmax VE 2001 and Ecosec HLC-8320GPS respectively. IR-ATR measurements were performed on Nicolet i550 FT-IR.

---

<sup>i</sup> Shriver, D. F.; Drezdon, M. A. Inert-Atmosphere Glove Boxes. *The Manipulation of Air-Sensitive Compounds*, 2nd ed.; John Wiley & Sons: New York, 1986; pp. 45-67

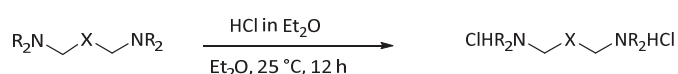
<sup>ii</sup> Pangborn, A. B.; Giardello, M. A.; Grubbs, R. H.; Rosen, R. K.; Timmers, F. J. *Organometallics* **1996**, 15, 1518-1520

Finally, *in-situ* IR-drift experiments were realized on a Thermo Fisher Nicolet 6700 apparatus. TPD (temperature programmed desorption) was performed on BEL JAPAN apparatus. The sample was placed into a quartz-cell then into a furnace. The cell was connected to an activated cryogenic zeolite trap. Hydrogen release was detected by a thermal conductivity detector (TCD) with argon as a vector gas. Quantitative measurements were performed, doing previously a calibration by the H<sub>2</sub>-pulsation technic. A blank experiment performed using Helium as gas vector confirms that dihydrogen is the only gas detected during the experiment.

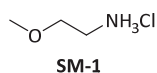
## II. Polyboramines: synthesis and characterization

### II.1. Synthesis of precursors: experimental procedures and characterizations

#### Procedure 1: synthesis of ammoniums chloride from aliphatic diamines

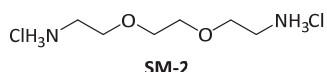


Representative procedure from 2-methoxyethylamine: a solution of HCl in Et<sub>2</sub>O (2M, 7.5 mL, 15.0 mmol) has been added dropwise to a solution of 2-methoxyethylamine (435 μL, 5 mmol) in diethylether (30 mL) under vigorous stirring at r.t. After 12 hours, a white precipitate was formed. Volatiles were removed and the solid was washed several times with dry pentane under argon until pH became neutral. The residual volatiles were removed under vacuum and the product was recovered as a white powder or crystalline solid to store and handle under argon because of its high hygroscopicity.



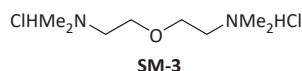
**3-methoxyamine hydrochloride (SM-1)** has been synthesized from 3-methoxyamine (870 μL, 10 mmol) and HCl in Et<sub>2</sub>O 2 M solution (15 mL) following Procedure 1, to yield a white crystalline solid, highly hygroscopic. Yield = 90 %, 1.00 g.

NMR Spectroscopy: <sup>1</sup>H NMR. (300 MHz, CDCl<sub>3</sub>, 25 °C, δ): 8.25 (s, 3H), 3.72 (t, *J* = 5 Hz, 2H), 3.41 (s, 3H), 3.25 (t, *J* = 5 Hz, 2H). <sup>13</sup>C NMR. (75 MHz, DMSO-*d*<sub>6</sub>, 25 °C, δ): 69.2, 66.3, 38.1.



**3, 3'-dioxetriethylenediamine dihydrochloride (SM-2)** has been synthesized from 3, 3'-dioxetriethylenediamine (1.44 mL, 10 mmol) and HCl in Et<sub>2</sub>O 2M solution (15 mL) following Procedure 1, to yield a white powder. Yield = 72 %, 1.585 g.

NMR Spectroscopy:  $^1\text{H}$  NMR. (300 MHz,  $\text{DMSO-}d_6$ , 25 °C,  $\delta$ ): 8.09 (s, 6H), 3.63 (t,  $J$  = 5.3 Hz, 4H), 3.59 (s, 4H), 2.95 (t,  $J$  = 5.3 Hz, 4H).  $^{13}\text{C}$  NMR. (75 MHz,  $\text{DMSO-}d_6$ , 25 °C,  $\delta$ ): 68.0, 58.0, 38.2.



**N, N'-(tetramethyl)diethylenediamine dihydrochloride (SM-3)** has been synthesized from N, N'-(tetramethyl)diethylenediamine (1.00 mL, 5 mmol) and HCl 2M in  $\text{Et}_2\text{O}$  (7.5 mL) following Procedure 1, to yield a white powder. Yield = 76 %, 821 mg.

NMR Spectroscopy:  $^1\text{H}$  NMR. (300 MHz,  $\text{DMSO-}d_6$ , 25 °C,  $\delta$ ): 3.47 (t,  $J$  = 6 Hz, 4H), 3.10 (s, br, 2H), 2.41 (t,  $J$  = 6 Hz, 4H), 2.18 (s, 12H).  $^{13}\text{C}$  NMR. (75 MHz,  $\text{DMSO-}d_6$ , 25 °C,  $\delta$ ): 63.6, 55.5, 42.1.

## II.2. Synthesis of pinacol bisboranonates monomers

### II.2.a. Procedure 2: Diboration of 1,2-hexene<sup>iii</sup>

Synthesis of **2,2'-(hexane-1,2-diyl)bis(4,4,5,5-tetramethyl-1,3,2-dioxaborolane) (4e)**:

Into an oven-dried Schlenk tube, provided with stir bar, under argon,  $\text{Cs}_2\text{CO}_3$  (582 mg, 17.8/ mmol) and bis(pinacolato)diboron (17.8 mmol, 3.32 g) were transferred. THF (20 ml) was added to dissolve the mixture. After that, 1,2-hexene (1.03 g, 11.9 mmol) and MeOH (2.7 mL, 59.5 mmol) were added, and the reaction mixture was stirred at 70 °C for 6 hours. The reaction mixture was cooled to room temperature. The reaction mixture was concentrated on a rotary evaporator. After all the volatiles were evaporated, the sample was purified by silica gel chromatography. Colorless oil. Yield: 3.9 g, 98 %.

NMR Spectroscopy:  $^1\text{H}$  NMR. (300 MHz,  $\text{CDCl}_3$ , 25 °C,  $\delta$ ): 1.43 (m, 1H), 1.27 (m, 8H), 1.23 (s, 12H), 1.11 (m, 2H), 0.86 (t, 3H,  $J$  = 2.4 Hz), 0.78 (dd, 3H,  $J$  = 15.5 Hz, 6 Hz).  $^{11}\text{B}$  NMR. (96 MHz,  $\text{CDCl}_3$ , 25 °C,  $\delta$ ): 35.0 (s).  $^{13}\text{C}$  NMR (75 MHz,  $\text{CDCl}_3$ , 25 °C,  $\delta$ ): 82.8, 82.7, 33.9, 31.9, 29.5, 28.8, 24.9, 24.8, 24.7, 22.6, 14.1. GC-MS:  $m/z$  = 374.3 ( $\text{M}^+$ -15).

<sup>iii</sup> Bonet, A.; Pubill-Ulldemolins, C.; Bo, C.; Gulyás, H.; Fernández, E., *Angew. Chem. Int. Ed.* **2011**, 50, 7158-7161.

**II.2.b. Procedure 3: Diboration of 4-octyne<sup>iv</sup>**

Synthesis of **(Z)-2,2'-(oct-4-ene-4,5-diyl)bis(4,4,5,5-tetramethyl-1,3,2-dioxaborolane) (4h)**: Into an oven-dried Schlenk tube, provided with stir bar, under argon, Cu(OAc)<sub>2</sub> (16.3 mg, 0.09 mmol), (t-Bu)<sub>3</sub>P 1M in toluene (0.315 mL, 0.32 mmol) and bis(pinacolato)diboron (1.48 g, 5.85 mmol) were transferred. Toluene 5 ml) was added to dissolve the mixture. After that, 4-octyne (500 mg, 4.5 mmol) was added, and the reaction mixture was stirred at 80 °C for 6 hours. The reaction mixture was cooled to room temperature. The reaction mixture was concentrated on a rotary evaporator. After all the volatiles were evaporated, the sample was purified by silica gel chromatography. Colorless oil. Yield: 1.54 g, 94 %.

NMR Spectroscopy: <sup>1</sup>H NMR. (300 MHz, CDCl<sub>3</sub>, 25 °C,  $\delta$ ): 0.88 (t, 6H,  $J$  = 7.4 Hz), 1.23-1.38 (m, 4H), 1.26 (s, 12H), 2.11-2.17 (m, 4H). <sup>11</sup>B NMR. (96 MHz, CDCl<sub>3</sub>, 25 °C,  $\delta$ ): 34.1 (s). <sup>13</sup>C NMR (75 MHz, CDCl<sub>3</sub>, 25 °C,  $\delta$ ): 172.4, 81.3, 31.1, 23.0, 21.0, 12.7. GC-MS:  $m/z$  = 364.30 (M<sup>+</sup>).

**II.2.c. Procedure 4: Diboration of dibromohexene<sup>v</sup>**

Synthesis of **1,6-bis(4,4,5,5-tetramethyl-1,3,2-dioxaborolan-2-yl)hexane (4k)**: In air, CuI (191 mg, 1 mmol), PPh<sub>3</sub> (341 mg, 1.3 mmol), LiOMe (760 mg, 20 mmol), and bis(pinacolato)diboron (3.81 g, 15 mmol) were added to a Schlenk tube equipped with a stir bar. The vessel was evacuated and filled with argon (three cycles). DMF (30 mL), the alkyl bromide (5 mmol, 0.77 mL) were added in turn by syringe under an argon atmosphere. The resulting reaction mixture was stirred vigorously at 25 °C for 18 h. The reaction mixture was then diluted with Et<sub>2</sub>O, filtered through silica gel with copious washings of Et<sub>2</sub>O, concentrated, and purified by column chromatography. Colorless oil. Yield : 1.40 g, 83 %.

NMR Spectroscopy: <sup>1</sup>H NMR. (300 MHz, CDCl<sub>3</sub>, 25 °C,  $\delta$ ): 1.40-1.24 (m, 32H), 0.77 (t, 4H,  $J$  = 6 Hz), 1.35 (m, br, 3H). <sup>11</sup>B NMR. (96 MHz, CDCl<sub>3</sub>, 25 °C,  $\delta$ ): 34.0 (s). <sup>13</sup>C NMR (75 MHz, CDCl<sub>3</sub>, 25 °C,  $\delta$ ): 82.8, 24.8, 24.0, 16.0. GC-MS:  $m/z$  = 323.27 (M<sup>+</sup>-15)

---

<sup>iv</sup> Yoshida, H.; Kawashima, S.; Takemoto, Y.; Okada, K.; Ohshita, J.; Takaki, K., *Angew. Chem.* **2012**, *124*, 239-242.

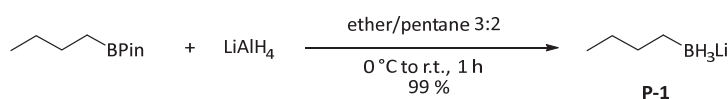
<sup>v</sup> Yang, C.-T.; Zhang, Z.-Q.; Tajuddin, H.; Wu, C.-C.; Liang, J.; Liu, J.-H.; Fu, Y.; Czyzewska, M.; Steel, P. G.; Marder, T. B.; Liu, L., *Angew. Chem. Int. Ed.* **2012**, *51*, 528-53



### II.3. Synthesis of amine-borane molecular bricks: experimental procedures and characterizations

---

#### II.3.a. Procedure 5: synthesis of borohydride derivatives from aliphatic boronic acids or pinacol boronates



**Lithium[butyl(trihydrido)borate] (P-1)<sup>vi</sup>:** a suspension of  $\text{LiAlH}_4$  in  $\text{Et}_2\text{O}$  (1 M, 9 mL, 9.0 mmol) was added dropwise with stirring at 0 °C to a solution of butylboronic acid pinacol ester (639  $\mu\text{L}$ , 3 mmol) in ether/pentane 3:2 (15 mL). After 30 min, the mixture was allowed to warm up to r.t. and stirred for 1 h. The insoluble part was precipitated by centrifugations or was filtered out (4G fritted glass) and washed with diethylether (3 x 10 mL). The volume of the filtrate was removed under vacuum ( $10^{-3}$  bars) to give white crystalline solid containing strongly associated  $\text{Et}_2\text{O}$  molecules. Yield > 99% (determined by NMR).

NMR Spectroscopy:  $^1\text{H}$  NMR. (300 MHz,  $\text{C}_6\text{D}_6$ , 25 °C,  $\delta$ ): 3.65 (m, br, 2H), 1.75 (m, br, 4H), 1.35 (m, br, 3H).  $^{11}\text{B}$  NMR. (96 MHz,  $\text{C}_6\text{D}_6$ , 25 °C,  $\delta$ ): -27.02 (q,  $J = 74.8$  Hz).  $^{13}\text{C}$  NMR (75 MHz,  $\text{C}_6\text{D}_6$ , 25 °C,  $\delta$ ): 69.0, 36.6, 26.9, 25.3.

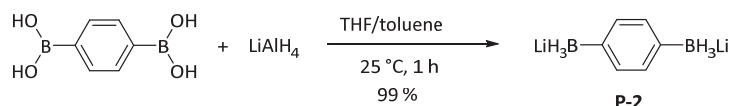
**3a** molecules formed a coordinated network as reported for **3b**<sup>vii</sup> in the literature (see below). It likely explain the aspect of the signals on the  $^1\text{H}$  NMR spectrum.  $^1\text{H}$  NMR signals of B-H are not visible, most probably because they are strongly broadened peaks.

---

<sup>vi</sup> B. Singaram, T. E. Cole, H. C. Brown, Addition compounds of alkali-metal hydrides, *Organometallics*, **1984**, 3, 774–777

<sup>vii</sup> Franz D., Bolte M., Lerner H-W and Wagner M., *Dalton Trans.*, **2011**, 40, 2433-2440.”

### II.3.b. Procedure 6: synthesis of borohydride derivatives from aromatic boronic acids / boronic acid pinacol ester.



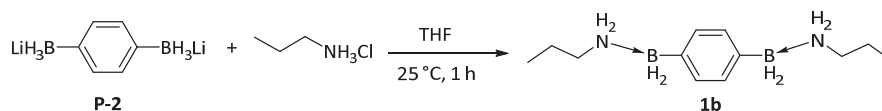
**Lithium [benzene-1,4-bis(trihydrido)borate] (P-2)<sup>i</sup>:** a suspension of  $\text{LiAlH}_4$  in THF (1 M, 9 mL, 9.0 mmol) was added dropwise at r.t. to a solution of benzene-1,4-diboronic acid (995 mg, 6 mmol) in THF/toluene 5:2 (34 mL). The reaction mixture was stirred for 1 h. The insoluble part was precipitated by centrifugations or was filtered out (4G fritted glass) and washed with THF (3 times, 10 mL). The resulting clear filtrate was evaporated under vacuum (down to  $10^{-3}$  bar). Then, solvent residue was removed under high vacuum (down to  $10^{-9}$  bar at 30 °C for 12 h) to give white crystalline solid containing strongly associated THF molecules. Yield > 99 % (determined by NMR).

NMR Spectroscopy:  $^{11}\text{B}$  NMR. (96 MHz,  $\text{C}_6\text{D}_6$ , 25 °C,  $\delta$ ): -26.8 (q,  $J = 77.8$  Hz).  $^1\text{H}$  NMR. (300 MHz,  $\text{C}_6\text{D}_6$ , 25 °C,  $\delta$ ): 7.02-7.18 (m, br, 4H).

**P-2** molecules form a coordination polymer<sup>i</sup> which likely explains the aspect of the signals on the  $^1\text{H}$  NMR spectrum.  $^1\text{H}$  NMR signals of B-H are not visible, most probably because they are strongly broadened peaks.

### II.3.c. Procedure 7: Synthesis of (N-alkyl)amine-(B-alkyl or aryl)boranes by salt metathesis / $\text{H}_2$ release.

Representative procedure from **P-2**: *n*-propylamine hydrochloride (29 mg, 0.3 mmol) was added in one batch at 0 °C to a stirred suspension of **P-2** (45 mg, 0.3 mmol determined by NMR) in THF (1 mL). Thin fizzy gas release was observed for 20 min, then the reaction mixture was allowed to warm up to r.t. After 1.5 h, the reaction mixture became a clear solution. The solution was filtered out on a frit (4G) and volatiles were evaporated.



**Di-(*n*-propyl)amine-(1,4-benzene)bisborane (1b)** has been synthesized from **P-2** (45 mg, 0.3 mmol) and *n*-propylamine hydrochloride (29 mg, 0.3 mmol) following procedure 7 to yield **1b** as well as propylamine-borane (**prAB**) with a ratio **1b/prAB** = 3:1, determined by NMR (c.f. Figure S89). For NMR Spectroscopy data of isolated **1b**: see procedure 5.

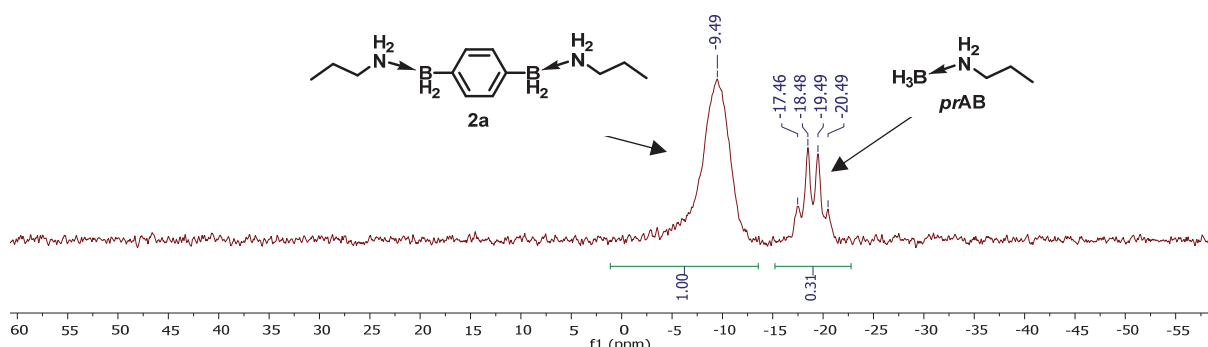
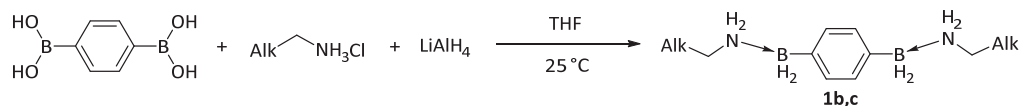


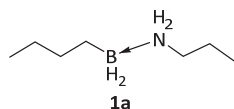
Figure S89.  $^{11}\text{B}$  NMR spectrum of **1b** synthesized from **P-2**. Presence of **prAB** deborylation-byproduct.

#### II.3.d. Procedure 8: one-pot synthesis of (N-alkyl)amine-(B-alkyl/aryl)boranes from (1,4-benzene)bisboronic acid and amines hydrochloride



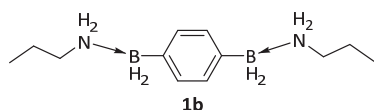
Representative procedure from (1,4-benzene)bisboronic acid : a mixture of 1,4-benzene bisboronic acid (332 mg, 2.0 mmol) and *n*-propylamine hydrochloride (384 mg, 4.0 mmol) in THF (8 mL) was first vigorously stirred to obtain a finely dispersed suspension. A suspension of  $\text{LiAlH}_4$  (226 mg, 3 mmol) in THF (6 mL) was added dropwise with vigorous stirring at r.t. During the addition, gas is evolved and the reaction mixture became foamy. At the end of the reaction foaming decreased and gas emission continued for about 30 min. After 4-12 h, the reaction mixture became a white suspension and was diluted in THF (30 mL), filtered on a 4G fritted glass. The solid was washed 3 times with THF. The resulting clear combined filtrates were evaporated under vacuum (down to  $10^{-3}$  bar) at r.t for 12 h then eventually under high vacuum (down to  $10^{-9}$  bars) at  $0^\circ\text{C}$  for 12-24 h. The product

**1b** included minute amounts of strongly associated THF molecules (quantified by NMR to determine the isolated yield).



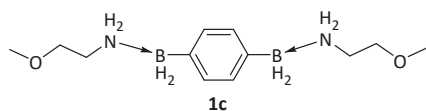
**(*n*-propyl)amine-(*n*-butyl)borane (1a)** has been synthesized from *n*-butylboronic acid pinacol ester (213  $\mu$ g, 1.0 mmol) and *n*-propylamine hydrochloride (95.6 mg, 1.0 mmol) in THF (3 mL) and  $\text{LiAlH}_4$  (57 mg, 1.5 mmol) in THF (2 mL) following procedure 7. Once isolated **1a** is unstable at room temperature making its characterization difficult. Conversion > 99 % according to *in situ*  $^{11}\text{B}$  NMR.

NMR Spectroscopy:  $^{11}\text{B}$  NMR. (96 MHz,  $\text{THF-}d_8$ , 25  $^\circ\text{C}$ ,  $\delta$ ): -10.8 (t,  $J = 93$  Hz).



**Di(*n*-propyl)amine-(1,4-benzene)bisborane (1b)** has been synthesized from 1,4-benzene bisboronic acid (332 mg, 2 mmol), *n*-propylamine hydrochloride (384 mg, 4 mmol), and  $\text{LiAlH}_4$  (226 mg, 3 mmol) following Procedure 8 to yield a white solid. Residual THF molecules were quantified by  $^1\text{H}$  NMR. Yield: 62 %, 273 mg.

NMR Spectroscopy:  $^{11}\text{B}$  NMR. (96 MHz,  $\text{THF-}d_8$ , 25  $^\circ\text{C}$ ,  $\delta$ ): -11.6 ( $h_{1/2} = 620$  Hz).  $^1\text{H}$  NMR. (300 MHz,  $\text{THF-}d_8$ , 25  $^\circ\text{C}$ ,  $\delta$ ): 7.08 (s, 4H), 4.77-4.60 (s, br, 4H), 2.84-2.54 (m, 4H), 2.84-2.54 (s, br, 4H), 1.61-1.53 (m, 4H), 0.99-0.86 (m, 6H).  $^{13}\text{C}$  NMR (75 MHz,  $\text{THF-}d_8$ , 25  $^\circ\text{C}$ ,  $\delta$ ): 131.4, 130.5, 45.7, 39.6, 20.4, 19.9, 8.8.



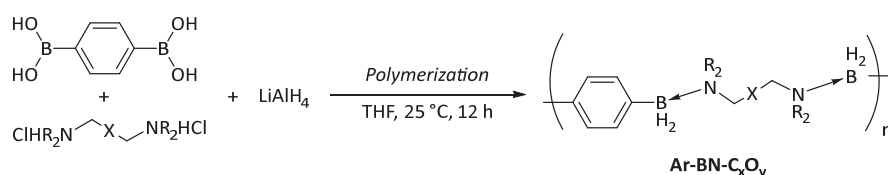
**Di(2-methoxyethyl)amine-(1,4-benzene)bisborane (1c)** has been synthesized from 1,4-benzene bisboronic acid (166 mg, 1 mmol), **SM-1** (223 mg, 2 mmol) and  $\text{LiAlH}_4$  (57 mg, 1.5 mmol) following Procedure 8. The reaction mixture was concentrated, and after addition of pentane (5 mL) the product precipitated at -20  $^\circ\text{C}$ . Precipitate was filtered and volatiles were removed to yield a clear yellow viscous oil at room temperature. Yield = 81 %, 202 mg.

NMR Spectroscopy:  $^{11}\text{B}$  NMR. (96 MHz,  $\text{THF-}d_8$ , 25 °C,  $\delta$ ): -9.86 ( $h_{1/2}$  = 353 Hz).  $^1\text{H}$  NMR. (300 MHz,  $\text{THF-}d_8$ , 25 °C,  $\delta$ ): 7.78-7.15 (m, 4H), 6.08 (s, br, 4H), 3.54-3.51 (m, 4H), 3.36-3.31 (m, 6H), 3.18-2.77 (m, 4H), 2.45 (s, br, 4H)  $^{13}\text{C}$  NMR (75 MHz,  $\text{THF-}d_8$ , 25 °C,  $\delta$ ): 133.4, 69.8, 57.9, 45.2.

## II.4. Synthesis of polyboramines: experimental procedures and characterizations

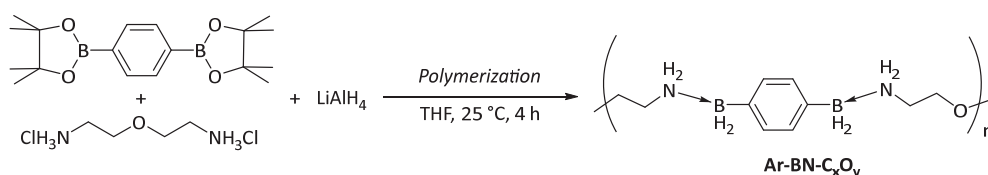
---

### II.4.a. Procedure A: synthesis of poly[(N,N'-alkylene)diamine-(1,4-benzene)bisborane] from (1,4-benzene)bisboronic acid and diamine hydrochloride.

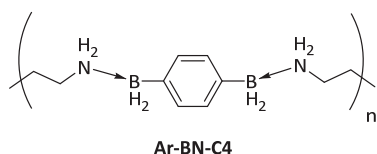


Representative procedure from (1,4-benzene)bisboronic acid and 2,2'-oxydiethyldiamine dihydrochloride : a mixture of benzene-1,4-diboronic acid (994 mg, 6.0 mmol) and 2,2'-oxydiethylamine dihydrochloride (1.060 g, 6.0 mmol) in THF (6 mL) was first vigorously stirred to obtain an finely dispersed suspension. A suspension of  $\text{LiAlH}_4$  (342 mg, 9 mmol) in THF (3 mL) was added dropwise under vigorous stirring at r.t. During the addition, gas release was observed. The mixture became white and foamy. At the end of the addition foaming decreased and gas emission continued for about 30 min to 1 h. After 4-12 h, the reaction mixture became a white suspension and was diluted with THF (100 mL), filtered on 4G a fritted glass and washed 3 times with THF. The resulting clear filtrate was evaporated under vacuum (down to  $10^{-3}$  bar) at r.t (12 h) then if required under high vacuum (down to  $10^{-9}$  bars) at 0 °C for 12-24 h. Polymers contain traces of strongly associated THF molecules (quantified determined by NMR to determine the isolated yield).

#### II.4.b. Procedure B: Synthesis of poly[(alkyl)diamine-(1,4-benzene)bisborane] from pinacol (1,4-benzene)bisboronate and diamine hydrochloride.

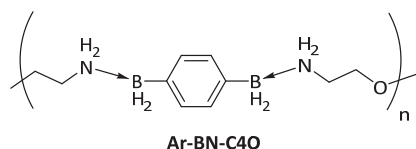


Representative procedure from pinacol (1,4-benzene)bisboronate and 2,2'-oxydiethyldiamine dihydrochloride : a mixture of 1,4-benzenediboronate bis(pinacol) ester (660 mg, 2.0 mmol) and 2,2'-oxydiethylamine dihydrochloride (354 g, 2.0 mmol) in THF (4 mL) was first vigorously stirred to obtain an finely dispersed suspension. A mixture of  $\text{LiAlH}_4$  (114 mg, 3 mmol) in THF (1 mL) was added dropwise under vigorous stirring at 0 °C. During the addition, gas evolved. The reaction was monitored by NMR (disappearance of the boron starting material) and additional  $\text{LiAlH}_4$  was added until completion if necessary. At the end of the addition, the reaction mixture was allowed to warm up to r.t. After 1-4 h, the reaction mixture featured a grey precipitate. It was filtered on a frit (4G) and washed 3 times with THF. The combined organics were evaporated under vacuum (down to  $10^{-3}$  bar) at r.t.



**Poly[diethylenediamine-(1,4-benzene)bisborane] (Ar-BN-C4)** has been synthesized from 1,4-benzene bisboronic acid (498 mg, 3.0 mmol), **1,4-butanediamine dihydrochloride** (480 mg, 3.0 mmol) and  $\text{LiAlH}_4$  (171 mg, 4.5 mmol) following the procedure A, and dried under vacuum overnight, to yield white solid. Yield 65 %, 510 mg.

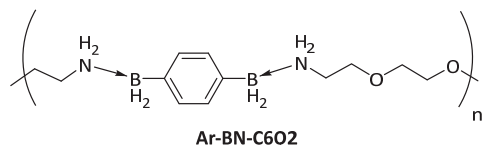
NMR Spectroscopy:  $^{11}\text{B}$  NMR. (96 MHz,  $\text{THF-}d_8$ , 25 °C,  $\delta$ ): -4.0 ( $h_{1/2}$  = 920 Hz).  $^1\text{H}$  NMR. (300 MHz,  $\text{THF-}d_8$ , 25 °C,  $\delta$ ): 7.08-6.9 (m, 4H), 4.60-4.00 (m, br, 4H), 2.58-2.50 (m, br, 4H), 2.28-2.19 (m, br, 4H), 1.54-1.51 (m, 4H).  $^{13}\text{C}$  NMR (75 MHz,  $\text{THF-}d_8$ , 25 °C,  $\delta$ ): 151.7, 137.3-124.9, 29.8, 25.4. IR-ATR:  $3390\text{ cm}^{-1}$  (N-H),  $2300\text{ cm}^{-1}$  (B-H),  $720\text{ cm}^{-1}$  (B--N).



**Poly[3-oxydiethylenediamine-(1,4-benzene)bisborane] (Ar-BN-C4O)** has been synthesized from (1,4-benzene)bisboronic acid (498 mg, 3.0 mmol), 2,2'-oxydiethyldiamine dihydrochloride (531 mg, 3.0 mmol) and  $\text{LiAlH}_4$  (171 mg, 4.5 mmol) following the procedure A, then dried under vacuum overnight, to yield white solid. Yield 52 %, 434 mg.

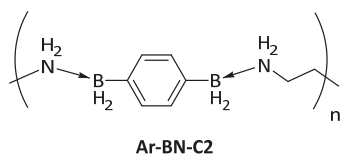
Oligomers **Ar-BN-C4O-olig** were synthesized from pinacol (1,4-benzene)bisboronate (660 mg, 2.0 mmol), 2,2'-oxydiethylamine dihydrochloride (354 mg, 2.0 mmol) and  $\text{LiAlH}_4$  (118 mg, 3.1 mmol), following the procedure B. The polymer can be precipitated in pentane to yield a white powder but poorly soluble in THF.

NMR Spectroscopy:  $^{11}\text{B}$  NMR. (96 MHz,  $\text{THF-}d_8$ , 25 °C,  $\delta$ ): -12.6 ( $h_{1/2}$  = 540 Hz).  $^1\text{H}$  NMR. (300 MHz,  $\text{THF-}d_8$ , 25 °C,  $\delta$ ): 7.23-7.11 (m, 4H), 4.71 (s, br, 4H), 3.47-3.43 (m, br, 4H), 2.86-2.77 (m, br, 4H), 2.36 (m, 4H).  $^{13}\text{C}$  NMR (75 MHz,  $\text{DMSO-}d_6$ , 25 °C,  $\delta$ ): 146.0, 68.1-67.8, 45.3. IR-ATR:  $3390\text{ cm}^{-1}$  (N-H),  $2300\text{ cm}^{-1}$  (B-H),  $720\text{ cm}^{-1}$  (B--N)



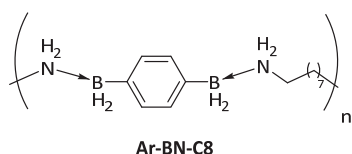
**Poly[3,3'-dioxydiethylenediamine-(1,4-benzene)bisborane] (Ar-BN-C6O4)** : has been synthesized from (1,4-benzene)bisboronic acid (498.2 mg, 3.0 mmol), **SM-2** (663.4 mg, 3.0 mmol) and  $\text{LiAlH}_4$  (172.0 mg, 4.5 mmol) following the procedure A, and dried under vacuum overnight, to yield white solid. Yield 48 %.

NMR Spectroscopy:  $^{11}\text{B}$  NMR. (96 MHz,  $\text{THF-}d_8$ , 25 °C,  $\delta$ ): -10.5 ( $h_{1/2}$  = 1540 Hz).  $^1\text{H}$  NMR. (300 MHz,  $\text{THF-}d_8$ , 25 °C,  $\delta$ ): 7.20-6.91 (m, 4H), 4.53 (s, br, 4H), 3.57-3.38 (m, br, 8H), 2.76 (m, br, 4H), 2.30 (m, 4H).  $^{13}\text{C}$  NMR (75 MHz,  $\text{THF-}d_8$ , 25 °C,  $\delta$ ): 137.4-125.0, 69.8, 67.8, 45.3, 43.1, 34.1, 28.8.



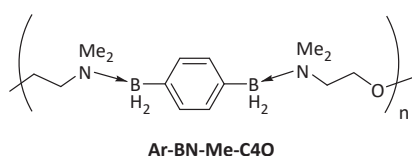
**Poly[ethylenediamine-(1,4-benzene)bisborane] (Ar-BN-C2)** has been synthesized from (1,4-benzene)bisboronic acid (498 mg, 3.0 mmol), **1,4-ethylenediamine dihydrochloride** (399 mg, 3.0 mmol) and  $\text{LiAlH}_4$  (171 mg, 4.5 mmol) following the procedure A. After filtration the polymer precipitated in THF. The material was dried under vacuum overnight, to yield white solid. Yield 31 %, 178 mg.

NMR Spectroscopy data were unable to be obtained due to the insolubility of the polymer. The comparison of IR data permitted to identify the polyboramine. IR-ATR:  $3375\text{ cm}^{-1}$  (N-H),  $2323\text{ cm}^{-1}$  (B-H),  $710\text{ cm}^{-1}$  (B--N).



**Poly[tetraethylenediamine-(1,4-benzene)bisborane] (Ar-BN-C8)** has been synthesized from (1,4-benzene)bisboronic acid (498 mg, 3.0 mmol), **1,4-tetraethylenediamine dihydrochloride** (651 mg, 3.0 mmol) and  $\text{LiAlH}_4$  (171 mg, 4.5 mmol) following the procedure A. The material was dried under vacuum overnight, to yield white solid. Yield 43 %, 318 mg.

NMR Spectroscopy:  $^{11}\text{B}$  NMR. (96 MHz,  $\text{THF-}d_8$ ,  $25\text{ }^\circ\text{C}$ ,  $\delta$ ): -12.7 ( $h_{1/2} = 277\text{ Hz}$ ).  $^1\text{H}$  NMR. (300 MHz,  $\text{THF-}d_8$ ,  $25\text{ }^\circ\text{C}$ ,  $\delta$ ): 8.03-7.01 (m, 4H), 5.48-5.07 (m, br, 4H), 2.19 (m, br, 4H), 2.86-2.39 (m, br, 4H), 1.45-0.63 (m, 12H). IR-ATR:  $3380\text{ cm}^{-1}$  (N-H),  $2304\text{ cm}^{-1}$  (B-H),  $712\text{ cm}^{-1}$  (B--N).



**Poly[3-oxydiethylene-N, N'-dimethyldiamine-(1,4-benzene)bisborane] (Ar-BN-Me-C4O)** : has been synthesized from (1,4-benzene)bisboronic acid (498.2 mg, 3.0 mmol), **SM-3** (699.5 mg, 3.0 mmol) and  $\text{LiAlH}_4$  (172 mg, 4.5 mmol) following the procedure A, and dried under vacuum overnight, to yield white solid. Yield 20 %.

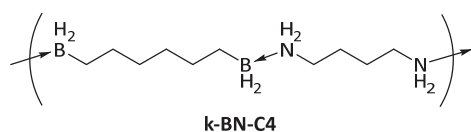


NMR Spectroscopy:  $^{11}\text{B}$  NMR. (96 MHz,  $\text{THF-}d_8$ , 25 °C,  $\delta$ ): -3.3 ( $h_{1/2}$  = 820 Hz).  $^1\text{H}$  NMR. (300 MHz,  $\text{THF-}d_8$ , 25 °C,  $\delta$ ): 7.20-6.91 (m, 4H), 4.53 (s, br, 4H), 3.57-3.38 (m, br, 8H), 2.76 (m, br, 4H), 2.30 (m, 4H).  $^{13}\text{C}$  NMR (75 MHz,  $\text{THF-}d_8$ , 25 °C,  $\delta$ ): 136.5, 69.1, 58.7, 45.2.

#### II.4.c. Procedure C: Synthesis of other poly[(diethylenediamine-(aliphatic)-bisborane] from a pinacol bisboronate and diethylenediamine hydrochloride

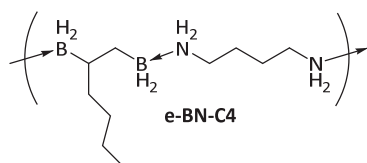
Representative procedure from **4k** and diethylenediamine dihydrochloride: a mixture of **4k** (500 mg, 1.47 mmol) and diethylenediamine dihydrochloride (238 mg, 1.47 mmol) in THF (4 mL) was first vigorously stirred to obtain an finely dispersed suspension. A mixture of  $\text{LiAlH}_4$  (84 mg, 2.21 mmol) in THF (1 mL) was added dropwise under vigorous stirring at 0 °C. During the addition, gas evolved. After 1-4 h, the reaction mixture was allowed to warm up to r.t., then filtered on a frit (4G) and washed 3 times with THF. The combined organics were evaporated under vacuum (down to  $10^{-3}$  bar).

*This procedure can be improved according to discussion in section 2. Consequently following data doesn't feature pure compounds but are indicative for the following of the study.*



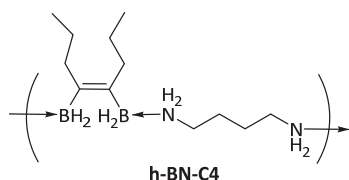
**Poly[tetraethylenediamine-(1,6-hexylene)bisborane] (k-BN-C4)** has been synthesized from **4k** (500 mg, 1.47 mmol), **1,4-tetraethylenediamine dihydrochloride** (238 mg, 1.47 mmol) and  $\text{LiAlH}_4$  (84 mg, 2.21 mmol) following the procedure C. The material was dried under vacuum overnight, to yield white solid.

NMR Spectroscopy:  $^{11}\text{B}$  NMR. (96 MHz,  $\text{THF-}d_8$ , 25 °C,  $\delta$ ): -13.0 ( $h_{1/2}$  = 1507 Hz).  $^1\text{H}$  NMR. (300 MHz,  $\text{THF-}d_8$ , 25 °C,  $\delta$ ) typical signals: 4.40 (s, br, 4H,  $\text{NH}_2$ ), 2.61 (s, br, 4H,  $\text{BH}_2$ ), 1.59-0.26 (m, br,  $\text{CH}_2$ -aliphatic). IR-ATR:  $3397\text{ cm}^{-1}$  (N-H),  $2299\text{ cm}^{-1}$  (B-H).



**Poly[tetraethylenediamine-((1-butyl)-1,2-ethylene)bisborane] (e-BN-C4)** has been synthesized from **4e** (1.2 g mg, 3.55 mmol), **1,4-tetraethylenediamine dihydrochloride** (575 mg, 1.47 mmol) and  $\text{LiAlH}_4$  (202 mg, 5.33 mmol) following the procedure C. The material was dried under vacuum overnight, to yield white solid.

NMR Spectroscopy:  $^{11}\text{B}$  NMR. (96 MHz,  $\text{THF-}d_8$ , 25 °C,  $\delta$ ): -6.5 ( $h_{1/2}$  = 1640 Hz). IR-ATR: 3397  $\text{cm}^{-1}$  (N-H), 2299  $\text{cm}^{-1}$  (B-H).



**Poly[tetraethylenediamine-(4,5-(di-*n*-propyl)-4,5-ethynylene)bisborane] (h-BN-C4)** has been synthesized from **4h** (300 mg mg, 0.83 mmol), **1,4-tetraethylenediamine dihydrochloride** (133 mg, 0.83 mmol) and  $\text{LiAlH}_4$  (47 mg, 1.24 mmol) following the procedure C. The material was dried under vacuum overnight, to yield white solid.

NMR Spectroscopy:  $^{11}\text{B}$  NMR. (96 MHz,  $\text{THF-}d_8$ , 25 °C,  $\delta$ ): -13.8 ( $h_{1/2}$  = 2352 Hz). IR-ATR: 3230  $\text{cm}^{-1}$  (N-H), 2300  $\text{cm}^{-1}$  (B-H).

## II.5. NMR spectra

### II.5.a. Amines hydrochloride

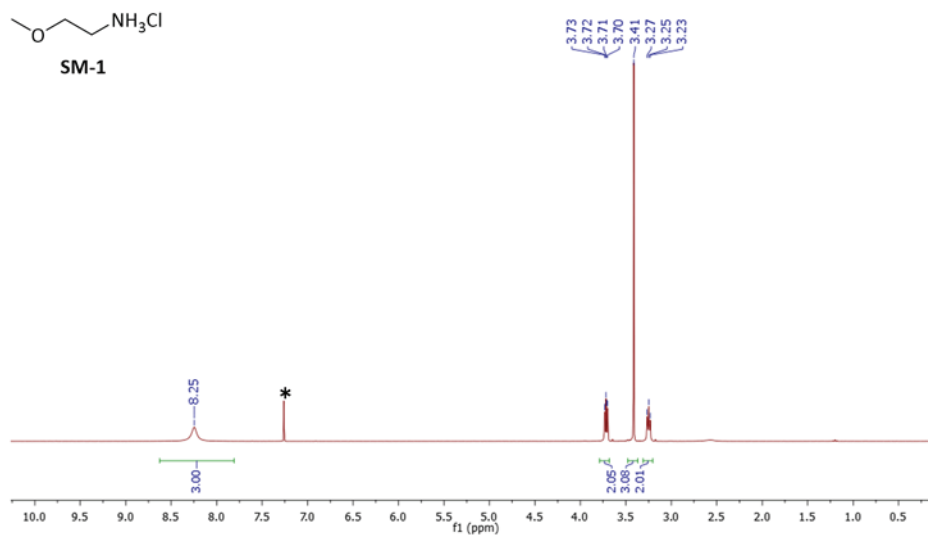


Figure S90.  $^1\text{H}$  NMR spectrum of 3-methoxyamine hydrochloride (SM-1)

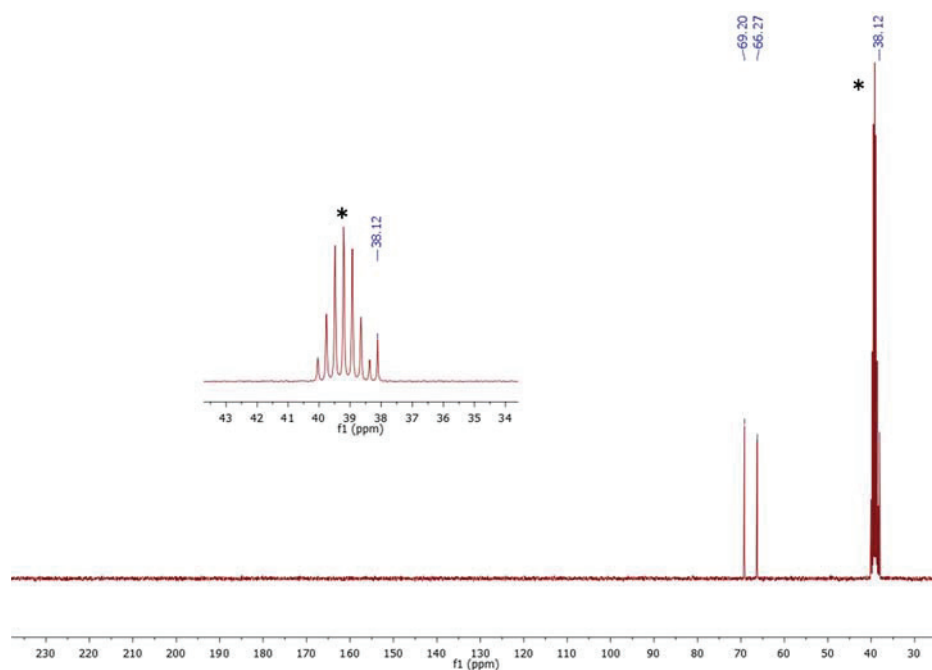


Figure S91.  $^{13}\text{C}$  NMR spectrum of 3-methoxyamine hydrochloride (SM-1)

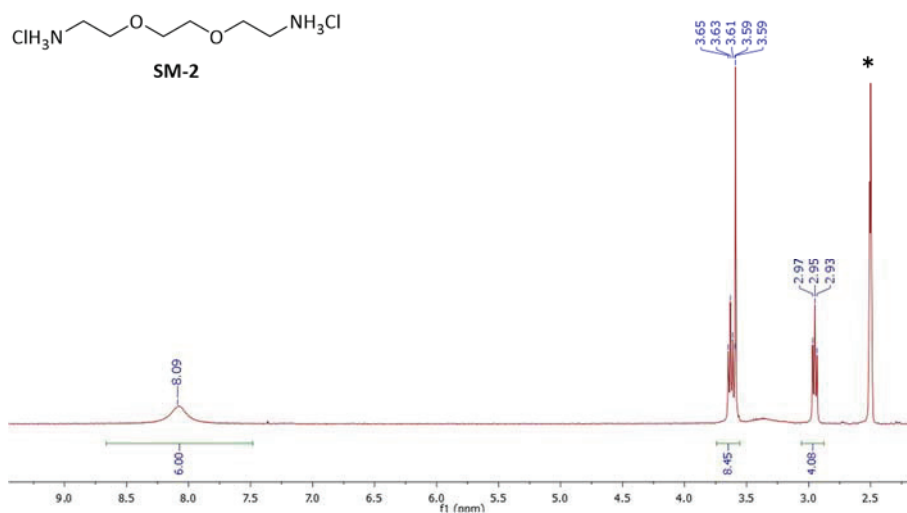


Figure S92.  $^1\text{H}$  NMR spectrum of 3,3'-dioxytriethylenediamine dihydrochloride (SM-2)

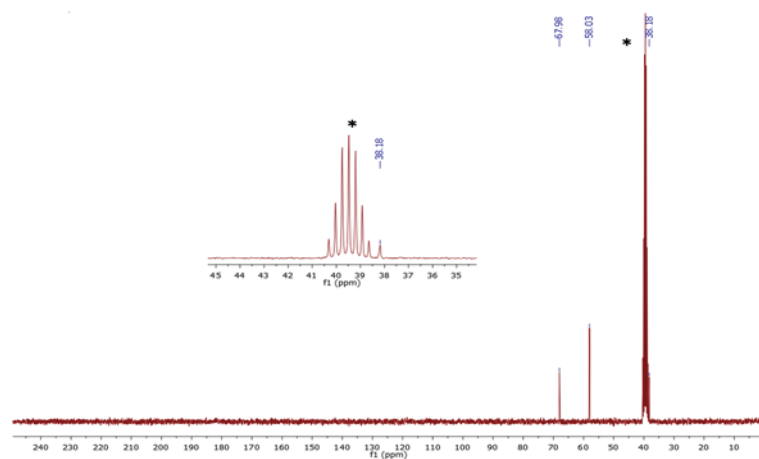


Figure S93.  $^{13}\text{C}$  NMR spectrum 3,3'-dioxytriethylenediamine dihydrochloride (SM-2)

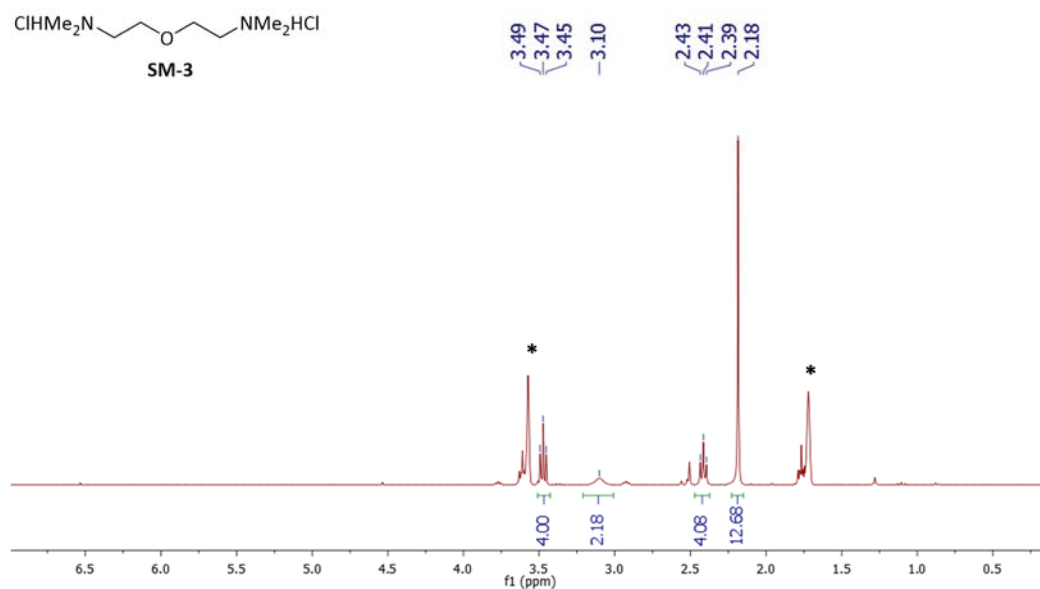


Figure S94.  $^1\text{H}$  NMR spectrum of *N,N'*-(tetramethyl)diethylenediamine dihydrochloride (SM-3)

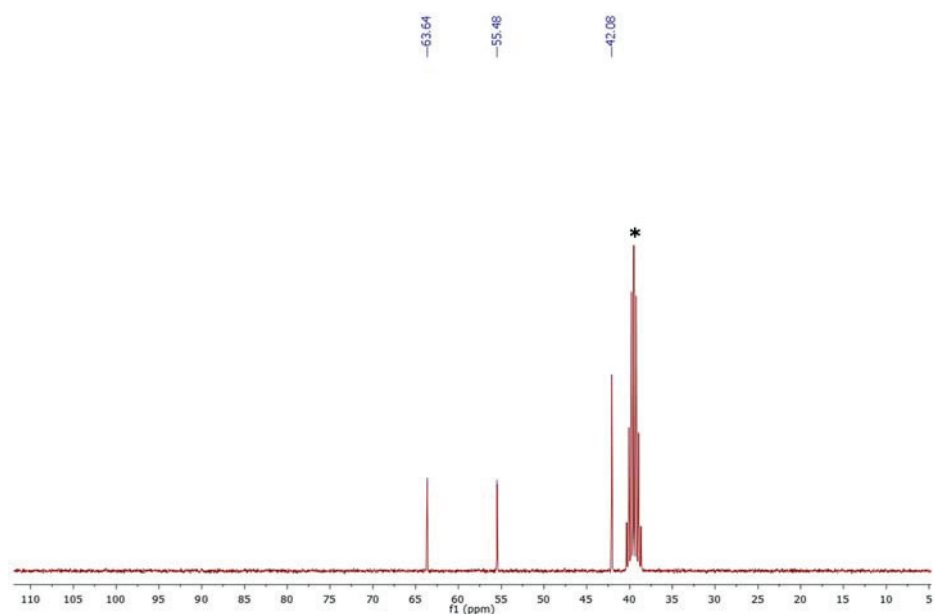
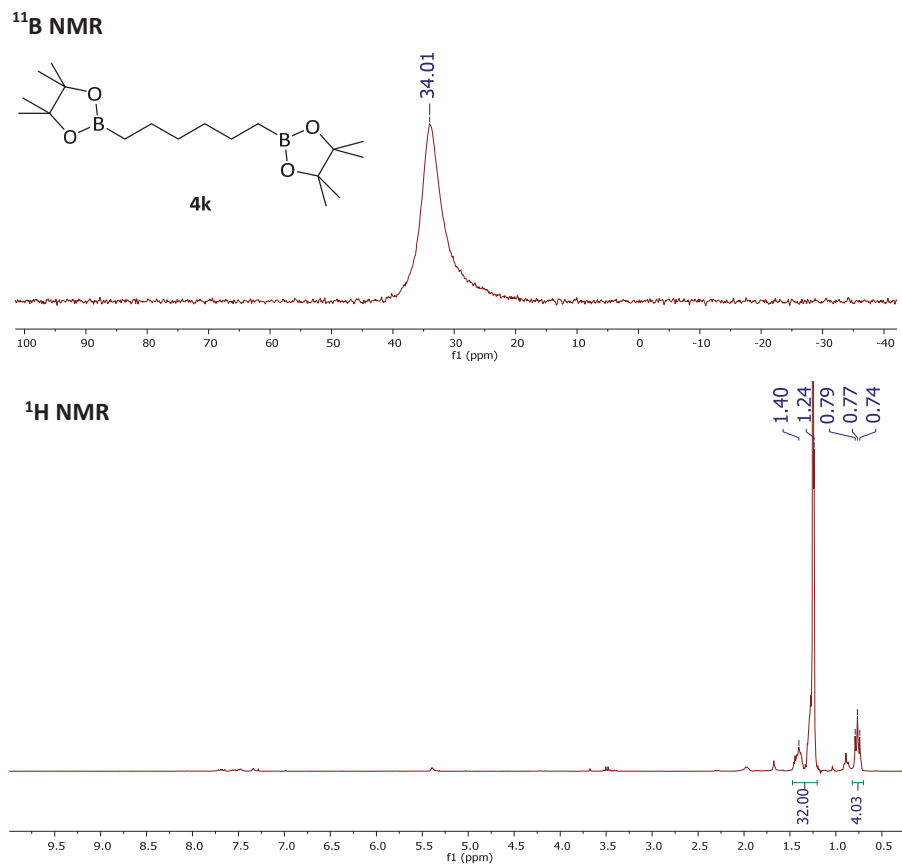
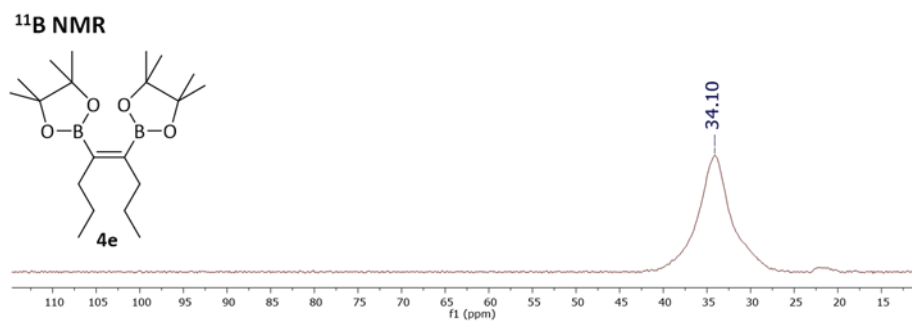
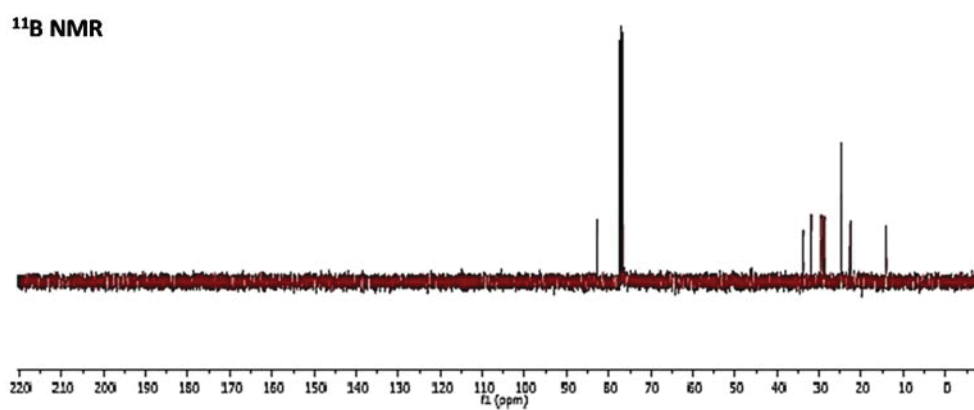
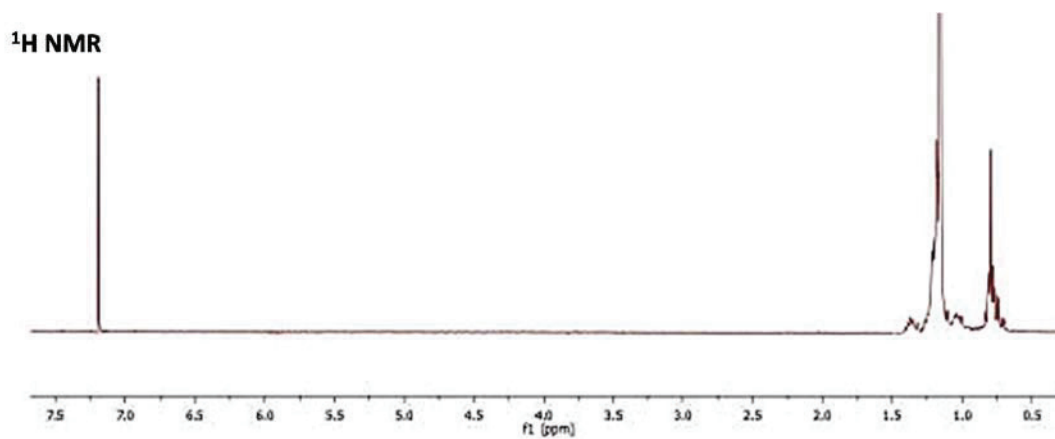
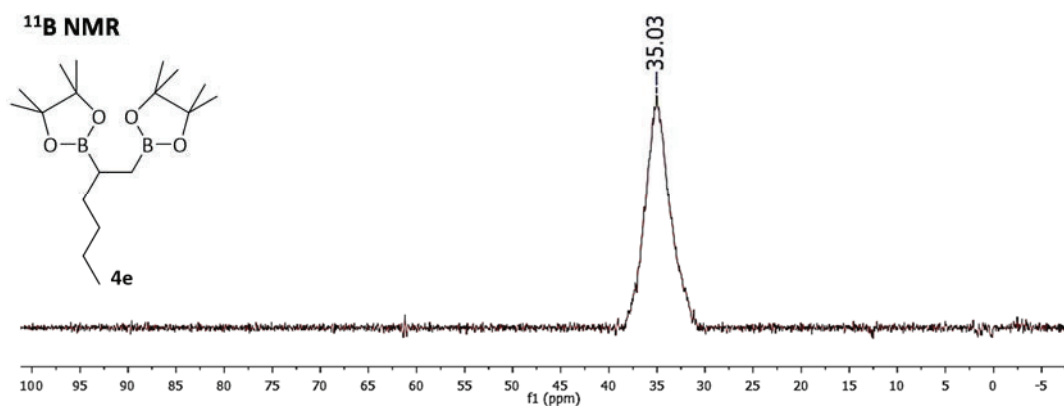
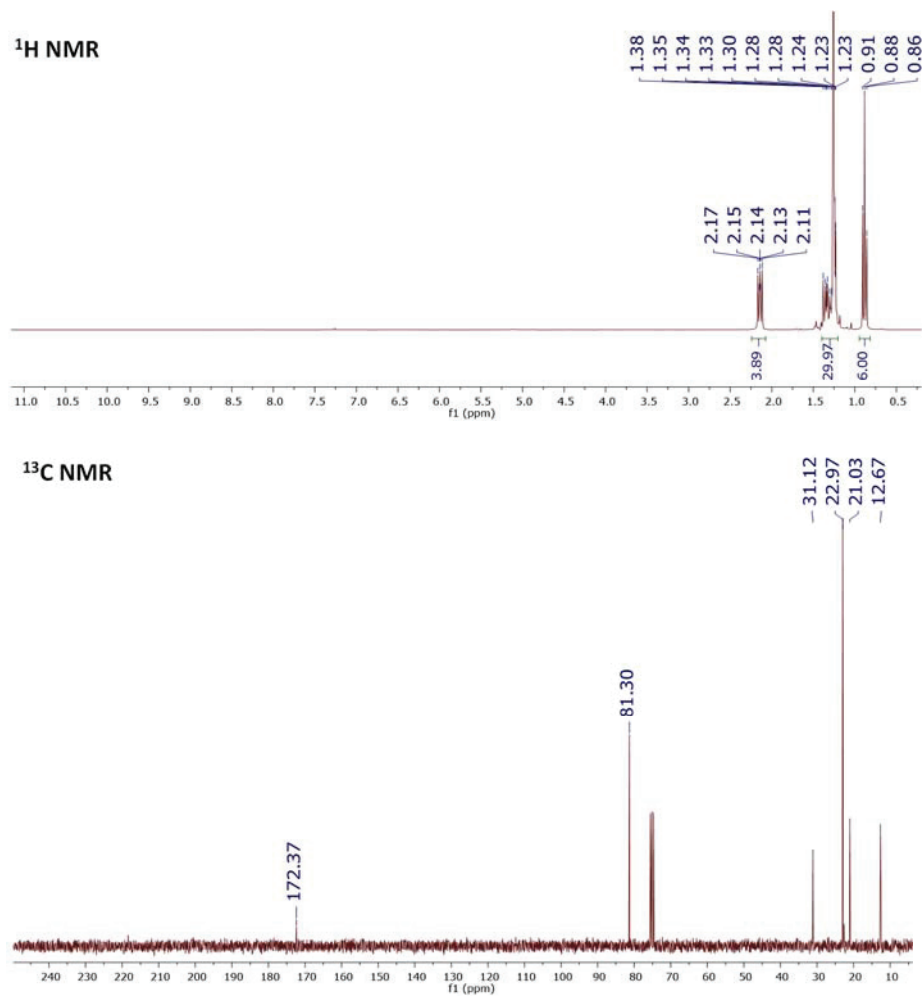


Figure S95. <sup>13</sup>C NMR spectrum of *N,N'*-(tetramethyl)diethylenediamine dihydrochloride (SM-3)

II.5.b. Pinalcol bisboronate monomers







II.5.c. Lithium trihydridoborates

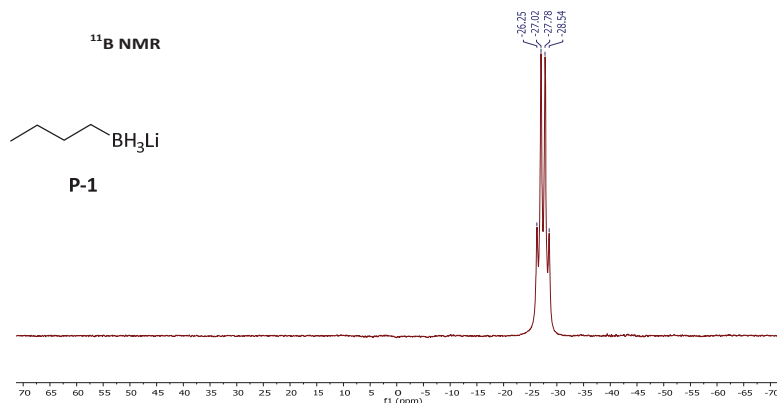
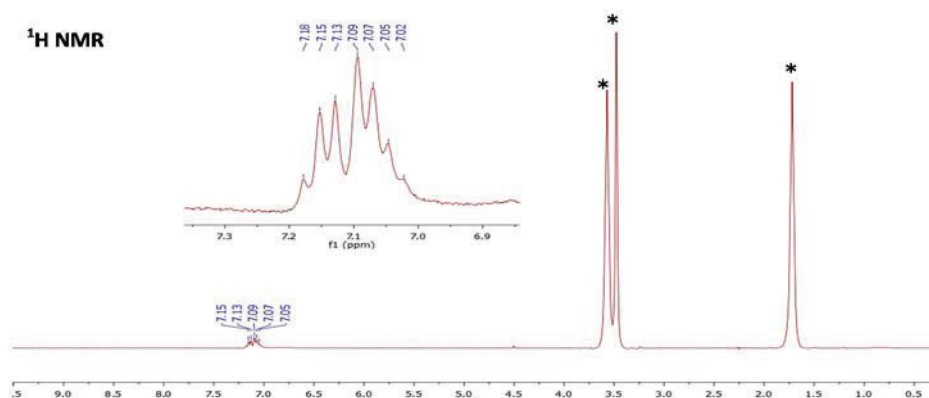
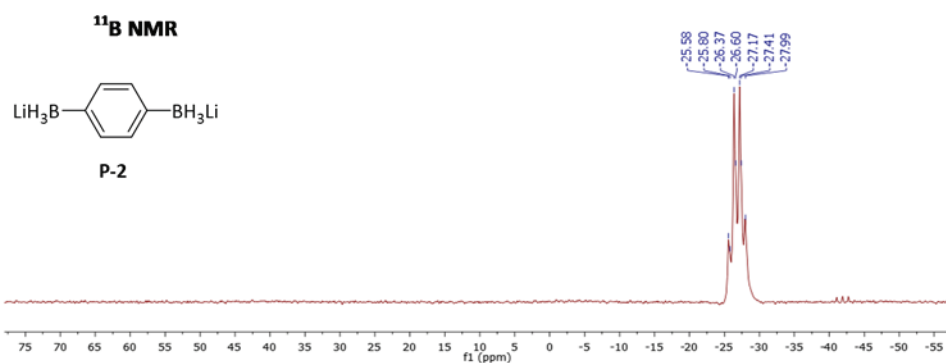
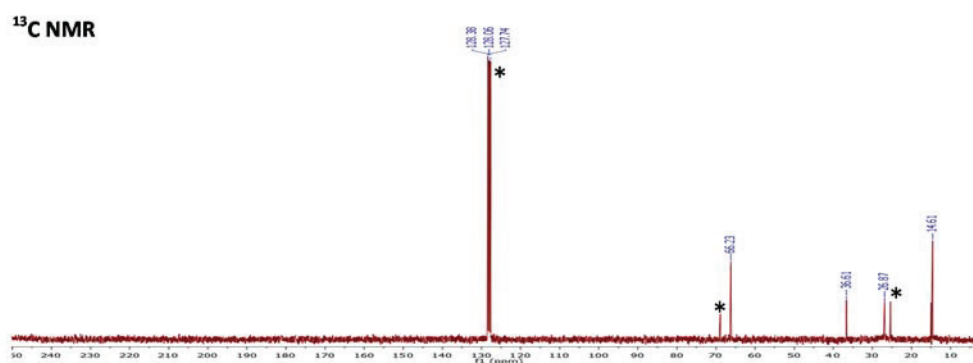
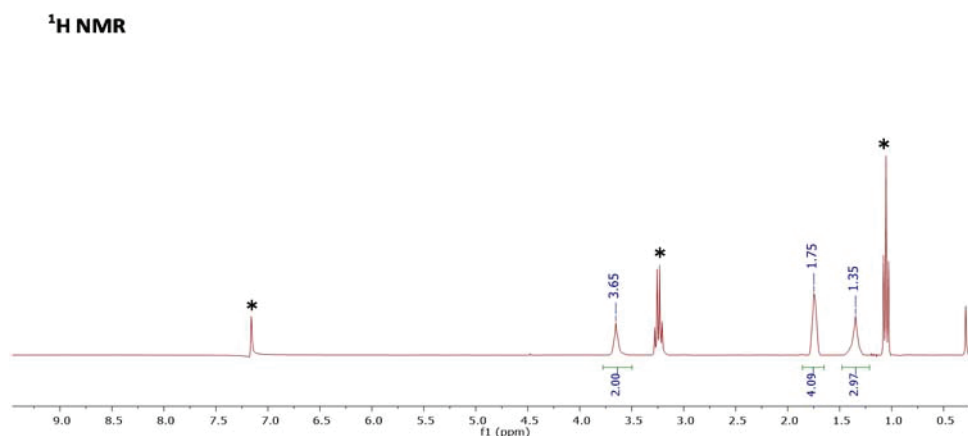
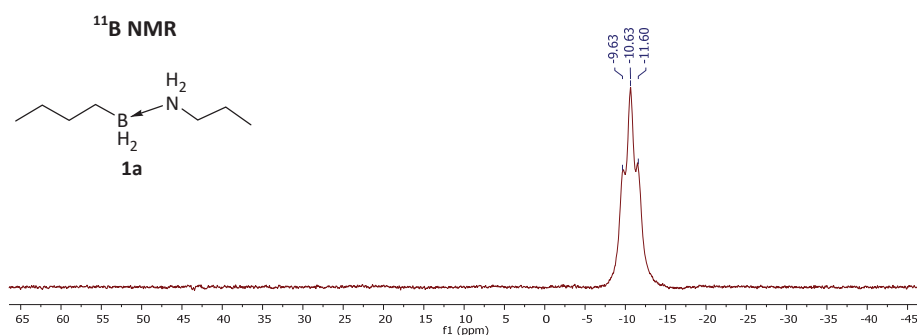
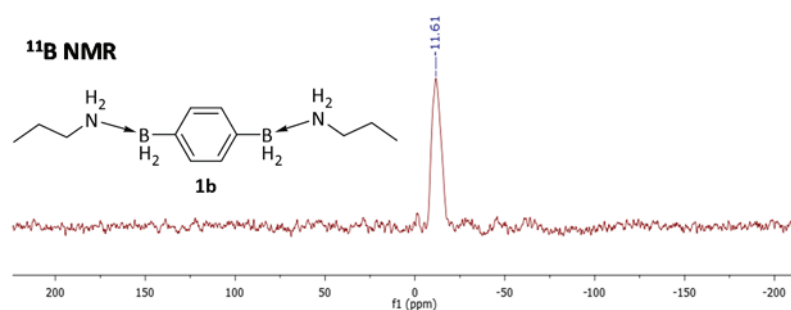
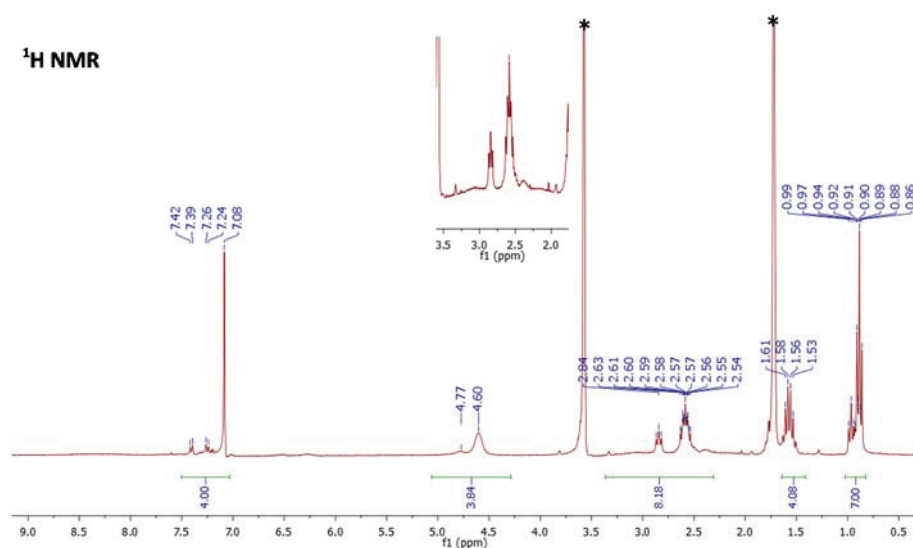


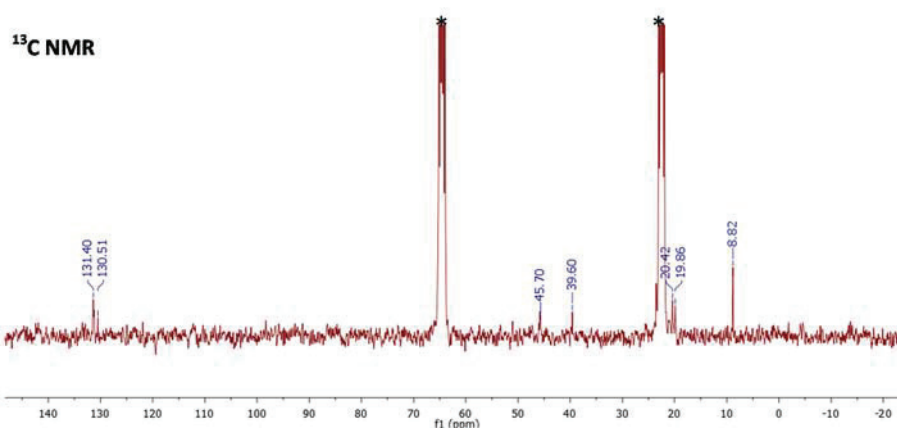
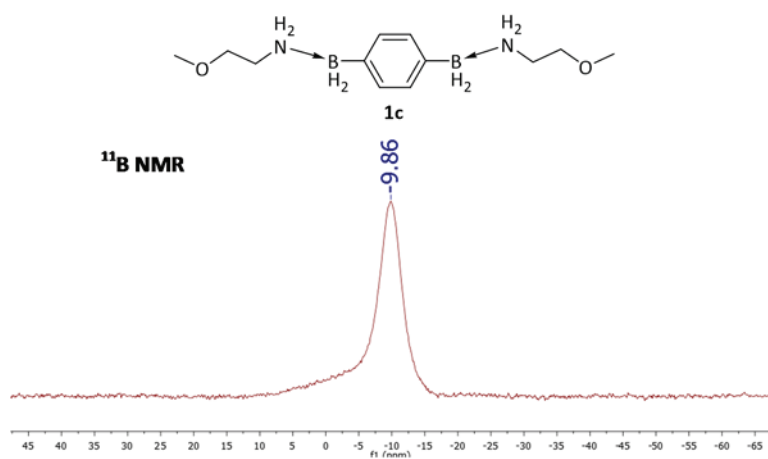
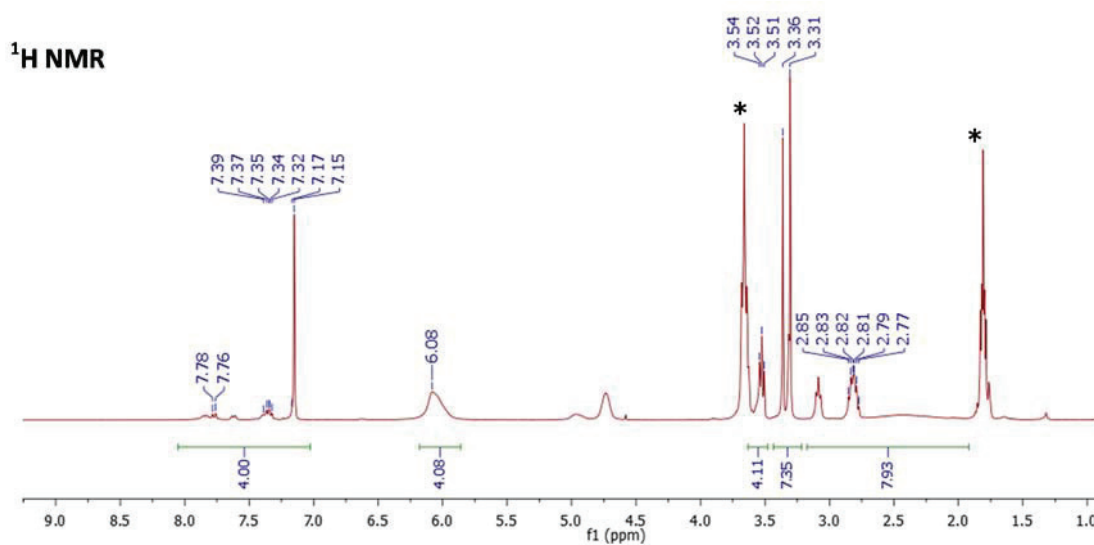
Figure S96. <sup>11</sup>B NMR spectrum of Lithium[butyl(trihydrido)borate] (P-1)





## II.5.d. Amine-boranes N and B mono-substituted

Figure S101. <sup>11</sup>B NMR spectrum of Propylamine-butylborane (1a)Figure S102. <sup>11</sup>B NMR spectrum of Dipropylamine-(1,4-benzene)bisborane (1b)Figure S103. <sup>1</sup>H NMR spectrum of Dipropylamine-(1,4-benzene)bisborane (1b)

Figure S104.  $^{13}\text{C}$  NMR spectrum of Dipropylamine-(1,4-benzene)bisborane (1b)Figure S105.  $^{11}\text{B}$  NMR spectrum of di(2-methoxyethyl)amine-(1,4-benzene)bisborane (1c)Figure S106.  $^1\text{H}$  NMR spectrum of di(2-methoxyethyl)amine-(1,4-benzene)bisborane (1c)

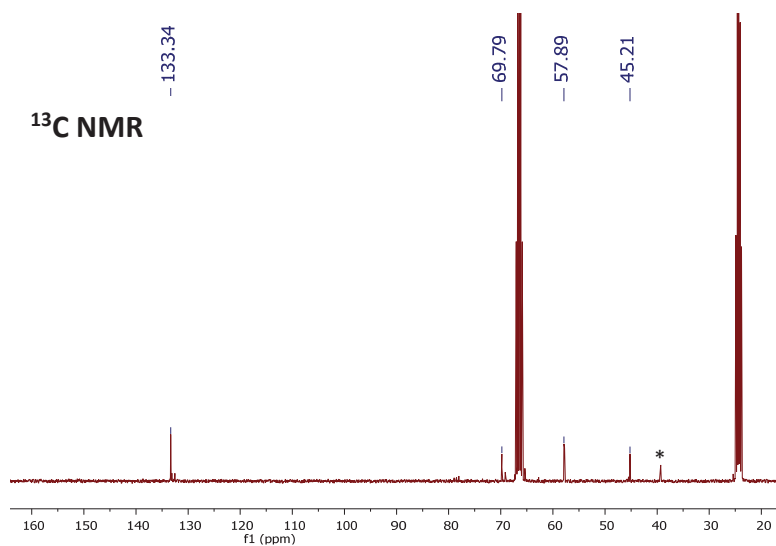


Figure S107. <sup>13</sup>C NMR spectrum of di(2-methoxyethyl)amine-(1,4-benzene)bisborane (1c)

## II.5.e. Polyboramines

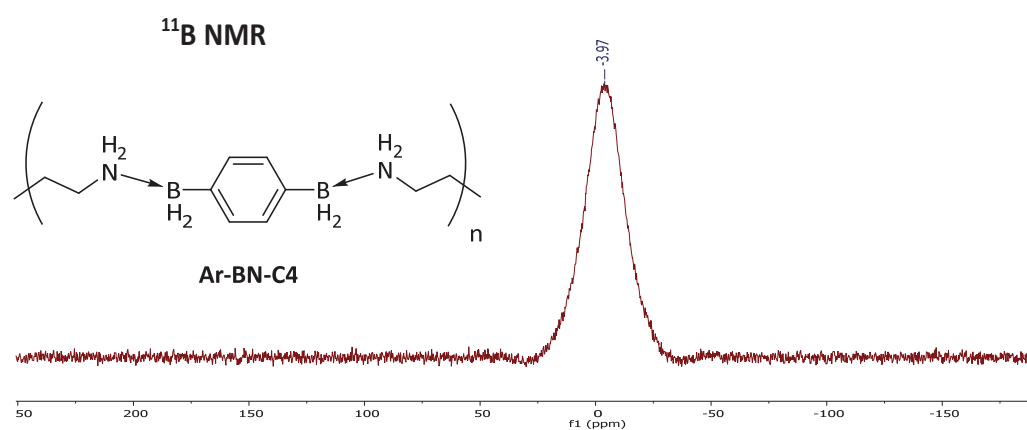


Figure S108. <sup>11</sup>B NMR spectrum of poly[diethylenediamine-(1,4-benzene)bisborane] (Ar-BN-C4)

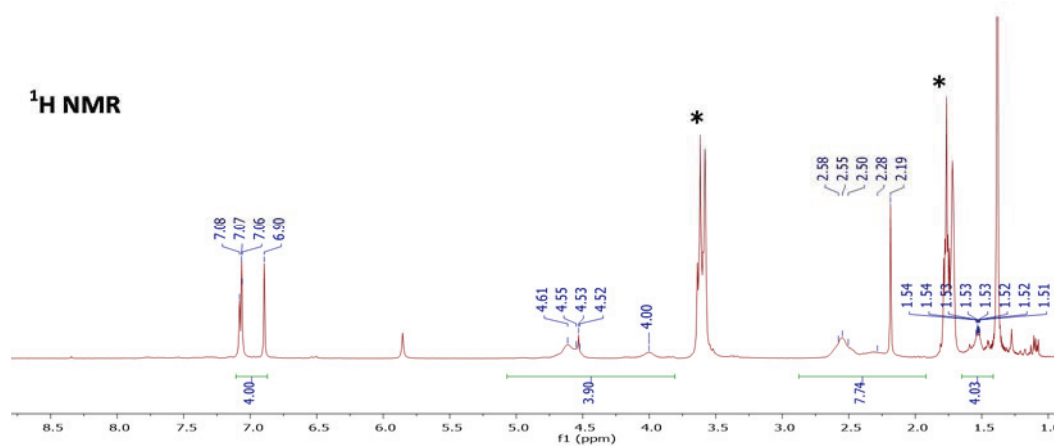


Figure S109. <sup>1</sup>H NMR spectrum of poly[diethylenediamine-(1,4-benzene)bisborane] (Ar-BN-C4)

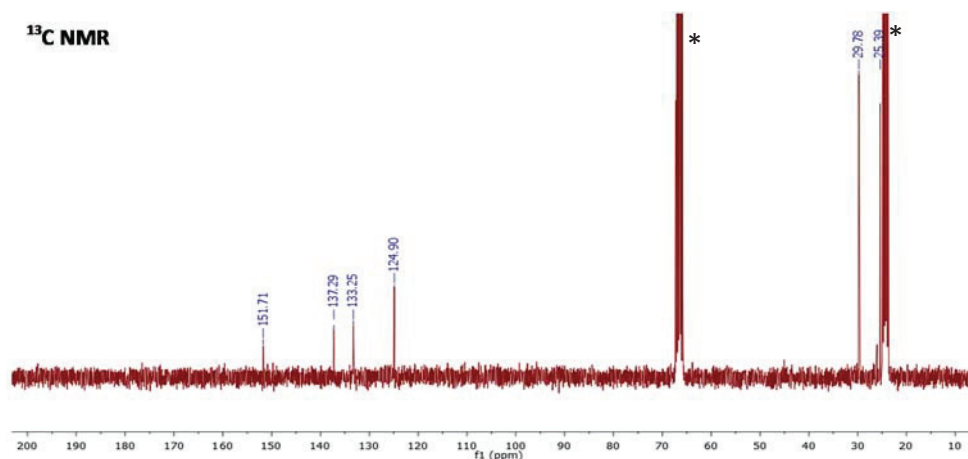


Figure S110.  $^{13}\text{C}$  NMR spectrum of poly[diethylenediamine-(1,4-benzene)bisborane] (Ar-BN-C4)

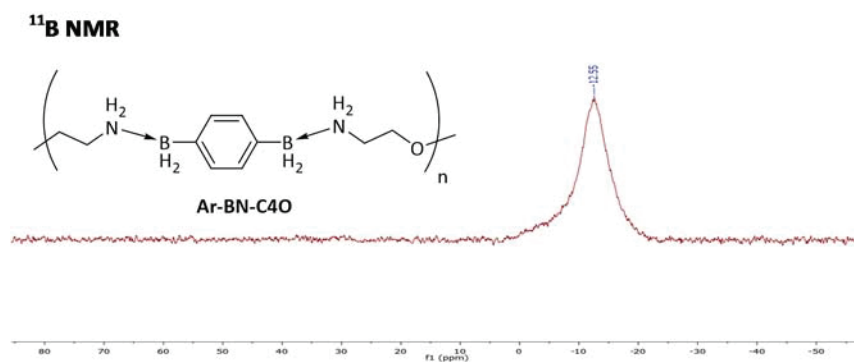


Figure S111.  $^{11}\text{B}$  NMR spectrum of poly[3-oxidiethylenediamine-(1,4-benzene)bisborane] (Ar-BN-C4O)

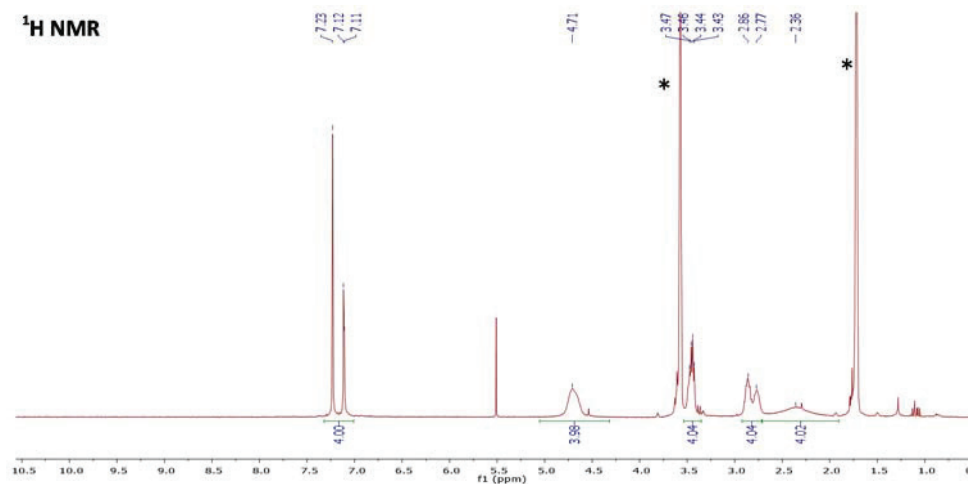


Figure S112.  $^1\text{H}$  NMR spectrum of poly[3-oxidiethylenediamine-(1,4-benzene)bisborane] (Ar-BN-C4O)

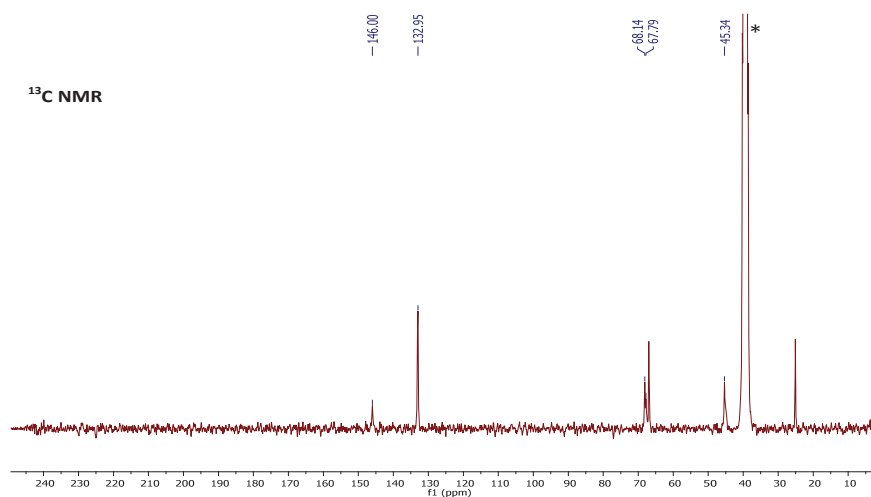


Figure S113. <sup>13</sup>C NMR spectrum of poly[3-oxydiethylenediamine-(1,4-benzene)bisborane] (Ar-BN-C4O)

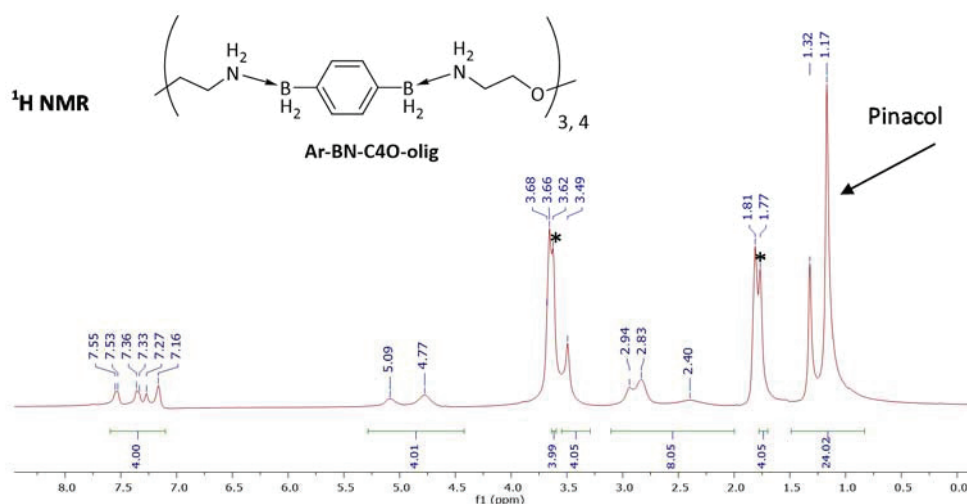


Figure S114. <sup>1</sup>H NMR spectrum of [3-oxydiethylenediamine-(1,4-benzene)bisborane]oligomers (Ar-BN-C4O-olig)

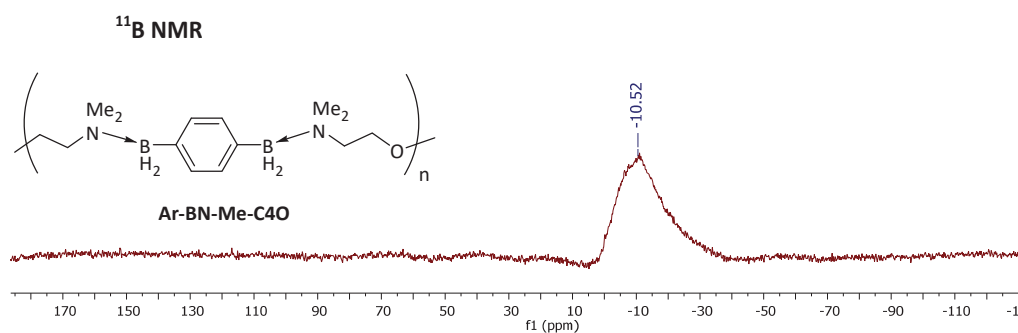


Figure S115. <sup>11</sup>B NMR spectrum of poly[3,3'-dioxydiethylenediamine-(1,4-benzene)bisborane] (Ar-BN-Me-C4O)

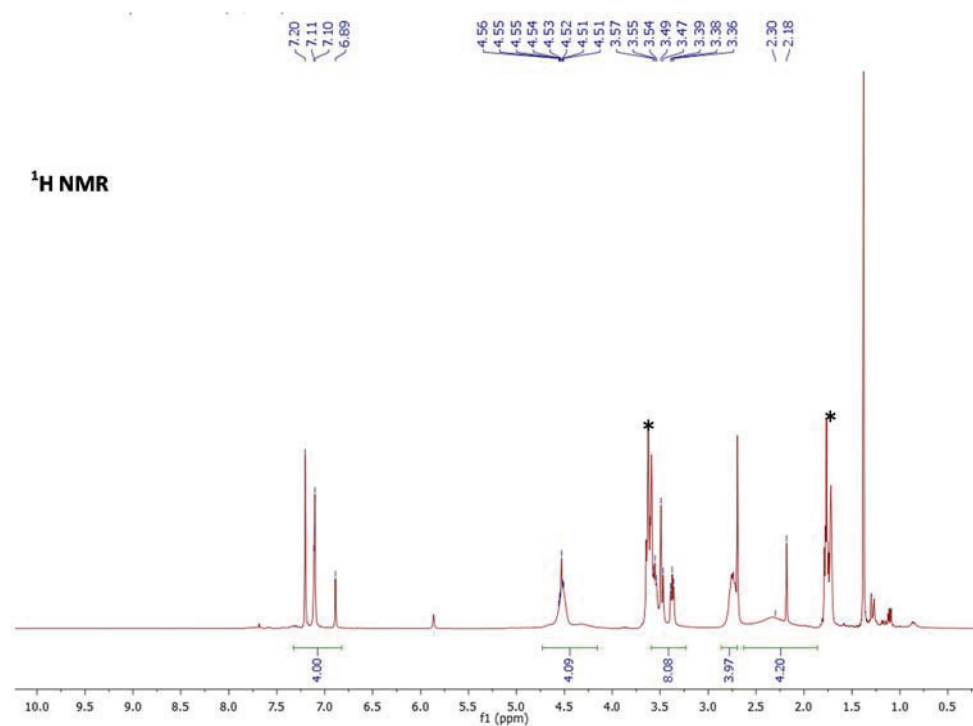


Figure S116.  $^1\text{H}$  NMR spectrum of poly[3,3'-dioxydiethylenediamine-(1,4-benzene)bisborane] (Ar-BN-Me-C4O)

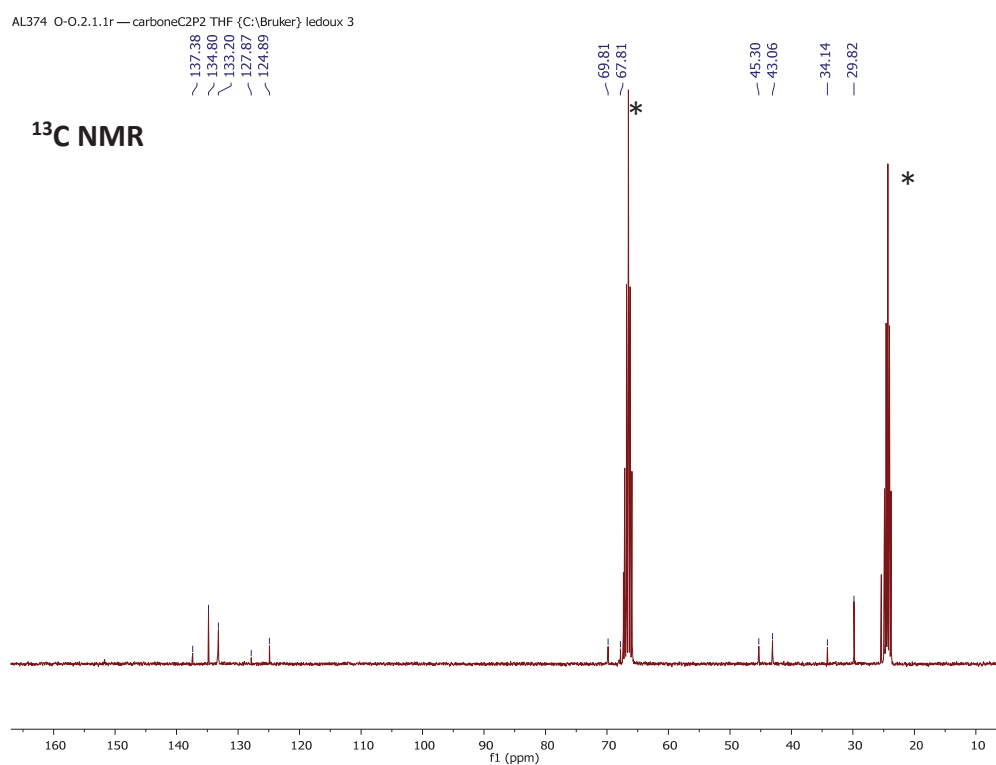


Figure S117.  $^{13}\text{C}$  NMR spectrum of poly[3,3'-dioxydiethylenediamine-(1,4-benzene)bisborane] (Ar-BN-Me-C4O)

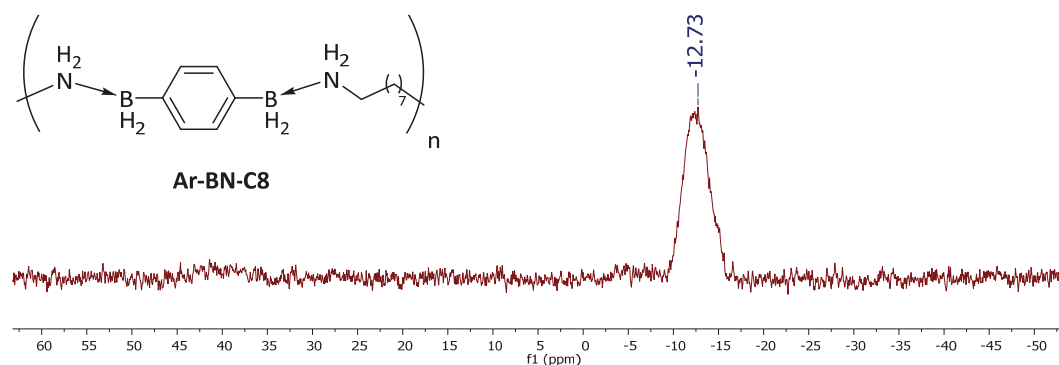
**$^{11}\text{B}$  NMR**

Figure S118.  $^{11}\text{B}$  NMR spectrum of poly[tetraethylenediamine-(1,4-benzene)bisborane] (Ar-BN-C8)

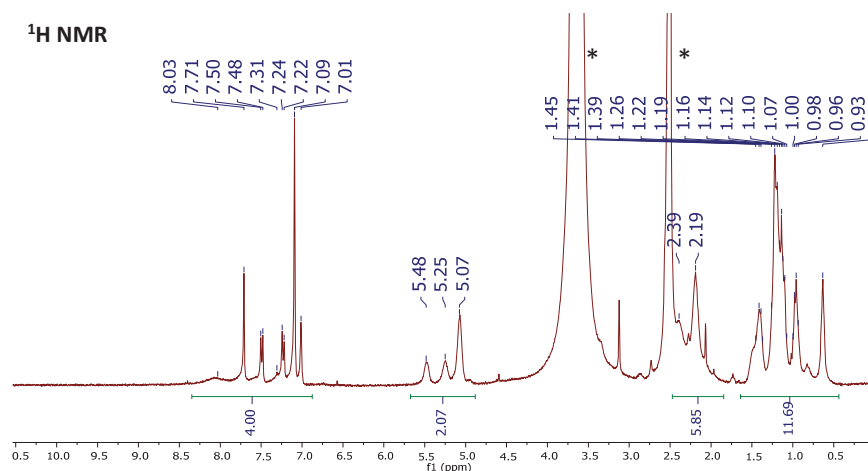
 **$^1\text{H}$  NMR**

Figure 119.  $^1\text{H}$  NMR spectrum of poly[tetraethylenediamine-(1,4-benzene)bisborane] (Ar-BN-C8)

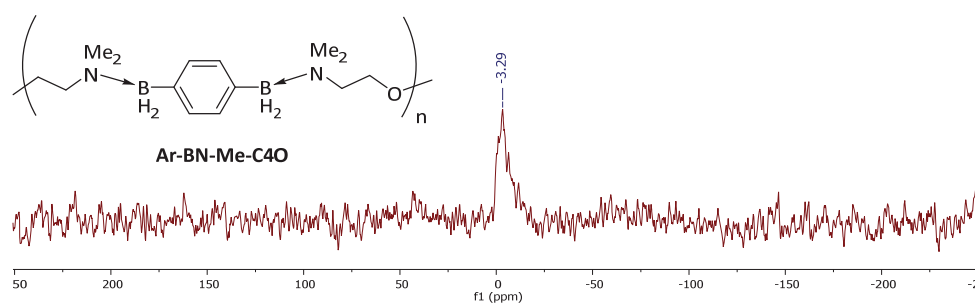
 **$^{11}\text{B}$  NMR**

Figure S120.  $^{11}\text{B}$  NMR spectrum of poly[3-oxydiethylene-N,N'-dimethyldiamine-(1,4-benzene)bisborane] (Ar-BN-Me-C4O)

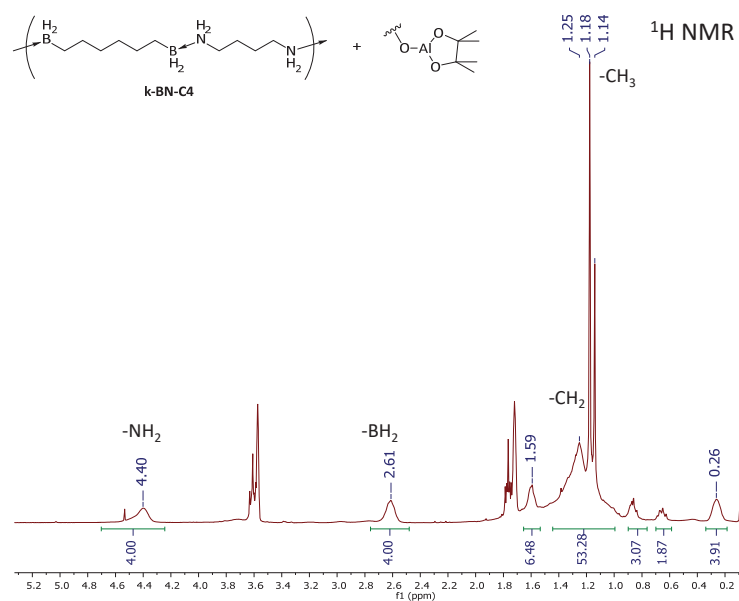
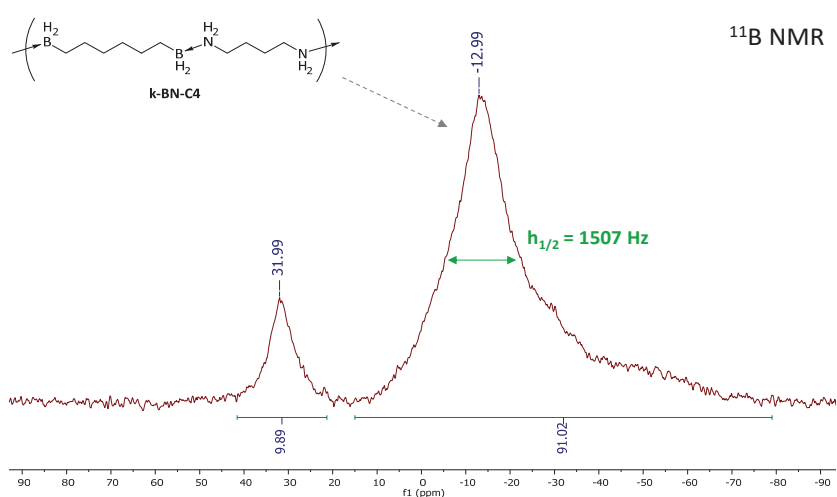
**$^{13}\text{C}$  NMR**

Chemical shift (ppm): 240, 230, 220, 210, 200, 190, 180, 170, 160, 150, 140, 130, 120, 110, 100, 90, 80, 70, 60, 50, 40, 30, 20, 10.

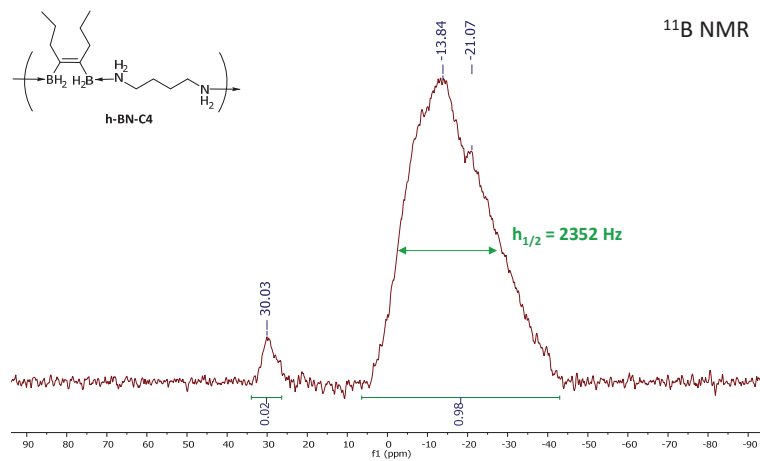
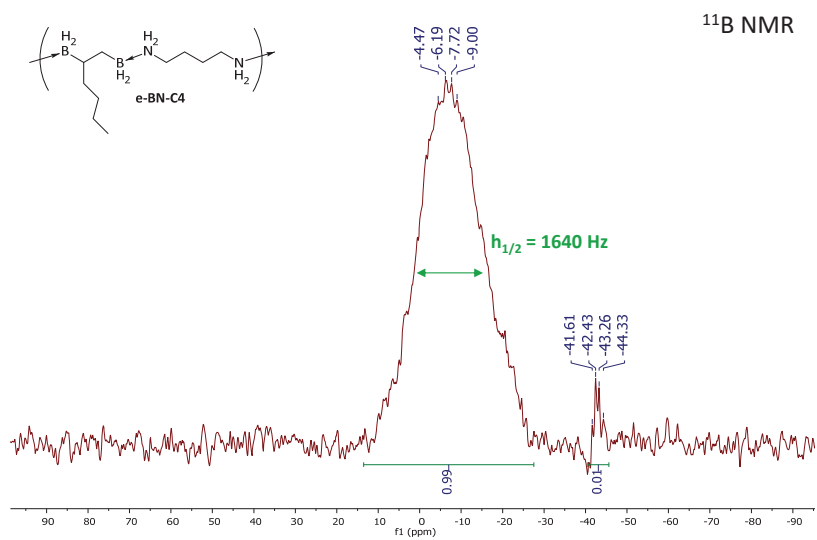
Peak labels (ppm): 136.50, 69.12, 68.68, 58.73, 58.49, 45.24, 45.04, 24.50.

**Figure S121.**  $^{13}\text{C}$  NMR spectrum of poly[3-oxydiethylene-N, N'-dimethyldiamine-(1,4-benzene)bisborane] (Ar-BN-Me-C4O)

*Following data doesn't feature pure compounds but are indicatives. Improvement are ongoing.*

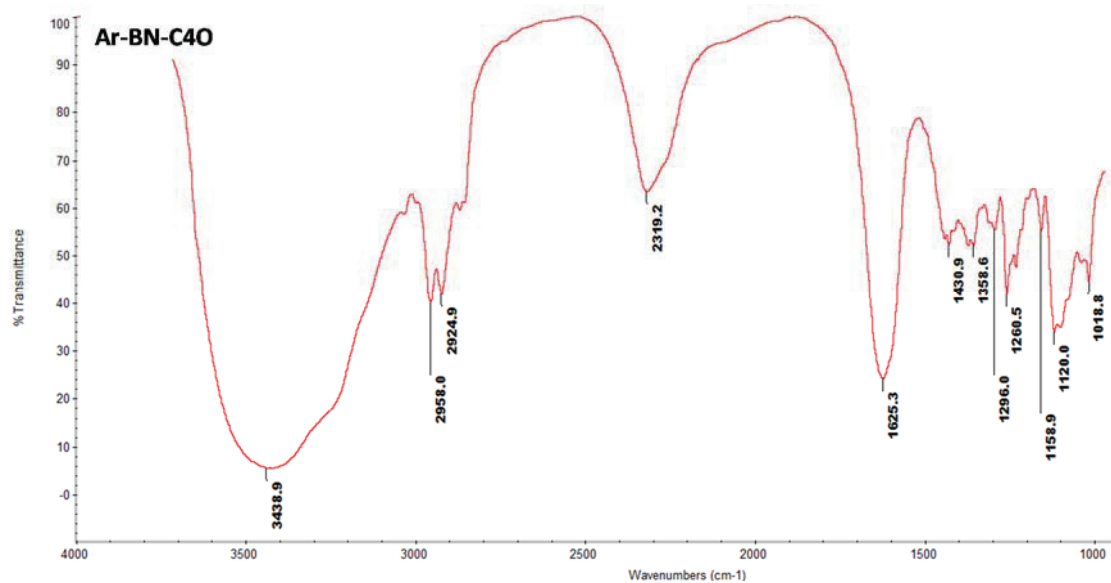
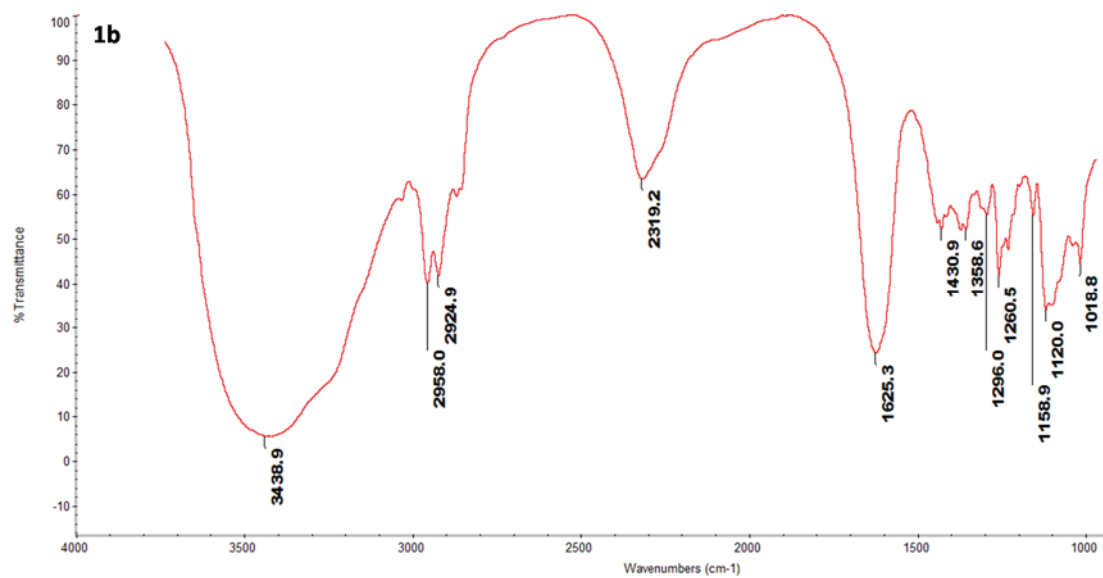


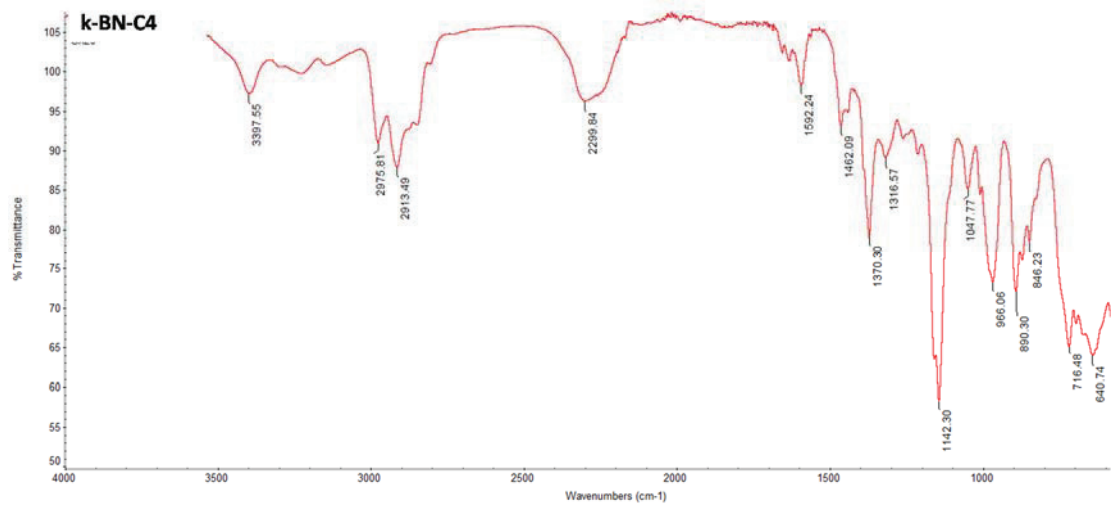
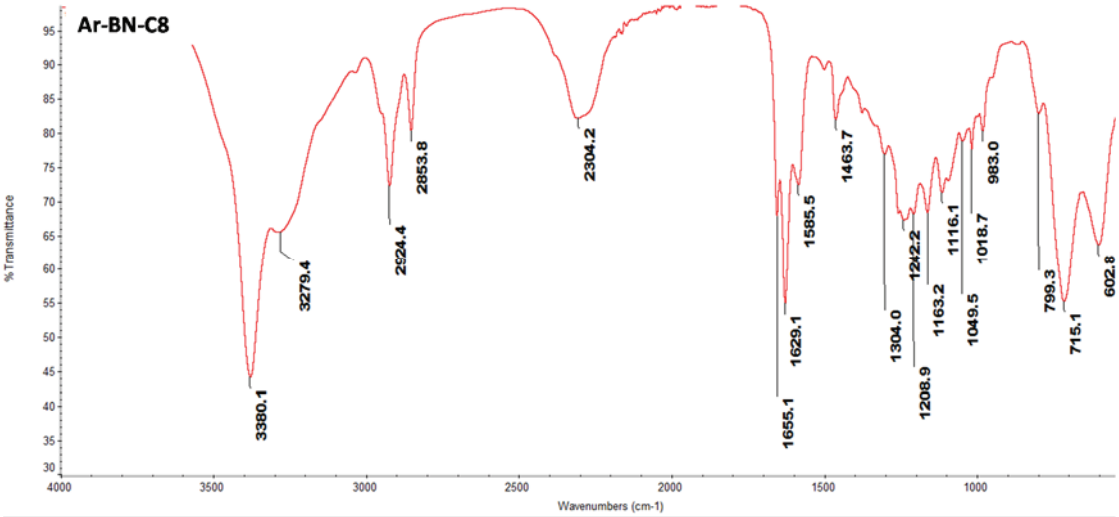
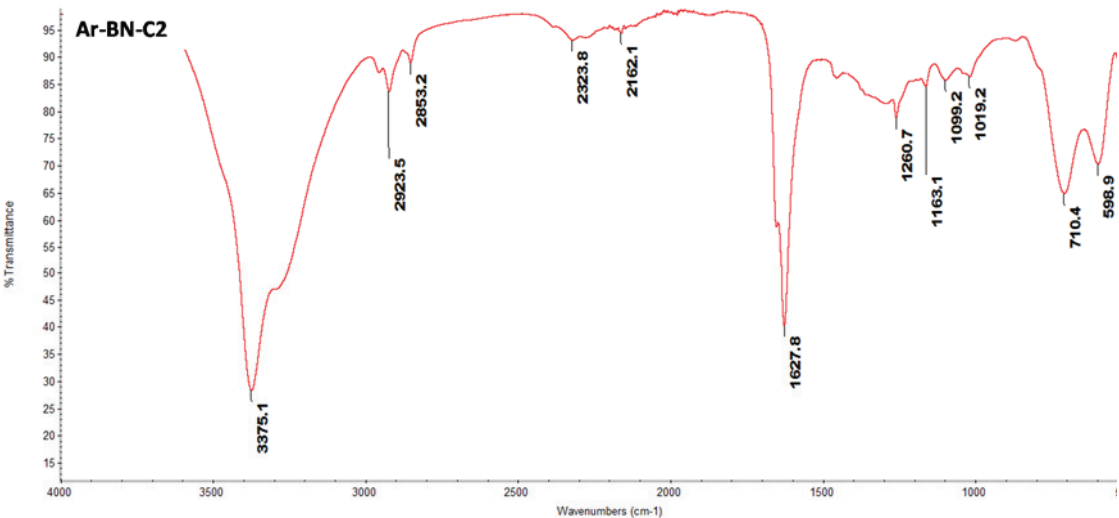


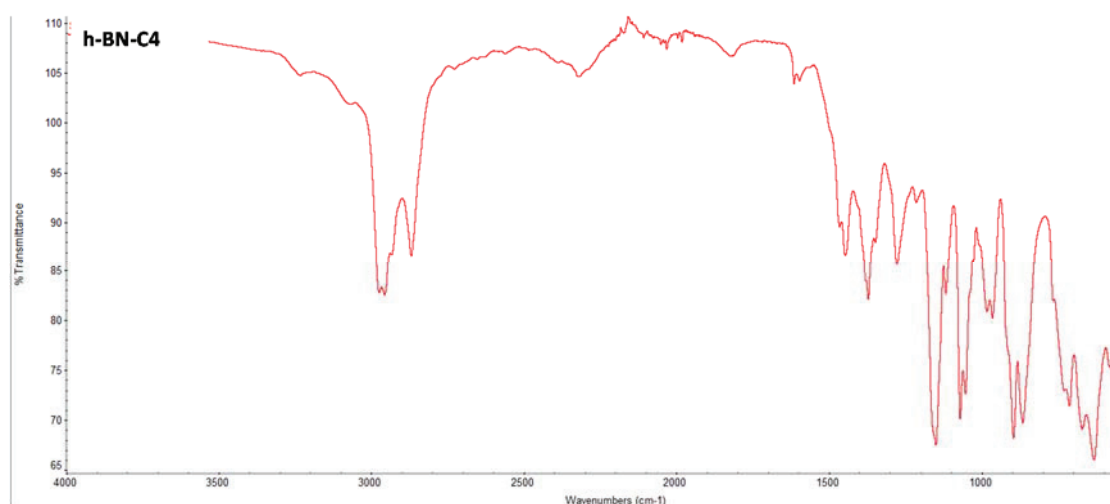


## II.6. ATR-IR spectra

### II.6.a. Polyboramines and molecular analogues







## II.6.b. Transfer hydrogenation

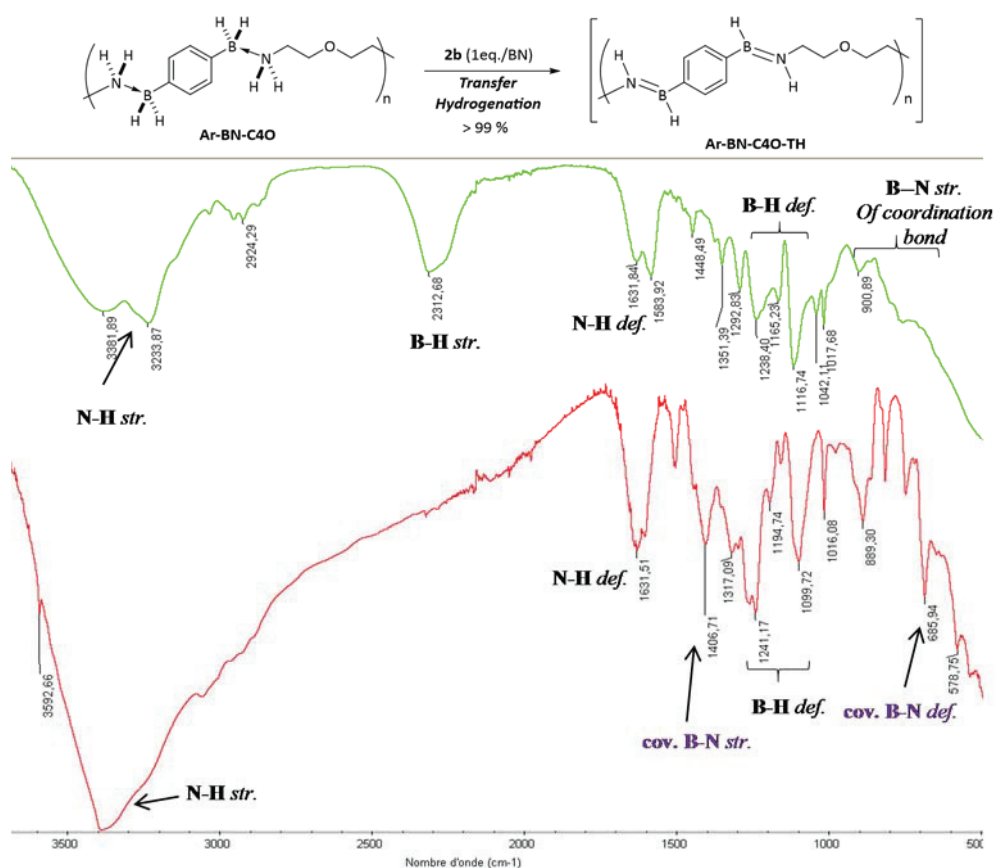


Figure S122. Hydrogen transfer reaction using Ar-BN-C4O polyboramine and 2b substrate. ATR-IR of polymer before (Ar-BN-C4O, up) and after (Ar-BN-C4O-TH, down).

II.7. SEC (steric exclusion chromatography)

II.7.a. SEC-THF of polymer Ar-BN-C4O

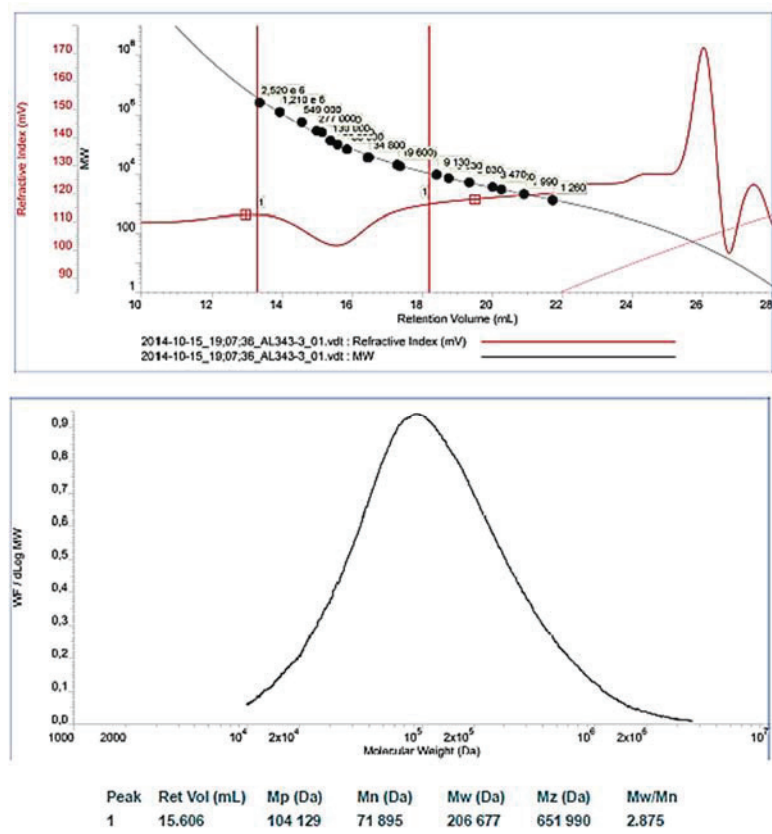


Figure S123. SEC of polymer Ar-BN-C4O. Eluent THF + 1w% TBAB, Temperature column 30°C.

II.7.b. SEC-THF of oligomer Ar-BN-C4O-olig

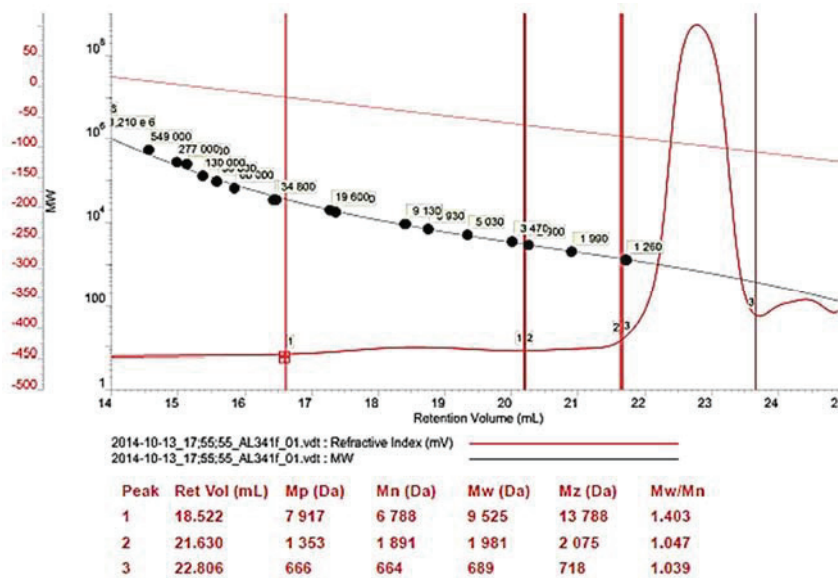


Figure S124. SEC of oligomers Ar-BN-C4O-olig. Eluent THF + 1w% TBAB, Temperature column 30°C.

II.7.c. SEC-DMF of a dehydrogenated polymer: Ar-BN-C4O-Dh

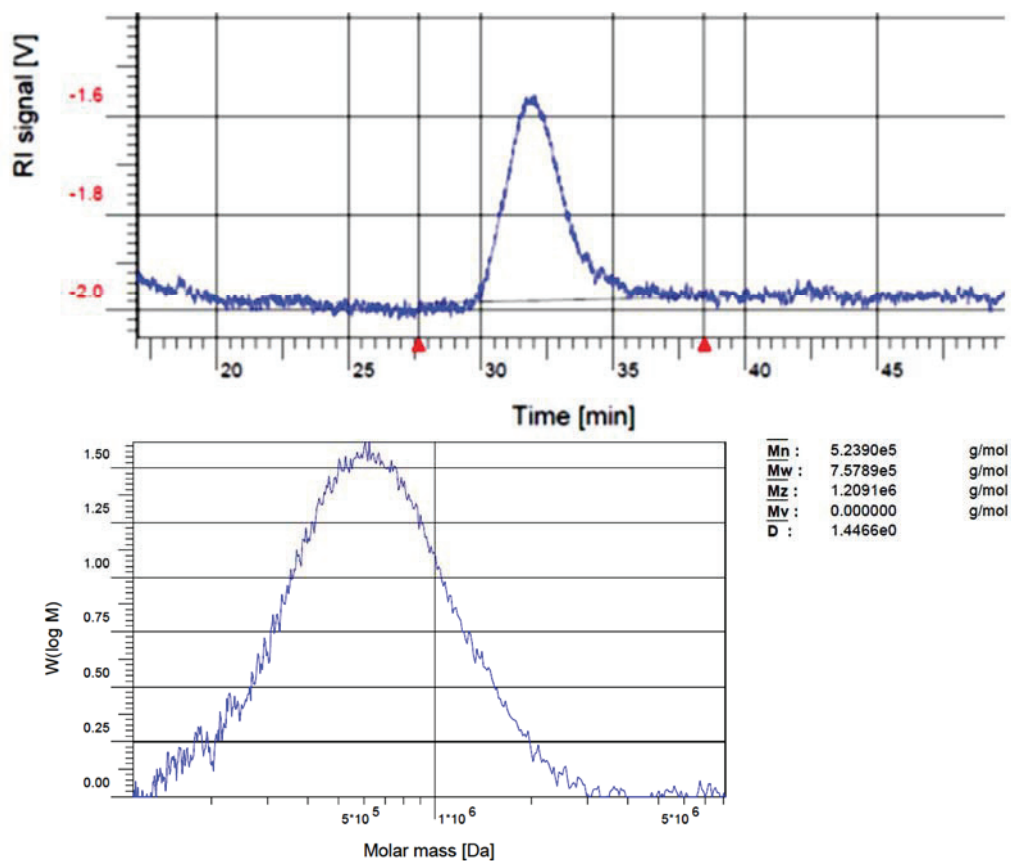


Figure S125. SEC of polymer Ar-BN-C4O after thermal treatment at 160 °C, 1 h to yield Ar-BN-C4O-Dh. Eluent: DMF + 0.5 w% LiBr. Temperature of column 60°C.

### III. Polyboramines: transfer hydrogenation on carbonyls

---

All reactions were carried out in duplicate and results were reported in tables below. Reactions were monitored by  $^{11}\text{B}$  NMR and/or  $^1\text{H}$  NMR until completion, using 1,1,2,2-tetrachloroethane as an internal standard. For polymer, the amount of product was expressed in mmol/unit, considering the mole number of 1 unit of polymer (n) as a *separated* molecule. All products were characterized by NMR spectroscopy and further identified by MS.

#### III.1. Experimental procedures of transfer hydrogenation

---

Imine starting materials for transfer hydrogenation reaction such as *N*-Benzylideneaniline, *N*-Benzylidenebenzenesulfonamide, *N*-Benzylidenemethylamine, *N*-Benzylidene-*tert*-butylamine have been obtained from Sigma-Aldrich and used without any further purification.

##### III.1.a. Procedure 9

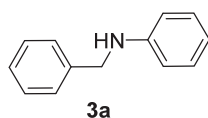
Representative procedure for the reduction of *N*-Benzylidenebenzenesulfonamide **2b** by Poly[3-oxydiethylenediamine-(1,4-benzene)bisborane] (**Ar-BN-C4O**): a vial equipped with a screw cap was loaded with **Ar-BN-C4O** (0.04 mmol/unit, 21 mg), **2b** (0.08 mmol, 19.6 mg) in THF- $d_8$  (0.6 mL) and stirred from r.t. to 40 °C for a desired time (5 min to 12 h).  $^1\text{H}$  NMR analysis were performed after addition of the internal standard (4.7  $\mu\text{L}$ , 0.045 mmol). According to the internal standard ( $\delta = 6.57$  ppm (s, 2H,  $-\text{CH}_2-\text{Cl}_2$ )), the typical chemical shift of the starting material ( $\delta = \text{ppm}$  (s, 1H,  $-\text{CH}-\text{N}$ )) decreased, and a new signal of the hydrogenated product ( $\delta = 4.02$  ppm (d, 2H,  $-\text{CH}_2-\text{NH}$ )) gradually appeared until the system reach a stationary state. The resulting hydrogenated substrate (amine) can be isolated by dissolution in EtOAc and filtration on short pad of silica. Identical conditions are used for other carbonyls.  $^1\text{H}$  NMR monitoring is performed as following: for benzaldehyde the typical chemical shift of the starting material ( $\delta = 10.0$  ppm (s, 1H,  $-\text{CH}-\text{O}$ )) decreased, while a new signal of the hydrogenated product ( $\delta = 4.57$  ppm (d, 2H,  $-\text{CH}_2-\text{OH}$ )) gradually appeared until completion. For acetophenone the typical chemical shift of

the starting material ( $\delta = 2.53$  ppm (s, 3H,  $-\text{CH}_3$ )) decreased, while a new signal of the hydrogenated product ( $\delta = 4.76$  ppm (q, 1H,  $-\text{CH}(\text{OH})-\text{CH}_3$ )) gradually appeared until completion. Dehydrogenated product of amine-borane can be recovered by precipitation into cold ether and analyzed by  $^{11}\text{B}$  NMR, and IR spectroscopy.

### III.1.b.Procedure 10: for viscous amine-boranes

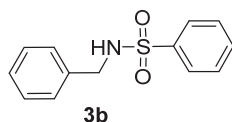
Representative procedure for the reduction of *N*-benzylideneaniline **2a** by di(2-methoxyethyl)amine-(1,4-benzene)bisborane (**1c**): A vial equipped with a screw cap was loaded with fresh **1c** in solution in  $\text{THF-}d_8$  (0.035 mmol, 0.6 mL) (filtrate never isolated from volatiles. See **1c** synthesis). The exact molarity is first determined by  $^1\text{H}$  NMR spectroscopy after addition of the internal standard (4.7  $\mu\text{L}$ , 0.045 mmol). Then **2a** (12.5 mg, 0.069 mmol) were added and the mixture were stirred from r.t. to 40 °C. Experiment is monitored by  $^1\text{H}$  NMR as described in procedure 9.

## III.2. Characterization of transfer hydrogenation products



### *N*-benzylaniline (**3a**)<sup>viii</sup>

NMR spectroscopy :  $^1\text{H}$  NMR (300 MHz,  $\text{THF-}d_8$ , 25 °C,  $\delta$ ): 4.29 (d,  $J = 6$  Hz, 2H), 5.30 (s, br, N-H), 6.51-6.60 (m, 3H), 7.00-7.40 (m, 7H);  $^{13}\text{C}$  NMR (75 MHz,  $\text{THF-}d_8$ , 25 °C,  $\delta$ ): 48.6, 113.4, 117.2, 127.6, 128.1, 129.2, 129.7, 141.5, 150.0; GC-MS:  $m/z = 183.10$  ( $\text{M}^+$ )



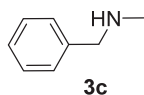
### *N*-(benzyl)benzenesulfonamide (**3b**)<sup>ix</sup>

$^1\text{H}$  NMR spectroscopy (300 MHz,  $\text{THF-}d_8$ , 25 °C,  $\delta$ ): 4.05 (d,  $J = 6$  Hz, 2H), 7.01 (s, br, N-H), 6.18-6.24 (m, 5H), 7.47-7.56 (m, 3H), 7.84-7.88 (m, 2H);  $^{13}\text{C}$  NMR (75 MHz,  $\text{THF-}d_8$ , 25 °C,  $\delta$ ): 47.4, 127.2, 127.9, 128.1, 128.8, 129.2, 132.8, 136.3, 140.0; GC-MS:  $m/z = 247.07$  ( $\text{M}^+$ ).

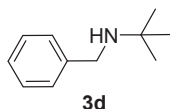
<sup>viii</sup> Yang, X.; Zhao, L.; Fox, T.; Wang, Z.-X.; Berke, H. *Angew. Chem. Int. Ed.* **2010**, 49(11), 2058–2062

<sup>ix</sup> Moore, J. D.; Herpel, R. H.; Lichtsinn, J. R.; Flynn, D. L.; Hanson, P. R. *Org. Lett.* **2003**, 5(2), 105-107.

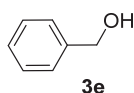


**N-benzylmethanamine (3c)<sup>x</sup>**

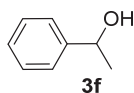
<sup>1</sup>H NMR spectroscopy (300 MHz, THF-*d*<sub>8</sub>, 25 °C,  $\delta$ ): 7.12–7.38 (m, 5H), 3.68 (s, 2H), 2.35 (s, 3H); <sup>13</sup>C NMR (**75** MHz, THF-*d*<sub>8</sub>, 25 °C,  $\delta$ ): 139.9, 128.1, 128.0, 127.9, 58.2, 38.4; GC-MS *m/z* = 121.09 (*M*<sup>+</sup>).

**N-benzyl-tert-butylamine (3d)<sup>viii</sup>**

NMR spectroscopy: <sup>1</sup>H NMR (300 MHz, THF-*d*<sub>8</sub>, 25 °C,  $\delta$ ): 1.15 (s, 9H), 3.71 (d, *J* = 6 Hz, 2H), 7.11–7.38 (m, 5H); <sup>13</sup>C NMR (**75** MHz, THF-*d*<sub>8</sub>, 25 °C,  $\delta$ ): 29.6, 47.9, 51.0, 127.2, 128.8, 128.9, 143.5; GC-MS: *m/z*: 163.14 (*M*<sup>+</sup>)

**benzylalcohol (3e)<sup>viii</sup>**

NMR spectroscopy: <sup>1</sup>H NMR (300 MHz, THF-*d*<sub>8</sub>, 25 °C,  $\delta$ ): 4.26 (s, br, O-H), 4.56 (d, *J* = 6 Hz, 2H), 7.15–7.20 (m, 1H), 7.24–7.34 (m, 4H); <sup>13</sup>C NMR (**75** MHz, THF-*d*<sub>8</sub>, 25 °C,  $\delta$ ): 65.2, 127.5, 128.1, 129.4, 142.8, GC-MS: *m/z* = 108.06 (*M*<sup>+</sup>).

**1-phenylethylalcohol (3f)<sup>viii</sup>**

NMR spectroscopy: <sup>1</sup>H NMR (300 MHz, THF-*d*<sub>8</sub>, 25 °C,  $\delta$ ): 1.37 (d, 3H, *J* = 7 Hz, 3H), 4.76 (q, *J* = 6 Hz, 1H), 4.19 (s, br, O-H), 7.18–7.31 (m, 5H); <sup>13</sup>C NMR (**75** MHz, THF-*d*<sub>8</sub>, 25 °C,  $\delta$ ): 25.0, 69.9, 125.4, 127.4, 128.4, 146.1; GC-MS: *m/z* = 122.07 (*M*<sup>+</sup>).

<sup>x</sup> (a) K. Nishiwaki, T. Ogawa, K. Shigeta, K. Takahashi, K. Matsuo, *Tetrahedron*. **2006**, 62, 7034–7042; (b) I. K. Nishiwaki, T. Ogawa, K. Shigeta, K. Takahashi, K. Matsuo, *Tetrahedron*. **2006**, 62, 7034–7042.

### III.3. Representative NMR spectra

#### III.3.a. $^1\text{H}$ NMR monitoring

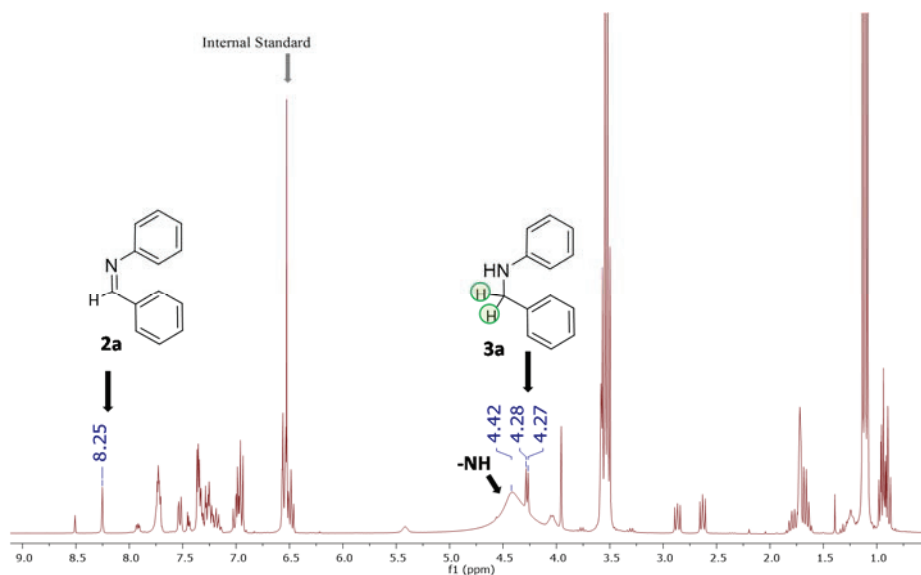


Figure S126. Transfer hydrogenation reaction on *N*-benzylidene aniline (**2a**) using **1b**.  $^1\text{H}$  NMR monitoring.

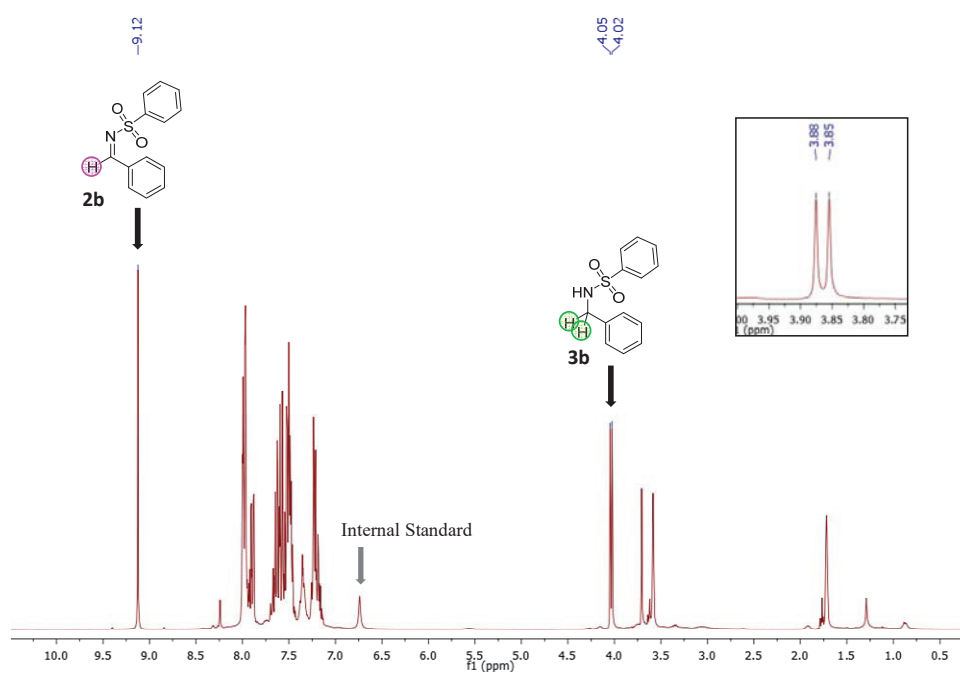


Figure S127. Transfer hydrogenation reaction on *N*-phenylsulfonylideneaniline (**2b**) using **Ar-BN-C4O**.  $^1\text{H}$  NMR monitoring.

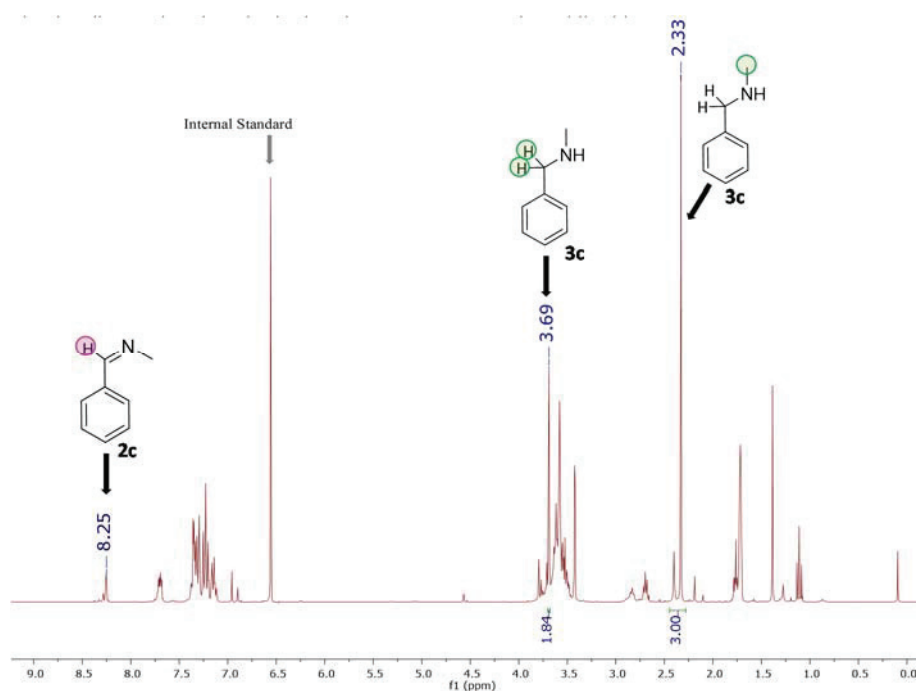


Figure S128. Transfer hydrogenation reaction on N-methyldene aniline (2c) using Ar-BN-C4O.  $^1\text{H}$  NMR monitoring.

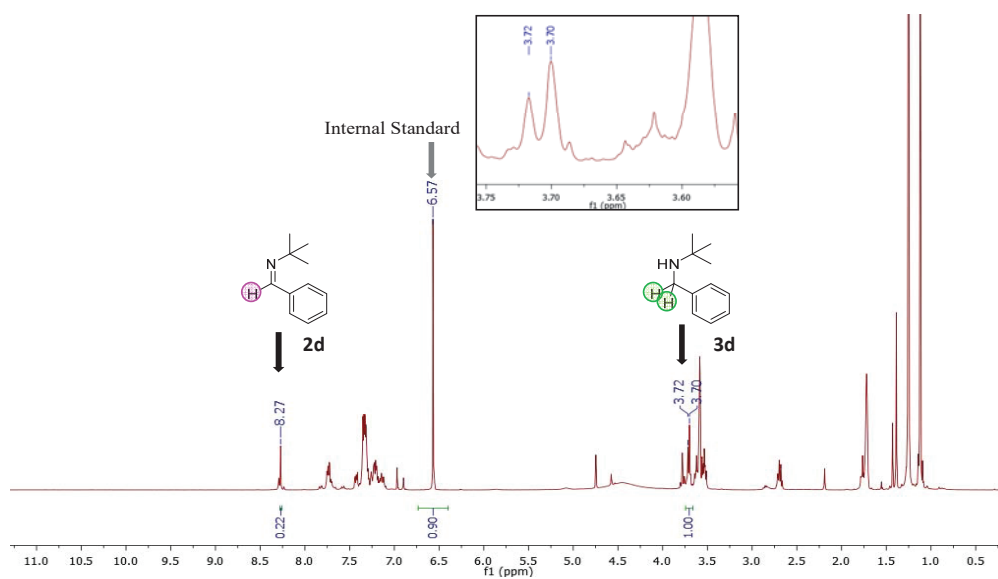


Figure S129. Transfer hydrogenation reaction on N-terbutyldene aniline (2d) using Ar-BN-C4O.  $^1\text{H}$  NMR monitoring.

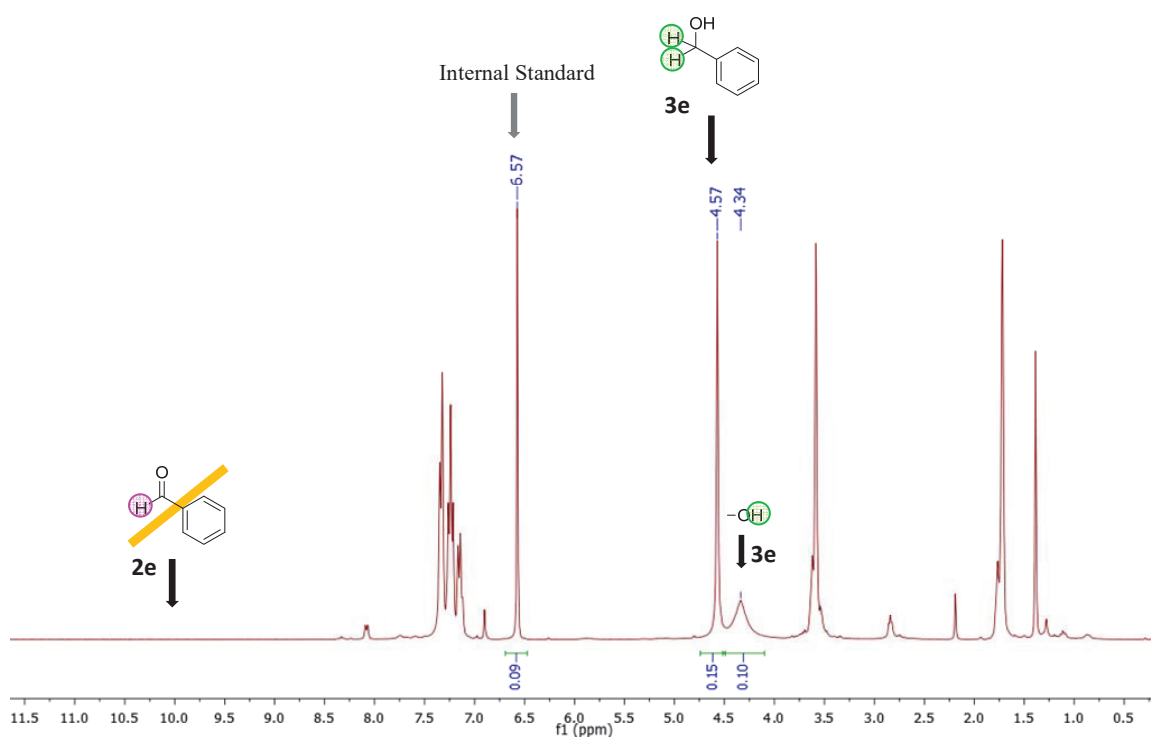


Figure S130. Transfer hydrogenation reaction on benzaldehyde (2e) using Ar-BN-C4O.  $^1\text{H}$  NMR monitoring.

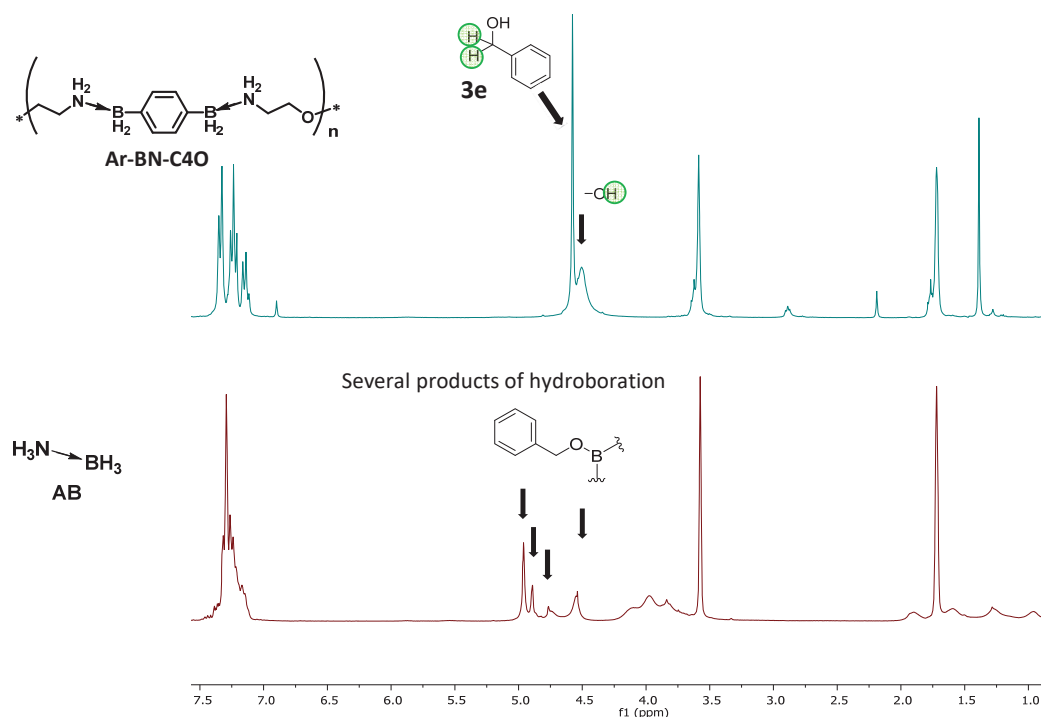


Figure S131. Transfer hydrogenation reaction performed by Ar-BN-C4O on benzaldehyde yielded benzylalcohol (c.f., e.g.,  $\delta(\text{CH}_2) = 4.56\text{ppm}$  (d,  $J = 6\text{ Hz}$ , 2H,  $m/z = 108.6$ ) versus hydroboration performed by ammonia-borane yielded boron-bounded alcoholates as tribenzylborate (c.f., e.g.,  $\delta(\text{CH}_2) = 4.99\text{ppm}$  (s, br). A comparative  $^1\text{H}$  NMR study.

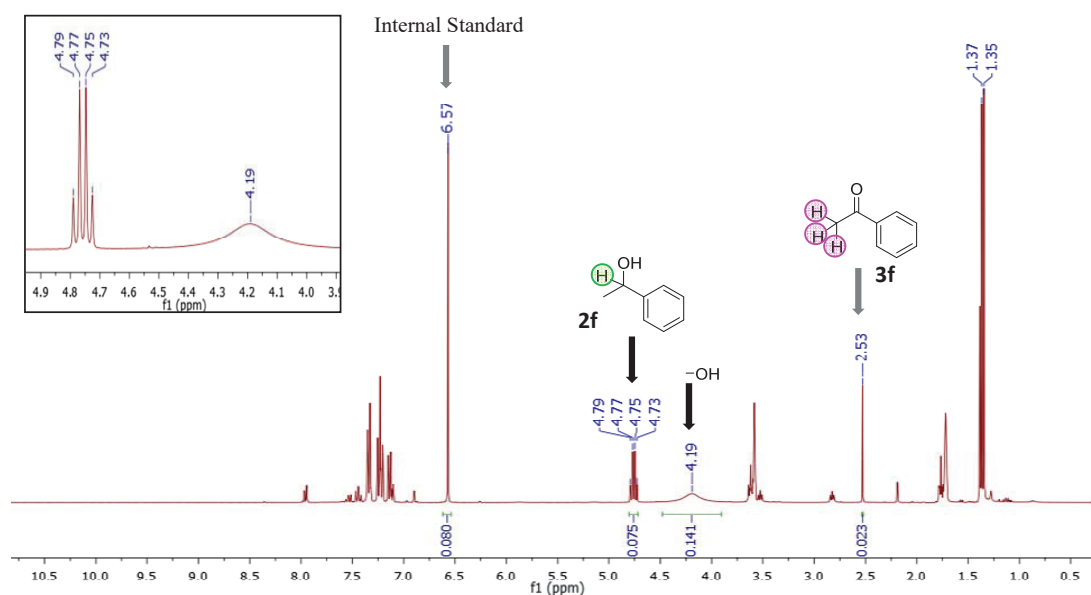


Figure S132. Transfer hydrogenation reaction on acetophenone (2f) using Ar-BN-C4O.  $^1\text{H}$  NMR monitoring.

### III.3.b. $^{11}\text{B}$ NMR monitoring

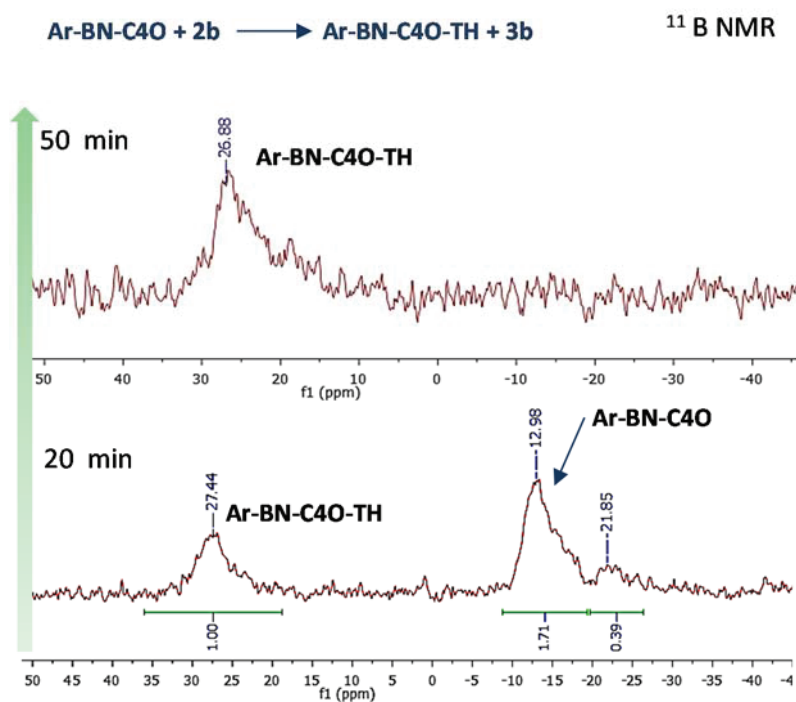


Figure S133.  $^{11}\text{B}$  NMR monitoring of polymer Ar-BN-C4O.

## IV. Polyboramines: Thermal dehydrogenation studies

*Note: A measurement uncertainty of  $\pm 5$  °C has to be taken into account between different type of experiments, due to both internal apparatus precision and possible differences in the detection system (e.g. location of the thermocouple).*

### IV.1. DSC (differential scanning calorimetry)

#### IV.1.a. Polymers

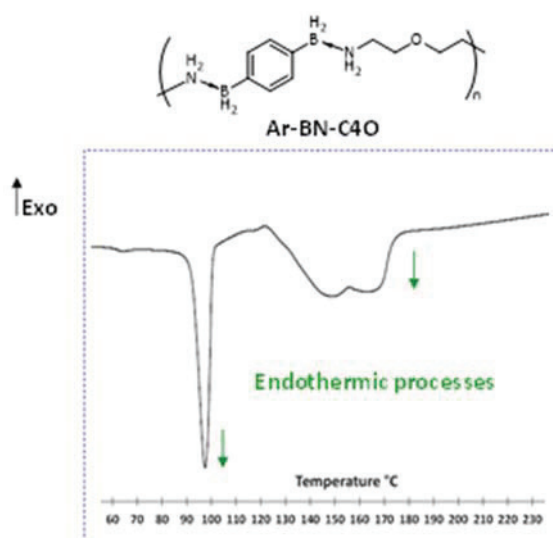


Figure S134. . DSC of polymer Ar-BN-C4o. 30 °C to 250 °C, 5 K.min<sup>-1</sup>. Endothermic peak during the dehydrogenation

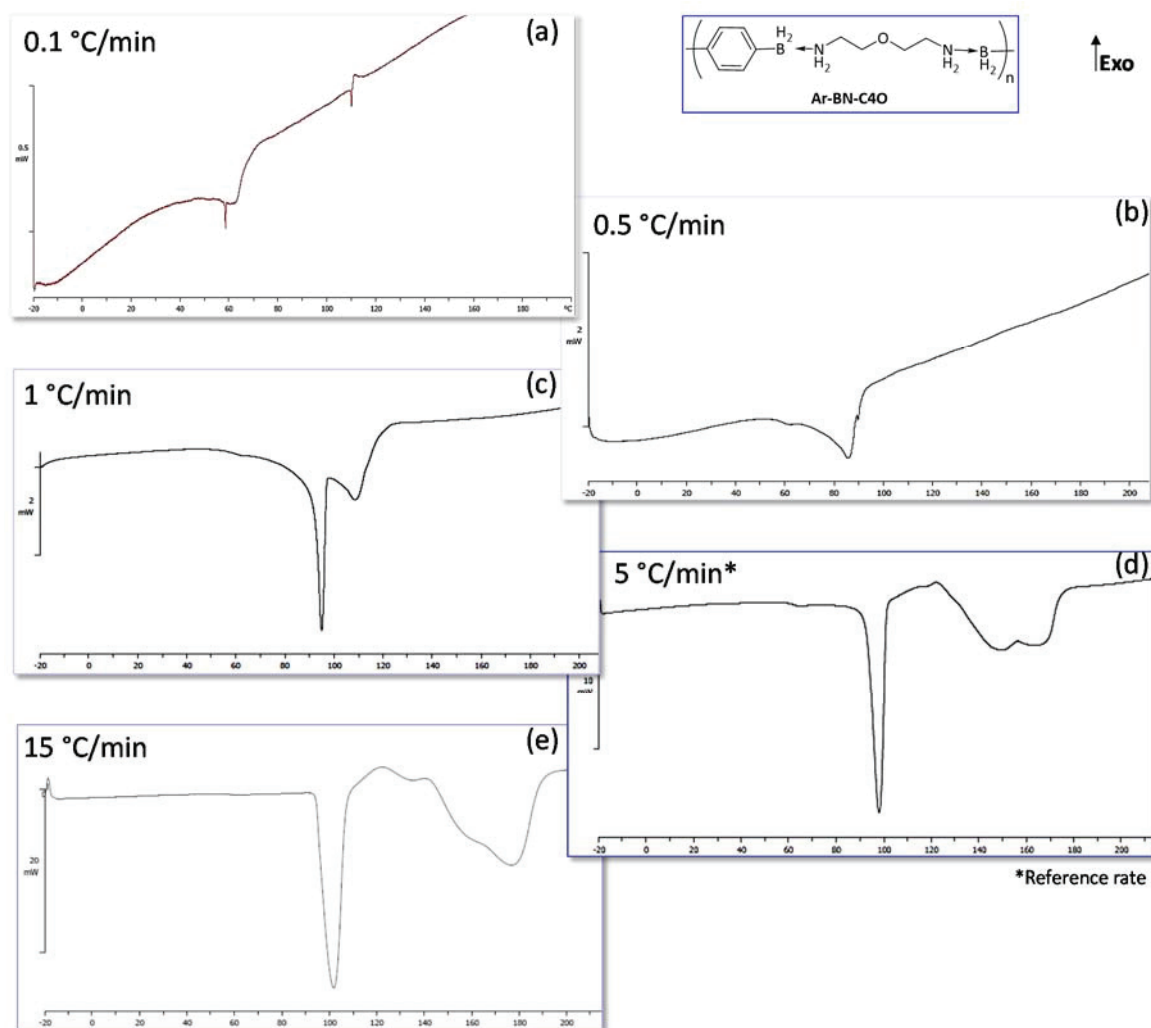


Figure S135. Dehydrogenation of Ar-BN-C4O at different temperature rates. (a) 0.1 °C/min, (b) 0.5 °C/min, (c) 1 °C/min, (d) 5 °C/min, (e) 15 °C/min. Reference conditions: 5 °C/min.

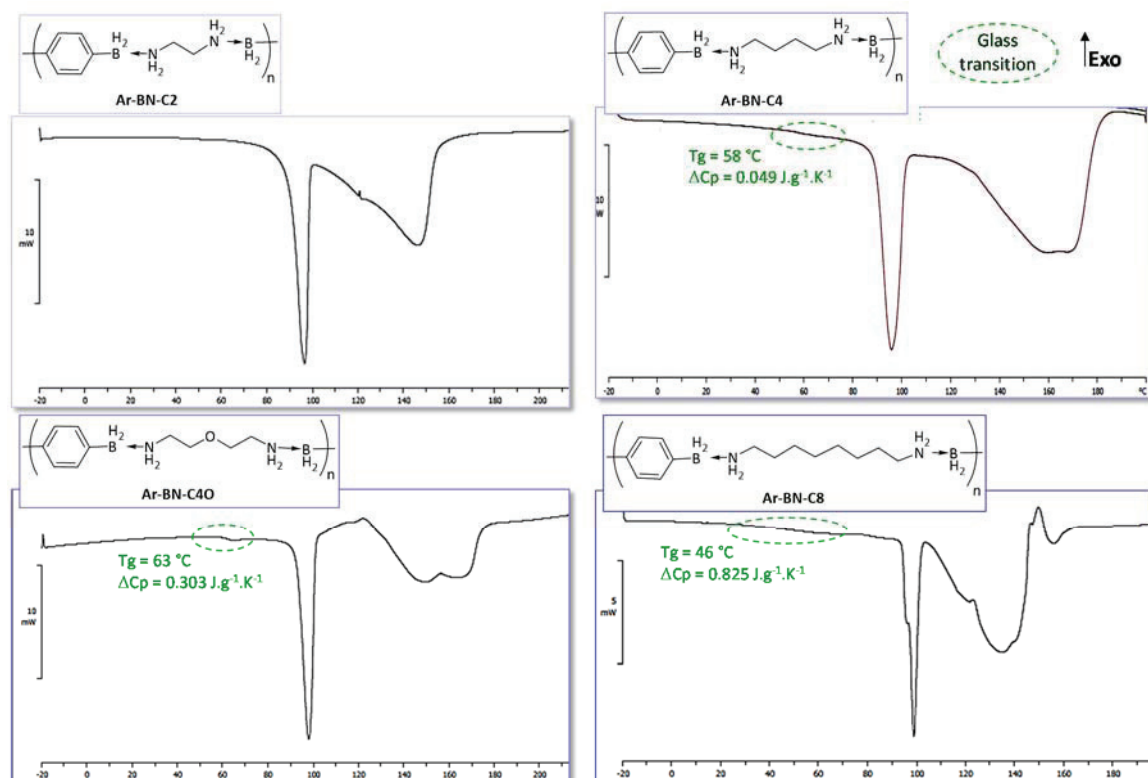


Figure S136. DSC profiles of polyboramines containing variable aliphatic chains, at a temperature rate of 5 °C/min.

#### IV.1.b.Molecular brick:

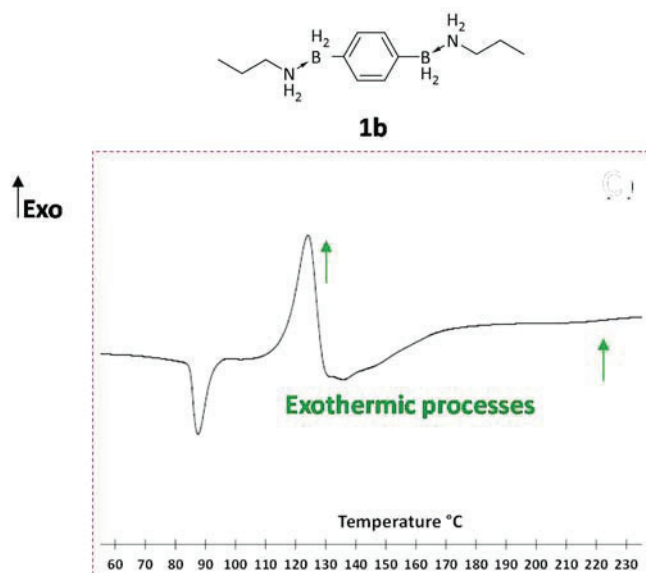


Figure S137. Identification of dehydrogenation peaks





#### IV.1.c. Oligomer:



#### IV.2. TPD ( $H_2$ temperature-programmed desorption)

#### IV.2.a.Polymer (Ar-BN-C4O)

Sample weight : 0.0230 g  
MFC total flow rate : 30 SCCM  
CF(count/nmol) : -749,000,742

Integration of H<sub>2</sub>

No.	Start time (sec)	End time (sec)	Time width (sec)	Peak position (sec)	Area (count)	nmol	nmol/g	log(W/F)+3
1	1440	2761	1322	1848	-1.575E+8	0.210	7.509	-4.472

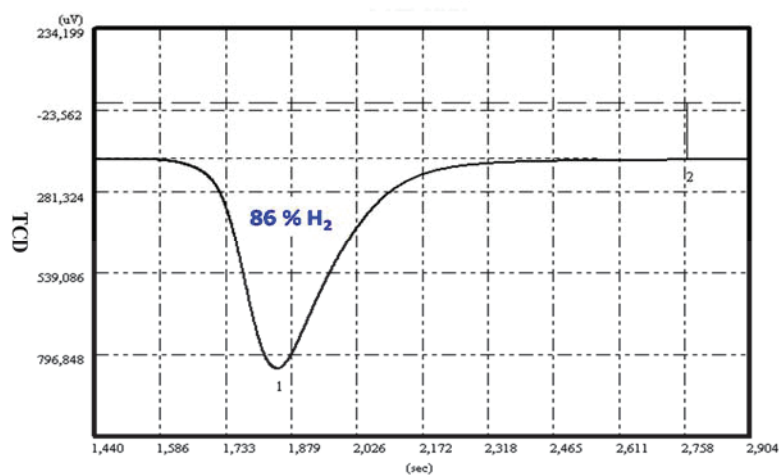


Figure S140. TPD Ar-BN-C4O. Temperature program: 30 °C to 160 °C, 15 °C/min then 160 °C, 1 h.

#### Integration:

Ideal molecular weight for one unit (n):  $MW_{th} = 206 \text{ g/mol-unit (n)}$

Real molecular after NMR quantification (considering THF coordinated):  $MW_{exp} = 460 \text{ g/mol}$

Amount of unit (n):  $n(\text{Ar-BN-C4O}) = 28.0/460 = 0.061 \text{ mmol}$

Theoretical amount of  $H_2$ :  $n(H_2)_{th} = 4 \cdot n(\text{Ar-BN-C4O}) \Leftrightarrow 4 \cdot 0.061 = 0.243 \text{ mmol } H_2$

Quantification of hydrogen released (TPD):  $n(H_2)_{exp} = 0.210 \text{ mmol } H_2 / 28.0 \text{ mg material}$

%  $H_2$ :  $n(H_2)_{exp}/n(H_2)_{th} = 0.210/0.243 \Leftrightarrow \% H_2 = 86 \%$

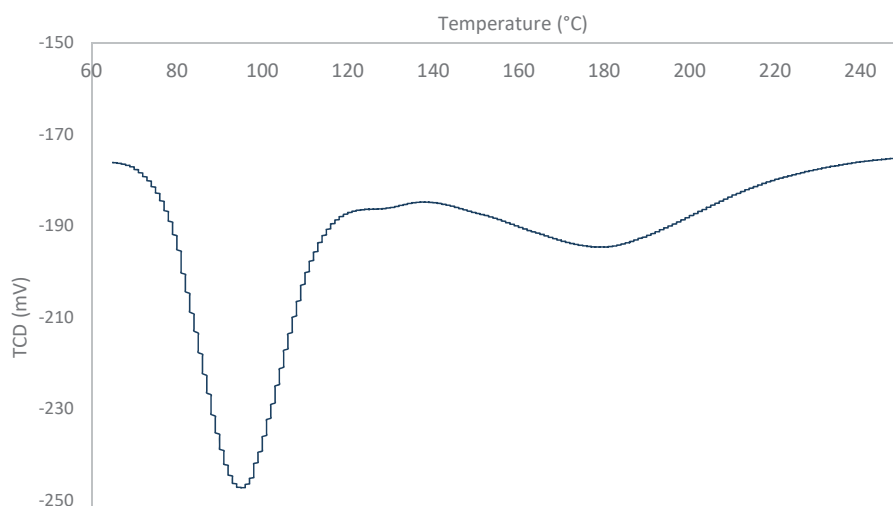


Figure S141. TPD Ar-BN-C4O. Temperature program: 30 °C to 250 °C, 5 °C/min.

## IV.2.b.Molecular brick (1b)

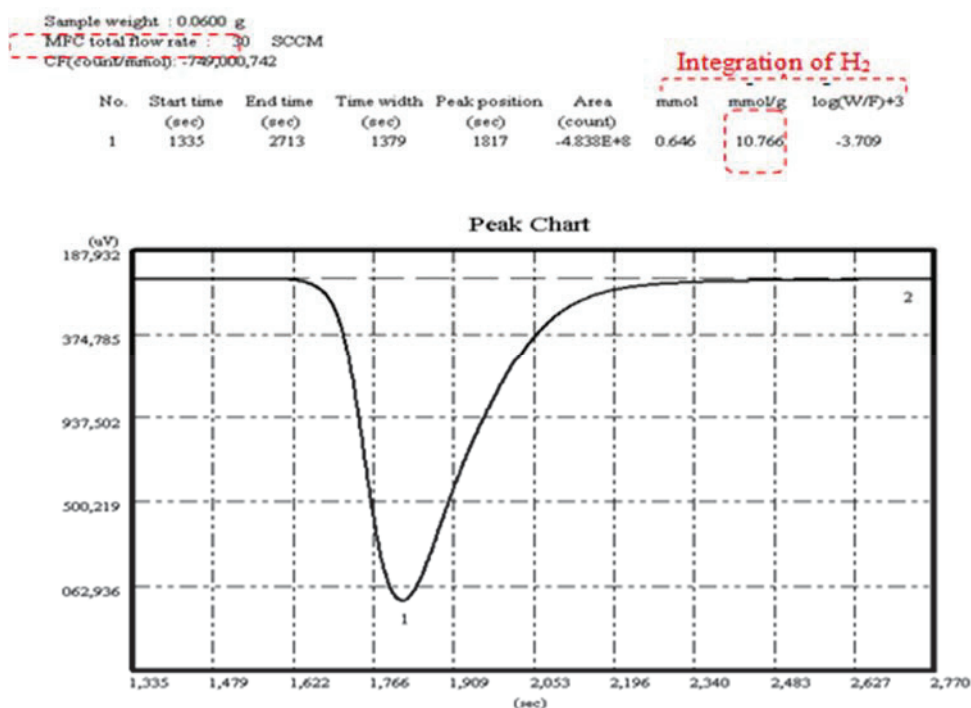


Figure S142. TPD 1b. Temperature program: 30 °C to 160 °C, 15 °C/min then 160 °C, 1 h.

### Integration:

Ideal molecular weight for one unit (n):  $MW_{th} = 220 \text{ g/mol}$

Real molecular after NMR quantification (considering THF coordinated):

$MW_{exp} = 360 \text{ g/mol}$

$n(\mathbf{2b}) = 60/360 = 0.167 \text{ mmol}$

Theoretical amount of H<sub>2</sub>:  $n(\text{H}_2)_{th} = 4 \cdot n(\mathbf{2b}) \Leftrightarrow 4 \cdot 0.167 = 0.667 \text{ mmol H}_2$

Quantification of hydrogen released (TPD):  $n(\text{H}_2)_{exp} = 0.646 \text{ mmol H}_2 / 60 \text{ mg material}$

$\% \text{ H}_2 = n(\text{H}_2)_{exp} / n(\text{H}_2)_{th} = 0.646/0.667 \Leftrightarrow \% \text{ H}_2 = 97 \%$ .

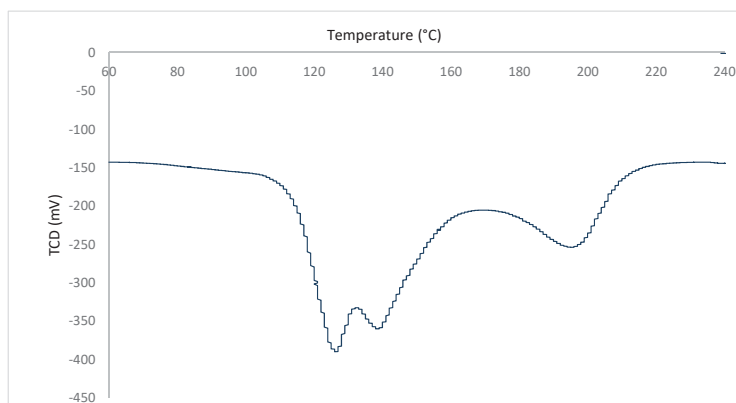


Figure S143. TPD of 1b. Temperature program: 30 °C to 250 °C, 5 °C/min.

### IV.2.c. Oligomer (Ar-BN-C4O-olig)

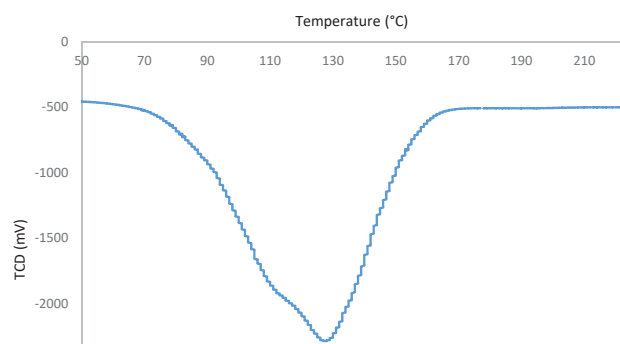
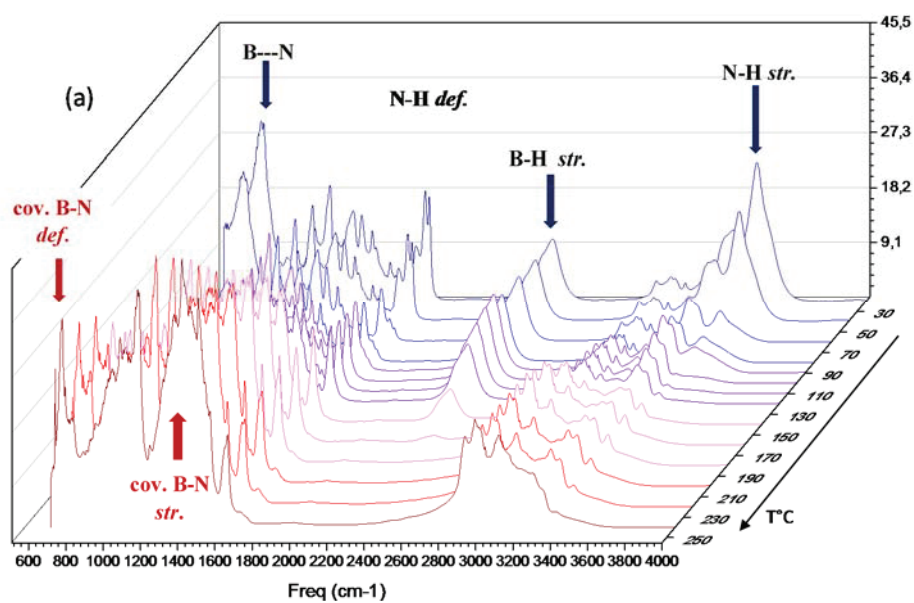


Figure S144. TPD of Ar-BN-C4O-olig. Temperature program: 30 °C to 250 °C, 5 °C/min.

## IV.3. IR-in situ

### IV.3.a. Polymer



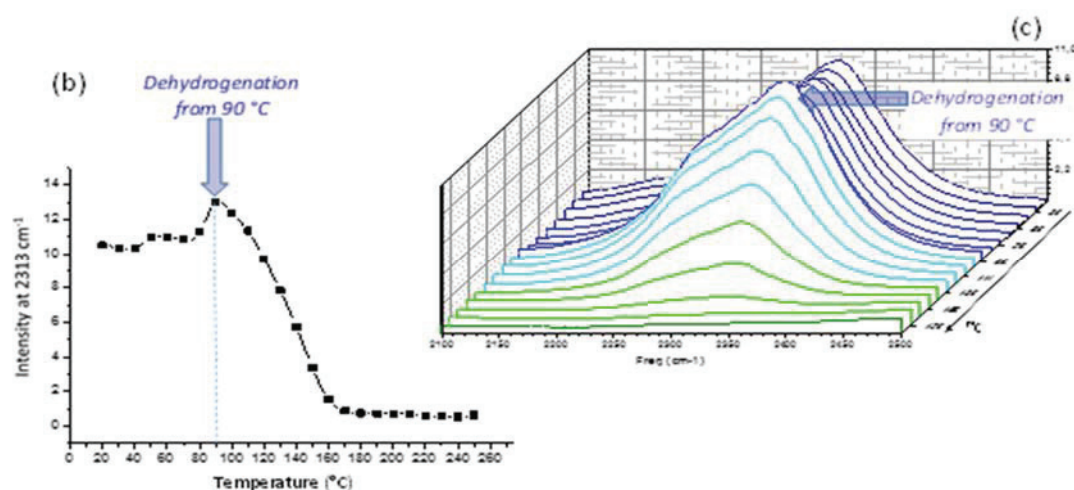


Figure S145. Dehydrogenation process of polyboramine Ar-BN-C4O followed by in situ IR spectroscopy. Complete disappearance of B-H stretches ( $\nu = 2200 - 2400 \text{ cm}^{-1}$ ).

### IV.3.b.Oligomer

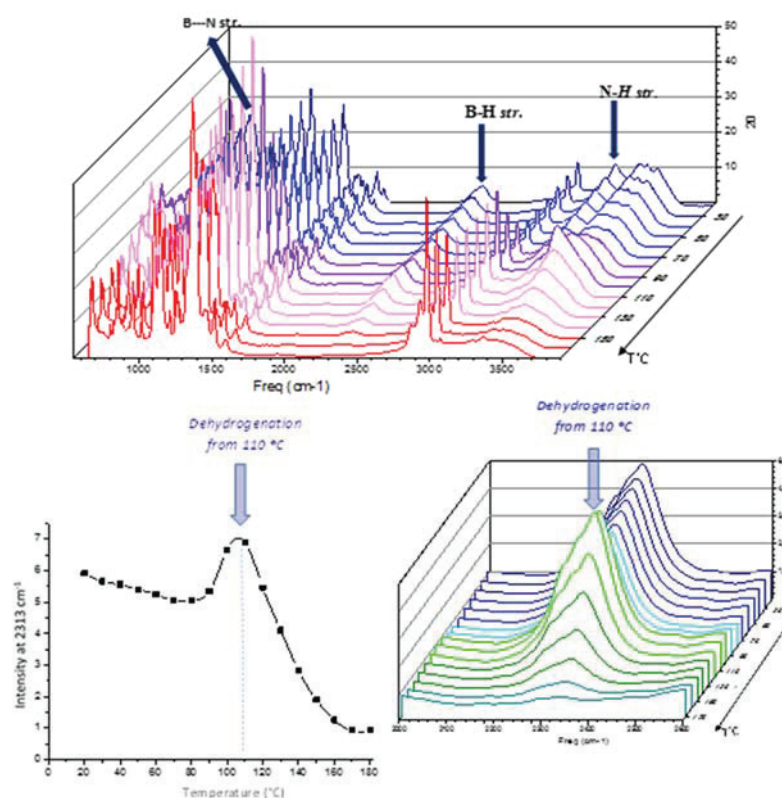


Figure S146. . Thermal dehydrogenation of Ar-BN-C4O-olig. IR-In situ monitoring.

## IV.4. TGA (thermal gravimetric analysis)

### IV.4.a.Hydrogen quantification.

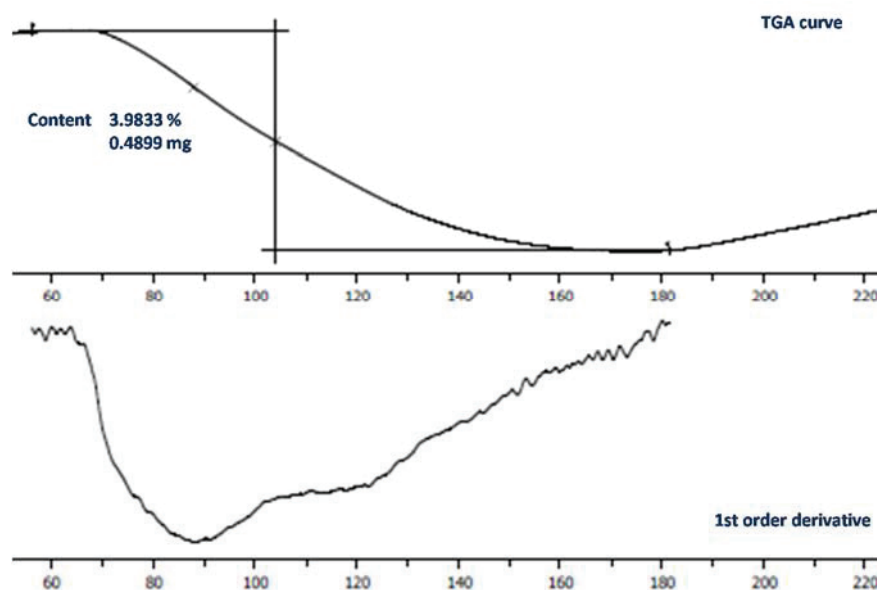


Figure S147. Thermal dehydrogenation of Ar-BN-C4O. Temperature program: 5 °C/min. Quantification of hydrogen released.

#### IV.4.b. Calcination

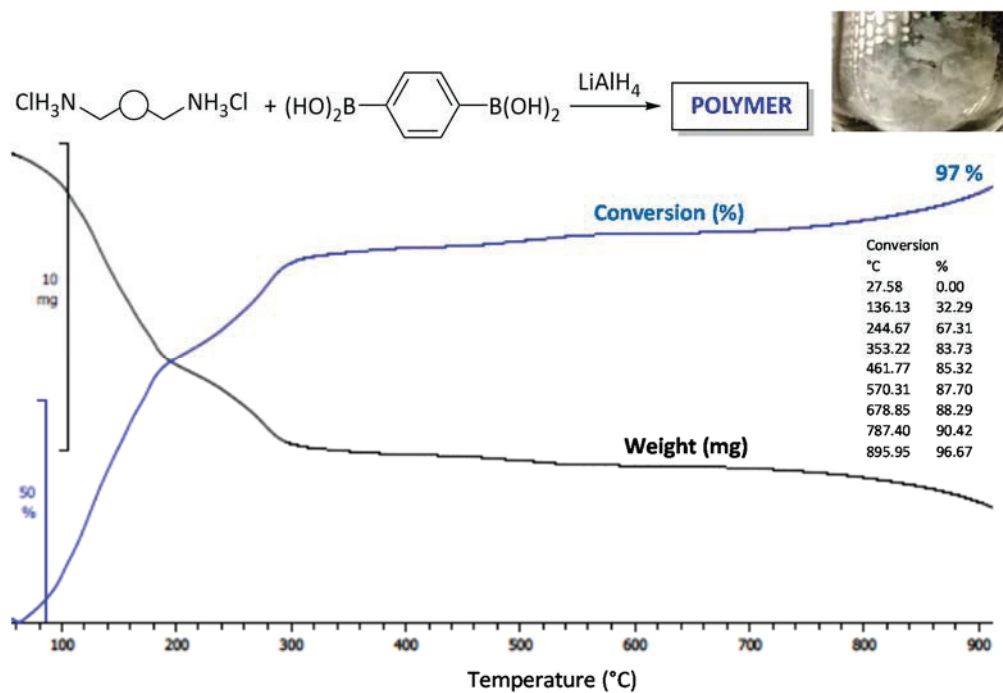


Figure S148. Gravimetric determination of residual salts present in Ar-BN-C4O polymer synthesized from boronic acid precursor.

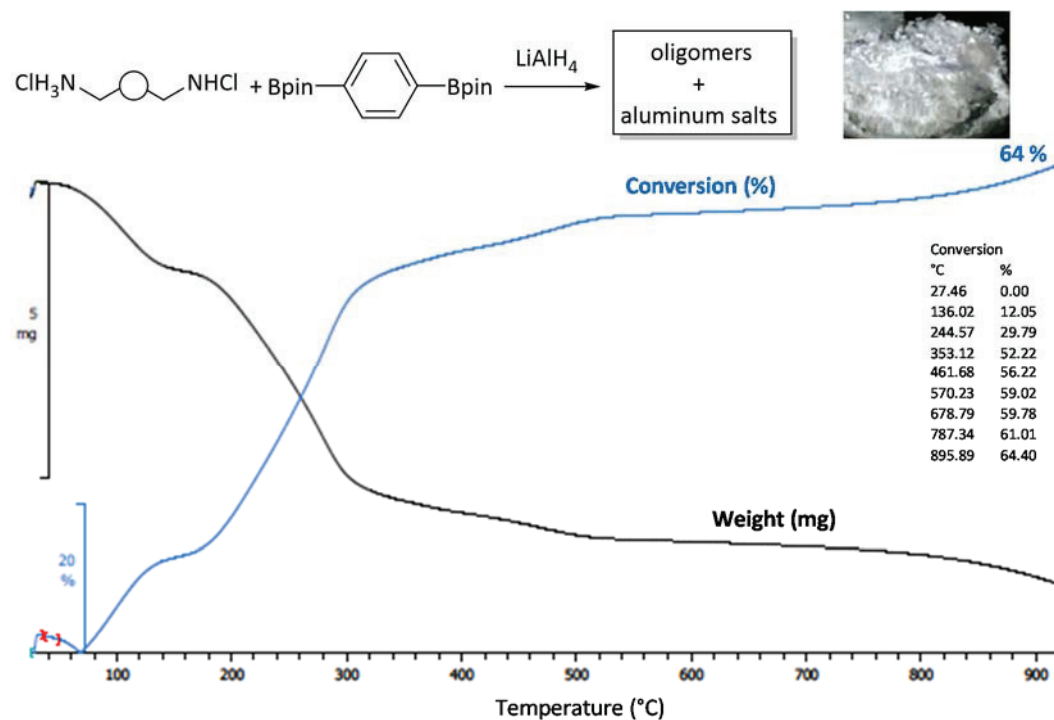


Figure 149. Gravimetric determination of residual salts present in oligomers of Ar-BN-C4O-olig synthesized from pinacol boronate precursor.

## IV.5. $^{11}\text{B}$ MAS-NMR of dehydrogenated materials

Due to the quadrupolar nature of the boron nucleus, chemical shifts are not to be taken in account with accuracy. Nevertheless, a comparative approach is possible.

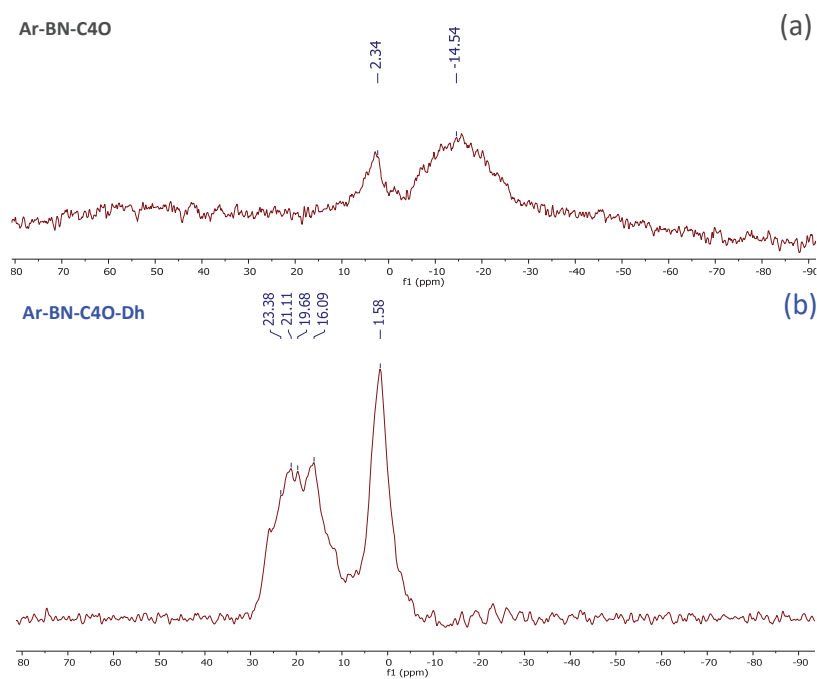


Figure S150.  $^{11}\text{B}$  MAS NMR spectra monitoring of thermally dehydrogenated. Starting material Ar-BN-C4O (a) and dehydrogenated material Ar-BN-C4O-Dh (b). Temperature program: 120 °C, 1h.

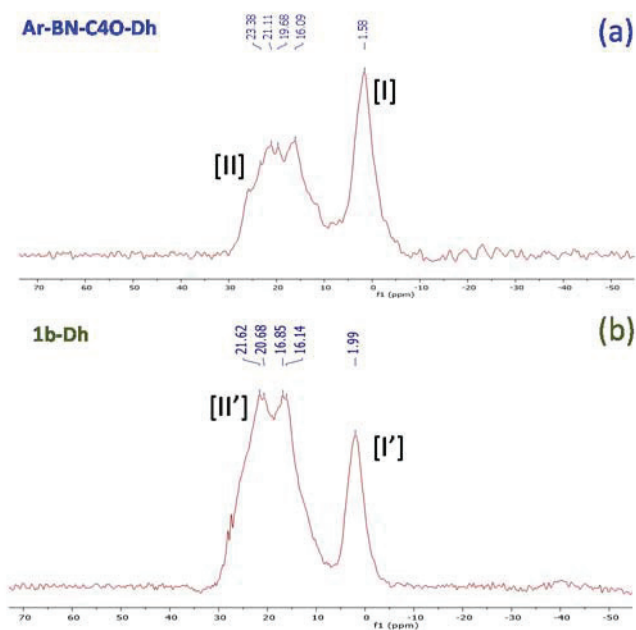


Figure S151.  $^{11}\text{B}$  MAS NMR spectra of thermally dehydrogenated Ar-BN-C4O and 1b to give (a) Ar-BN-C4O-Dh and (b) 1b-Dh. Temperature program: 120 °C, 1h.

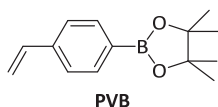


## V. Functional polystyrenes: synthesis and characterization

### V.1. Synthesis of precursors: experimental procedures and characterizations

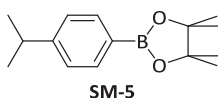
#### V.1.a. Procedure 9: esterification of boronic acids with pinacol

Representative procedure for the synthesis of pinacol 4-vinylphenylboronate **VBP**: 4-vinylphenylboronic acid (10.0 g, 67.6 mmol) and pinacol (8.03 g, 68.0 mmol) as well as 0.05 mL distilled water were stirred in THF (100 mL) at room temperature for 30 min. Then four spatula tips of magnesium sulphate were added to the solution and stirred at room temperature for 2 h. The mixture was filtered and volatiles were removed to yield the pure product in quantitative yield.



**Pinacol 4-vinylphenylboronate (VBP)**: has been synthesized according to procedure 9, from 4-vinylphenylboronic acid (10.0 g, 67.6 mmol) and pinacol (8.03 g, 68.0 mmol) to yield a clear yellow oil. Yield: 14.7 g, 95 %.

NMR Spectroscopy:  $^{11}\text{B}$  NMR. (96 MHz,  $\text{THF-}d_8$ , 25 °C,  $\delta$ ): 26.3 ( $h_{1/2}$  = 230 Hz).  $^1\text{H}$  NMR. (300 MHz,  $\text{THF-}d_8$ , 25 °C,  $\delta$ ): 7.68 (d,  $J$  = 15.6 Hz, 2H, CH-aromatic), 7.30 (d,  $J$  = 8.0 Hz, 2H, CH-aromatic), 6.61 (dd,  $J$  = 17.6, 10.9 Hz, 1H,  $\text{CH}=\text{CH}_2$ ), 5.73 (d,  $J$  = 17.5, 1H,  $\text{CH}_2=\text{CH}$ ), 5.18 (d,  $J$  = 10.8 Hz, 1H), 1.23 (s, 12H,  $\text{CH}_3$ ),  $^{13}\text{C}$  NMR. (400 MHz,  $\text{THF-}d_8$ , 25 °C,  $\delta$ ): 140.3, 136.9, 135.1, 125.6, 114.9, 83.8, 24.9. GC-MS:  $m/z$  = 230.15 ( $\text{M}^+$ )



**Pinacol 4-isopropylphenylboronate (SM-5)**: has been synthesized according to procedure 9 from isopropylphenylboronic acid (328 mg, 2 mmol) and pinacol (238 mg, 2.02 mmol) to yield a white solid. Yield: 400 mg, 80 %.

NMR Spectroscopy:  $^{11}\text{B}$  NMR. (96 MHz,  $\text{THF-}d_8$ , 25 °C,  $\delta$ ): 30.9 ( $h_{1/2}$  = 382 Hz).  $^1\text{H}$  NMR. (300 MHz,  $\text{THF-}d_8$ , 25 °C,  $\delta$ ): 7.64 (d,  $J$  = 8.0 Hz, 2H, CH-aromatic), 7.17 (d,  $J$  = 7.9 Hz, 2H, CH-aromatic), 2.97 (sept,  $J$  = 7.0 Hz, 1H,  $\text{CH-CH}_3$ ), 1.29 (s, 12H, C- $\text{CH}_3$ ), 1.22 (d,  $J$  = 6.9 Hz, 6H),  $^{13}\text{C}$  NMR. (400 MHz,  $\text{THF-}d_8$ , 25 °C,  $\delta$ ): 147.3, 130.8, 135.1, 121.2, 78.5, 29.7, 20.0, 19.0. GC-MS:  $m/z$  = 246.18 ( $\text{M}^+$ )

#### V.1.b. Procedure 10: Gabriel reaction on 4-vinylbenzene moieties<sup>xi</sup>

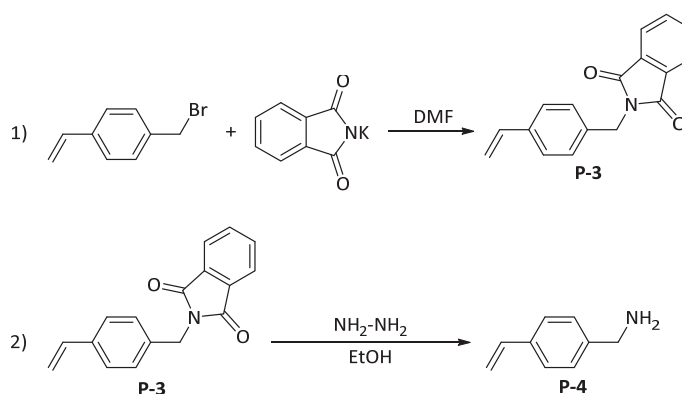
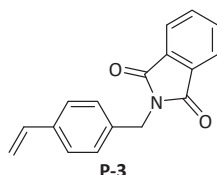


Figure S152. Gabriel reaction.

**Procedure 10 – step 1:** 4-vinylbenzyl chloride (14.13 mL, 100 mmol) and potassium phthalimide (18.5 g, 100 mmol) were added into DMF (50 mL) to give an orange suspension. The reaction mixture was stirred for 17 h at room temperature. The solution was added to 1.7 M NaOH (1 L) and the formed product was collected *via* filtration under vacuum, dissolved in EtOAc (100 mL) to give a cloudy white suspension. The solvent was removed under reduced pressure and the product was recrystallized in cold MeOH. **P-3** was isolated as a white solid.

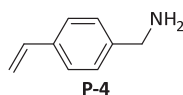


**4-vinylbenzylphthalimide (P-3):** has been synthesized following procedure 9 – step 1. Yield: 27.10 g, > 99 %.

<sup>xi</sup> Thielbeer, F.; Chankeshwara, S. V.; Bradley, M., *Biomacromolecules* **2011**, 12, 4386-4391.

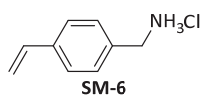
NMR Spectroscopy:  $^1\text{H}$  NMR. (300 MHz,  $\text{THF-d}_8$ , 25 °C,  $\delta$ ): 7.83 (m, 4 H), 7.38 (m, 4 H), 6.67 (dd,  $J = 17.2$  Hz,  $J = 10.5$  Hz, 1 H), 5.74 (d,  $J = 17.2$ , 1 H), 5.24 (d,  $J = 10.5$ , 1H), 4.83 (s, 2 H). GC-MS:  $m/z = 263.09$  ( $\text{M}^+$ ). In accordance with literature data.<sup>xi</sup>

**Procedure 10 – step 2:** 4-vinylbenzylphthalimide (**P-3**) (520 mg, 2.1 mmol) was dissolved in nitrogen-flushed ethanol (7 mL) and heated under reflux until dissolution of the starting material. Hydrazine hydrate (236 mg, 4 mmol) was added and the reaction mixture was stirred for 3 h. The solution was filtered and washed twice with EtOH (10 mL). The filtrate was concentrated under vacuum to give a white solid, which was treated with 1.5M KOH (200 mL) and extracted with  $\text{Et}_2\text{O}$ . The combined organic phases were washed with 2 %  $\text{K}_2\text{CO}_3$  (50 mL), dried over  $\text{MgSO}_4$ , and concentrated under reduced pressure to give the product as a white solid.



**4-vinylbenzylamine (P-4):** has been synthesized following procedure 9 – step 2. Yield: 173 mg, 64 %.

NMR Spectroscopy:  $^1\text{H}$  NMR. (300 MHz,  $\text{THF-d}_8$ , 25 °C,  $\delta$ ): 7.32 (m, 4H), 6.71 (dd, 4H,  $J = 17.6$  Hz,  $J = 11.0$  Hz), 5.73 (d, 1H,  $J = 17.6$  Hz) 5.22 (d, 1H,  $J = 11.0$ ), 3.76 (s, 2H). GC-MS:  $m/z = 133.09$  ( $\text{M}^+$ ). In accordance with literature data.<sup>xi</sup>



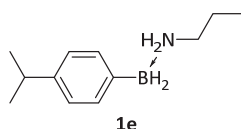
**4-vinylbenzylamine hydrochloride (SM-6):** has been synthesized according to procedure 1, from **P-4** (580 mg, 439 mmol) and HCl 6 M in *i*PrOH (1.2 mL, 7.4 mmol) at 0 °C. Yield: 452 mg, 70 %.

NMR Spectroscopy:  $^1\text{H}$  NMR. (300 MHz,  $\text{THF-d}_8$ , 25 °C,  $\delta$ ): 7.44 (m, 4H), 6.74 (dd, 4H,  $J = 17.7$  Hz,  $J = 11.0$  Hz), 5.80 (d, 1H,  $J = 17.7$  Hz) 5.27 (d, 1H,  $J = 11.0$ ), 4.10 (s, 2H). In accordance with literature data.<sup>xi</sup>

## V.2. Synthesis of molecular bricks: characterizations

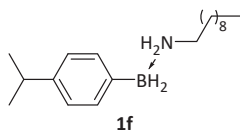
### Procedure 11: synthesis of amine-(aryl)boranes.

Representative procedure for the synthesis of 4-isopropylphenylborane-decylamine (**1f**): To a stoichiometric mixture of **SM-5** (300 mg, 1.32 mmol) and *n*-decylammonium chloride (294 mg, 1.32 mmol) in THF/Toluene 1:4 (15 mL), were added dropwise  $\text{LiAlH}_4$  (42 mg, 1.056 mmol) in THF (3 mL). The reaction mixture was kept vigorously stirring for 2h. The resulting mixture was centrifuged (10 min) to recover the supernatant that was further filtered with a 22 $\mu\text{m}$ -PTFE filter. The resulting clear solution was concentrated and dried under vacuum to yield quantitatively a white solid. To remove residual coordinated THF and traces of starting material, the powder can be dissolved in a minimum of THF (3 mL) and filtrated.



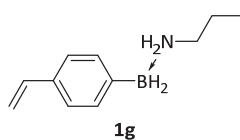
**4-isopropylphenylborane-propylamine (1e)** has been synthesized according to procedure 11 from **SM-5** (100 mg, 0.41 mmol), *n*-propylammonium chloride (39 mg, 0.41 mmol) and  $\text{LiAlH}_4$  (13 mg, 0.33 mmol) to yield a white solid (74mg, 94%). Yield: 164 mg, 86 %.

NMR Spectroscopy:  $^{11}\text{B}$  NMR. (96 MHz,  $\text{THF-d}_8$ , 25 °C,  $\delta$ ): -12.1 ( $h_{1/2}$  = 241 Hz).  $^1\text{H}$  NMR. (300 MHz,  $\text{THF-d}_8$ , 25 °C,  $\delta$ ): 7.22 (d,  $J$  = 8.0 Hz, 2H, CH-aromatic), 6.93 (d,  $J$  = 7.8 Hz, 2H, C-H aromatic), 4.74 (s, br, 2H, NH), 2.75 (m, 1H,  $\text{CH}-(\text{CH}_3)_2$ ,  $J$  = 6.9 Hz), 2.60 (m, 2H,  $-\text{CH}_2-\text{NH}_2$ ), 2.96 – 1.81 (m, br, 2H, BH), 1.58 (m, 2H,  $\text{CH}_2-\text{CH}_2-\text{NH}_2$ ), 1.19 (d, 6H,  $\text{CH}-(\text{CH}_3)_2$ ,  $J$  = 6.9 Hz), 0.87 (t, 3H,  $\text{CH}_2-\text{CH}_3$ ,  $J$  = 7.5 Hz).  $^{13}\text{C}$  NMR. (75 MHz,  $\text{THF-d}_8$ , 25 °C,  $\delta$ ): 141.9, 132.5, 122.4, 46.0, 32.0, 22.0, 20.4, 8.9.



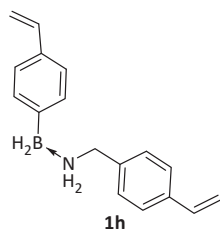
**4-isopropylphenylborane-decylamine (1f)** has been synthesized following procedure 11 from **SM-5** (300 mg, 1.32 mmol) and *n*-decylammonium chloride (294 mg, 1.32 mmol) and LiAlH<sub>4</sub> (42 mg, 1.056 mmol) to yield a white solid. Yield: 374 mg, 98 %.

NMR Spectroscopy: <sup>11</sup>B NMR. (96 MHz, THF-*d*<sub>8</sub>, 25 °C,  $\delta$ ): -12.1 ( $h_{1/2}$  = 241 Hz). <sup>1</sup>H NMR. (300 MHz, THF-*d*<sub>8</sub>, 25 °C,  $\delta$ ): 7.21 (d,  $J$  = 7.9 Hz, 2H, CH-aromatic), 6.93 (d,  $J$  = 7.8 Hz, 2H, C-H aromatic), 4.67 (s, br, 2H, NH), 2.75 (m, 1H, CH-(CH<sub>3</sub>)<sub>2</sub>), 2.63 (m, 2H, -CH<sub>2</sub>-H<sub>2</sub>N), 2.96 – 1.93 (m, br, 2H, BH), 1.56 (m, 2H, CH<sub>2</sub>-CH<sub>2</sub>-NH<sub>2</sub>), 1.29 (s, 14H, CH<sub>2</sub>), 1.18 (d, 6H, 18.3, CH<sub>3</sub>-CH), 0.96 – 0.80 (m, 3H, CH<sub>2</sub>-CH<sub>3</sub>). <sup>13</sup>C NMR. (75 MHz, THF-*d*<sub>8</sub>, 25 °C,  $\delta$ ): 143.9, 134.8, 134.3, 125.4, 124.3, 46.1, 34.3, 33.9, 31.9, 29.6, 29.5, 29.3, 29.2, 26.8, 24.9, 23.8, 23.2, 22.6. ATR-IR:  $\nu$  = 3281 cm<sup>-1</sup> (N-H), 2327 cm<sup>-1</sup> (B-H), 720 cm<sup>-1</sup> (B---N).



**4-vinylphenylborane-propylamine (1g)** has been synthesized according to procedure 8 from 4-vinylphenylboronic acid (1.48 g, 10 mmol) and *n*-propylammonium chloride (960 mg, 10 mmol), and LiAlH<sub>4</sub> (275 mg, 7.5 mmol) at 0°C, to give a white powder. Yield: 1.29 g, 98 %.

NMR Spectroscopy: <sup>11</sup>B NMR. (96 MHz, THF-*d*<sub>8</sub>, 25 °C,  $\delta$ ): -10.5 (t,  $J$  = 100 Hz). <sup>1</sup>H NMR. (300 MHz, THF-*d*<sub>8</sub>, 25 °C,  $\delta$ ): 7.93-7.12 (m, 4H, CH-aromatic), 6.77-6.56 (m, 1H, CH=CH<sub>2</sub>), 5.81-5.56 (m, 1H, CH=CH<sub>2</sub>), 5.21-4.95 (m, 1H, CH=CH<sub>2</sub>), 4.81 (s, br, NH), 2.64-2.55 (m, 2H, -CH<sub>2</sub>-NH<sub>2</sub>), 2.38 (s, br, BH), 1.69-1.54 (m, 2H, CH<sub>2</sub>-CH<sub>2</sub>-NH<sub>2</sub>), 0.81-0.93 (m, 3H, CH<sub>2</sub>-CH<sub>3</sub>). <sup>13</sup>C NMR. (75 MHz, THF-*d*<sub>8</sub>, 25 °C,  $\delta$ ): 138.2, 137.6, 134.2, 133.7, 124.9, 124.6, 124.4, 109.4, 47.8, 24.2, 10.6.



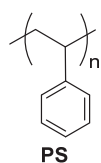
**4-vinylphenylborane-(4-vinylbenzyl)amine (1h)** has been synthesized according to procedure 8 from 4-vinylphenylboronic acid (148 mg, 1 mmol) **SM-6** (170 mg, 1 mmol) and LiAlH<sub>4</sub> (28.5 mg, 0.75 mmol) at 0°C, to give a white powder. Yield: 200 mg, 80 %.

NMR Spectroscopy: <sup>11</sup>B NMR. (96 MHz, THF-*d*<sub>8</sub>, 25 °C, δ): -9.8 (s, *h*<sub>1/2</sub> = 200 Hz). <sup>1</sup>H NMR. (300 MHz, THF-*d*<sub>8</sub>, 25 °C, δ): 7.93-7.12 (m, 8H, CH-aromatic), 6.74-6.54 (m, 2H, CH=CH<sub>2</sub>), 6.74-6.54 (m, 2H, CH=CH<sub>2</sub>), 5.17-4.97 (m, 2H, CH=CH<sub>2</sub>), 5.28 (s, br, NH), 3.74-3.70 (m, 2H, -CH<sub>2</sub>-NH<sub>2</sub>), 3.21-2.52 (s, br, BH). <sup>13</sup>C NMR. (75 MHz, THF-*d*<sub>8</sub>, 25 °C, δ): 138.4, 138.2, 137.5, 137.3, 137.2, 136.6, 136.4, 134.3, 133.8, 133.5, 128.5, 126.2, 124.9, 124.5, 113.1, 109.5, 49.7.

### V.3. Free radical polymerization: Synthesis PS-BPin-x%. Experimental procedures and characterizations.

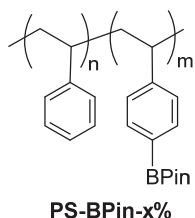
#### Procedure D: Free radical copolymerization of styrene and PVB

Representative procedure for the synthesis of **PS-BPin-10%**: styrene (1 mL, 9 mmol), **PVB** (246 mg, 1 mmol) were dissolved in THF (3 mL), and the mixture was degassed by three freeze-pump-thaw cycles. After addition of benzoyl peroxide (40 mg, 1.6 %), the system was closed and the reaction mixture was then heated to 60°C for 12 h. After <sup>1</sup>H NMR control of the conversion the mixture was precipitated into pentane (200 mL). The white solide was recovered by centrifugation, washed twice with pentane and dried overnight under vacuum (1 g, 85 % yield).



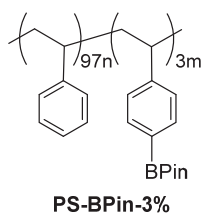
**Polystyrene (PS)** has been synthesized according to procedure D from styrene (1.1 g, 10.6 mmol). White powder. Yield: 860 mg, 78 %.

$^1\text{H}$  NMR. (400 MHz, toluene- $d_8$ , 25°C,  $\delta$ ): 7.06-6.96 (3H, CH-aromatic), 6.73-6.47 (2H, CH-Ph), 2.08 (1H,  $\underline{\text{CH}}\text{-CH}_2$ ), 1.62 ( $\underline{\text{CH}}_2\text{-CH}$ ).  $^{13}\text{C}$  NMR (100 MHz, toluene- $d_8$ , 25°C,  $\delta$ ): 145.3 (C-Ph), 128.1, 128.0, 125.7 (CH-Ph), 44.2-42.6 ( $\underline{\text{CH}}\text{-CH}_2$ ), 40.7 ( $\underline{\text{CH}}_2\text{-CH}$ ). DSC:  $T_g = 105^\circ\text{C}$ . TGA:  $T_{\text{dec}} = 900^\circ\text{C}$ , 100 wt% loss.

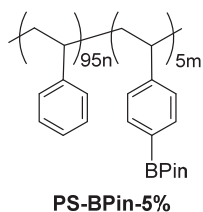


**[poly(styrene-*ran*-PVB)] ; [x PVB%] (PS-BPin- $x\%$ )**

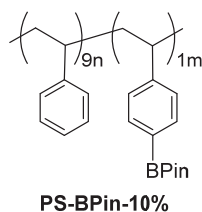
$^{11}\text{B}$  NMR. (128 MHz, toluene- $d_8$ , 25°C,  $\delta$ ): 29.0 ( $h_{1/2} = 1800$  Hz).  $^1\text{H}$  NMR. (400 MHz, toluene- $d_8$ , 25°C,  $\delta$ ): 7.92 (2H, CH-Ar(B)), 7.05 (2H, CH-Ar(B) + 3H, CH-Ph), 6.72 (2H, CH-Ph), 2.03 (1H,  $\underline{\text{CH}}\text{-CH}_2$ ), 1.55 (2H,  $\underline{\text{CH}}_2\text{-CH}$ ).  $^{13}\text{C}$  NMR (100 MHz, toluene- $d_8$ , 25°C,  $\delta$ ): 149.2 (C-Ar(B)), 145.3 (C-Ph), 135.3 (CH-Ar(B)), 128.1 (CH-Ph), 127.9 (CH-Ph), 126.6 (CH-Ar(B)), 125.6 (CH-Ph), 83.1 (C-pinacol), 46.0-42.4 ( $\underline{\text{CH}}\text{-CH}_2$ ), 40.7 ( $\underline{\text{CH}}_2\text{-CH}$ ), 24.7 ( $\underline{\text{CH}}_3\text{-pinacol}$ ). Chemical shifts are identical for all heteropolymers **PS-BPin- $x\%$** . Proton attributions corresponds to isolated units. Integration of chemical shifts is proportional the value of  $x$ . (see NMR spectra).



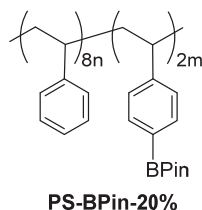
**[poly(styrene-*ran*-PVB)] ; [3 PVB%] (PS-BPin-3%)** has been synthesized according to procedure D from styrene (1 g, 9.7 mmol) and PVB (69 mg, 0.3 mmol). White powder. Yield: 960 mg, 90 %. GPC:  $M_w = 15\,989$  Da,  $\bar{M}_n = 1.81$ .



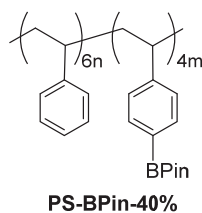
**[poly(styrene-*ran*-PVB)] ; [5 PVB%] (PS-BPin-5%)** has been synthesized according to procedure D from styrene (1.08 mL, 9.5 mmol) and PVB (115 mg, 0.5 mmol). White powder. Yield: 1 g, 92 %.



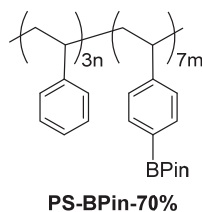
**[poly(styrene-*ran*-PVB)] ; [10 PVB%] (PS-BPin-10%)** has been synthesized according to procedure D from styrene (1.03 mL, 9.0 mmol) and PVB (246 mg, 1.0 mmol). White powder. Yield: 1 g, 85 %.



**[poly(styrene-*ran*-PVB)] ; [20 PVB%] (PS-BPin-20%)** has been synthesized according to procedure D from styrene (0.915 mL, 8.0 mmol) and PVB (492 mg, 2.0 mmol). White powder. Yield: 1.1 g, 83 %. GPC:  $M_w = 25\,145$  Da,  $\bar{M}_n = 2.05$ .

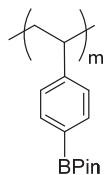


**[poly(styrene-*ran*-PVB)] ; [40 PVB%] (PS-BPin-40%)** has been synthesized according to procedure D from styrene (0.624 mL, 6.0 mmol) and PVB (984 mg, 4.0 mmol). White powder. Yield: 1.23 g, 87 %. GPC:  $M_w = 31\,546$  Da,  $\bar{M}_n = 2.31$ .





**[poly(styrene-*ran*-PVB)] ; [70 PVB%] (PS-BPin-70%)** has been synthesized according to procedure D from styrene (0.340 mL, 3.0 mmol) and PVB (1.61 g, 7.0 mmol). White powder. Yield: 1.77 g, 92 %. GPC:  $M_w = 32\,567$  Da,  $\bar{M}_n = 2.19$ .



**PS-BPin-100%**

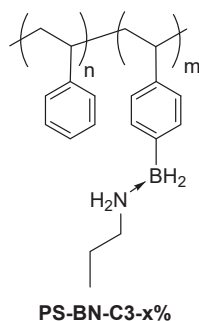
**Poly(PVB) (PS-BPin-100%)** has been synthesized according to procedure D from PVB (2.3 g, 10.0 mmol). White powder. Yield: 2.0 g, 87 %.

$^{11}\text{B}$  NMR. (128 MHz, toluene- $d_8$ , 25°C,  $\delta$ ): 29 ( $h_{1/2} = 1800$  Hz).  $^1\text{H}$  NMR. (400 MHz, toluene- $d_8$ , 25°C,  $\delta$ ): 7.92 (2H, CH-Ar(B)), 7.05 (2H, CH-Ar(B) + 3H, CH-Ph), 6.72 (2H, CH-Ph), 2.03 (1H,  $\text{CH}_2\text{-CH}_2$ ), 1.55 (2H,  $\text{CH}_2\text{-CH}$ ).  $^{13}\text{C}$  NMR (100 MHz, toluene- $d_8$ , 25°C,  $\delta$ ): 149.0 (C-Ar(B)), 135.3 (CH-Ar(B)), 126.5 (CH-Ar(B)), 83.0 (C-pinacol), 46.1 ( $\text{CH}_2\text{-CH}_2$ ), 41.2 ( $\text{CH}_2\text{-CH}$ ), 24.7 ( $\text{CH}_3\text{-pinacol}$ ). GPC:  $M_w = 40\,211$  Da,  $\bar{M}_n = 2.83$ .

#### V.4. Post-functionalization: Synthesis PS-BN-C3-x% and PS-BN-C10-x%. Experimental procedures and characterizations

##### Procedure E: post-functionalization of PS-BPin-x% into PS-BN-C3-x% or PS-BN-C10-x%

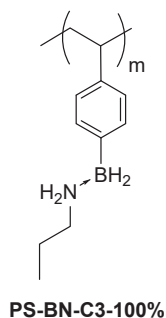
Representative procedure for the synthesis of poly(4-vinylphenyldihydro)borane-(*n*-decyl)amine (**PS-BN-C10-100%**): To a stoichiometric mixture of **PS-BPin-100%** (400 mg, 1.74 mmol) and *n*-decylammonium chloride (386 mg, 1.74 mmol) in THF/Toluene 1:4 (15 mL), were added dropwise  $\text{LiAlH}_4$  (53 mg, 1.40 mmol) in THF (3 mL). The reaction mixture was kept vigorously stirring for 2h. The resulting mixture was centrifuged (10 min) to recover the supernatant that was further washed with a THF/Toluene 1:2 solution. The resulting clear solution was concentrated and dried under vacuum to yield quantitatively a white solid. To remove eventual residual coordinated THF the polymer can be dropped in pentane and dried by centrifugation.



**Poly[styrene-*ran*-(4-vinylphenyldihydro)borane-(*n*-propyl)amine]]; $[x \text{ BN}\%]$  (PS-BN-C3-x%)**

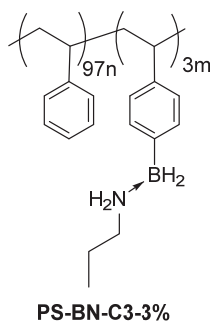
$^{11}\text{B}$  NMR. (128 MHz, toluene- $d_8$ , 25°C,  $\delta$ ): -13.9 ( $h_{1/2} = 395$  Hz).  $^1\text{H}$  NMR. (400 MHz, toluene- $d_8$ , 25°C,  $\delta$ ): 7.39-6.47 (m, br, 4H,  $\text{CH-Ar(B)}$  + 4H,  $\text{CH(Ph)}$ ), 4.59 (s, br, 2H,  $\text{NH}$ ), 2.83-2.59 (m, br, 2H,  $\text{CH}_2\text{-NH}$ ), 2.30 (s, br, BH), 2.0 ( $\text{CH-CH}_2$  styrene) 1.58-1.06 (m, br, 2H,  $\text{CH}_2\text{-CH}$  + 1H,  $\text{CH-CH}_2$  aryl), 1.29 (m, br, 2H,  $\text{CH}_2$ ), 0.89 (s, br, 3H,  $-\text{CH}_2\text{-CH}_3$ ).  $^{13}\text{C}$  NMR (100 MHz, toluene- $d_8$ , 25°C,  $\delta$ ): 148.5, 145.9, 141.3, 134.1, 128.7, 127.9, 126.2, 125.1, 47.9, 40.3, 22.1, 10.9.

Chemical shifts are identical for all heteropolymers **PS-BN-C3-x%**. Proton attributions corresponds to isolated units. Integration of chemical shifts is proportional the value of  $x$ . (see NMR spectra).

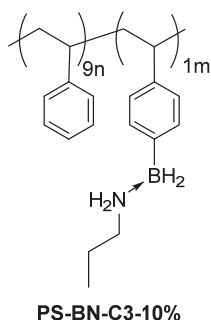


**Poly(4-vinylphenyldihydro)borane-(*n*-propyl)amine (PS-BN-C3-100%)** has been synthesized according to procedure D from **PS-BPin-100%** (100 mg, 0.43 mmol), *n*-propylammonium chloride (42 mg, 1.74 mmol) and  $\text{LiAlH}_4$  (13 mg, 0.35 mmol). White powder. Yield: 11.4 mg, 15 %.

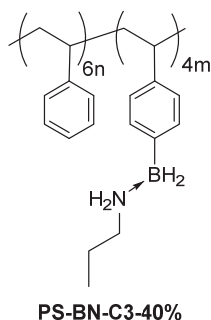
ATR-IR:  $\nu = 3219 \text{ cm}^{-1}$  (N-H),  $2323 \text{ cm}^{-1}$  (B-H),  $712 \text{ cm}^{-1}$  (B---N).



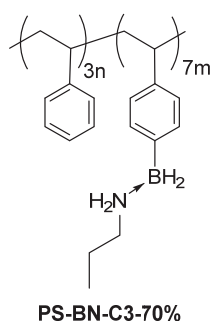
**Poly[styrene-*ran*-(4-vinylphenyldihydro)borane-(*n*-propyl)amine];[3 BN%] (PS-BN-C3-3%)** has been synthesized according to procedure D from **PS-BPin-3%** (500 mg, 0.14 mmol), *n*-propylammonium chloride (13 mg, 0.14 mmol) and  $\text{LiAlH}_4$  (5 mg, 0.12 mmol). White powder. Yield: 482 mg, 98 %.



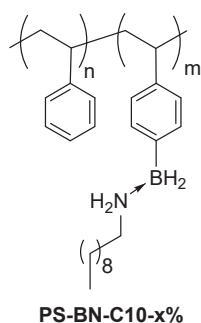
**Poly[styrene-*ran*-(4-vinylphenyldihydro)borane-(*n*-propyl)amine];[10 BN%] (PS-BN-C3-10%)** has been synthesized according to procedure D from **PS-BPin-10%** (500 mg, 0.43 mmol), *n*-propylammonium chloride (41 mg, 0.43 mmol) and  $\text{LiAlH}_4$  (14 mg, 0.34 mmol). White powder. Yield: 460 mg, 97 %.



**Poly[styrene-*ran*-(4-vinylphenyldihydro)borane-(*n*-propyl)amine];[40 BN%] (PS-BN-C3-40%)** has been synthesized according to procedure D from **PS-BPin-40%** (300 mg, 0.78 mmol), *n*-propylammonium chloride (74 mg, 0.78 mmol) and  $\text{LiAlH}_4$  (24 mg, 0.63 mmol). White powder. Yield: 172 mg, 67 %.



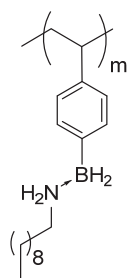
**Poly[styrene-*ran*-(4-vinylphenyldihydro)borane-(*n*-propyl)amine];[70 BN%] (PS-BN-C3-70%)** has been synthesized according to procedure D from **PS-BPin-70%** (300 mg, 1.57 mmol), *n*-propylammonium chloride (150 mg, 1.57 mmol) and  $\text{LiAlH}_4$  (48 mg, 1.26 mmol). White powder. Yield: 67 mg, 28 %.



**Poly[styrene-*ran*-(4-vinylphenyldihydro)borane-(*n*-decyl)amine];[ $x$  BN%] (PS-BN-C10- $x\%$ )**

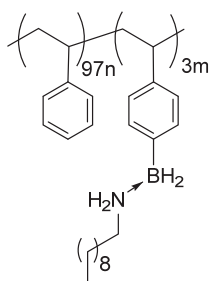
$^{11}\text{B}$  NMR. (128 MHz, toluene- $d_8$ ,  $25^\circ\text{C}$ ,  $\delta$ ): -13.9 ( $h_{1/2} = 395$  Hz).  $^1\text{H}$  NMR. (400 MHz, toluene- $d_8$ ,  $25^\circ\text{C}$ ,  $\delta$ ): 7.43-6.47 (m, br, 4H,  $\text{CH-Ar(B)} + 4\text{H, CH(Ph)}$ ), 4.54 (s, br, 2H,  $\text{NH}$ ), 2.63 (m, br, 2H,  $\text{CH}_2\text{-NH}$ ), 2.30 (s, br, BH), 1.95 ( $\text{CH-CH}_2\text{styrene}$ ) 1.77-1.29 (m, br, 2H,  $\text{CH}_2\text{-CH} + 1\text{H, CH-CH}_2\text{aryl}$ ), 1.29 (m, br, 16H,  $\text{CH}_2$ ), 0.88 (t, br, 3H,  $-\text{CH}_2\text{-CH}_3$ ).  $^{13}\text{C}$  NMR (100 MHz, toluene- $d_8$ ,  $25^\circ\text{C}$ ,  $\delta$ ): 149.2-145.4, 140.9, 134.0, 127.7-125.4, 46.3, 40.4, 31.9, 29.7-29.1, 27.1, 26.9, 26.8, 25.4, 22.6, 13.4

*Chemical shifts are identical for all heteropolymers PS-BN-C10- $x\%$ . Proton attributions corresponds to isolated units. Integration of chemical shifts is proportional the value of  $x$ . (see NMR spectra).*

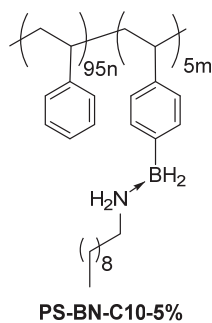
**PS-BN-C10-100%**

**Poly(4-vinylphenyldihydro)borane-(*n*-decyl)amine) (PS-BN-C10-100%)** has been synthesized according to procedure D from PS-BPin-100% (400 mg, 1.74 mmol), *n*-decylammonium chloride (386 mg, 1.74 mmol) and  $\text{LiAlH}_4$  (53 mg, 1.40 mmol). White powder. Yield: 2.0 g, 87 %.

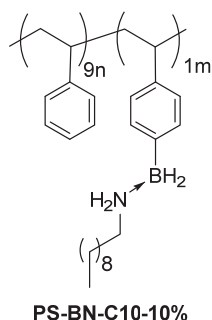
$^{11}\text{B}$  NMR. (128 MHz, toluene- $d_8$ , 25°C,  $\delta$ ): -13.9 ( $h_{1/2}$  = 395 Hz).  $^1\text{H}$  NMR. (400 MHz, toluene- $d_8$ , 25°C,  $\delta$ ): 7.48-6.41 (m, br, 4H, CH-Ar(B)), 4.54 (s, br, 2H, NH), 2.63 (m, br, 2H,  $\text{CH}_2\text{-NH}$ ), 2.30 (s, br, BH), 1.77-1.29 (m, br, 2H,  $\text{CH}_2\text{-CH}$  + 1H,  $\text{CH-CH}_2$ ), 1.29 (m, br, 16H,  $\text{CH}_2$ ), 0.88 (t, br, 3H,  $\text{-CH}_2\text{-CH}_3$ ).  $^{13}\text{C}$  NMR (100 MHz, toluene- $d_8$ , 25°C,  $\delta$ ): 148.3, 140.9, 134.0, 127.0, 126.2, 46.3, 40.0, 31.9, 29.7-29.1, 27.0, 22.6, 13.4. ATR-IR:  $\nu$  = 3389  $\text{cm}^{-1}$  (N-H), 2323  $\text{cm}^{-1}$  (B-H), 719  $\text{cm}^{-1}$  (B---N).

**PS-BN-C10-3%**

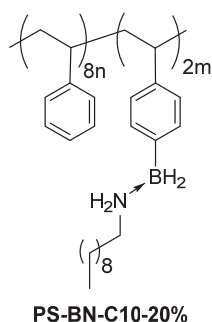
**Poly[styrene-*ran*-(4-vinylphenyldihydro)borane-(*n*-decyl)amine];[3 BN%] (PS-BN-C10-3%)** has been synthesized according to procedure D from **PS-BPin-3%** (500 mg, 0.14 mmol), *n*-decylammonium chloride (31 mg, 0.14 mmol) and  $\text{LiAlH}_4$  (5 mg, 0.12 mmol). White powder. Yield: 482 mg, 89 %.



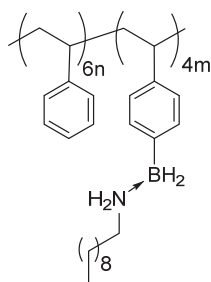
**Poly[styrene-*ran*-(4-vinylphenyldihydro)borane-(*n*-decyl)amine)];[5 BN%] (PS-BN-C10-5%)** has been synthesized according to procedure D from **PS-BPin-5%** (200 mg, 0.09 mmol), *n*-decylammonium chloride (20 mg, 0.09 mmol) and LiAlH<sub>4</sub> (3 mg, 0.07 mmol). White powder. Yield: 200 mg, 95 %.



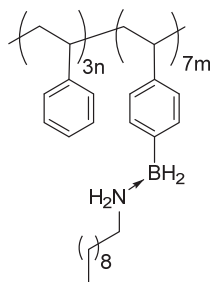
**Poly[styrene-*ran*-(4-vinylphenyldihydro)borane-(*n*-decyl)amine)];[10 BN%] (PS-BN-C10-10%)** has been synthesized according to procedure D from **PS-BPin-10%** (500 mg, 0.43 mmol), *n*-decylammonium chloride (95 mg, 0.43 mmol) and LiAlH<sub>4</sub> (14 mg, 0.34 mmol). White powder. Yield: 492 mg, 95 %.



**Poly[styrene-*ran*-(4-vinylphenyldihydro)borane-(*n*-decyl)amine)];[20 BN%] (PS-BN-C10-20%)** has been synthesized according to procedure D from **PS-BPin-20%** (300 mg, 0.48 mmol), *n*-decylammonium chloride (107 mg, 0.48 mmol) and LiAlH<sub>4</sub> (15 mg, 0.38 mmol). White powder. Yield: 370 mg, 99 %.

**PS-BN-C10-40%**

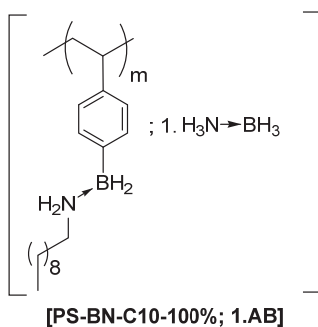
**Poly[styrene-*ran*-(4-vinylphenyldihydro)borane-(*n*-decyl)amine]];**[40 BN%] (**PS-BN-C10-40%**) has been synthesized according to procedure D from **PS-BPin-40%** (400 mg, 1.04 mmol), *n*-decylammonium chloride (231 mg, 1.04 mmol) and LiAlH<sub>4</sub> (32mg, 0.83 mmol). White powder. Yield: 235 mg, 89 %.

**PS-BN-C10-70%**

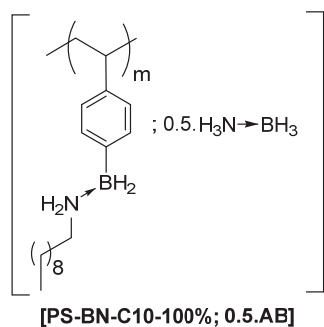
**Poly[styrene-*ran*-(4-vinylphenyldihydro)borane-(*n*-decyl)amine]];**[70 BN%] (**PS-BN-C10-70%**) has been synthesized according to procedure D from **PS-BPin-70%** (200 mg, 0.73 mmol), *n*-decylammonium chloride (162 mg, 0.73 mmol) and LiAlH<sub>4</sub> (23mg, 0.58 mmol). White powder. Yield: 203 mg, 88 %.

## V.5. Ammonia-borane doping

### Procedure F: doping of PS-BN-C10-100% with AB



Representative procedure for the synthesis of **[poly(4-vinylphenyldihydro)borane-(*n*-decyl)amine)];[1.AB]** (**[PS-BN-C10-100%; 1.AB]**): To a THF solution of **PS-BN-C10-100%** (100 mg, 0.27 mmol) were added ammonia-borane (8.4 mg, 0.27 mmol) in THF (3 mL). The reaction mixture was kept vigorously stirring for 1h. The resulting mixture was dried under vacuum to yield quantitatively a white solid.

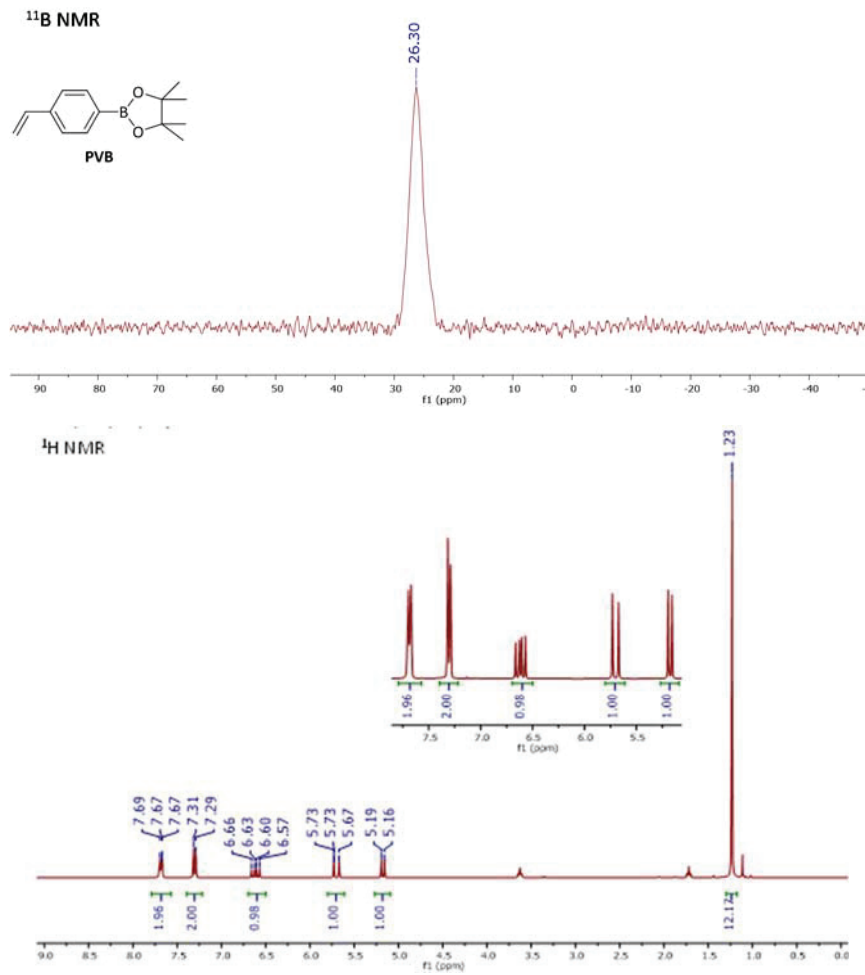


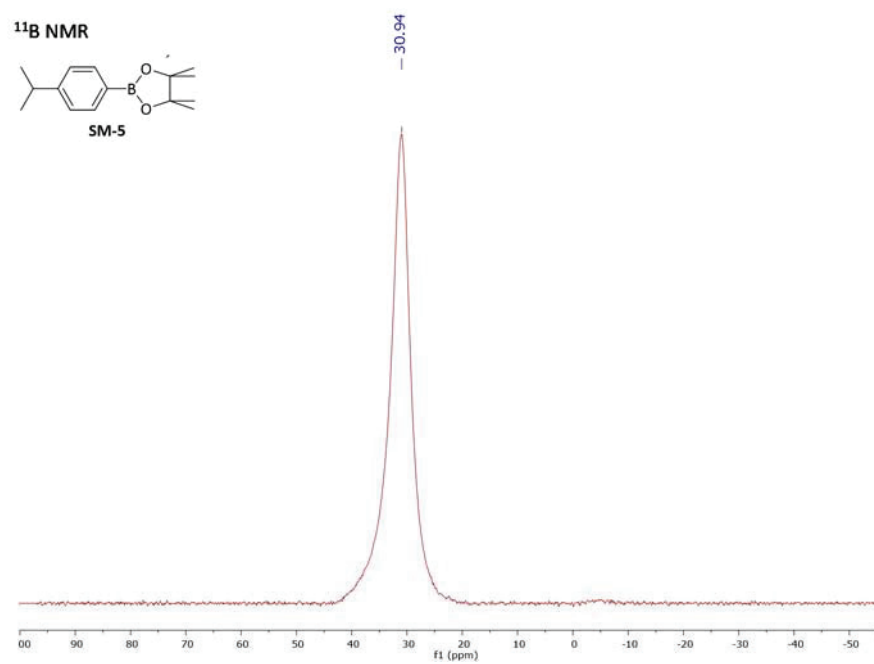
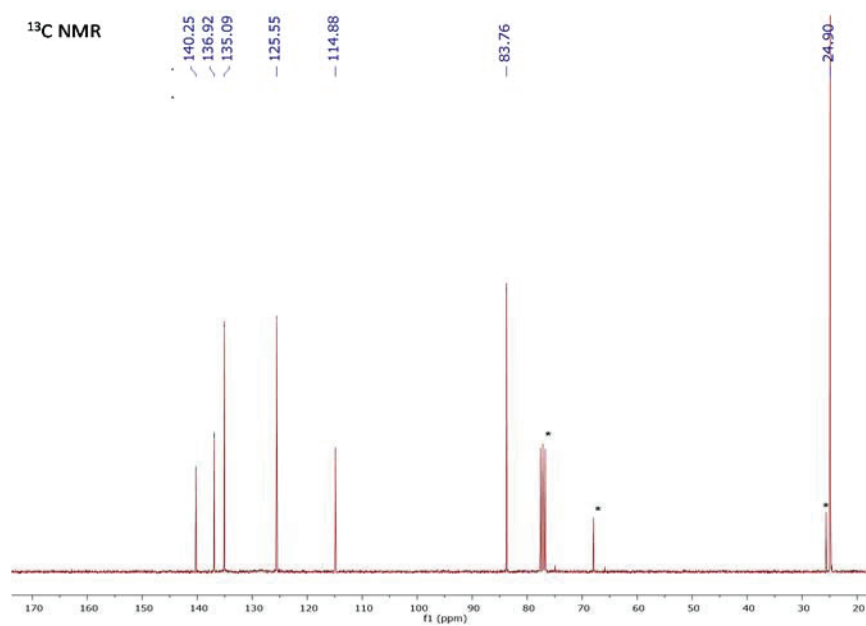
**[poly(4-vinylphenyldihydro)borane-(*n*-decyl)amine)];[0.5.AB]** (**[PS-BN-C10-100%; 0.5.AB]**): has been synthesized according to procedure F with **PS-BN-C10-100%** (100 mg, 0.27 mmol) and ammonia-borane (4.2 mg, 0.13 mmol).

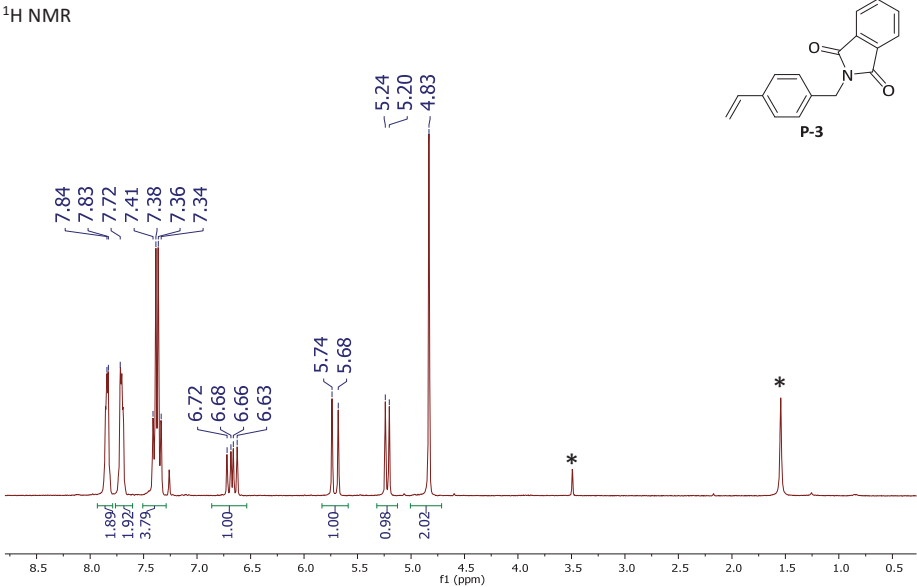
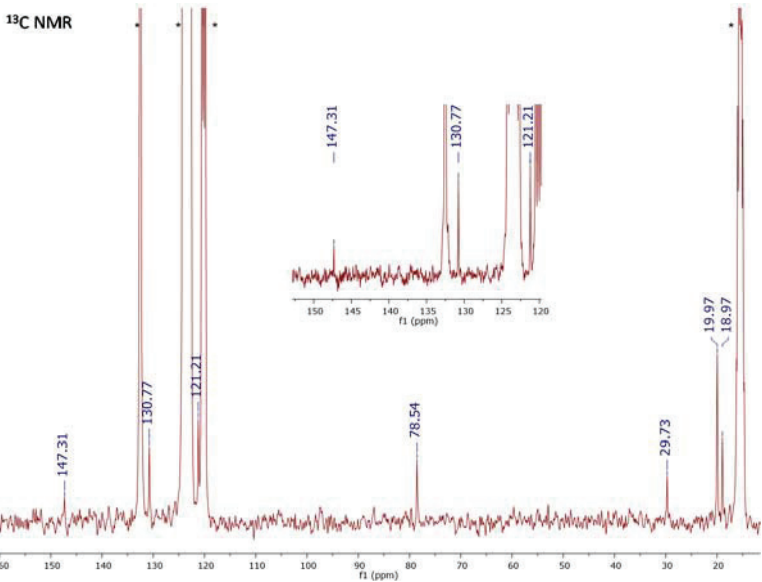
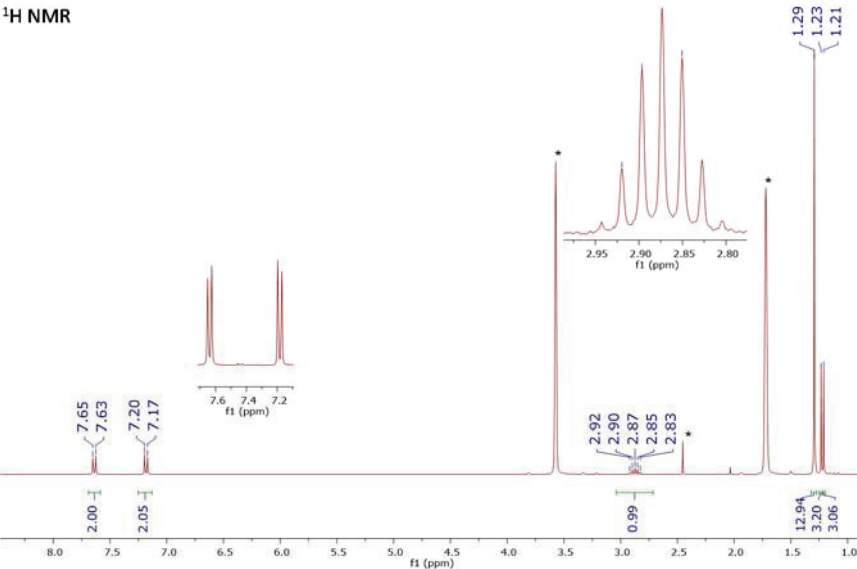


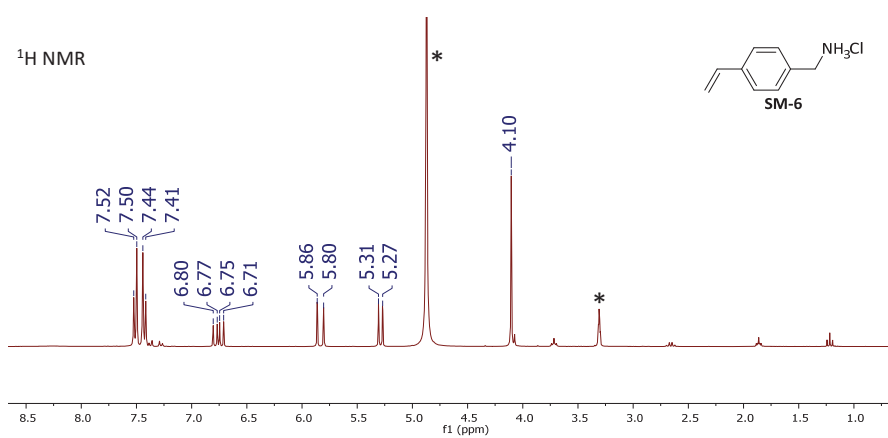
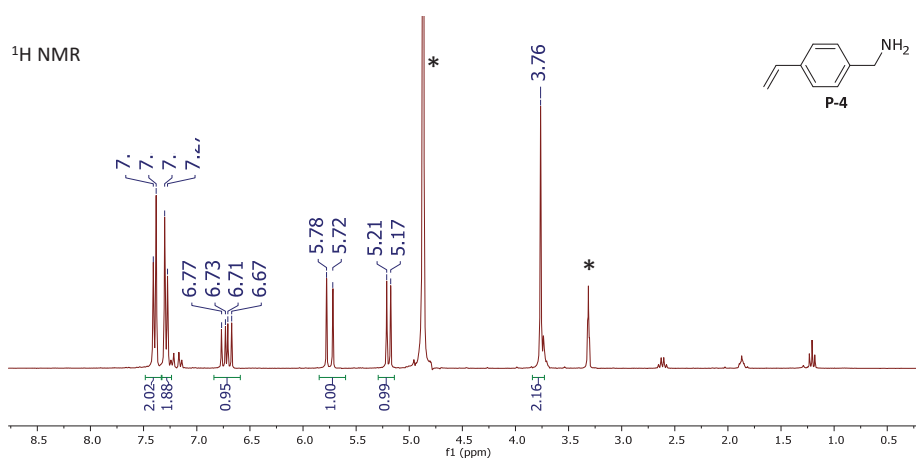
V.6. NMR Spectra

V.6.a. Precursors

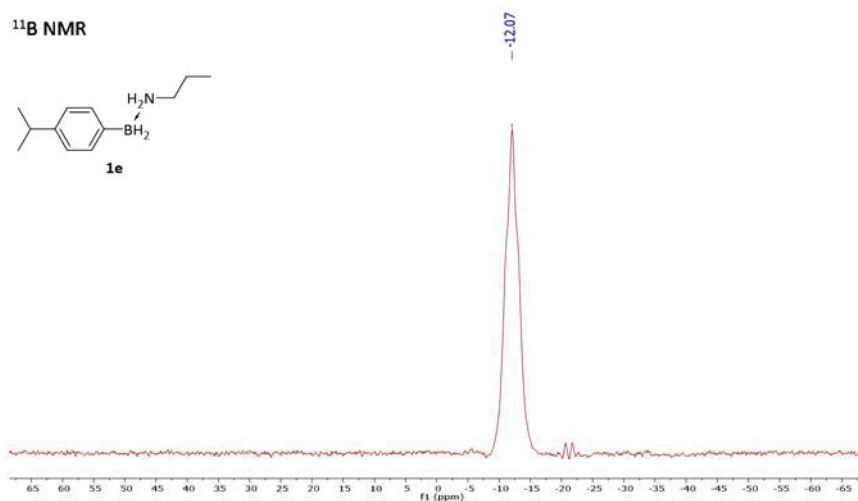




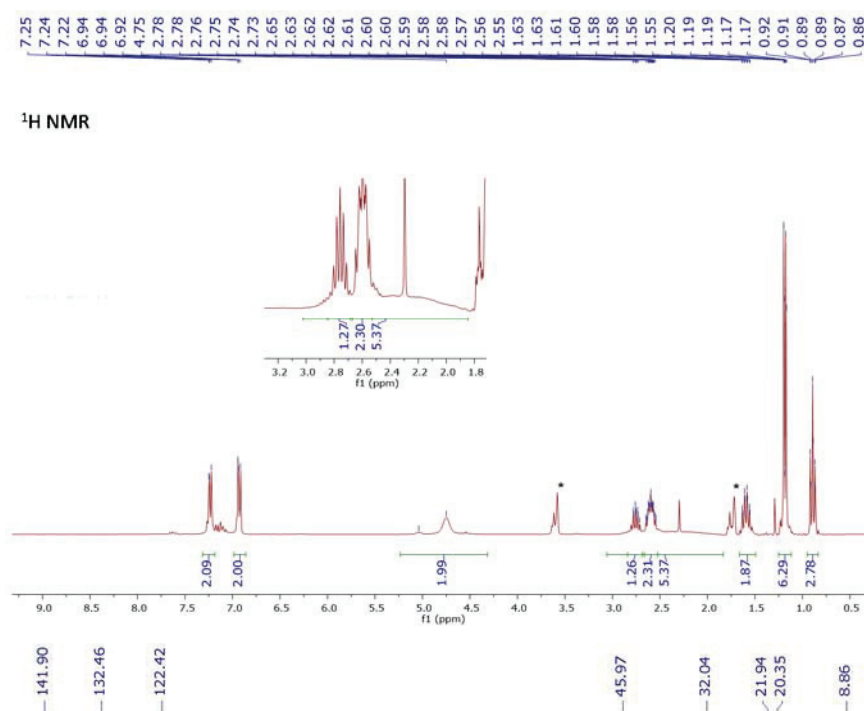
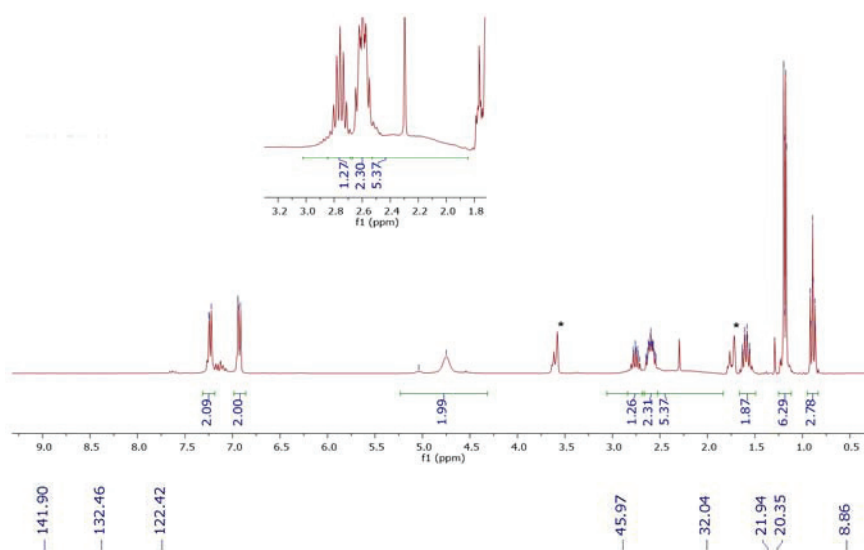
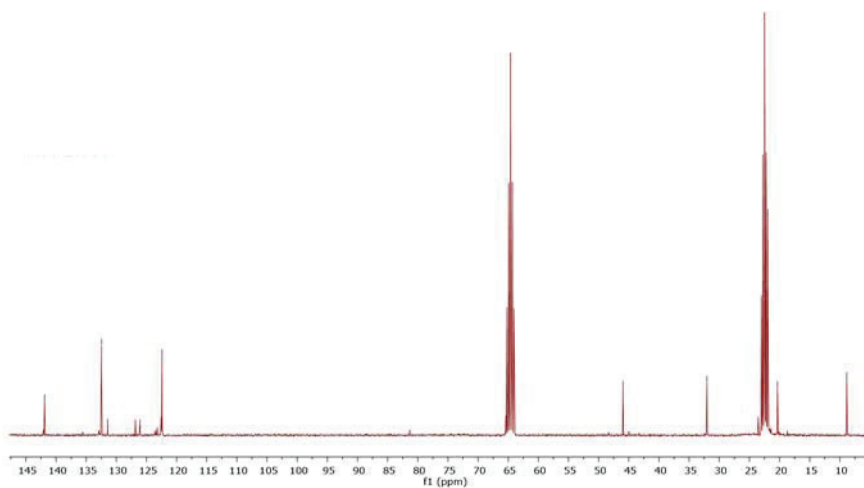
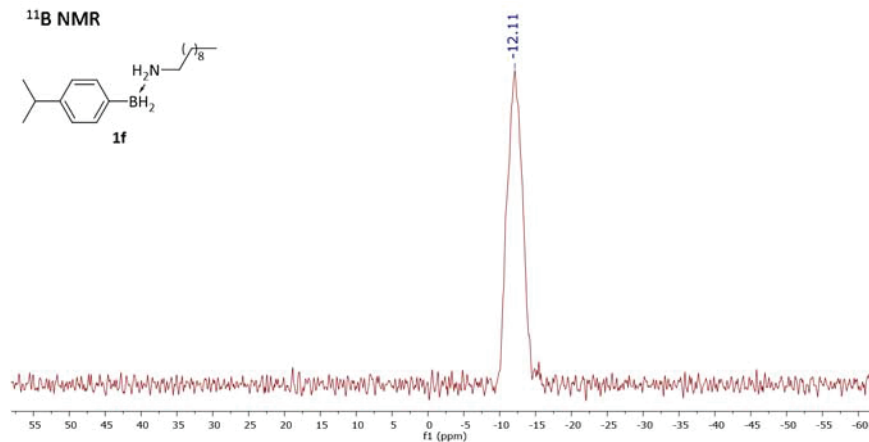
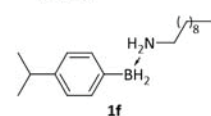


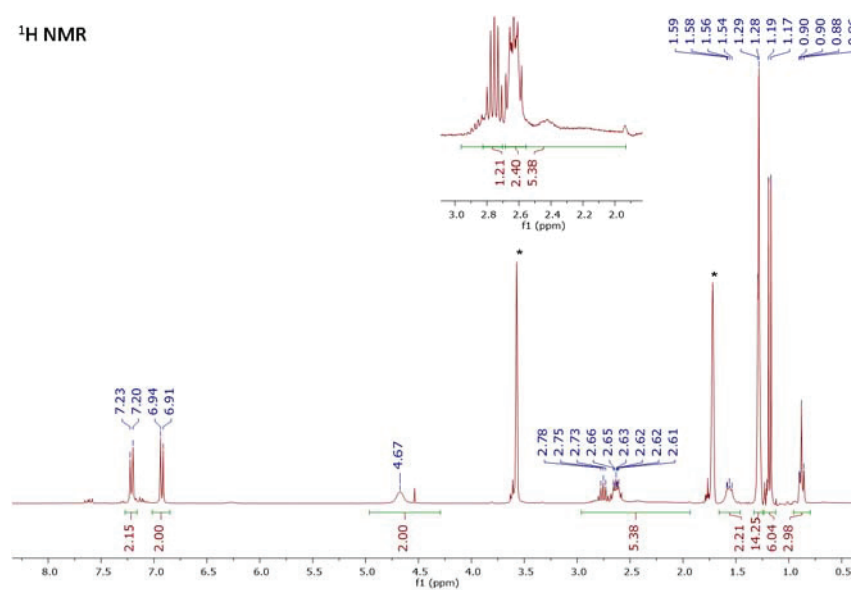
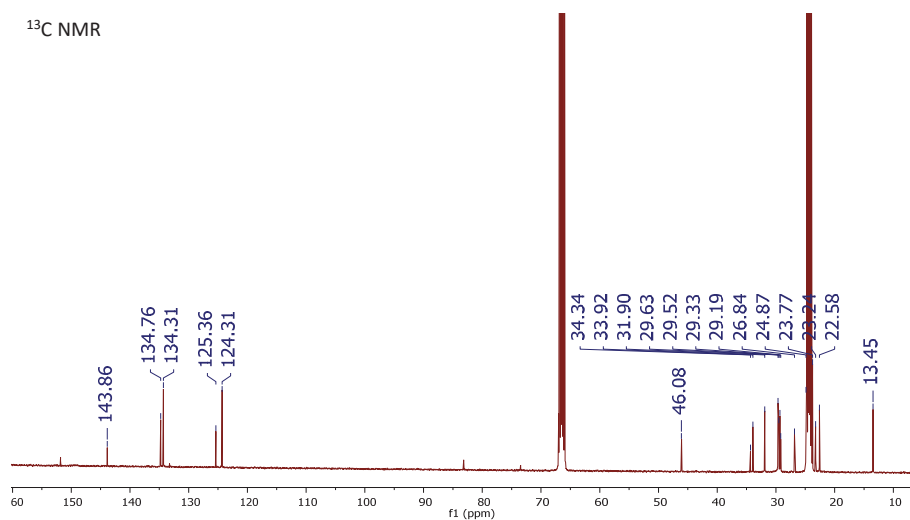
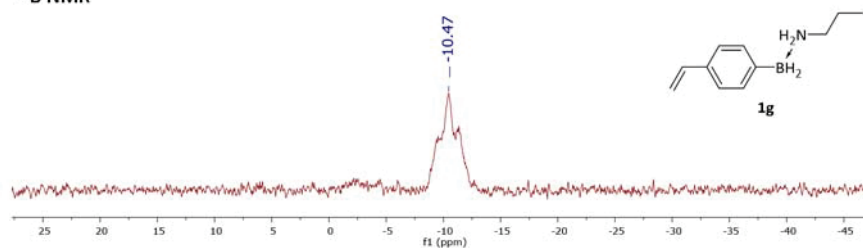


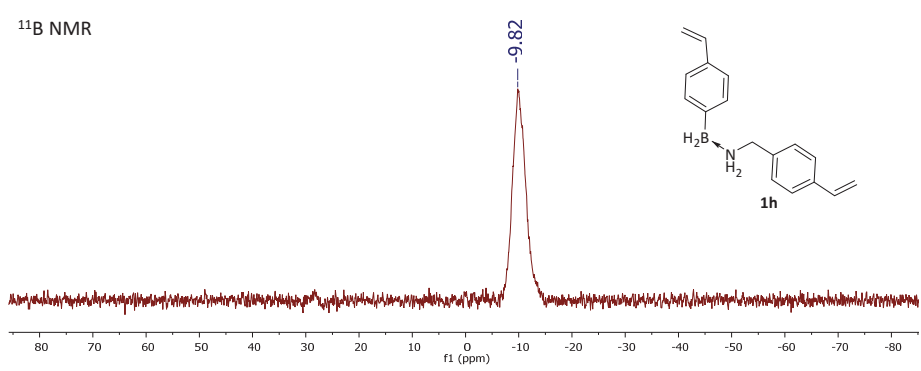
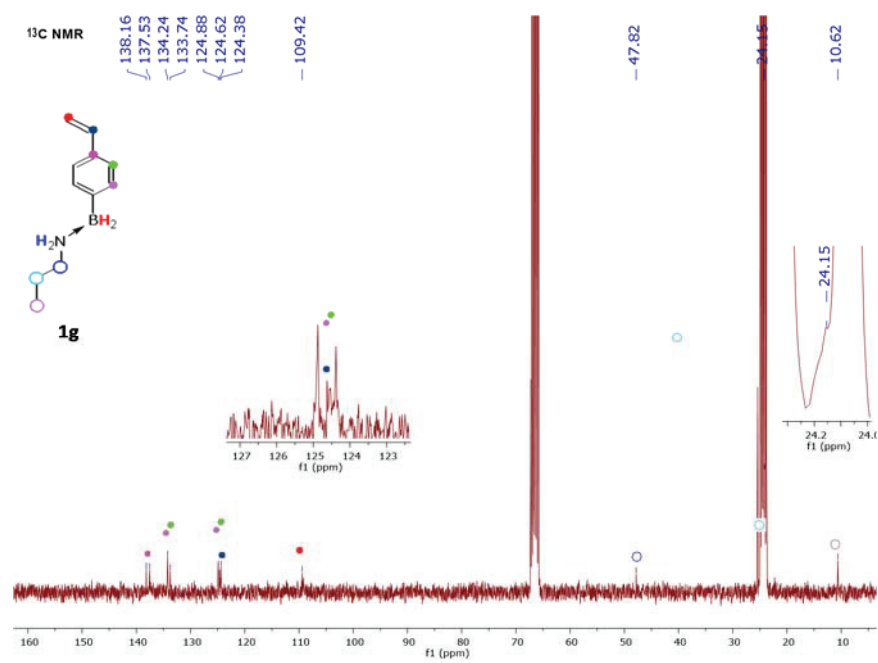
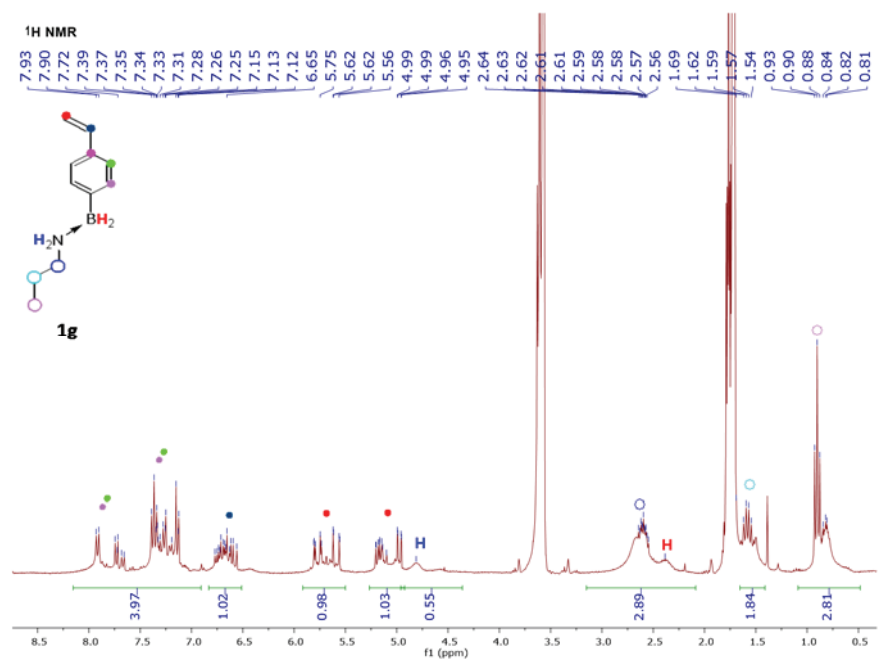
## V.6.b. Molecular bricks

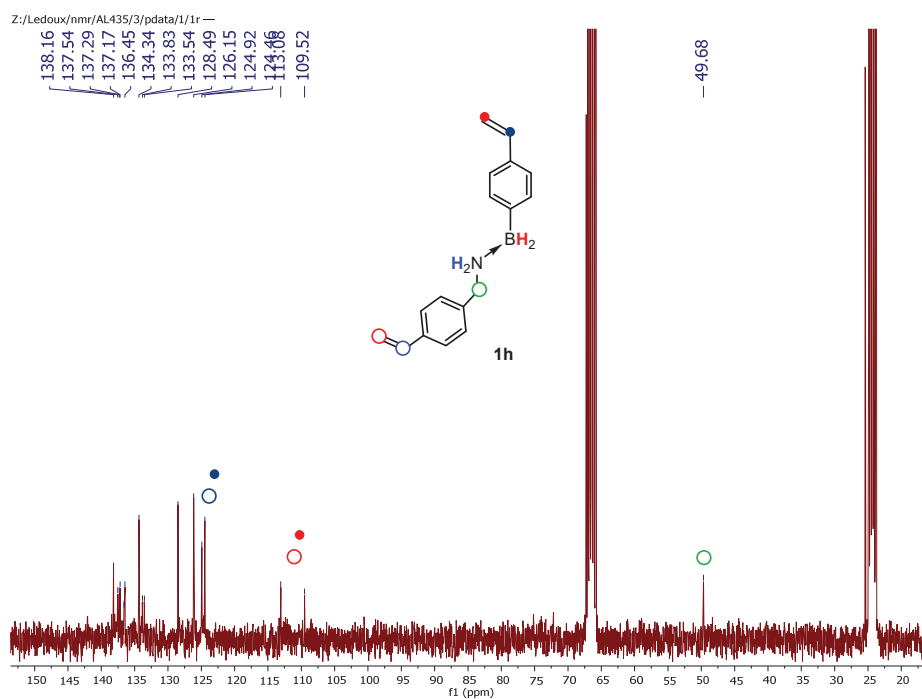
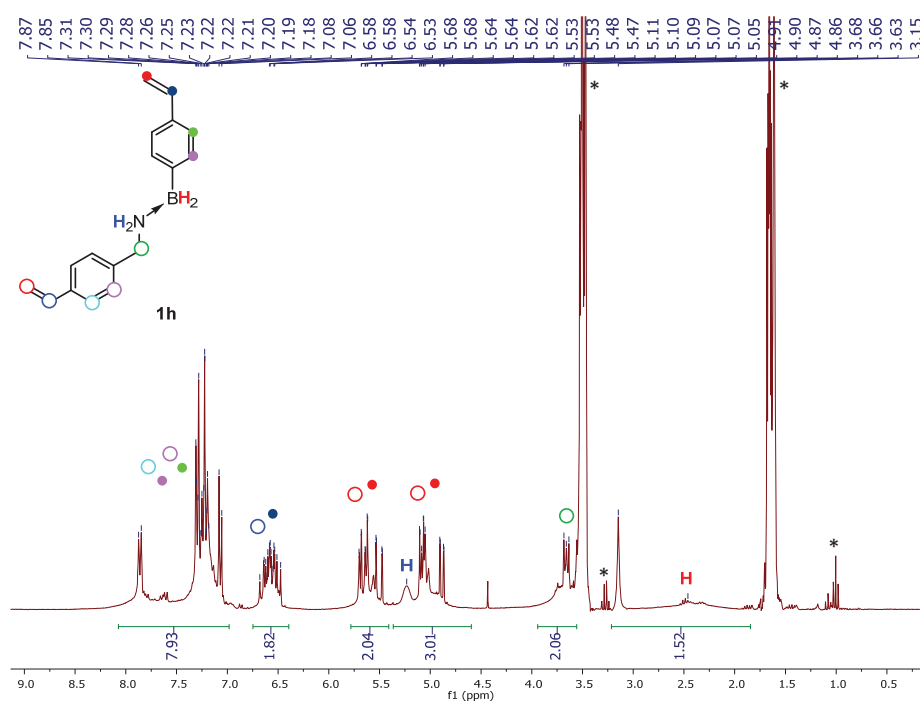


## Section 4: Experimental data

<sup>1</sup>H NMR<sup>13</sup>C NMR<sup>11</sup>B NMR

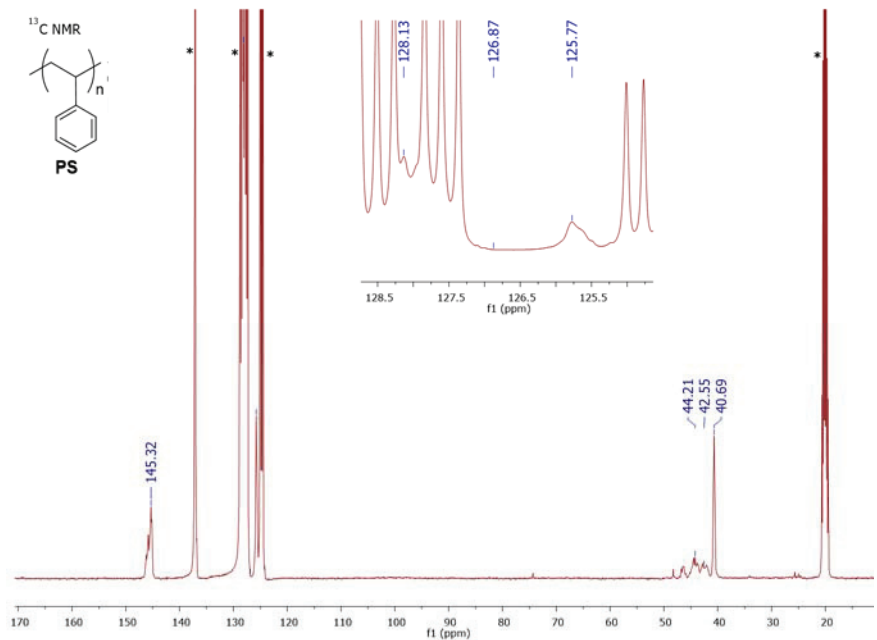
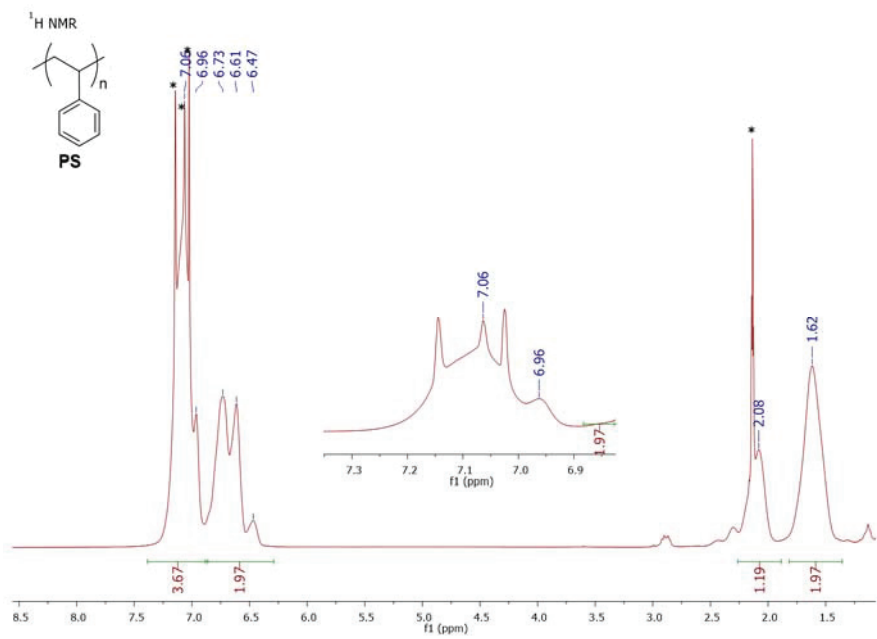
$^1\text{H}$  NMR $^{13}\text{C}$  NMR $^{11}\text{B}$  NMR

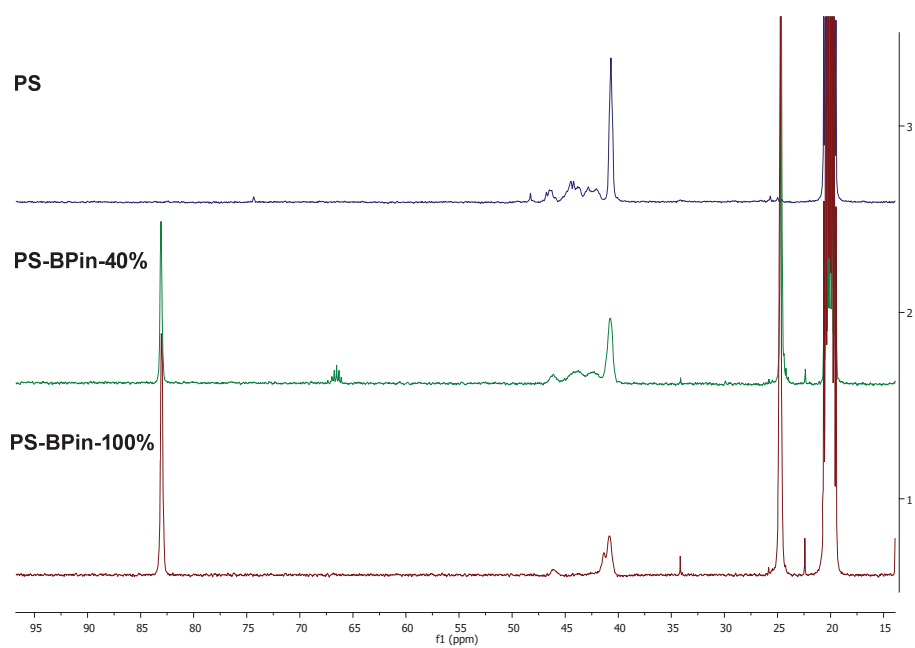
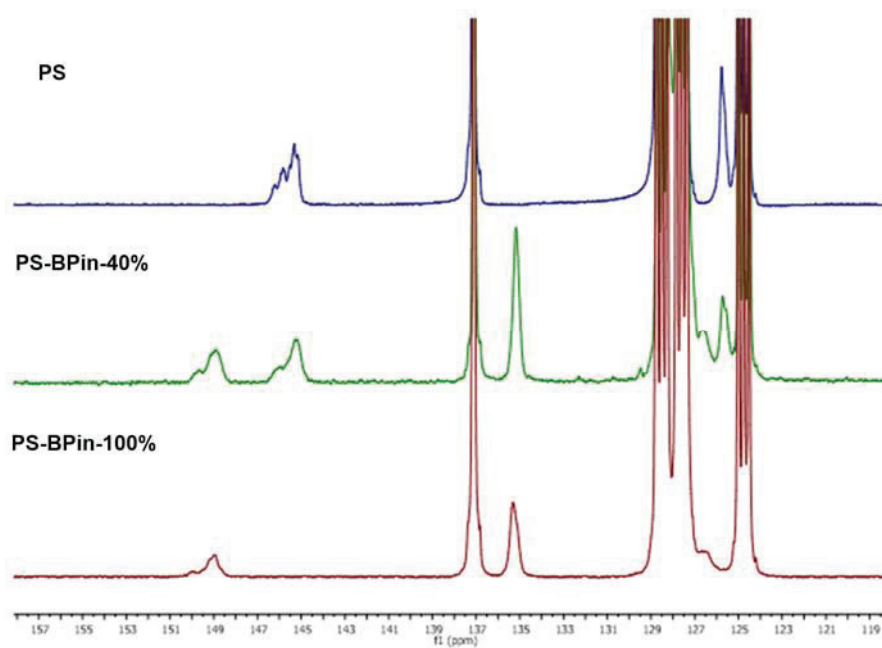
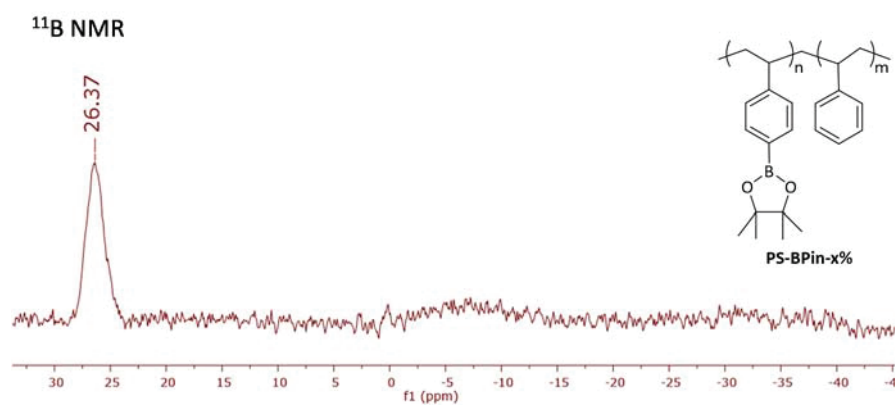




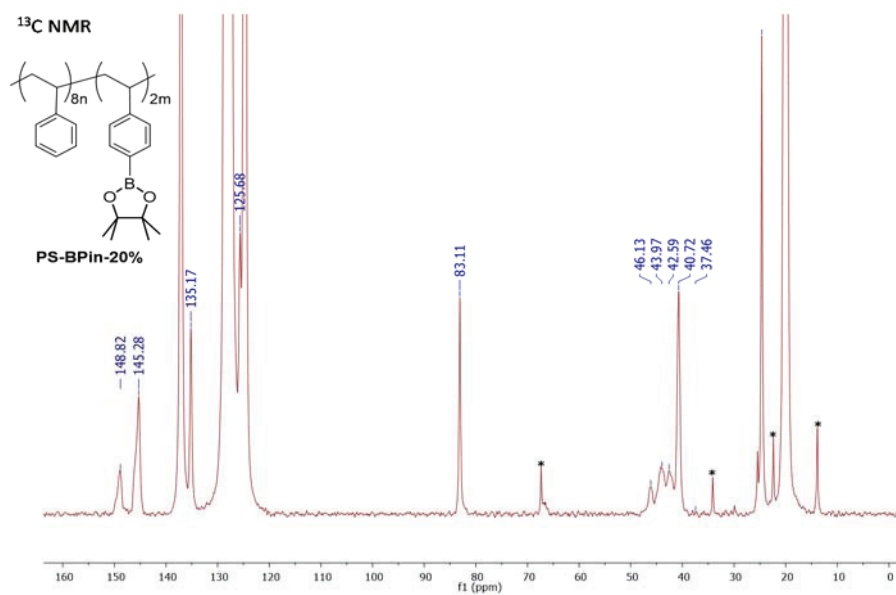
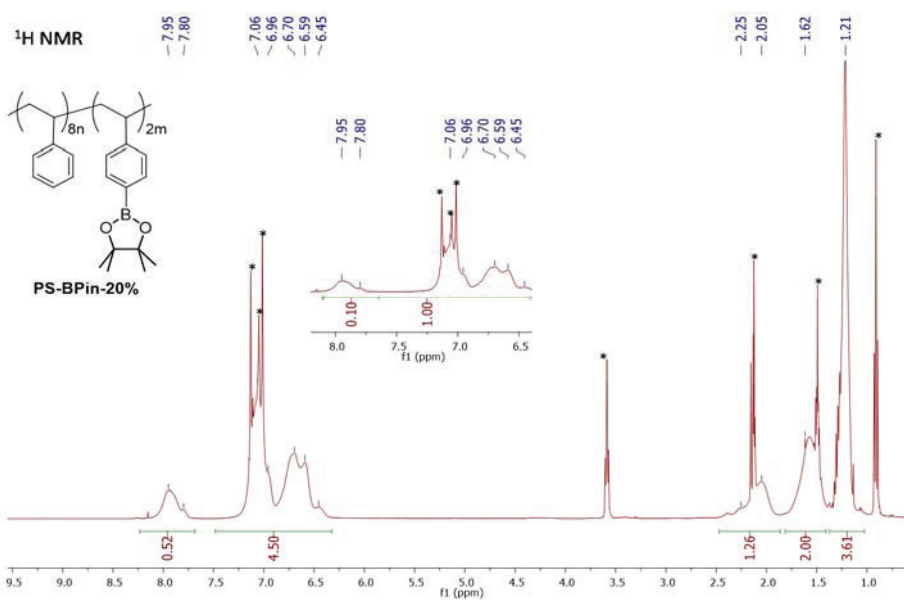
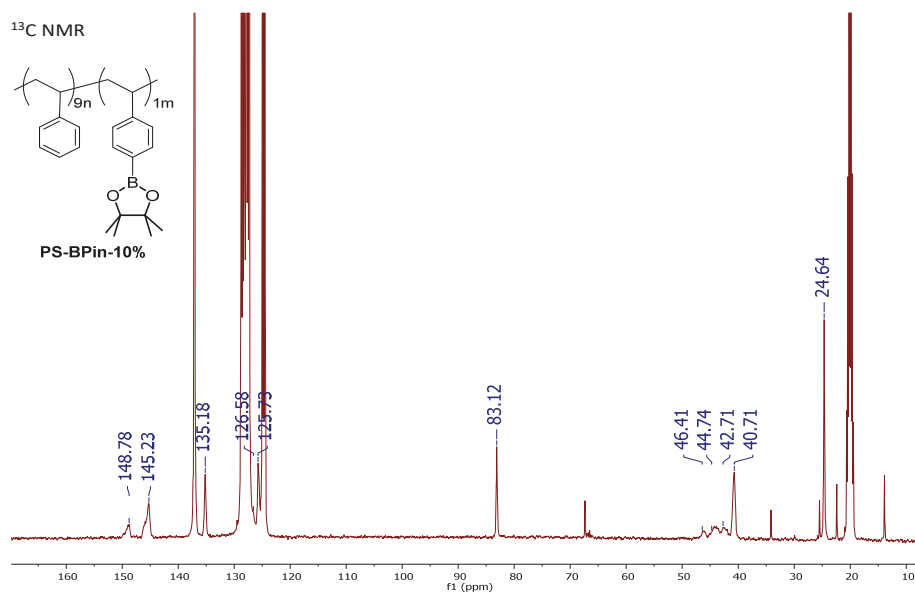
### V.6.c. Polymers PS and PS-BPin-x%

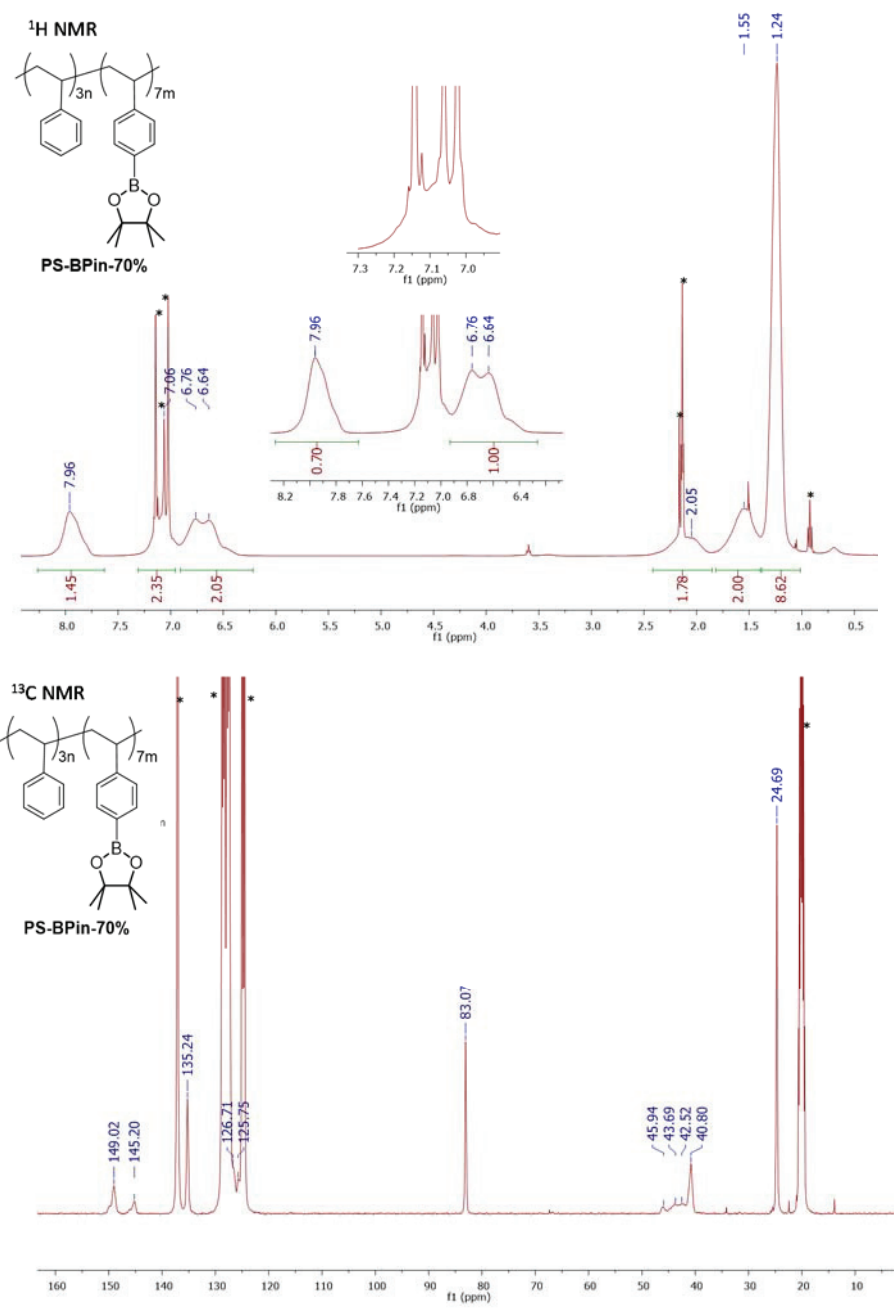


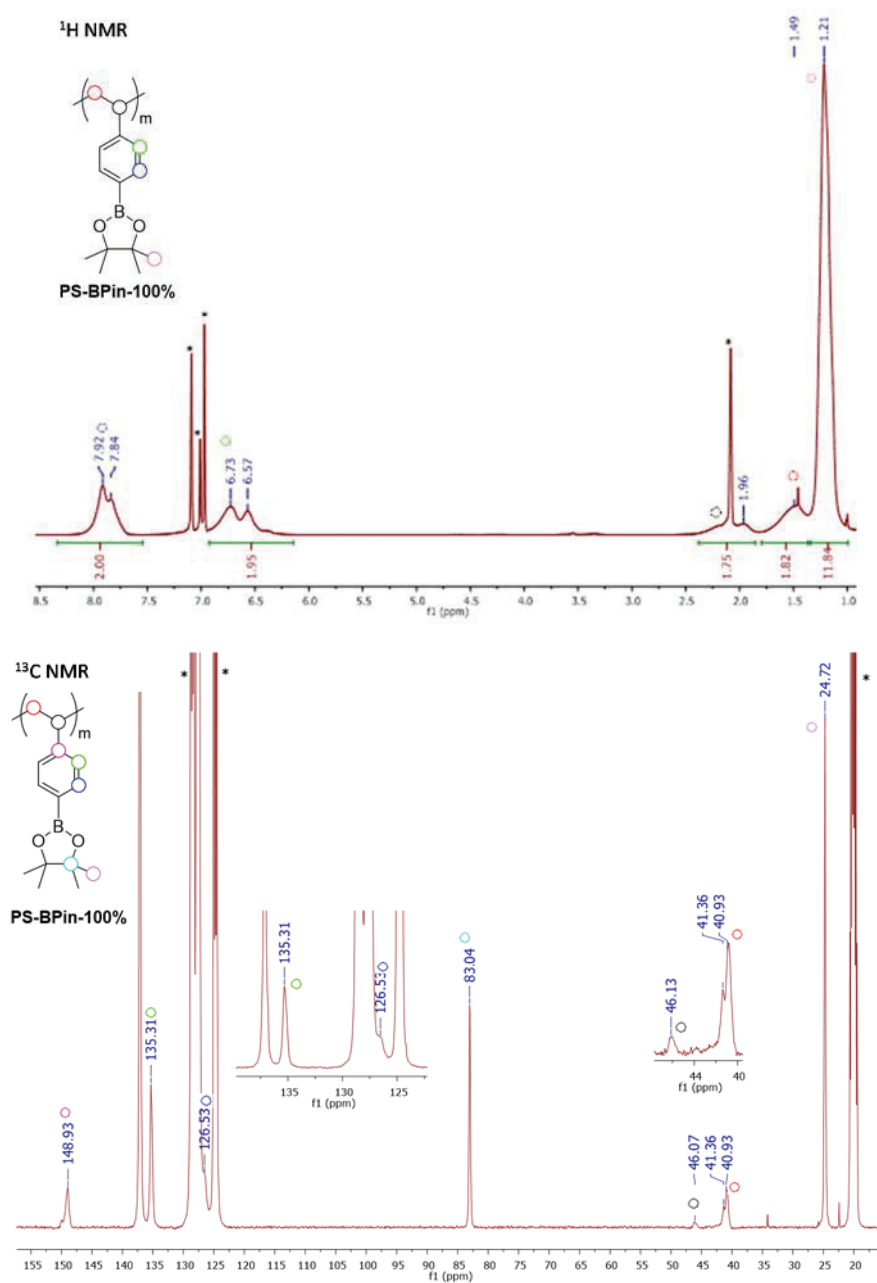




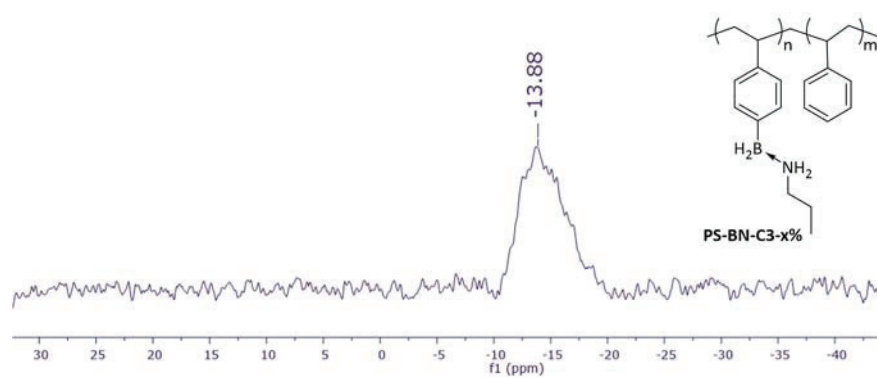


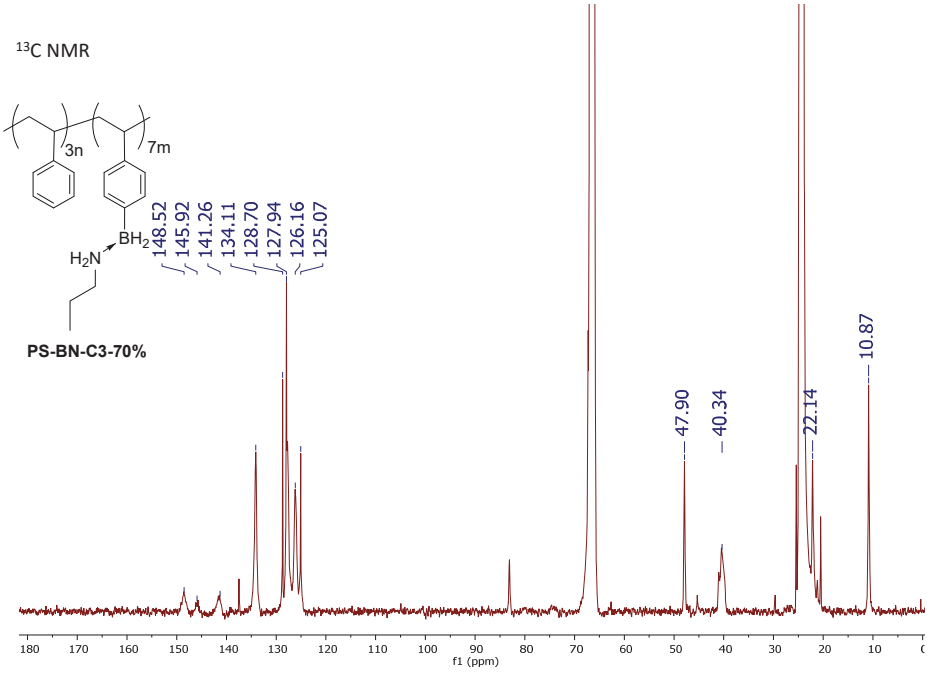
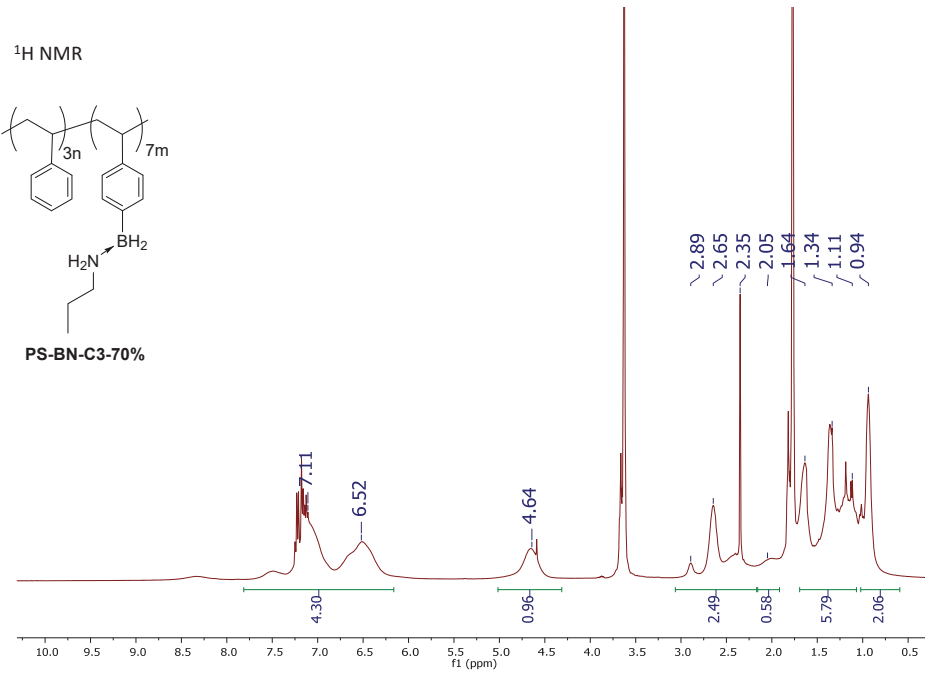


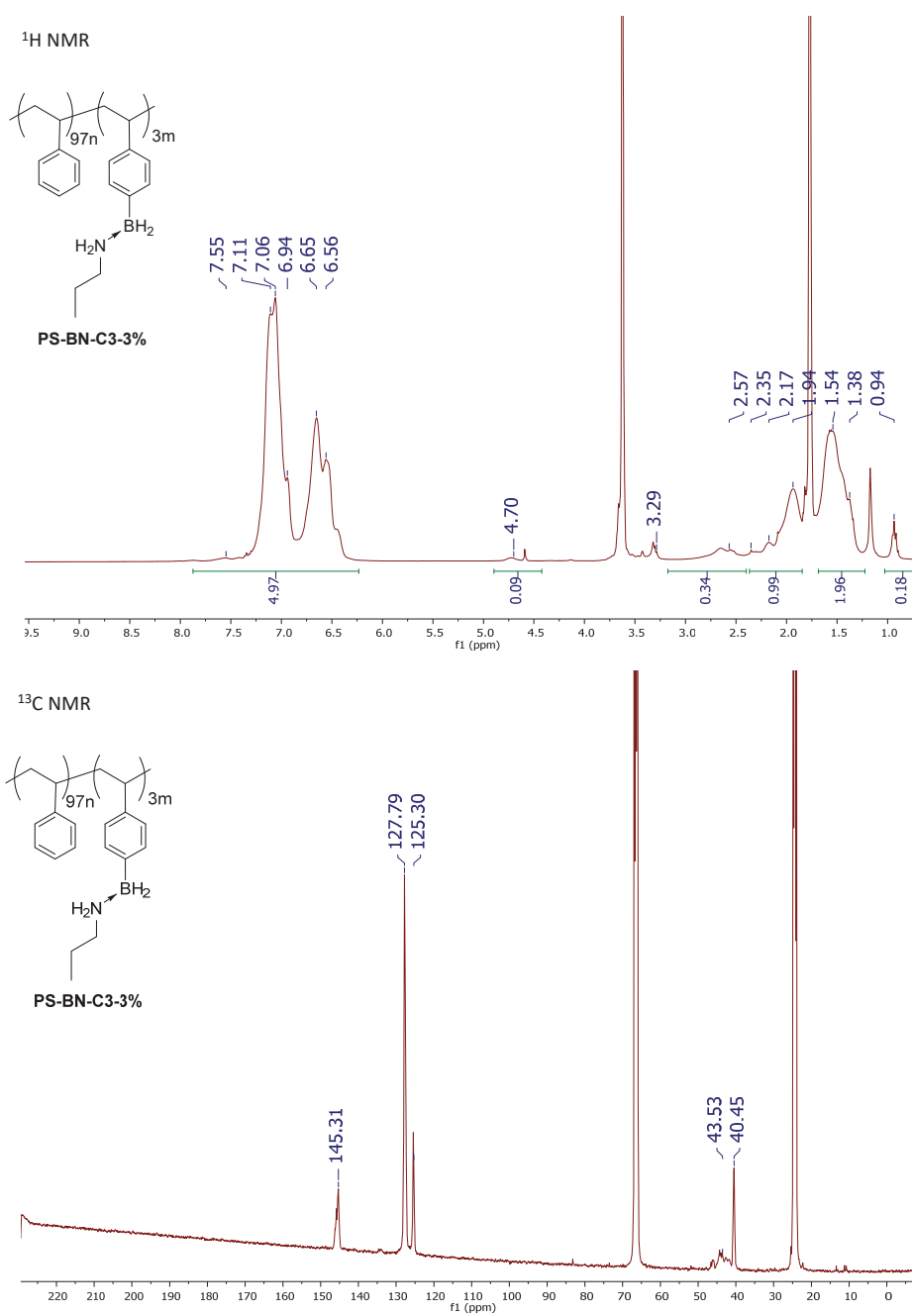




## V.6.d. PS-BN-C3-x%

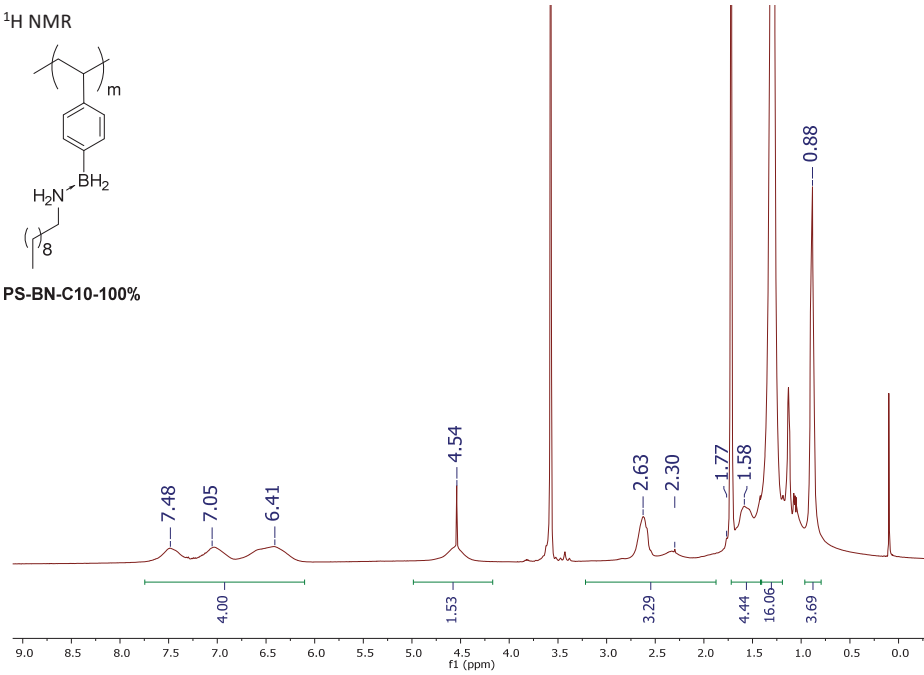
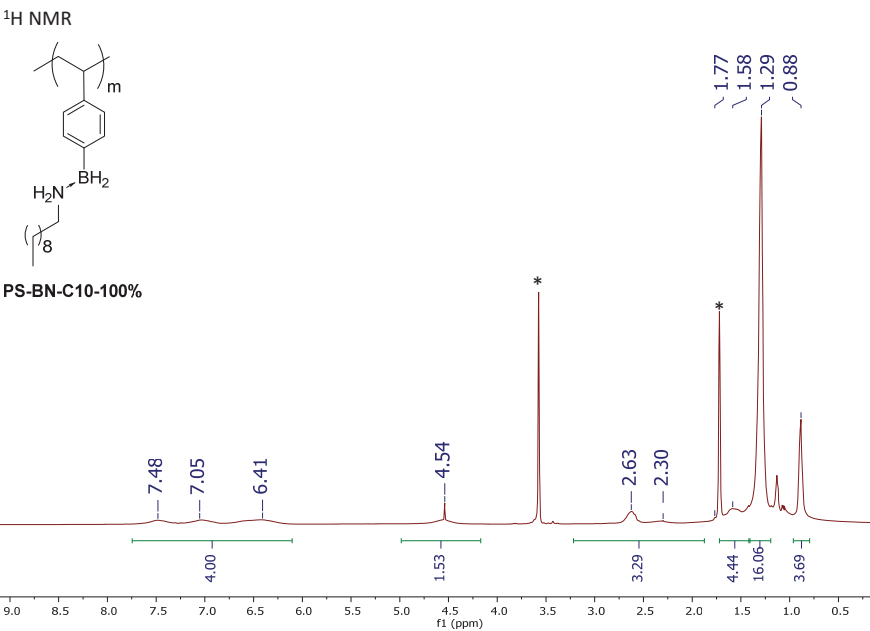


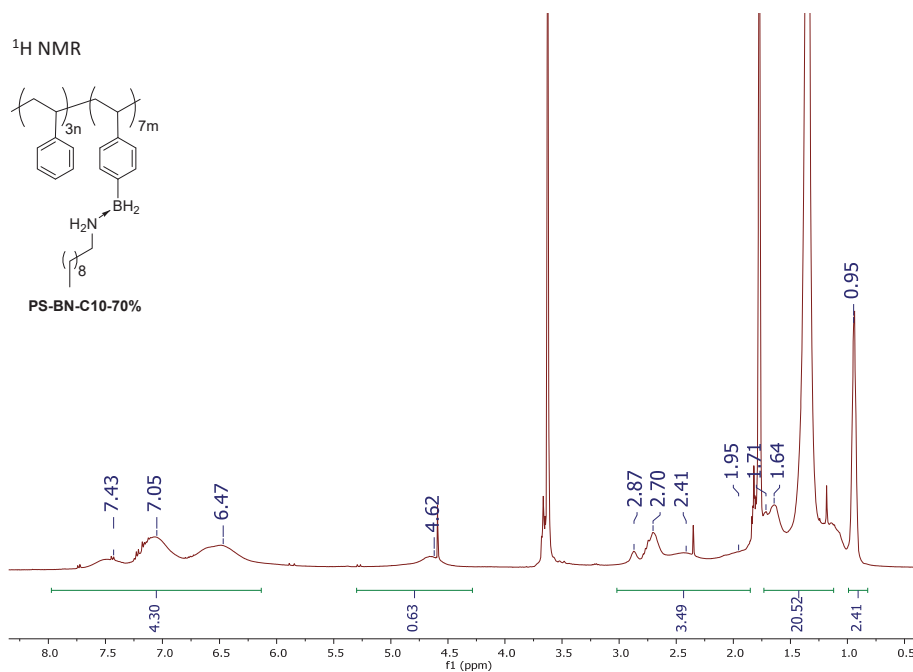
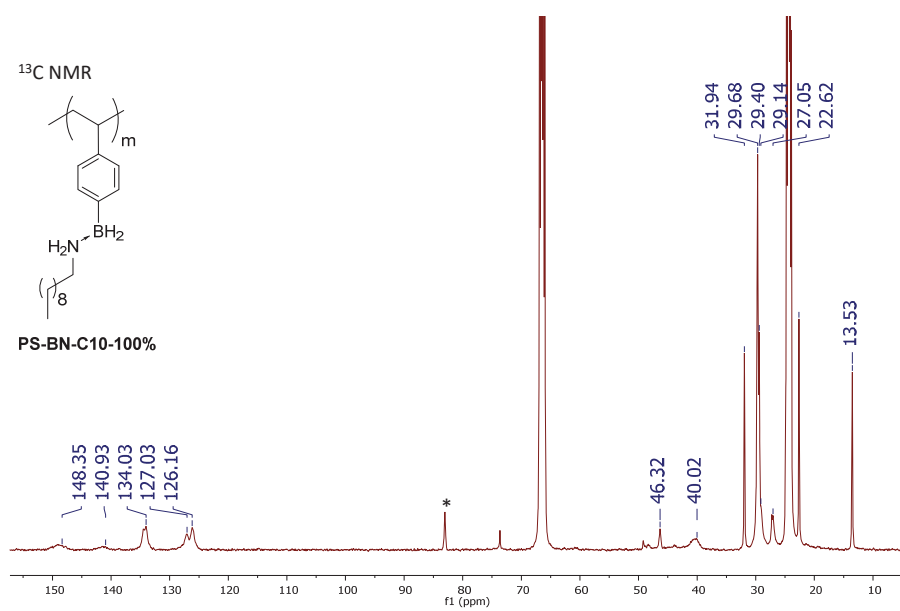


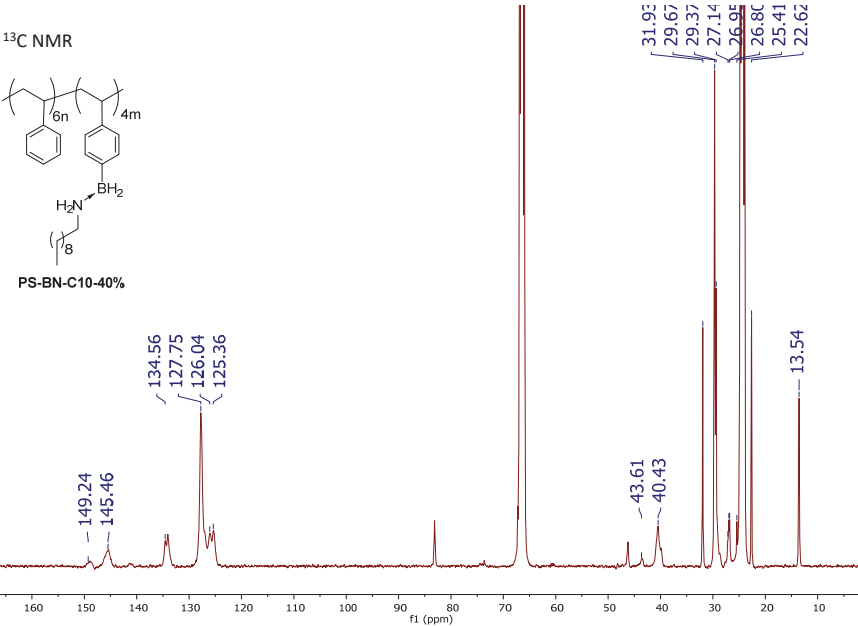
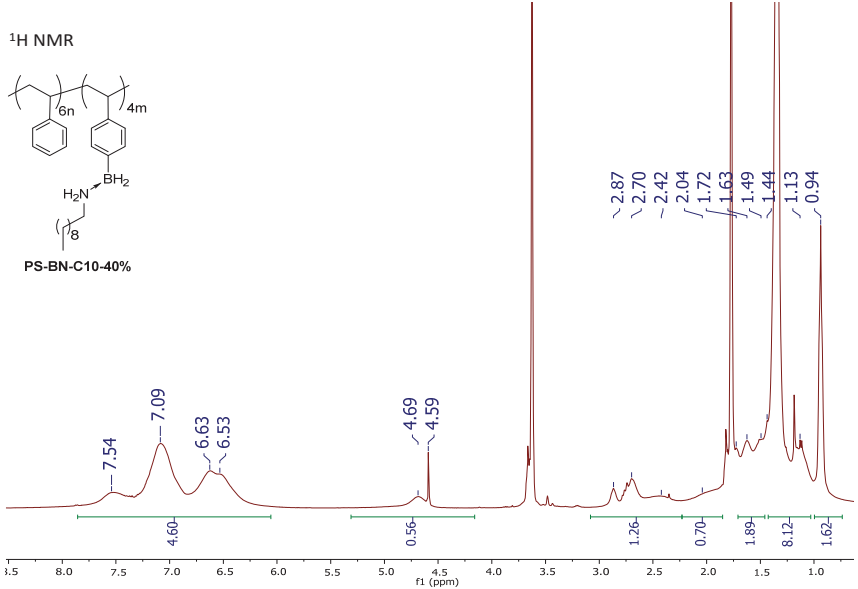
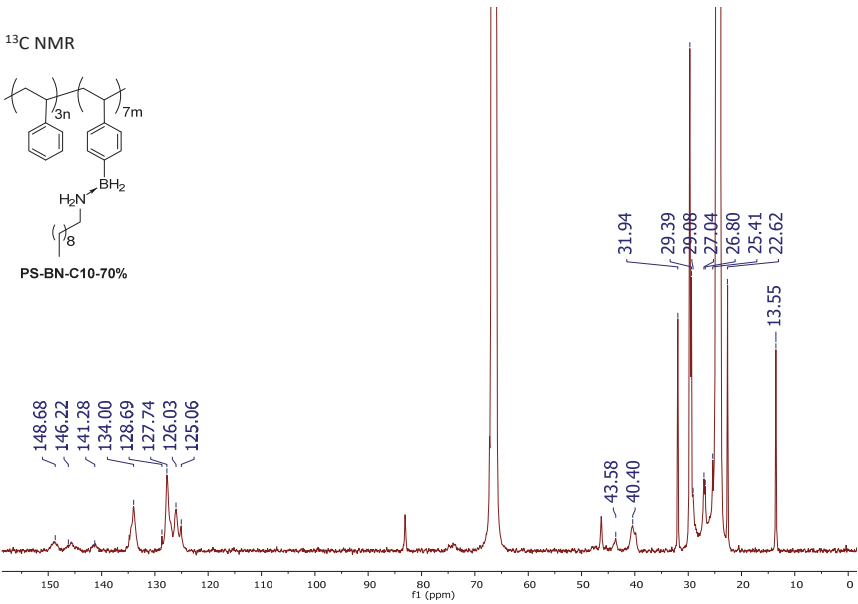


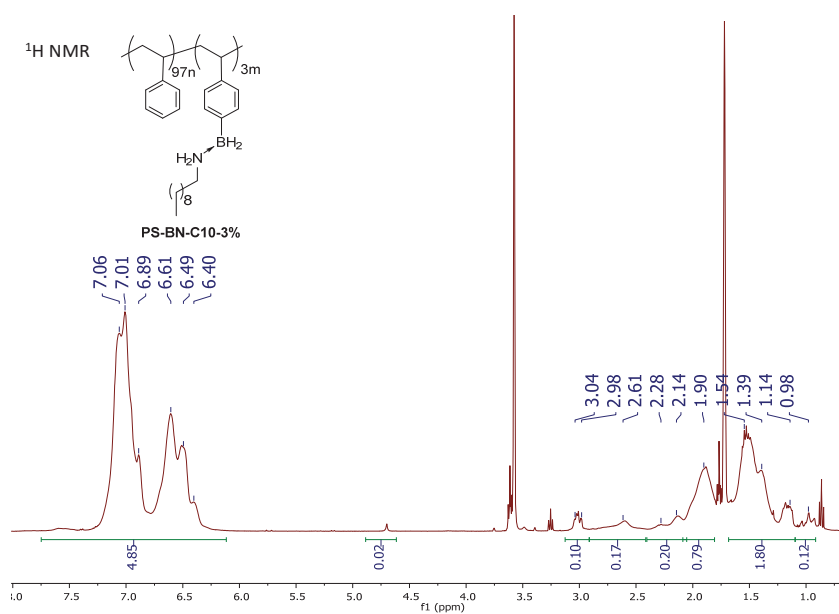
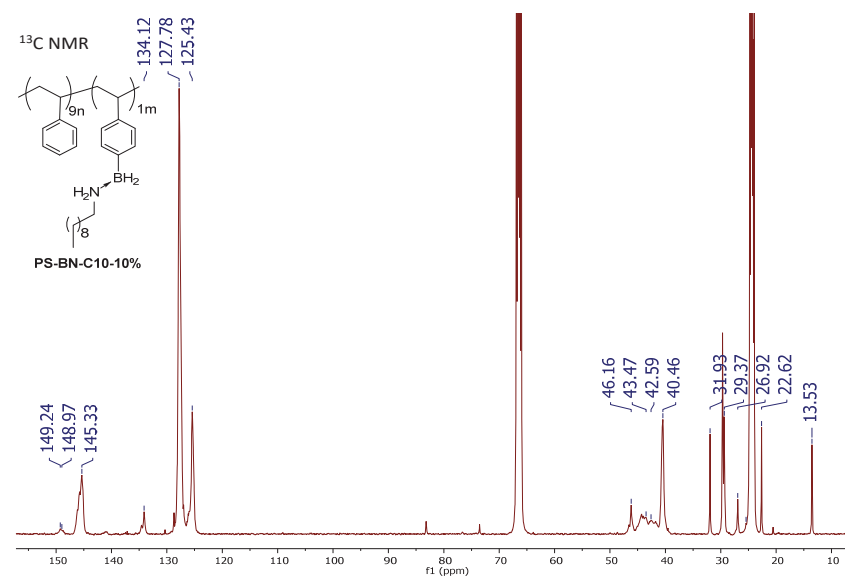
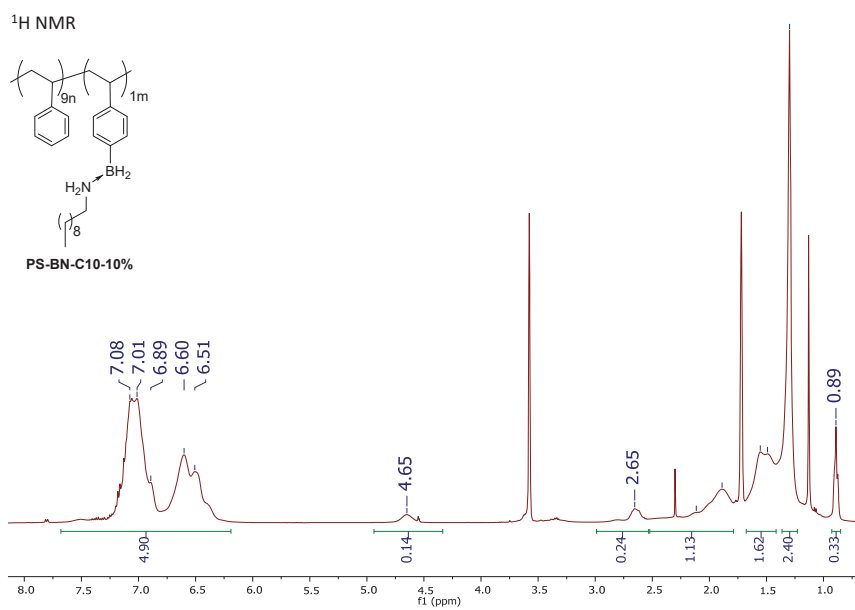
## V.6.e. PS-BN-C10-x%





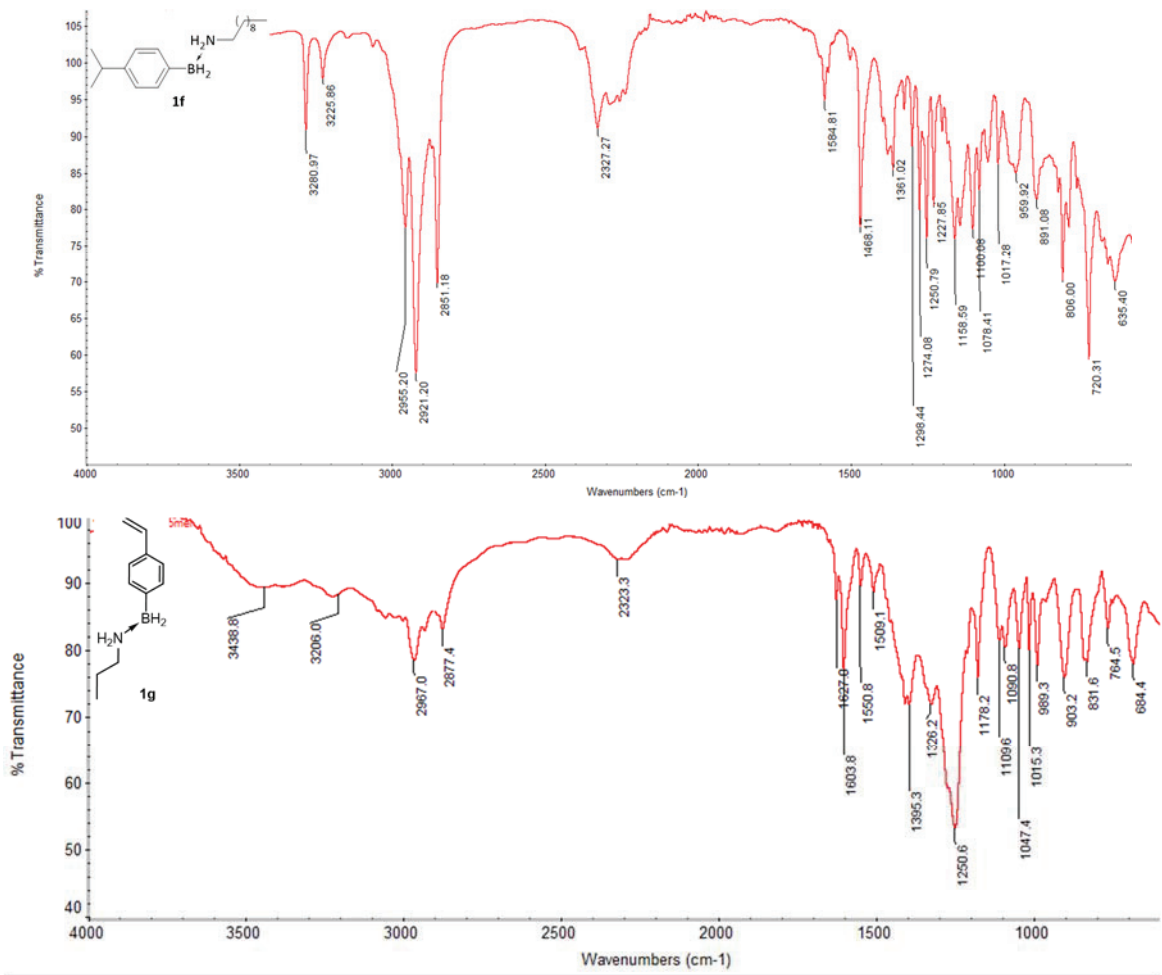




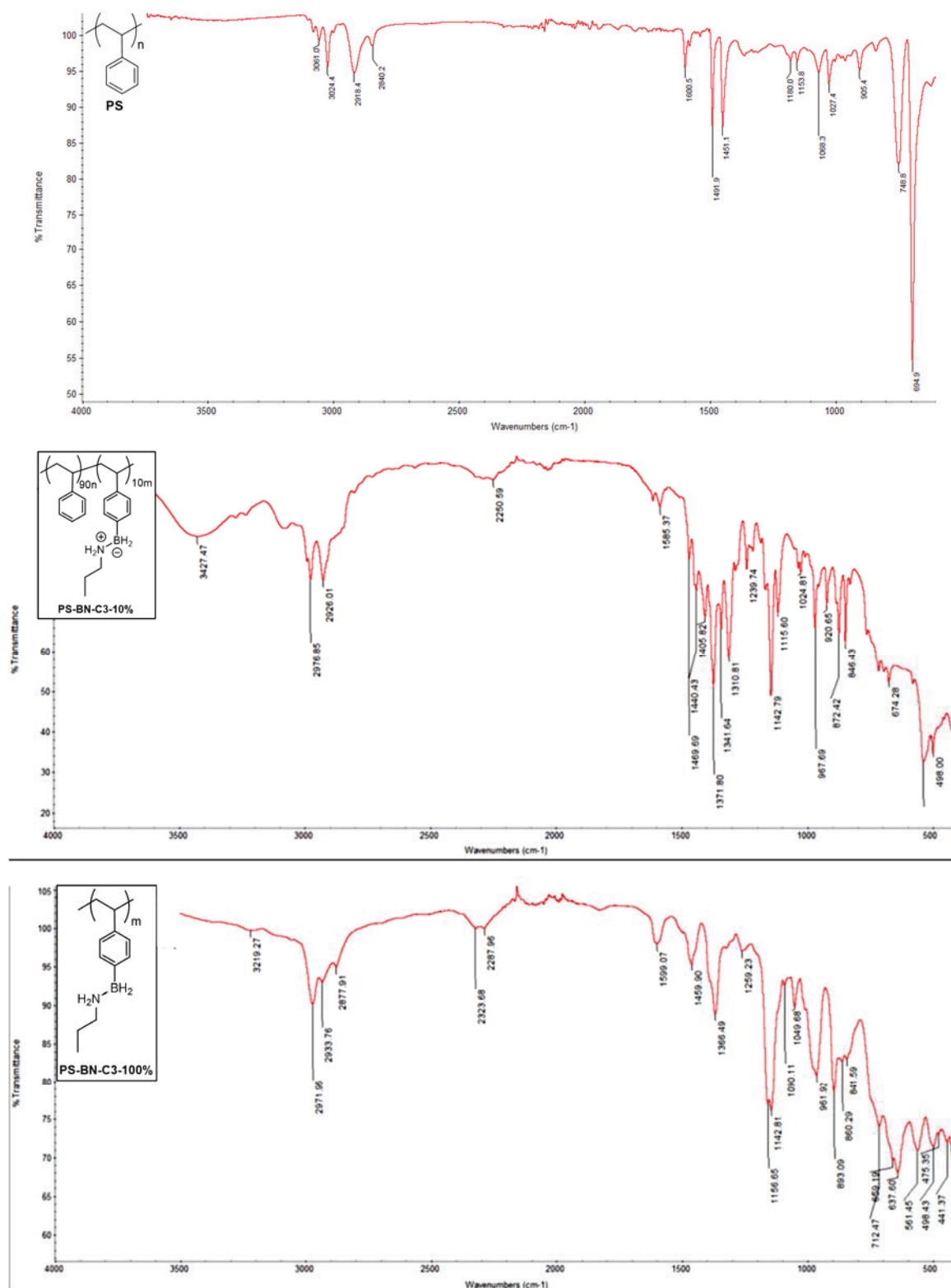


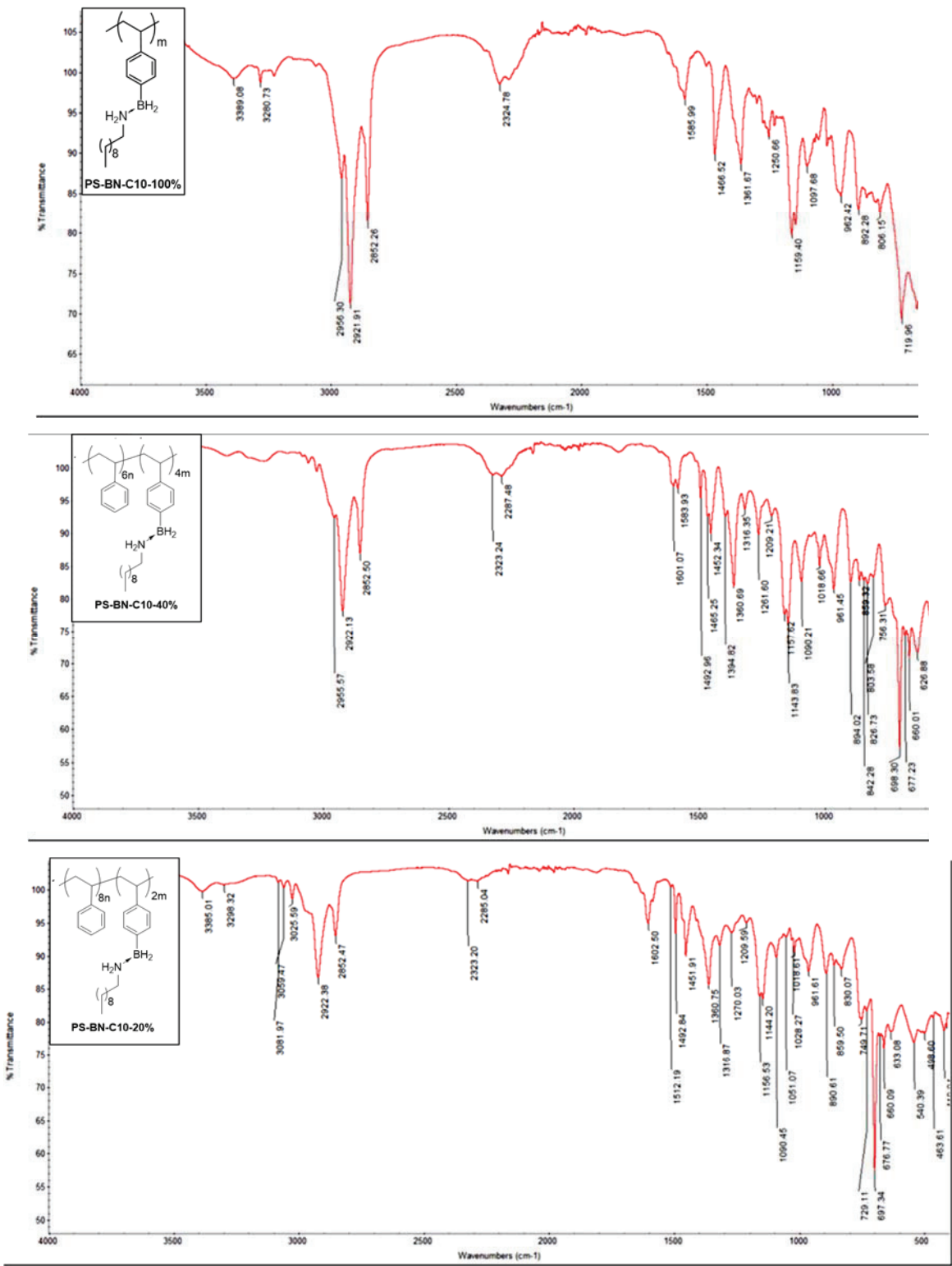
V.7. ATR-IR

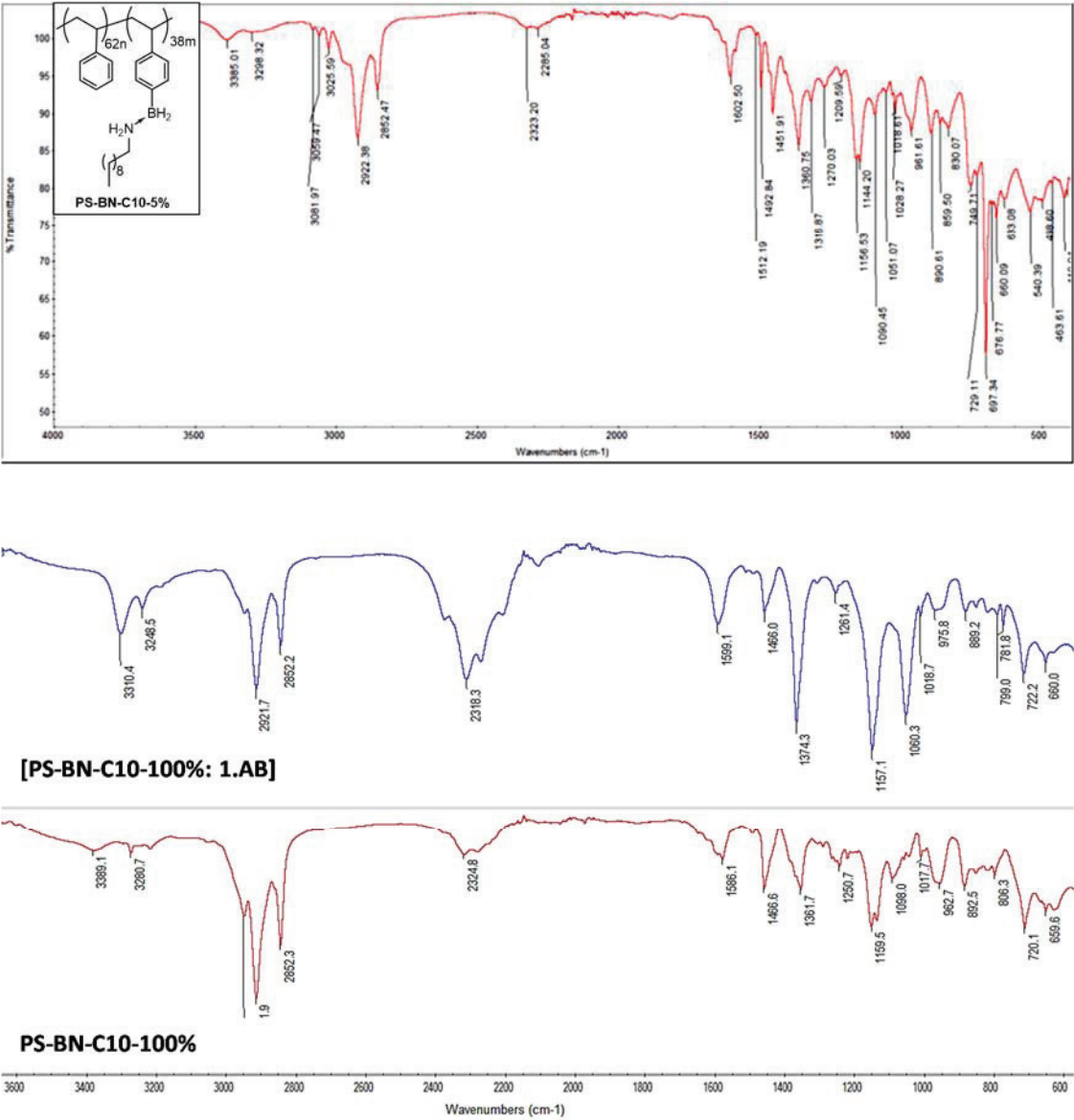
V.7.a. Molecular bricks



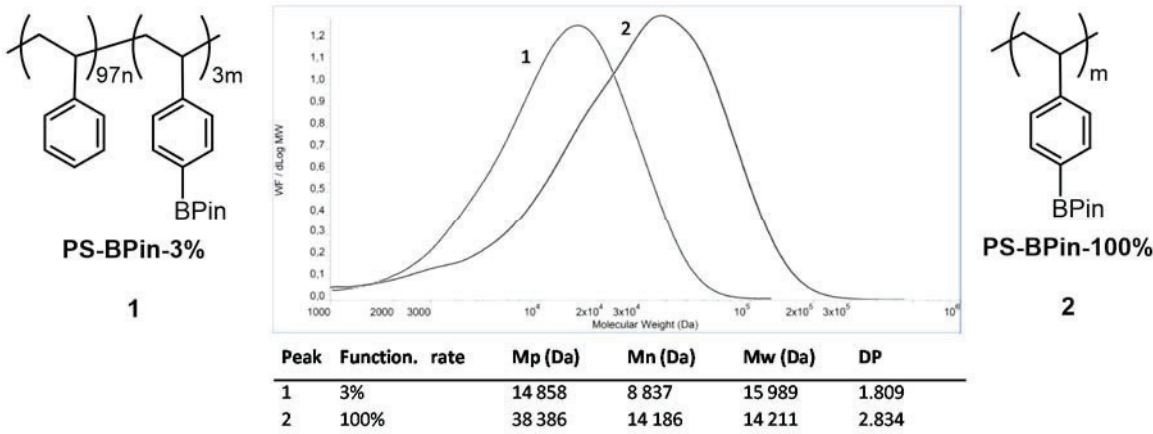
## V.7.b. Polymers



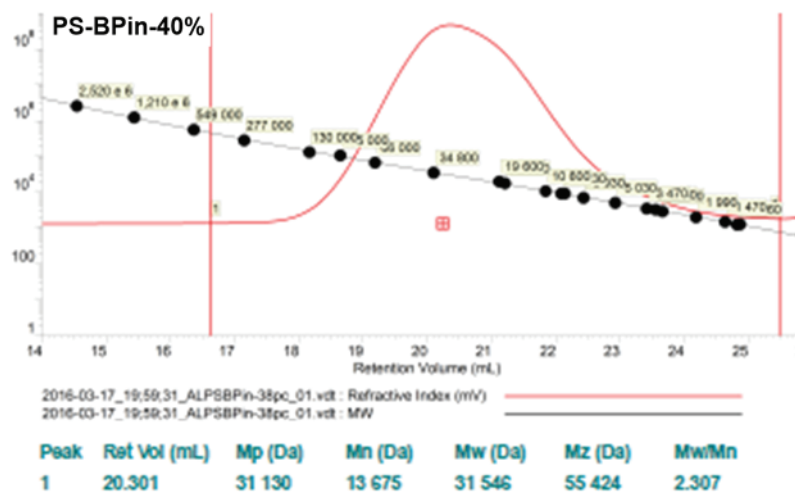
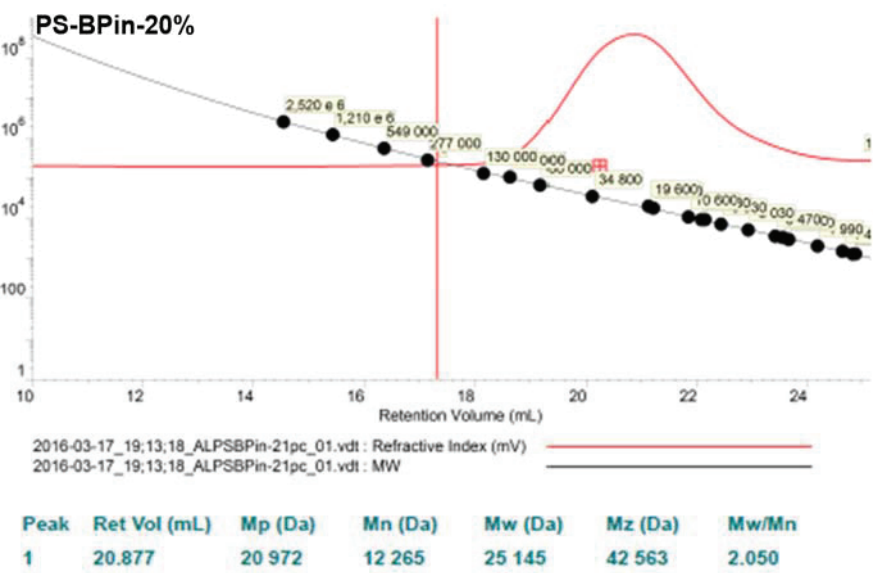
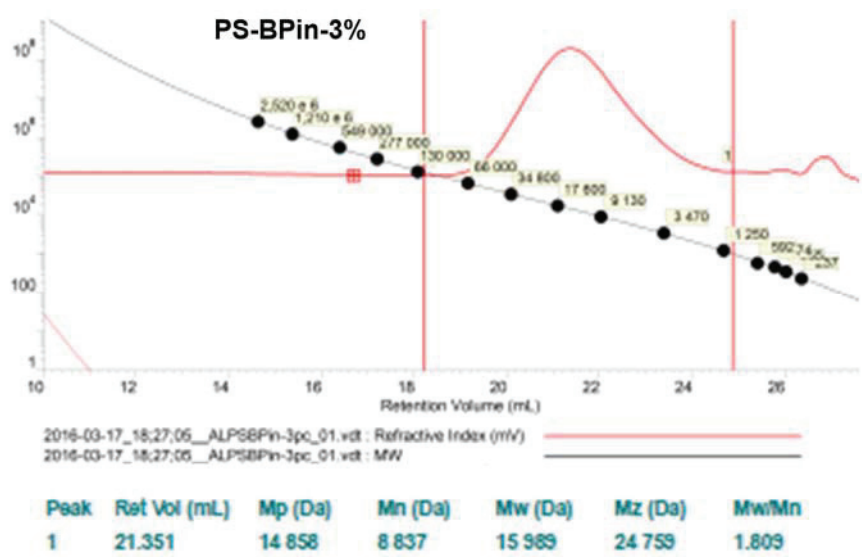




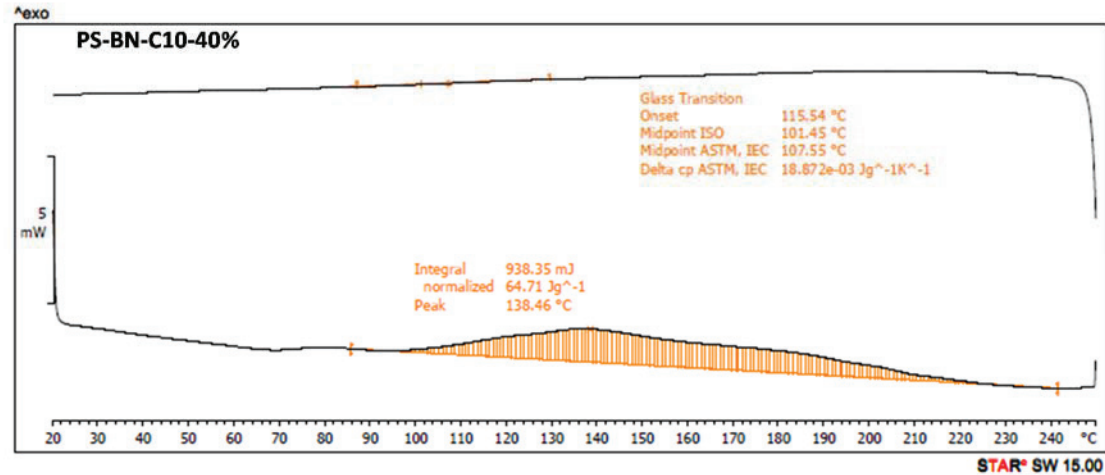
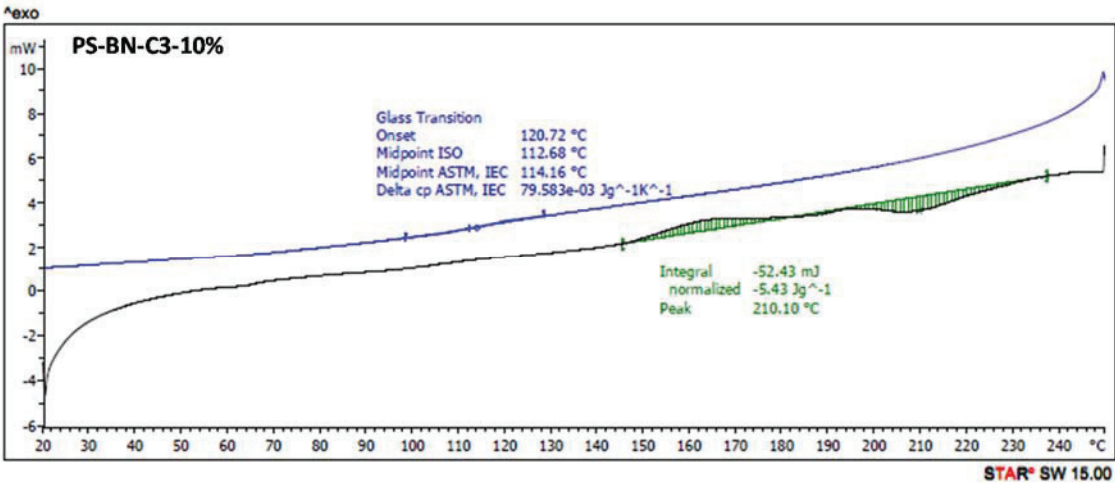
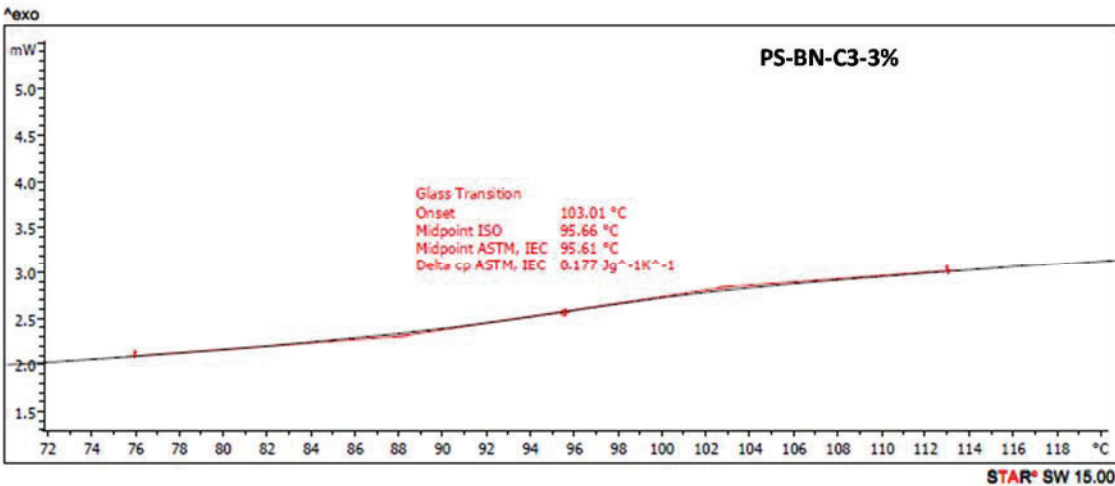
V.8. SEC (steric exclusion chromatography)

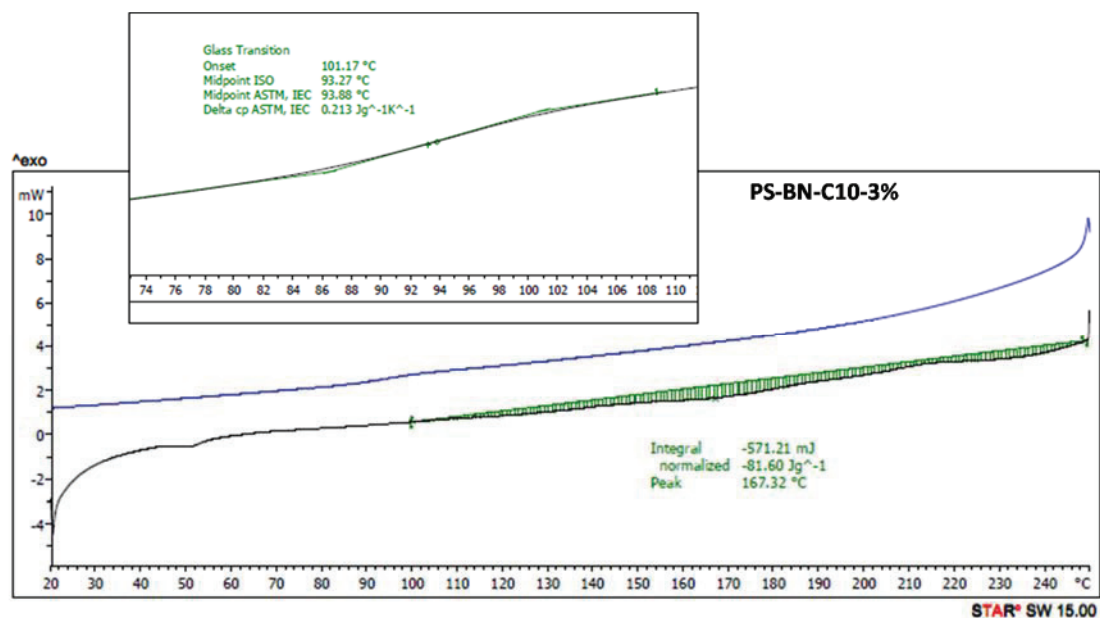
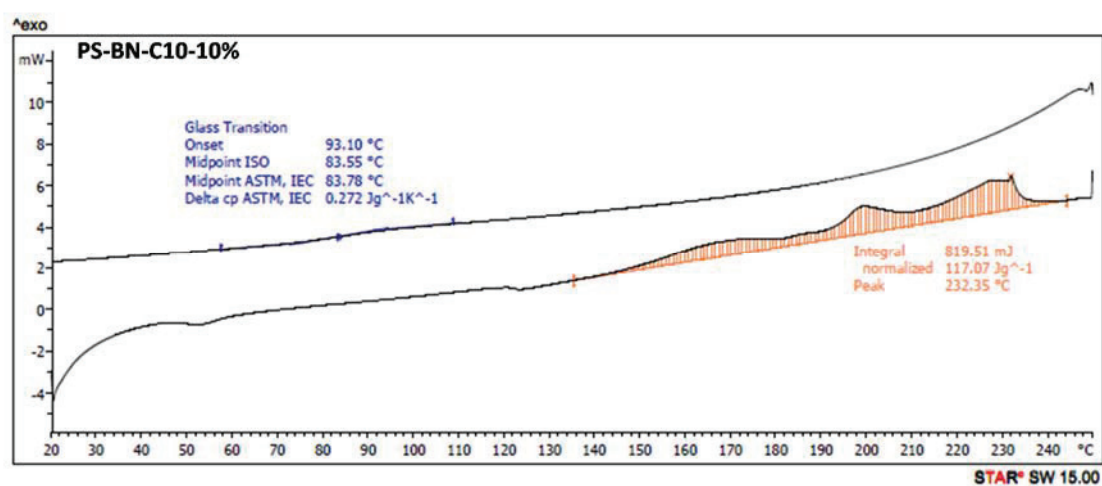
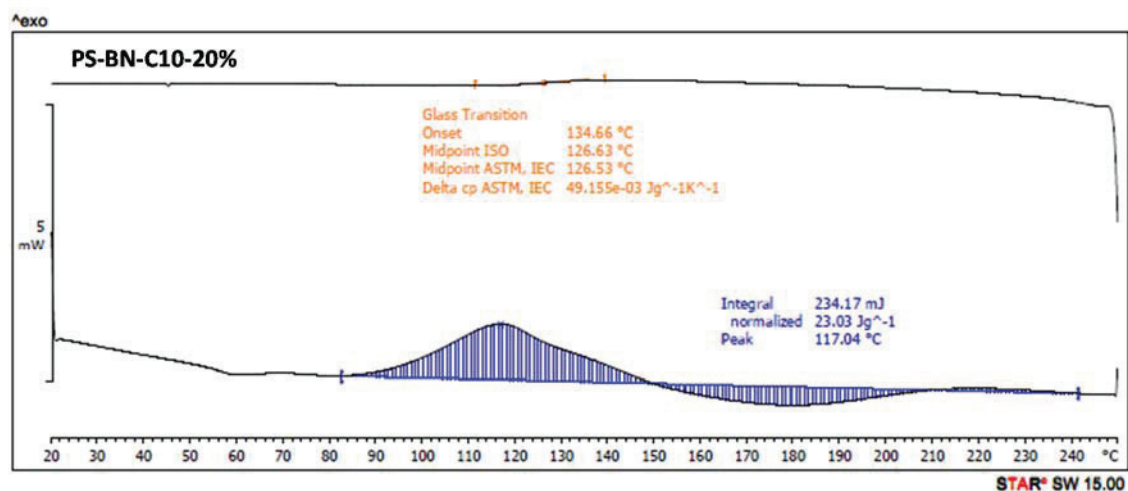




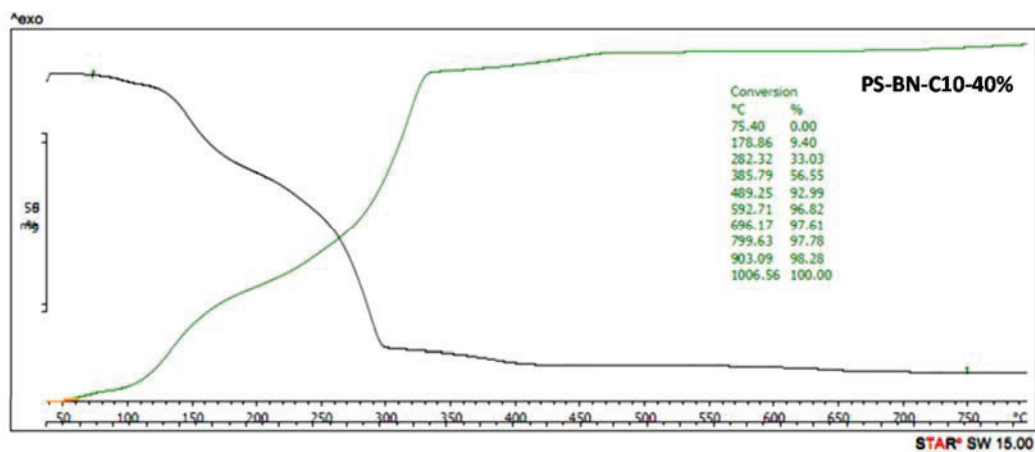
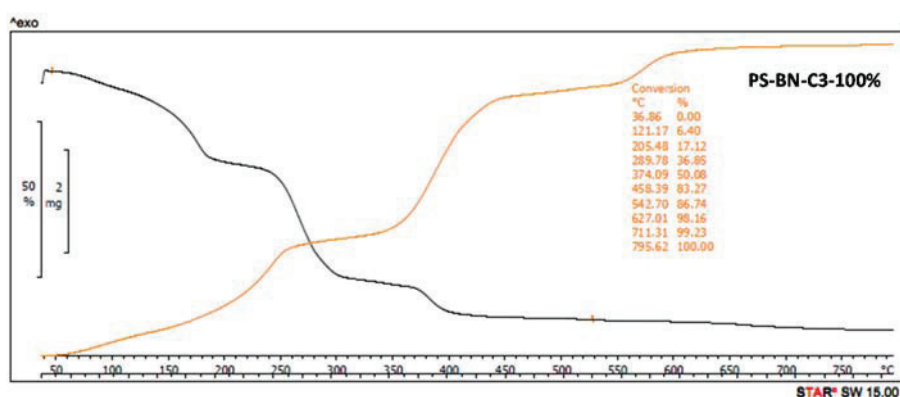
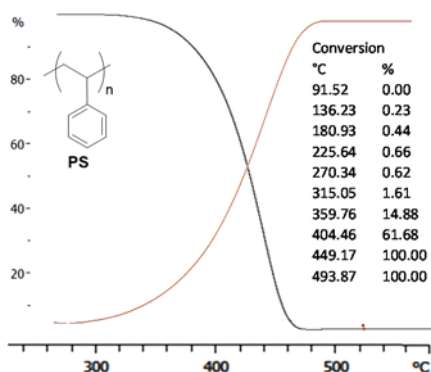


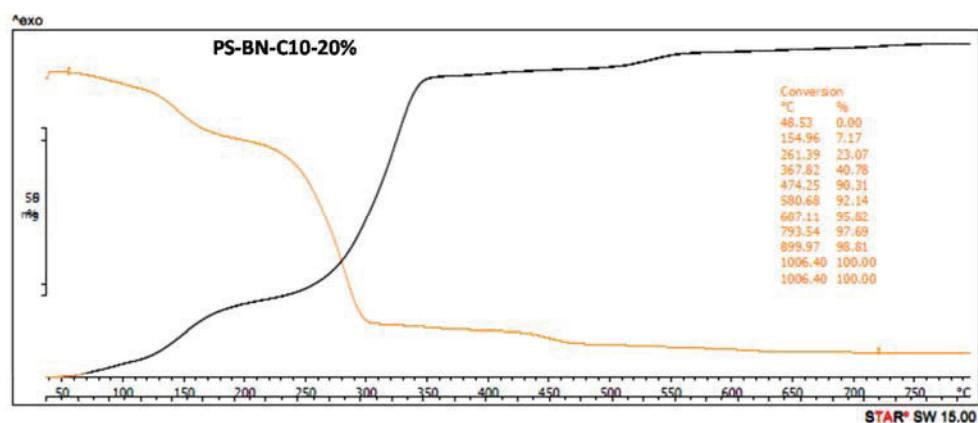






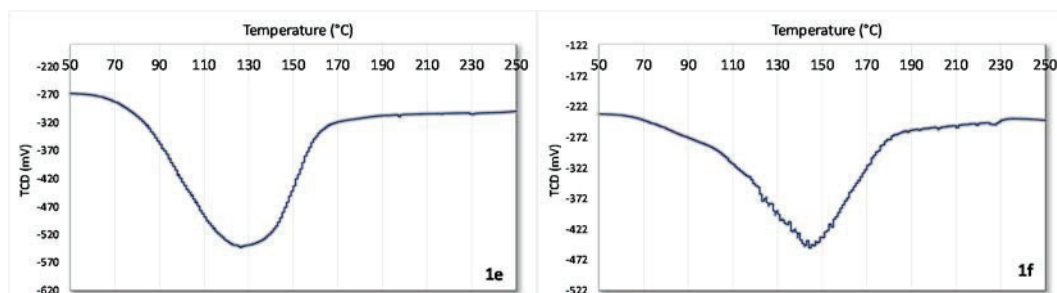
### V.10. TGA (thermal gravimetric analysis)



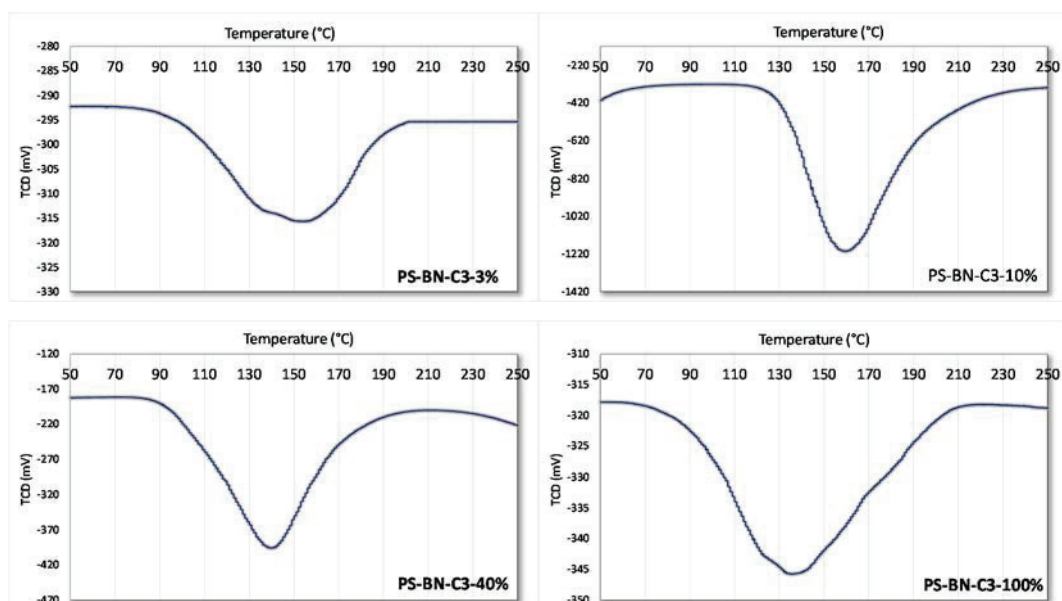


## V.11. TPD

### V.11.a. Molecular bricks

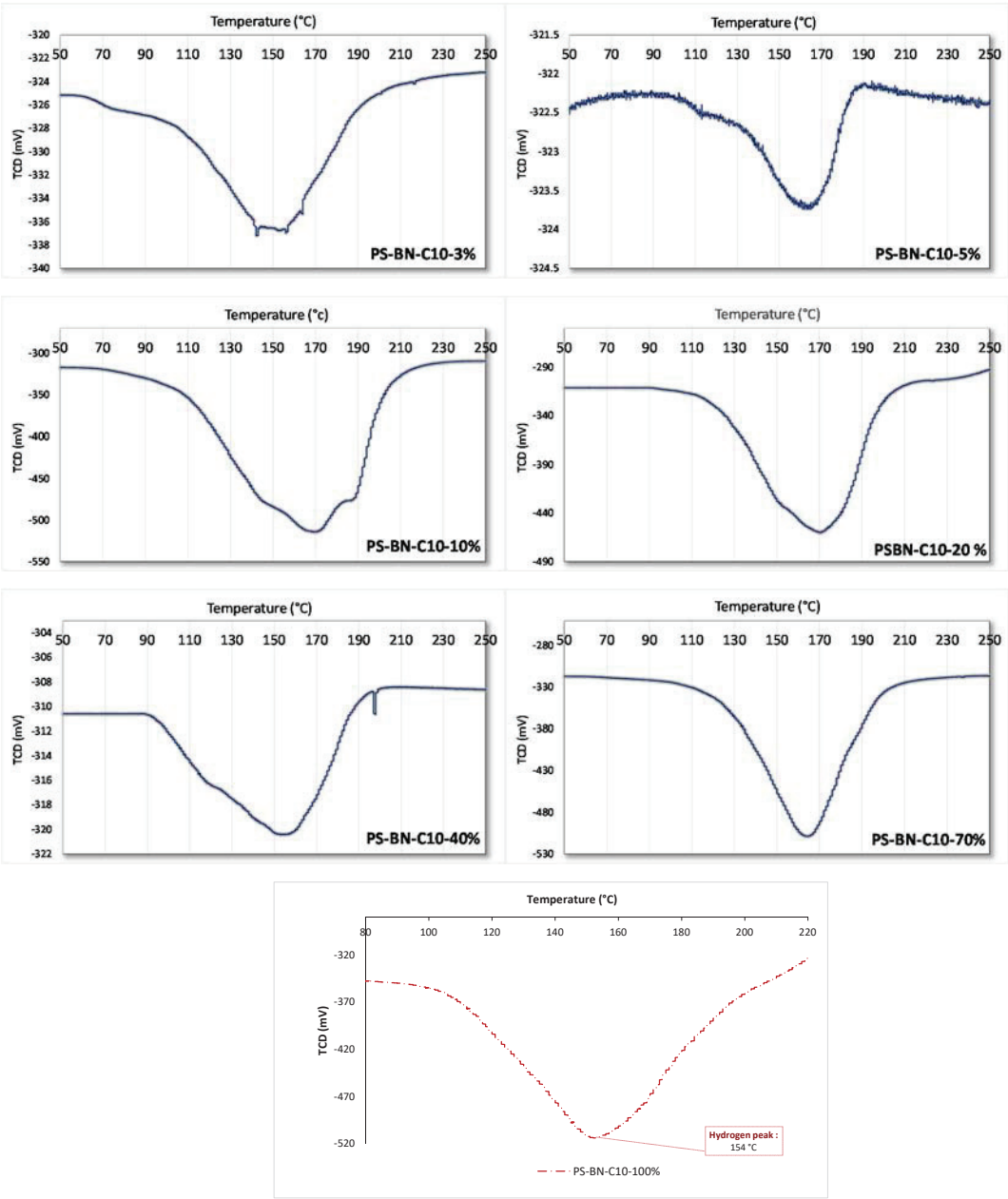


### V.11.b. Polymers PS-BN-C3-x%





V.11.c.      Polymers PS-BN-C10-x%



**V.11.d. AB-doped PS-BN-C10-100%**